Role of ABC transporters in *Candida* species

Thesis submitted to
Jawaharlal Nehru University
New Delhi, India
for the award of the degree of

Doctor of Philosophy

by

Sonam Kumari

Registration number: ICGEB/2015/019

International Centre for Genetic Engineering and Biotechnology (ICGEB)
Aruna Asaf Ali Marg
New Delhi-110 067
India

Year- 2020

ICGEB International Centre for Genetic Engineering and Biotechnology | Developing Knowledge

Declaration

I hereby declare that the work towards this thesis entitled "**Role of ABC transporters in *Candida* species**" has been carried out by me under the supervision of Dr. Naseem A. Gaur, Group Leader, Yeast Biofuel Group, at the International Centre for genetic engineering and biotechnology (ICGEB), New Delhi and under the co-supervision of Prof. Rajendra Prasad, Amity University, Gurugram. This work is original and has not been submitted in part or full for any other degree or diploma of any other university or institution.

Sonam Kumari

Sonam Kumari

ICGEB | *New Delhi*
Tel: +91-11-26741358
Fax: +91-11-26742316
E-mail: icgeb@icgeb.res.in
Trieste, ITALY - New Delhi, INDIA - Cape Town, SOUTH AFRICA
ICGEB Campus Aruna Asaf Ali Marg |110 067 New Delhi INDIA - www.icgeb.org

Certificate

This is to certify that this thesis entitled, "**Role of ABC transporters in *Candida* species**", submitted by Sonam Kumari for the Degree of Doctor of Philosophy to Jawaharlal Nehru University (JNU) is based on the work carried out at International Centre for Genetic Engineering and Biotechnology (ICGEB), New Delhi and Amity University, Gurugram. This work is original and has not been submitted in part or full for any other degree or diploma of any other University or Institution.

02-09-22

Dr. Naseem A. Gaur

Thesis Supervisor
Group Leader
Yeast Biofuel Group
ICGEB, New Delhi, India

International Centre For Genetic Engg. & Biotechnology Director New Delhi

Dr. Dinakar M. Salunke

Director
ICGEB,
New Delhi, India

Prof. Rajendra Prasad

Thesis Co-Supervisor
Dean, Faculty of Science, Engineering and Technology
Director, Amity Institute of Integrative Sciences and Health
Director, Amity Institute of Biotechnology
Amity University Haryana, India

Dedicated to ★★★

My Loving Family

Table of Contents

ACKNOWLEDGMENT

"The pursuit of Ph.D. is indeed a daring adventure," **and its sprouting and completion cannot be completed without the help of kind peoples and physical resources. With immense pleasure, I want to utilize this space to show my gratitude to all those concerned persons who have stood by me directly or indirectly during this journey. This accomplishment would be incomplete without a note of thanks to all of you.**

The most important factor for making a successful researcher is proper guidance that shapes the infant ideas. First and foremost, I would be to express my gratitude to my supervisors Dr. Naseem A. Gaur Sir and Prof. Rajendra Prasad Sir, for their continuous and invaluable guidance, encouragement, and support. Naseem Sir's tenacity and creativity have lead me to develop a deep sense of knowledge in the scientific field. Being his first PhD student, also provided me with an excellent opportunity to learn from his professional, scientific attitude. His constructive criticism and frequent discussions always inspired me to go ahead hastily. With him, I have learnt how to solve problems and think beyond. Our experiments have never suffered because of his administrative skills. I feel very happy to express myself as his first PhD student, and I consider myself very fortunate for being a part of his research group.

RP sir is the most wonderful scientist I have ever met. His scientific knowledge, focused and optimistic approach with exceptional enthusiasm are some of the qualities that are accomplished with excellent managerial skills that I admire the most. He is a masterpiece in science and has a problem-solving attitude that makes me feel truly blessed to get a chance to work with him. Not only in the scientific field, but he also supported me mentally and emotionally with his great advice. It was a learning experience to work with him as he himself works harder than anybody else, and that kept me charged all the time. I will always be thankful to him for shaping up my boat before a long voyage into the infinite ocean of science. I am also thankful to Vibha Ma'am for all the encouragement and best wishes during these years.

I am thankful to the ICGEB director Dr. Dinakar M. Salunke, for providing me the necessary infrastructure and resources. I am also profoundly thankful to ICGEB faculty members, ICGEB instrument handling staffs who have provided me a great lab space and working environment. I would like to say special thanks to Purnima ma'am for assisting me during confocal studies. I am thankful to ICGEB administration and IT members, library personals especially, Nidhi ma'am, Mayank Sir, Shravana Sir, Prathibha ma'am for their enormous help in these many years. I am thankful to Sachin sir for helping me in getting timely fellowships.

I am thankful to ICGEB Bioenergy centre for proving me space and instruments for my work. All scientists in the group were very helpful during these years. Dr. Brajesh Barese sir need special acknowledgement for solving our issues. I would like to thank Girish for helping in instruments issues. I would like to extend my thanks to Dr. Shireesh Srivastva from systems biology for biofuel group and Dr. Asif Mohmmed from parasitic cell biology group, ICGEB for being my doctoral committee member and critically accessing my study.

No work has been completed if I have not been gained the support from my Lab members. I have learnt a lot from my seniors from lab especially, Rameshwar Sir, Piyush Sir, Ajay Sir, Priya Ma'am and Farnaz Ma'am. I have found a very good friend Sonakhshi from the lab who has helped me with so many things that can't be explained in words. I would always remember the tea time spent you and the gossips that we did over these years. Other lab members and juniors Juhi, Mahendra, Sonu, Kiran, Anup, Shahid for their support. They helped me in all ways and always. I am fortunate to have all of you and the bonding which we have developed over these years will always stay in my heart, and I am sure a smile will come on your face while you are reading this. I am also thankful to the ICGEB trainees for making me learn several things.

"Ph.D. is a very cumbersome journey where failures are inevitable." **I am extremely extremely fortunate to have Mohit as a constant support system with me as my labmate, friend and my love of life. He is the source of my happiness, my origin of**

ideas. His immense love, faith and selfless support have always boosted my confidence. Since the day I met him, he quietly helped me with all his effort unconditionally. He became an inspiration for me in both my personal life and professional career. His consistent problem-solving attitude kept me working through these years.

During these long years, I couldn't have come this far without the constant support, suggestions from friends and ICGEB batchmates. I would like to extend my indebtedness and accord my heartful thanks to Amita, Ruchi, Danish, Sandeep, Subia, Suman and other ICGEB batchmates for their constant and unconditional emotional and scientific support in these years. The time spent with you guys and all the gossips that we did in ICGEB is memorable and very special to me, and I will miss the presence of all of you. I fell very indebted to the support of other group members of biofuel groups for their support during these years.

I was very fortunate that I have gained a chance to have access to three labs at the same time. I am deeply indebted and thankful to Nitesh Sir, senior from JNU, who have helped me to stand during my initial years of Ph.D. He not only supported in research work but also helped me through the day to day problems in the research area. The other members of JNU Atanu Sir, Remya Ma'am, Archna Ma'am, Neha Ma'am for making me learn research works. I am thankful to Ashutosh Sir, Lucknow University, for encouraging me in writing works. A special thanks to Wasi for his unconditional help in my research works. I can not forget the good time spent with you guys.

I am also thankful to have access to the lab of Amity University, where I have gained a lot. I am thankful to find such a good lab members Garima, Suman, Ashok Sir, Praveen there. They helped me a lot. Thank you all.

I would like to extend my gratitude to Dr. Rupinder Kaur for providing me a chance to visit her lab during my initial stage of PhD. She provided me lab space and guidance to learn basic tricks for yeast works. I am also thankful to the Lab of fungal pathogenesis members especially, Vivek sir, Kundan Sir, Priyanka Ma'am for the great experience I have gained there.

I also would like to add heartfull thanks to Dr. Awinash Bajaj from RCB and his lab members for helping me during my research work. I would like to give a special thanks to Jyoti for being a friend during the lab visits.

I have no words to express my gratitude to my teachers and friends from BHU and VBU for being my well-wishers and being in contact with these cumbersome years. I can not forget the time that you have taken out for our party, the meetings and the visits to several moments, from your so busy schedules. I am thankful to every BHUians from whom I have met these years. It has always given a reason to smile to meet you guys.

I am also thankful to our lab attendants Amar Ji and Pan Singh, who have kept everything ready for continuous flow of works.

I would like to extend a huge thanks to my funding agency Council of Scientific & Industrial Research (CSIR), India, for providing me fellowship support during my Ph.D.

I must appreciate the dedicated reviewers and editors of the journals Plos One and FEMS Yeast Research for their scientific comments and valuable suggestions in improving the quality of this research work.

"Family is a compass to guide us and motivate us in every step of life". **I am at a loss for words to express my gratitude and indebtedness to my Parents Deepak Kumar Verma and Kusum Lata Devi, whose teaching since childhood, unconditional and unending affection and sacrifice has made me achieve this milestone today. My brother Sandeep Kumar Verma is always a source of motivation. I feel blessed to have my grandparents with me and constantly supporting me. I am super blessed and fortunate to have very nice and supportive in-laws. They never stopped me for doing anything and continuously supporting me to achieve more. I am very lucky to find the support of my all family members.**

This episode of acknowledgment would be incomplete without a huge thanks to almighty God for being kind to me and his blessings. Thank you to my Shiv Ji for being with me through hard times.

At last, I would like to apologize and acknowledge all whom I might have missed inadvertently because small support from anyone means a lot to me.

Thank you all…….

Abbreviations

ABC	ATP-binding cassette
MDR	Multi drug resistance
CDR	Candida drug resistance
MFS	Major facilitator superfamily
BLAST	Basic Local Alignment Search Tool
TMDs	Transmembrane domains
TMHs	Transmembrane helices
NBD1	Nucleotide binding domain 1
PDR	Pleiotropic drug resistance
PM	Plasma membrane
HphB	Hygromycin B
R6G	Rhodamine 6G
NYS	Nystatin
AmB	Amphotericin B
FLC	Fluconazole
ITZ	Itraconazole
MCZ	Miconazole
KTC	Ketoconazole
TER	Terbinafine
CHX	Cycloheximide
ANY	Anisomycin
YPD	Yeast extract peptone dextrose
DCFDA	2′,7′-dichlorofluorescein diacetate
ROS	Reactive oxygen species
PCR	Polymerase chain reaction
RT-PCR	Real time polymerase chain reaction
LB	Luria bertani
YNB	Yeast nitrogen base
SDS	Sodium dodecyl sulphate
EDTA	Ethylenediaminetetraacetic acid
DEPC	Diethylpyrocarbonate
PEG	Polyethylene glycol

DTT	Di-thiothreitol
AMP	Ampicillin
NTC	Nourseothricin
MYR	Myriocin
4-NQO	4-Nitroquinoline 1-oxide
CSF	Caspofungin
RAPA	Rapamycin
PBS	Phosphate Buffered Saline
NR	Nile Red
BEA	Beauvericin
OMY	Oligomycin
WT	Wild type

List of Figures

List of tables

INTRODUCTION AND REVIEW OF LITERATURE

1: Introduction and Review of literature

1.1 An Introduction to human fungal pathogens and associated diseases

1.1.1 Kingdom Fungi

Fungi, the most evolutionarily and ecologically diverse organisms evidenced to have first appeared around 1 billion years ago (Berbee et al. 2017). They are ubiquitous to this planet, estimated to be approximately 2.2 to 3.8 million species, which constitutes about a quarter of earth's biomass (Miller 1992; Webster and Weber 2007), but we know only about just 120,000 species (Hawksworth and Lücking 2017). Fig 1.1 represents the diversity of the fungal kingdom. These are non-photosynthetic, heterotrophic eukaryotic organisms and can reproduce both sexually and asexually (Moore-Landecker 1996; Taylor et al. 1999). The majority of fungi grow as filamentous fungi with multiple nuclei in contrast to that yeast-like fungi with uninucleus, which divide by budding or fission (Fincham 2001; Borkovich and Ebbole 2010). In the tree of life, the fungal kingdom is among the most diverse kingdoms which includes molds, yeasts, mushrooms, plant parasitic rusts, lichens, smuts and mildews (Blackwell 2011).

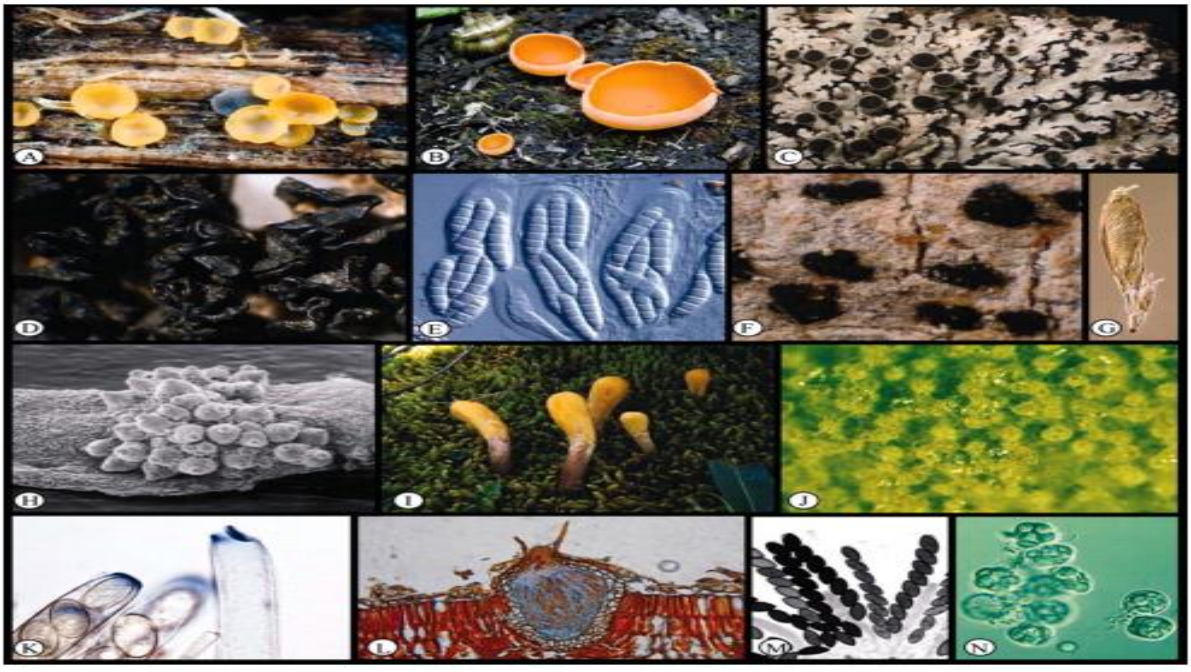

Fig1.1: Fungal diversity (Adapted from *Spatafora et al. 2017*)

During evolution, fungi adapted to survive a.nd propagate in any habitat, which could be considered as extreme (Raspor and Zupan 2006). Fungi play an intriguing role to support life on this planet (Walker and White 2017). Fungi are also a source of nutritious food and food additives, lifesaving medicines and antibiotics and probiotics, pigments, biofuels, vitamins, fatty acids, beverages and enzymes for biotechnology (Willis 2018). Table 1.1 represents the list of fungi important to humankind.

Table 1.1: Fungi important to man (compiled from *May and Adams, 1997* and *Kendrick, 2011*)

Human health and medicine	**Agriculture**	**Industrial biotechnology**	**Basic research**
Candida spp.	*Ustilago spp.*	*Saccharomyces cerevisiae*	*Saccharomyces cerevisiae*
Aspergillus spp.	*Magneporthe grisea*	*Pichia Pastoris*	*Schizosaccharomyces pombe*
Cryptococcus spp	*Fusarium spp.*	*Aspergillus niger*	*Neurospora crassa*
Pneumocystis carnii	*Erysipe spp.*	*Aspergillus oryzae*	*Aspergillus nidulans*
Coccidiodes immitis	*Aspergillus flavus*	*Aspergillus awamori*	*Ustilago maydis*
Histoplasma capsulatum	*Phytophthora infestans*	*Penicillium chrysogenum*	*Schizophyllum commune*
Blastomyces dermatitidis	*Agaricus bisporus*	*Trichoderma reesei*	*Coprinus cinereus*

1.1.2 Fungal pathogens and diseases: an underestimated problem

Even though fungi has extensive influence on human, animal, plant, ecosystem health and economic well-being, the threats posed by fungal pathogens from last three decades are often poorly underestimated (Olsen et al. 2011; de Pauw 2011). Fungi are the remarkable pathogen species in plants, animals as well as in humans. Out of 1,400 recognized human pathogens, a little more than 20 % (~ 325) are fungal, and less than a dozen are allied with “life-threatening” diseases (Taylor et al. 2001; Di Mambro et al. 2019). Primary fungal diseases (e.g., coccidioidomycosis, histoplasmosis) are very few that induce symptomatic disease in healthy people (Cutler et al. 2007; Casadevall 2007). Most pathogenic fungi infect susceptible individuals with already experiencing serious

illness, chemotherapy, autoimmune disease therapy, intensive care, and sophisticated surgery (Köhler et al. 2015). Nevertheless, once established, fungal diseases are often challenging to treat (Romani 2004; Casadevall 2007). Four essential conditions for infecting humans are high-temperature tolerance, capacity to enter the human body, human tissue lysis, and immunity to the human immune system (Gostinčar et al. 2018). While most of the fungal infections are subcutaneous and superficial infections affecting the skin, mucous membranes, and keratinous tissues, but some of the fungal infections can be fatal (Bajpai et al. 2019). Human pathogenic fungi belong to four major classes, namely zygomycetes, ascomycetes, deuteromycetes and basidiomycetes associated diseases (Al-Fakih 2014). The number of deaths attributed to fungal infections is equal to the mortality of the world's lethal illnesses, including malaria and tuberculosis, as stated by the CDC and WHO (Healey et al. 2016). The global burden of fungal infections is shown in Fig 1.2, which further explains why there is an urgency of combating these infections (Bongomin et al. 2017).

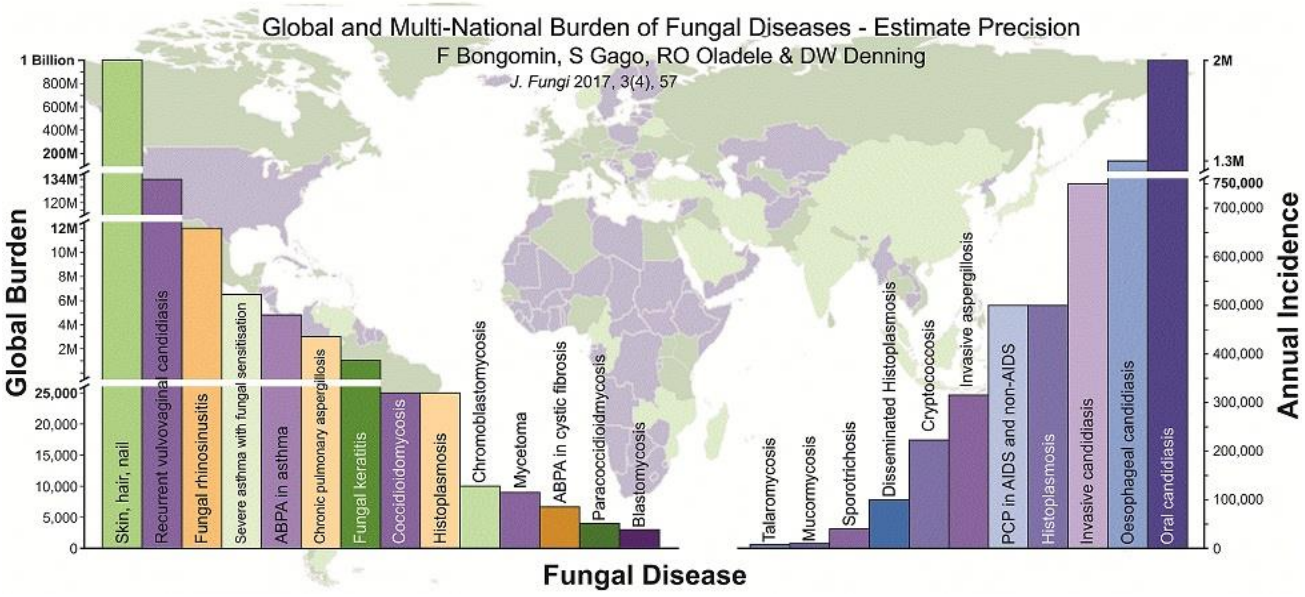

Fig 1.2: Global burden of fungal infections estimated recently (Adapted from *Bongomin et al. 2017*)

Overall, about one billion people develop fungal skin, nail or hair infections, millions from mucosal candidiasis, and over 150 million suffer from serious mycosal infections (Brown et al. 2012; Almeida et al. 2019; Bajpai et al. 2019). List of important pathogens and their etiologies are explained in Table 1.2.

Table 1.2: List of important human fungal pathogen and their distribution and etiological agents (Edited version of *Almeida et al. 2019*)

Fungal diseases	Distribution and etiological agent	References
Aspergillosis	Worldwide mycosis, caused by *Aspergillus spp.* Wide spectrum of infections in humans, but mainly in immunocompromised individuals. *Aspergillus fumigatus* and *Aspergillus flavus* are the most common.	Latge, 1999; Sugui et al., 2014
Blastomycosis	Endemic mycosis to the south central and north central United States, caused by *Blastomyces dermatitidis* and *Blastomyces gilchristii* in immunocompromised individuals.	Castillo et al., 2016; McBride et al., 2017
Candidiasis	Worldwide mycosis, caused by *Candida spp.* A major cause of mortality worldwide, and the main causative agent in systemic fungal infections. Among the *Candida spp., Candida albicans* and *Candida glabrata* are most common.	Pfaller and Diekema, 2007; Yapar, 2014
Coccidioidomycosis	Endemic to Southwestern United States and Central and South America, caused by *Coccidioides immitis* and *Coccidioides posadasii.*	Twarog and Thompson, 2015; Stockamp and Thompson, 2016
Cryptococcosis	Worldwide distribution, caused by *Cryptococcus neoformans*. Affects immunocompromised hosts, and is a major cause of HIV-related deaths. One noticeable outbreak in Vancouver Islands of *C. gattii* in immunocompetent patients.	Casadevall and Perfect, 1998; Heitman et al., 2011; Almeida et al., 2015
Dermatophytosis	Worldwide, *Trichophyton rubrum* and *Trychophyton interdigitale* have been described as the most common to cause dermatophytosis. The most frequent type of superficial mycosis in humans, attacking skin and nails.	Weitzman and Summerbell, 1995; Bitencourt et al., 2018; Persinoti et al., 2018
Histoplasmosis	Worldwide, *Histoplasma capsulatum* is the etiologic agent, mostly immunocompromised individuals, it is one of the most common invasive fungal pulmonary diseases.	Cano and Hajjeh, 2001; Guimaraes et al., 2006

Paracoccidiodomycosis	Endemic to Latin America, caused by thermodimorphic fungi of the *Paracoccidioides spp.*	Colombo et al., 2011; Theodoro et al., 2012
Pneumocystis	Worldwide, caused by *Pneumocystis jiroveci*, affects patients that are immunosuppressed, such as cancer patients receiving chemotherapy or HIV patients.	Thomas and Limper, 2004; Morris and Norris, 2012
Sporotrichosis	Worldwide, subcutaneous and subacute/chronic disease caused by dimorphic fungus of the genus *Sporothrix*.	Chakrabarti et al., 2015; Conceicao-Silva and Morgado, 2018

1.1.3 Candidiasis: fungal infection by genus *Candida*

Candidiasis is a broad term given to fungal infections due to species of *Candida* genus. Its scope covers a wide range of diseases from more superficial and milder clinical manifestations such as oral thrush, oropharyngeal candidiasis to serious infections such as bloodstream infections (BSI) and disseminated candidiasis (Hani et al. 2015). Invasive candidiasis includes severe diseases such as candidemia, endocarditis, central nervous system infections, endophthalmitis, and osteomyelitis (Fig 1.3) (Kullberg and Arendrup 2015). There have also been reports showing that older age people, diabetes mellitus patients and chronic renal failure patients are identified as risk factors for patients with invasive candidiasis (Wang et al. 2014). Genitourinary candidiasis is a widespread clinical complication from which ~ 75% of women suffer at least once during their child-bearing years (Achkar and Fries 2010). Pathogenesis and sites of infection due to *Candida spp*. are represented in Fig 3. According to the Centers for Diseases Control and Prevention (CDC) and the National Healthcare Safety Network data, *Candida* species ranked fifth among hospital-acquired pathogens and fourth among BSI patients. Surveillance studies based on population show incidence of *Candida* infections as 8 per 100,000 populations per year (Yapar 2014a), and 2500 cases of candidemia occur nationwide each year, according to CDC reports. Present challenges in the treatment of candidiasis include diagnostic delays, low sensitivity, difficulty in the discrimination of colonization from invasive candidiasis, limitations in current diagnostic techniques. Sometimes, the causative infection is only confirmed after autopsy (Pappas et al. 2018).

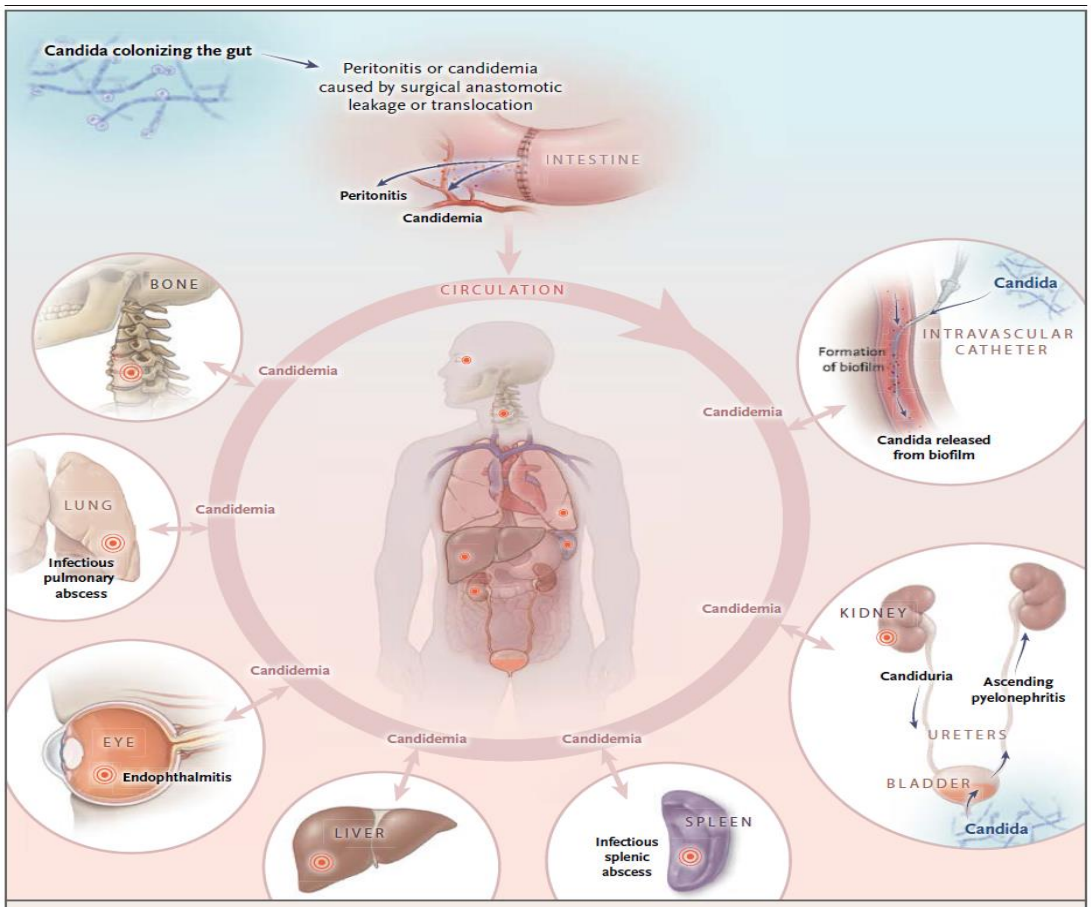

Fig 1.3: Pathogenesis of Invasive Candidiasis (Adapted from *Kulberg et al. 2015*)

About 200 *Candida* species have been described so far, but only a few have the pathogenic effect (Yapar 2014a; Zeng et al. 2019). These are *Candida albicans*, *Candida glabrata*, *Candida krusei*, *Candida tropicalis*, *Candida parapsilosis*, *Candida lusitaniae*, *Candida guilliermondii*, *Candida pelliculosa*, *Candida dubliniensis*, *Candida kefyr*, *Candida famata*, *Candida lipolytica*, *Candida rugosa*, *Candida inconspicua*, and *Candida norvegensis. Candida spp* can survive on inanimate surfaces, healthcare instruments and also in the hands of healthcare personnel, which increases the risk of outbreak and cross dissemination among susceptible hosts such as neonates, immunocompromised, intensive care, and surgical patients (Orozco et al. 2009; van Schalkwyk et al. 2018). In 95% cases of infections in both ICU and non-ICU settings, the pathogens involved are *C. albicans, C. parapsilosis*, *C. glabrata*, *C. tropicalis*, and *C. krusei* (Cortés and Corrales 2018). Rest of the 5% infections are due to twelve to fourteen other *Candida species,* including *C. krusei* (2 to 3%), *C. lusitaniae* (0.5 to 0.6%), *C. guilliermondii* (0.5 to 1%), *C.*

famata (0.08 to 0.5%), *C. rugosa* (0.03 to 0.7%), *C. dubliniensis* (0.01 to 0.1%) (Pfaller et al. 2010). Recently *Candida auris* have emerged as global threat to cause invasive candidiasis (Cortegiani et al. 2018).

1.1.4 Epidemiology of *Candida* infections

The third most common pathogen, *Candida* species, confer 20-34% bloodstream deaths (Fu et al. 2017). Globally, the majority of the isolate to cause candidiasis is *C. albicans,* but this varies from 35%-75% depending on the geographical locations (Doi et al. 2016; Pfaller et al. 2019; Zeng et al. 2019). The global surveillance programs SYNTRY surveillance program and ARTEMIS have reported geographical trends of *Candida spp* isolation and their distribution patterns. Global increase in non-*albicans Candida* (NAC) species are alarming and distribution of major NAC species are represented in Fig 1.14.

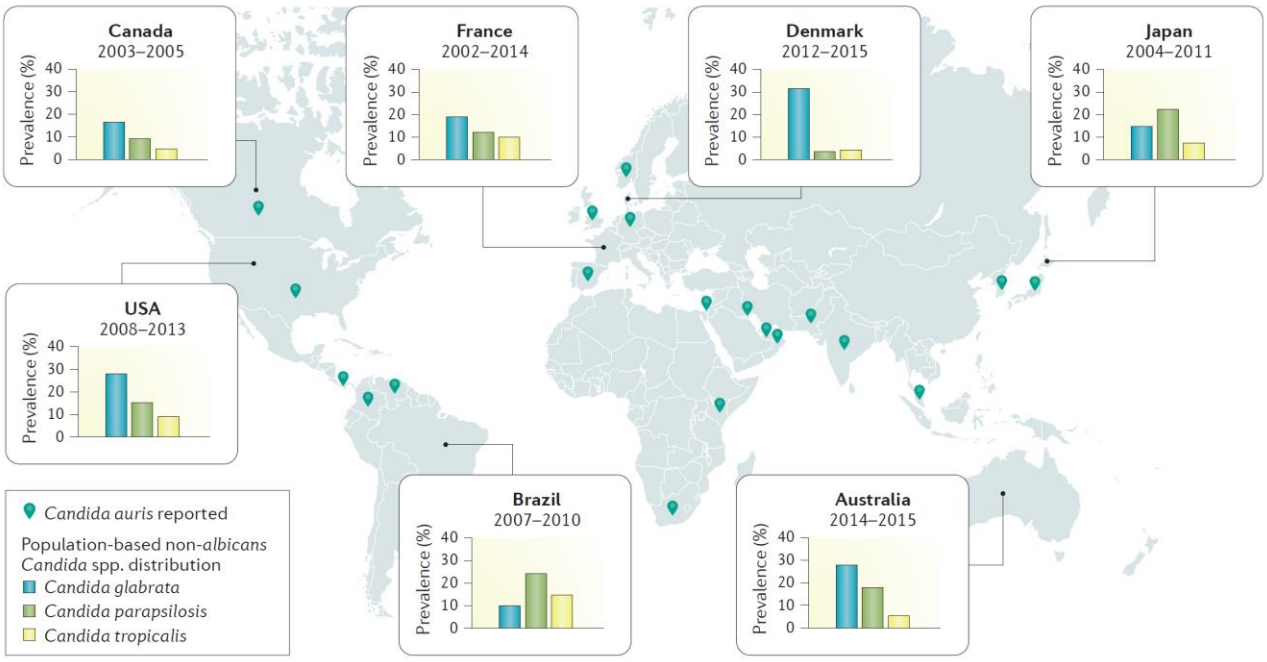

Fig 1.4: Scenario of NAC species globally (Adapted from *Pappas et al. 2018*)

The rise in candidemia due to NAC *spp.* has partly been associated with the use of fluconazole (FLC) prophylaxis and treatment of invasive fungal infections in susceptible and immunocompromised patients (Lamoth et al. 2018; Hassan et al. 2019). However, linking of FLC prophylaxis with changing epidemiological pattern of *Candida* infections

remain controversial as several reports claim no correlation between them (Lin et al. 2005). 30% of candidemia cases among newborns are due to *C. parapsilosis,* whereas the rate is 10%–15% among adults (Kothalawala et al. 2019). *C. parapsilosis* can colonize the skin and is a common isolate from catheter-related infections (Wang et al. 2016). *C. tropicalis* infections are frequently seen among leukaemia and neutropenic patients (Guarana and Nucci 2018). *C. krusei* infections are common among neutropenic leukaemia or hematopoietic stem cell recipients or receiving FLC prophylaxis (Yapar 2014b). *C. glabrata* is a more common infectious agent among older and neoplastic patients (Kothalawala et al. 2019; Kim et al. 2019b).

Candida species distribution varies with geographical location. A study conducted from 1999 to 2008 at Sri Ganga Ram Hospital, New Delhi, revealed a significant change in Candida's epidemiology that is marked by infection shifts caused by non-*albicans Candida spp*. (Oberoi et al. 2012). In Northern India, a study from Haryana hospital including 228 isolates collected between Dec 2015 to June 2018 showed *C. albicans* (67.0%) comprised the major part, followed by *C. tropicalis*, *C. auris*, *C. glabrata* and *C. parapsilosis* (Kumar et al. 2020). Another study from North India with a total of 136 isolates showed 80% prevalence of non-*albicans Candida spp*. with *C. tropicalis* at the top (39%) accompanied by *C. parapsilosis* (22.1%), *C. albicans* (14.7%) and *C. glabrata* (5.9%) (Singh et al. 2014). In a laboratory analysis performed at the Department of Microbiology, Manipal Hospital, *C. tropicalis* was causal for 39,7% of the patients in southern parts of India (Adhikary and Joshi 2011).

To summarize, globally changing epidemiological pattern of candidemia highlights the importance of close monitoring of the distribution of *Candida spp*. to optimize the therapies for *Candida* infections. Importantly, the emergence of a rare species, *C. rugosa*, both in India and in a tertiary care hospital in Sao Paulo, Brazil (Colombo et al. 2007), is alarming for the clinicians.

1.2 Current treatment landscape

Since 1960, after the introduction and development of antibiotics, a drastic rise in fungal infections was observed. At the present scenario, they represent a global health threat, also recognized by World Health Organization (WHO) (Vandeputte et al. 2012). The

increasing incidence of superficial and deep-seated Candida infections is not only due to chemotherapy or organ transplantation but also the use of broad-spectrum antibiotics, aggressive surgery and prosthetic devices (Di Mambro et al. 2019). These incidences aroused to the development of different therapies for the treatments. Currently, therapy includes anti-fungal agents, monoclonal antibodies and radioimmunotherapy.

1.2.1 Anti-fungal agents

There is a limited number of the armamentarium of antifungal drugs available despite extensive researches are going on in the development of new therapies. Indeed, only four molecular classes of antifungal are currently used that target three distinct fungal metabolic pathways to treat systemic fungal infections. These are polyenes, azoles, echinocandins, and fluoropyrimidine analog 5-flurocytosine (5-FC) (Canuto and Rodero 2002). Morpholines and allylamines class antifungals are only used as topical agents due to either their poor efficacy or adverse effects when administered systemically (Vandeputte et al. 2012). The currently available antifungals and their mechanism of action are demonstrated in Fig 1.5.

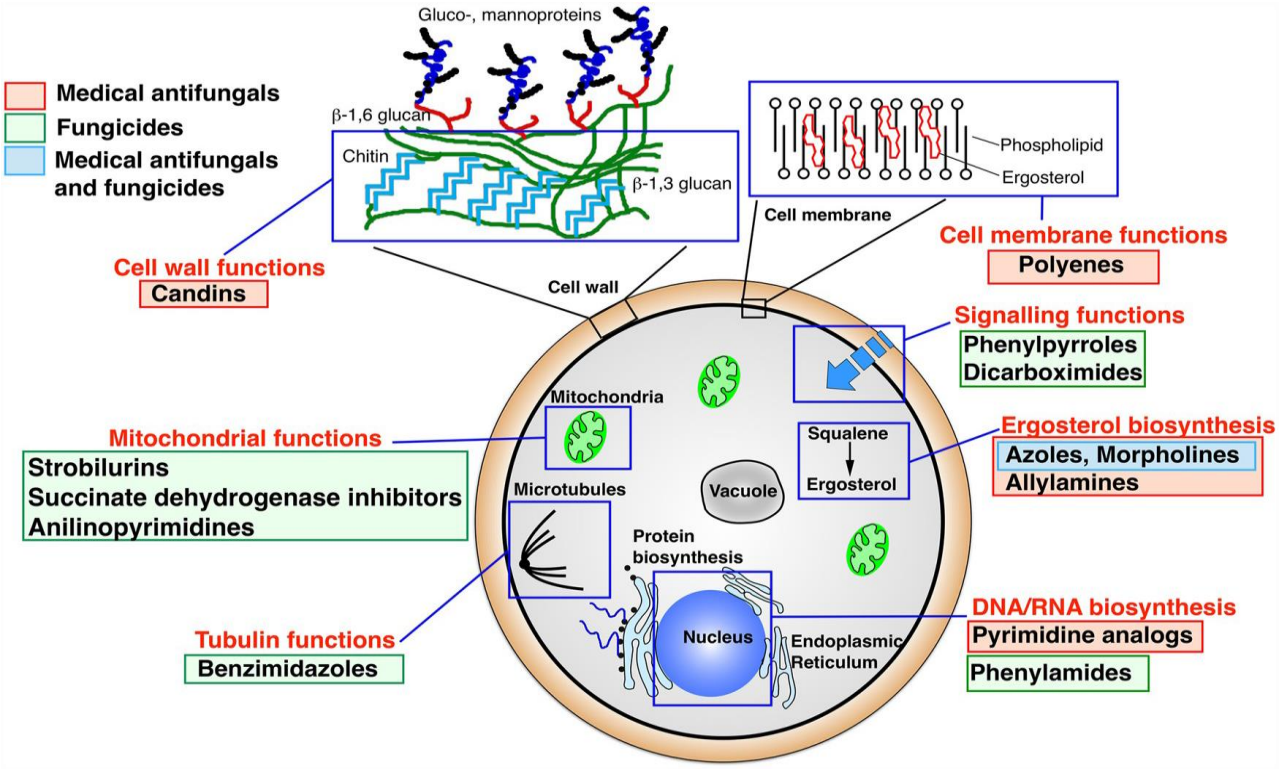

Fig 1.5: Antifungal agents and their mechanism of action (Adapted from Sanglard, *2019*)

1.2.1.1 Polyenes

Structurally polyenes are cyclic amphiphilic organic molecules, also known as macrolides with 20-40 carbons macrolactone rings conjugated with a d-mycosamine group. More than 200 molecules from polyenes class have antifungal activity, but only three of them, namely, amphotericin B (AmB), nystatin (NYS) and natamycin are being used in clinical practices (Vandeputte et al. 2012). Most of the polyenes are being produced by *Streptomyces* bacteria; however, these can be commercially produced. AmB is administered intravenously and the clinically approved dosage for AmB for all *Candida spp*. is 0.7 mg/kg/day except for *C. glabrata* and *C. krusei*, where approved dosage are ≥0.7 mg/kg/day and 1 mg/kg/day, respectively (Spellberg et al. 2006)

Polyenes target ergosterol, through binding the lipid bilayer and forming pores. Pore formation promotes destabilization of the plasma membrane (PM), leads to leakage of channels for intracellular components such as K^+ ions and cell lysis. However, AmB is also able to induce oxidative and nitrosative bursts in *Candida* and *Cryptococcus* to enhance its fungicidal property (Mesa-Arango et al. 2014, p.). AmB acquired or innate resistance occurrence among fungal pathogens is infrequent, and it has very severe effects on the kidney of the host (Adler-Moore and Proffitt 2008). Lipid-based formulations of AmB are less toxic, an effective treatment invasive candidiasis and are also less expansive (de Oliveira Santos et al. 2018). Polyenes also have a lower affinity for the human counterpart of ergosterol, cholesterol. This slight cholesterol affinity explains the high toxicity associated with antifungals and is responsible for several side effects. That is the reason why AmB is only given systemically, while NYS and natamycin are either used locally or orally (Vandeputte et al. 2012).

1.2.1.2 Azoles

Azoles are the most frequently used antifungal. Azoles inhibit *ERG11* gene, which codes for an enzyme of the cytochrome demethylase system of the fungal cells resulted in toxic sterol formation (14-α methylated sterol) and disrupt the membrane oxidative enzymes, retention of intracellular phospholipids, and ultimately fungal cell death (Nami et al. 2019). Since these compounds also react with the cytochrome P450 of the mammalian enzyme system, their oral and/or parenteral intake causes multiple disruptions and leads to multiple side effects. Azoles are cyclic organic molecules divided

into two groups the imidazoles [ketoconazole (KTC), clotrimazole (CTZ), miconazole (MCZ)] with two nitrogen atoms, and the triazoles [FLC, voriconazole (VRC), itraconazole (ITZ)] with three nitrogen atoms. The first azole was synthesized in 1944, but it was in the late 1960s when CTZ, econazole, and MCZ became available for treatment. KTC was permitted by the food and drug administration (FDA) in 1981, and FLC became available for use by clinicians only in 1990. ITZ was approved and made available by the FDA in 1992 (Di Mambro et al. 2019).

FLC is the most recommended for most *Candida* infections due to the low cost in patients (Paramythiotou et al. 2014). At present, there are a number of licensed azole antifungals; however, only four of them (FLC, ITZ, posaconazole, and VRC) are employed in clinical prophylaxis or treatment of fungal BSI (Van Daele et al. 2019). Oral formulations are available for all azoles; however, intravenous administrations are limited to FLC and VRC. FLC and VRC can be absorbed rapidly, but ITZ and MCZ are slow to be absorbed (Brüggemann et al. 2009). KTC was the first broad-spectrum oral antifungal agent available to treat systemic and superficial mycoses, but due to its hepatotoxic side effects, oral KTC was withdrawn in 2013 (Gupta and Lyons 2015). VT-1598, VT-1129 and VT-1161, some new azole antifungal under preclinical, phase1 and phase 3 clinical trials respectively with a longer half-life (Van Daele et al. 2019). NT-a9, a new triazoles and an analogue of isavuconazole is effective against several fungi including *C. albicans*, *C. glabrata* and *C. neoformans* (Lu et al. 2019)

Doses used for various azoles in clinical practice for FLC is 400-800 mg/day, for VRC is 600 mg/day for initial two days and then 400 mg/day, for ITZ is 400 mg/day and for posaconazole is 400-800 mg/day (Spellberg et al. 2006; Goldman and Green 2015). Although azoles are generally well tolerated, azole antifungals have limitations to their use. Limitations to use azole antifungal include adverse effects such as hepatotoxicity and the emergence of resistance (Patil et al. 2015). Azoles can be toxic, as they serve as substrates or inhibitors of the number of enzymes, such as cytochrome P450 enzymes (de Oliveira Santos et al. 2018).

1.2.1.3 Echinocandins

Echinocandins introduction in clinical practice was a ray of hope for candidiasis patients with a history of exposure to azoles, or intolerance to AmB (Rivero-Menendez et al. 2019; Nami et al. 2019). Echinocandins are synthetic derivatives of lipopeptides and are naturally produced by several fungal species *viz.*, *Aspergillus rugulovalvus* synthesizes caspofungin (CSF). Three echinocandins CSF, micafungin (MCF), and anidulafungin (ANF) are currently approved for clinical use by the FDA, in 2001, 2005 and 2006 respectively (Vandeputte et al. 2012). These molecules are fungicidal in *Candida* but only fungistatic in *Aspergillus* (Minnebruggen et al. 2010).

Echinocandins inhibits *β*(1-3)-glucan synthase, an enzyme that catalyzes the polymerization of *β*(1-3)-glucan from uridine diphosphate-glucose which is a structural component for maintaining the fungal cell-wall integrity and rigidity (Van Daele et al. 2019). Two *FKS* genes are present within the genome of most of the fungi with overlapping functions (Riquelme et al. 2018). Echinocandins can inhibit both the *FKS1* and *FKS2* gene in *S. cerevisiae* and *C. glabrata* (Johnson et al. 2011; Pham et al. 2014). Inhibition of *β*(1-3)-glucan synthase leads to cell wall destabilization, leakage of intracellular components, which results in fungal cell lysis (Parente-Rocha et al. 2017).

All three echinocandins are available only in the form of intravenous formulations, which limits their use (Perlin 2011). For CSF and MCF, clinically approved doses are administered at 70 mg/day and 75 mg/day, respectively, while ANF is given as a dose of 150 mg for the first day, followed by 75 mg/day (Denning 2003). As echinocandins target *β*(1-3)-glucan synthase, which is absent in mammalian cells, so these have a favourable safety profile (Perlin 2011).

1.2.1.4- 5- Fluorocytosine

5-FC was synthesized in 1957 as an antitumor therapy, and in 1963 its antifungal potential was discovered (Scorzoni et al. 2017). It has a broad range of activity and is active against *Candida* and *Cryptococcus* genera. It diffuses rapidly throughout the body when taken orally due to its high hydrosolubility and small size (Vandeputte et al. 2012). 5-FC interferes DNA replication, but it has no antifungal activity. Through specific transporters

(cytosine permeases or pyrimidine transporters), 5-FC enters the cell; it is then converted into 5-fluorouridine (5-FU) by the cytosine deaminase. Then, another enzyme, uridine phosphoribosyltransferase (UPRT), converts 5-FU into 5-fluorouracil monophosphate (5-FUMP). 5-FUMP can then either be converted into 5-fluorouracil triphosphate incorporating in RNA instead of UTP and inhibiting protein synthesis or converted into 5-fluorodeoxyuridine monophosphate (5-FUM). 5-FUM further inhibits DNA synthesis enzyme, thymidylate synthase, thereby inhibiting cell replication (de Oliveira Santos et al. 2018).

5-FC is not routinely used in monotherapy due to its limited activity spectrum and emergence of drug resistance, and it is usually used in combination with azoles and AmB. (Van Daele et al. 2019). Generally, it has negligible side effects, despite some severe adverse effects, such as hepatotoxicity or bone marrow suppression occurring in rare cases (Vandeputte et al. 2012).

1.2.1.5 Other antifungals

Three minor groups of antifungal, which inhibit ergosterol biosynthesis, are also used as a topical antifungal. The allylamines, such as terbinafine (TER), inhibit the squalene epoxidase encoded by *ERG1* (Ruckenstuhl et al. 2007). The morpholines such as amorolfine act as an inhibitor of two enzymes of ergosterol pathway: the *ERG24* encoded Δ7,8-isomerase and the *ERG2* encoded C14-reductase (Gebre et al. 2015). These are used to treat dermatophyte infections despite their wide spectrum effect. Griseofulvin, interfere with microtubule dynamics, ultimately inhibits mitosis (Rathinasamy et al. 2010). Phenylamides antifungals such as metalaxyl, cyprofuram, benalaxyl and oxadixyl target RNA polymerase I (Park et al. 2014). Benzimidazoles antifungals such as carbendazim bind to b-tubulin, which affect DNA synthesis (Zhou et al. 2016). Inhibitors of both strobilurins and succinate dehydrogenase inhibit both the electron transfer chain (ETC) of mitochondrial respiration by inhibiting complex III and complex II, respectively (Sanglard 2019; Zuccolo et al. 2019). Antnilinopyrimidines antifungals target mitochondrial signaling pathways (Fisher et al. 2018).

1.2.1.6 Potential targets for the new antifungal discovery

Ergosterol biosynthesis is targeted by most antifungal class; however, other possible targets could also be explored for further drug development.

1.2.1.6.1 Heat Shock protein 90 (HSP90)

A promising new strategy to improve the efficiency of antifungals and to block the evolution of drug resistance can be achieved by targeting molecular chaperone Hsp90 (Veri and Cowen 2014). Hsp90 is a conserved molecular chaperone with various physiological functions but is also associated with the rapid development of antifungal resistance in *Candida spp*. and *Aspergillus spp*. (Lamoth et al. 2015). Hsp90 is a part of a complex network that involves calcineurin, lysine deacetylases (KDAC), and other proteins, which organize compensatory repair mechanisms of the cell wall in response to the stress induced by antifungals (Veri and Cowen 2014). Disrupting Hsp90 circuitry by several agents (Hsp90 inhibitors and KDAC inhibitors) potentiates the antifungal activity of CSF and azoles, thus representing a promising novel antifungal approach (Cowen et al. 2009). Inhibitors of Hsp90 include geldanamycin, which is a benzoquinone ansamycin, its derivatives, and radicicol, a resorcyclic acid lactone produced by certain fungal species show the synergistic effect with known antifungal agents (Jacob et al. 2015).

1.2.1.6.2 Calcineurin signaling

Calcineurin signaling is a conserved signaling pathway, plays diverse roles in fungi such as morphogenesis, regulation of stress responses, and pathogenesis. Fungal pathogens are also shown to exploit this pathway to successfully survive in the host environment and to cause life-threatening infections (Liu et al. 2015). Calcineurin signaling also regulates growth at alkaline pH, increased temperature, membrane stress conditions, and virulence *C. albicans* and *C. neoformans* (Kozubowski and Heitman 2012; Yu et al. 2015). Calcineurin plays an important role in maintaining colony morphology and dimorphic switching and also regulates several downstream target genes, such as vacuolar calcium P-type ATPase CaPmc1p and β-(1,3)-glucan synthase subunit CaFks1p in *C. albicans* (Sanglard et al. 2003). In *Neurospora crassa*, calcineurin impacts the tip high calcium gradient important for the development of hyphal tip and normal vegetative growth

(Silverman-Gavrila and Lew 2000). In *A. fumigatus,* calcineurin is required for virulence in the host (Juvvadi et al. 2014).

In a genome-wide microarray analysis of the global response of iron deprivation in C. albicans displayed upregulation of several HSPs (HSP90, HSP70, HSP60, and HSP30) and calcineurin mediated drug resistance (Hameed et al. 2011). Although calcineurin is a non-essential gene in *C. albicans*, mutation in *CaCNB1*, a regulatory subunit of calcineurin, leads to hypersensitivity to FLC (Jia et al. 2012). The mechanism of calcineurin signing in stress is regulated through the dephosphorylation of the Zn-finger transcription factor CaCrz1p, which after activation, translocates into the nucleus to activate downstream genes expression (Karababa et al. 2006). The potential targets in the Ca2+-calcineurin pathway are represented in Fig 1.6.

Known immunosuppressive calcineurin inhibitors include FK506 and cyclosporine A which are active against several fungi, pointing to targeting the calcineurin can be a promising antifungal drug development strategy (Liu et al. 2015). Several azoles *viz.*, VRC and posaconazole, in combination with FK506 and cyclosporine A show a clear synergism against fungi (Borba-Santos et al. 2017).

However, the currently available calcineurin inhibitors are not ideal for treating fungal infections due to their immunosuppressive effects (Steinbach et al. 2007). It is unlikely in recent times that the current calcineurin inhibitors will gain clinical approval as antifungal agents, so new and more potent inhibitors are required that do not cross-react with the host and do not induce immunosuppression (Juvvadi et al. 2014).

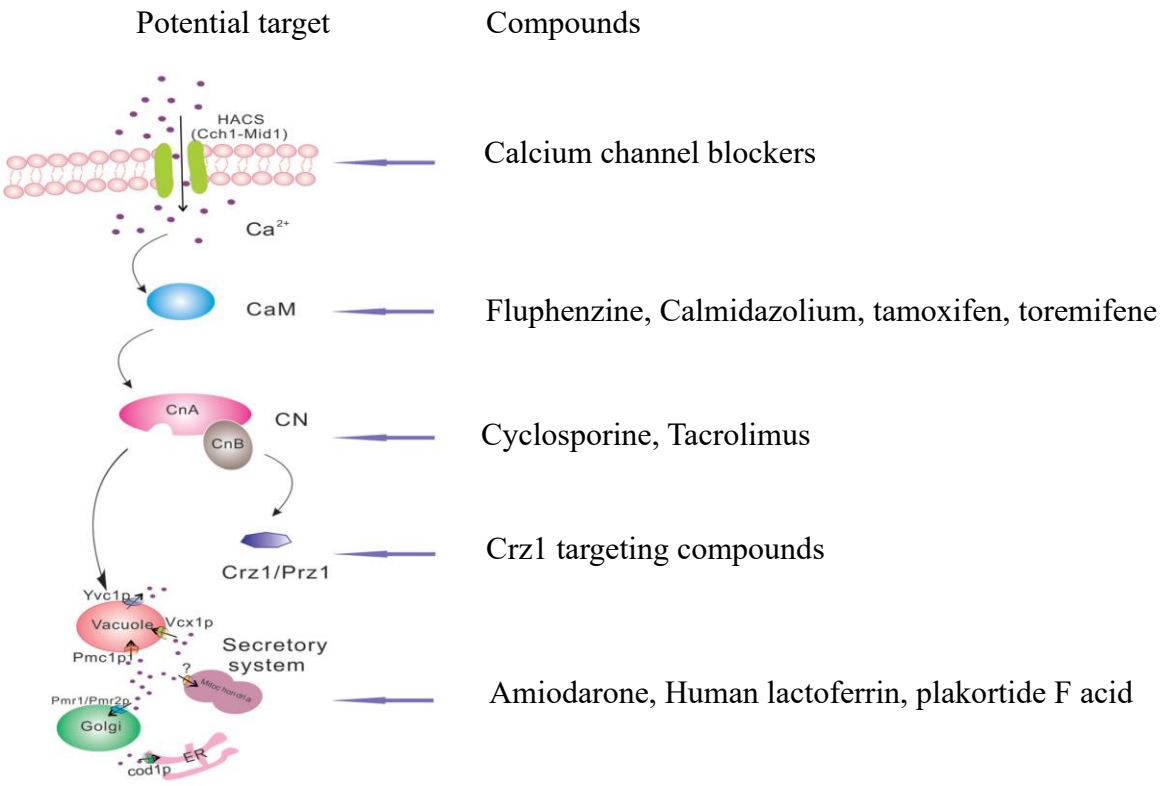

Fig 1.6: Antifungal targets in Ca2+- calcineurin pathway (Adapted from *Liu et al. 2015*)

1.2.1.6.3 TOR kinase

Two TOR paralogs exist and form distinct complexes in yeast belonging to *Saccharomyces* clade, namely TOR complex 1 (TORC1) and TOR complex 2 (TORC2). The TORC1 controls protein synthesis, inhibition of translation by regulating mRNA synthesis, repression of ribosomal gene expression, nitrogen catabolite response, stress response, and degradation, ribosome biogenesis, and induction of autophagy in *S. cerevisiae* (Loewith and Hall 2011). TORC2 is involved in the control of actin polarization and cell wall integrity (Shertz et al. 2010). *S. cerevisiae* Sc*TOR2* can complement the *Sctor1* loss generated function, but *ScTOR1* cannot complement the *Sctor2* loss generated functions (Shertz et al. 2010; Roelants et al. 2011). The TOR signaling activation is different in humans and yeasts (Inoue and Nomura 2017) (Fig 1.7), so it could be a good target for future drug designing.

In *C. albicans*, the deletion of a PM localized ABC transporter *Cdr6/Roa1*, hyperactivates CaTor1 kinase, which affects multiple cellular functions. CaTor1 activation in the mutant resulted in the activation of Hsp90 and ribosome biogenesis and suppression of complex

sphingolipid biosynthesis. The activation of CaTor1 kinase in the mutant and change in membrane permeability leads to increased resistance to azoles in the mutant (Khandelwal et al. 2018).

Tor kinases can be inhibited pharmacologically by the use of the immunosuppressant drug rapamycin, a natural secondary metabolite produced by *Streptomyces hygroscopicus* (Loewith and Hall 2011). Recently studies indicate that rapamycin decreases *erg3*-mediated azole resistance (Shapiro et al. 2011). Recently, small-molecule inhibitor of Pho84A is approved, which affects TORC1 signaling and enhances the activity of the antifungals AmB and MCZ (Liu et al. 2017). The molecular mechanism through which the TOR signaling cascade regulates responses to azoles remains an exciting area for future studies.

1.2.1.6.4 Casein kinase 2.

The casein kinase 2 (CK2) is a serine/threonine-protein kinase that controls cellular growth and proliferation of yeast (Litchfield 2003). In most of the fungi, CK2 kinase is composed of two catalytic subunits Cka1 and Cka2 and two regulatory subunits Ckb1 and Ckb2 (Ong et al. 2019). Insertion mutations in *CaCKA2* were found to be FLC resistant in *C. albicans,* and the molecular basis was due to the overexpression of the drug efflux pumps *CaCDR1* and *CaCDR2* (Bruno and Mitchell 2005). Although insertion mutation in *CaCKA1* had a slight effect on FLC resistance, but its overexpression in *CaCka2* mutant resulted in suppression of FLC resistance, indicating there might have some role of CaCka1p in azole resistance. Inhibition of calcineurin or *Cacrz1 deletion* also reversed the phenotype of *CaCKA2* mutant (Onyewu et al. 2004). Genetic interaction between HSP90 and CK2 complex was observed in genome-wide chemical-genetic screening in *S. cerevisiae* (Diezmann et al. 2012). It will be a matter of great interest to further dissect the role of CK2 in the development of azole resistance.

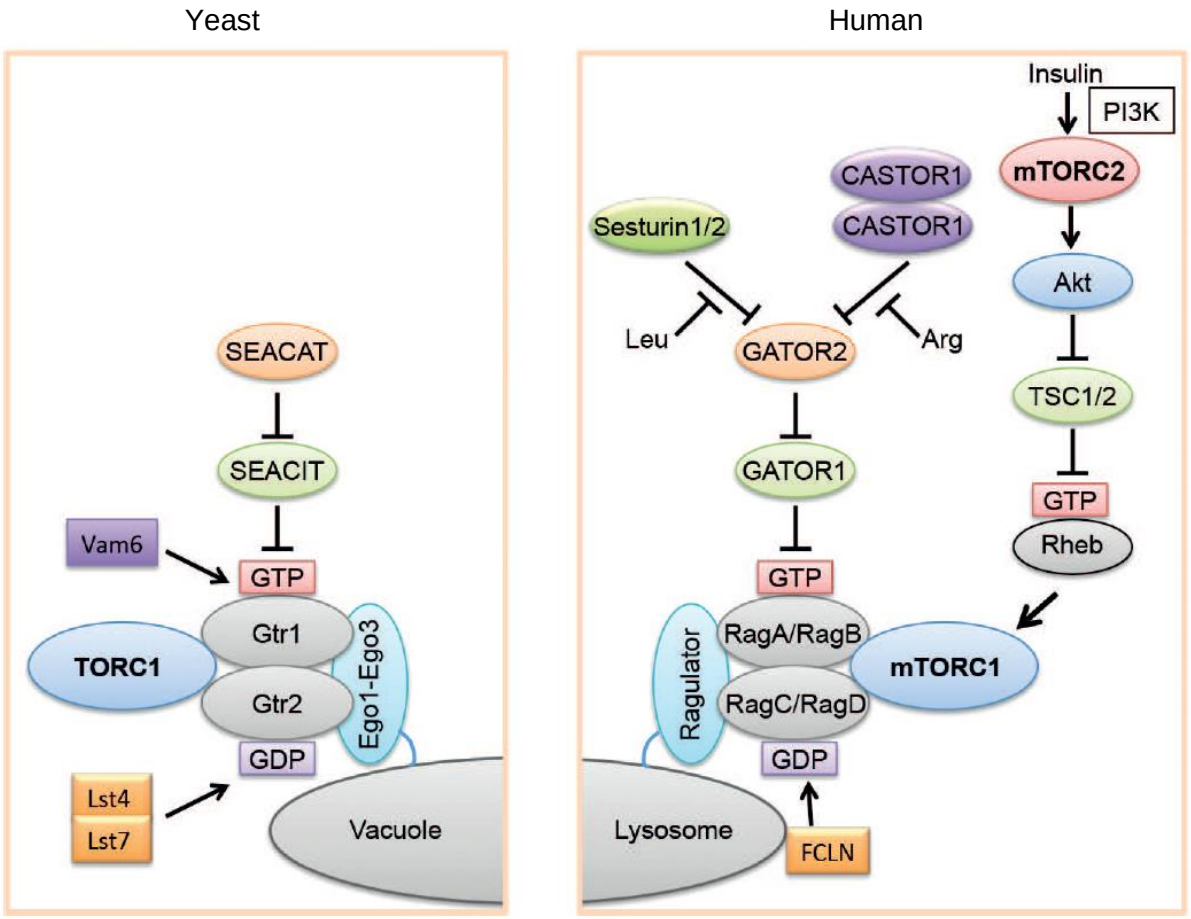

Fig 1.7: Circuitry of signing cascades in yeasts and humans (Adapted from *Inoue et al. 2017*)

1.2.1.6.5 Sphingolipids

Sphingolipids are major components of fungal cell membranes, playing a variety of roles such as heat stress response, signal transduction, endocytosis, apoptosis, fluidity, and domain organization (Heung et al. 2006). Both ergosterol and sphingolipids interact with each other in the membrane, and most of the antifungal target ergosterol synthesis, which suggests that sphingolipid can also interfere with the inhibition (Mukhopadhyay et al. 2004). Some sphingolipids attenuate the fungal pathogenesis by inhibiting or deleting enzymes involved in the biosynthetic pathways, for example, by inositolphosphoryl ceramide (IPC) and GlcCer (Rollin-Pinheiro et al. 2016).

Although the pathway of sphingolipid biosynthesis is conserved, still the structural complex lipids are different in fungal and mammalian cells and can be a potential target

for drug development. Several natural inhibitors of fungal GlcCer synthesis are known to attribute antifungal properties (Mor et al. 2015). *Caipt1* deletion in *C. albicans* which ultimately lead to depletion of $M(IP)_2C$, significantly increased susceptibility to azoles (Prasad et al. 2005). *FEN1* and *FEN12,* encode enzymes for the synthesis of very-long-chain fatty acids, null mutants of these also shown to be hypersensitive on AmB in both *S. cerevisiae* and *C. albicans* (Sharma et al. 2014). Upregulation of sphingolipid biosynthesis genes is also observed in FLC resistant *C. albicans* isolates. (Gao et al. 2018).

1.2.2 Immunotherapy

With increasing susceptible group, mortality and morbidity associated with invasive antifungals, prevention from fungal infection is a need. Advances in our knowledge to host defense system against fungal infection has provided a good platform for the development of effective vaccines. Several antifungal vaccines are in pre-clinical studies, although few trials have been performed on humans (Scorzoni et al. 2017). For invasive candidiasis treatment, two vaccines are promising and are in the clinical trial. The first is in phase IIa, containing the rAls3p-N antigen and prevents fungal adhesion and invasion in immunized hosts (Shahid 2016). The second vaccine in the clinical trial phase is a virosome-based vaccine containing a recombinant Sap2 antigen (Scorzoni et al. 2017). A monoclonal antibody was also tested pre-clinically, which binds to the immunodominant epitope of *C. albicans* Hsp90p. Mice vaccinated with Hsp90-CA DNA exhibited prolonged survival by 64% compared with the untreated control (Raska et al. 2005). Recently use of a live attenuated mutant strain of *C. neoformans* lacking sterol glucosidase enzyme (*Cnsgl1Δ*) shows a potential vaccine formulation (Rella et al. 2015). Only a few vaccines have been entered in the clinical trial phase; however, with ever-increasing infection and devastating results indicates an urgent need for new and improved vaccine production.

1.2.3 Combination therapy

Combination therapy is generally described for fungal infection difficult to treat, such as in aspergillosis and mucormycosis (Belanger et al. 2015). Numerous antifungal combinations are being studied *in vitro* by combining triazoles with echinocandins or AmB (Elefanti et al. 2013; Katragkou et al. 2014). A combination of CSF and VRC shows the in-vitro synergistic effect against *Aspergillus spp*. (Walsh et al. 2008). VRC and ANF

combination has improved effects against aspergillosis than their single counterparts (Marr et al. 2015). 5-FC in combination with azole or with AmB did not show synergistic activity for *Candida spp.* but was efficient for cryptococcal meningitis (Scheid et al. 2012).

Non-antifungal agent interactions have also been described as potentiating antifungal activity. Triclosan, a compound that displayed synergistic activity with FLC against *in vitro* in *C. albicans* and *C. neoformans* by switching on apoptotic pathways (Yu et al. 2011; Movahed et al. 2016). Recently, calcium channel blockers amlodipine, nifedipine, benidipine, and flunarizine showed synergistic activity with FLC in *C. albicans* (Liu et al. 2016).

Natural source molecules are also now gaining importance to enhance antifungal activity of available drugs. Use of the natural chemical beauvericin with conventional antifungals can be able to potentiate the action of FLC, inhibits efflux pumps, and morphogenesis in *C. albicans* (Shekhar-Guturja et al. 2016a).

1.3 *Candida glabrata*: overview and pathogenesis

1.3.1 History and evolutionary classification

C. glabrata was historically a nonpathogenic yeast, was first isolated from human stool and named as *Cryptococcus glabrata* by Anderson in 1917, later Lodder and deVries in 1938 called it *Torulopsis glabrata* (Anderson 1917). Meyer and Yarrow in 1978 introduced its present name when the *Torulopis* genus was merged with *Candida* due to the fact that pseudohyphae formation was not enough to factor for the genus determination. (Kurtzman et al. 2011; Tam et al. 2015). However, later *C. glabrata* was placed under the *Nakaseomyces* clade, with two other pathogenic *Candida* species; *Candida nivarensis* and *Candida bracarensis*, and three environmental species (Kurtzman and Robnett 2003). Nakaseomyces is the only group that has evolved the ability to infect humans among the post-WGD clade (Gabaldón and Carreté 2016).

From an evolutionary perspective, *C. glabrata* is more closely related to the baker's yeast *S. cerevisiae* than to *C. albicans* (Dujon et al. 2004a). The evolutionary status of *C. glabrata* is resented in Fig 1.8. Several genetically distinct clades of *C. glabrata* population have been shown based on few loci, reported to be enriched in same clade and are dependent on geographical origin (Gabaldón and Fairhead 2019).

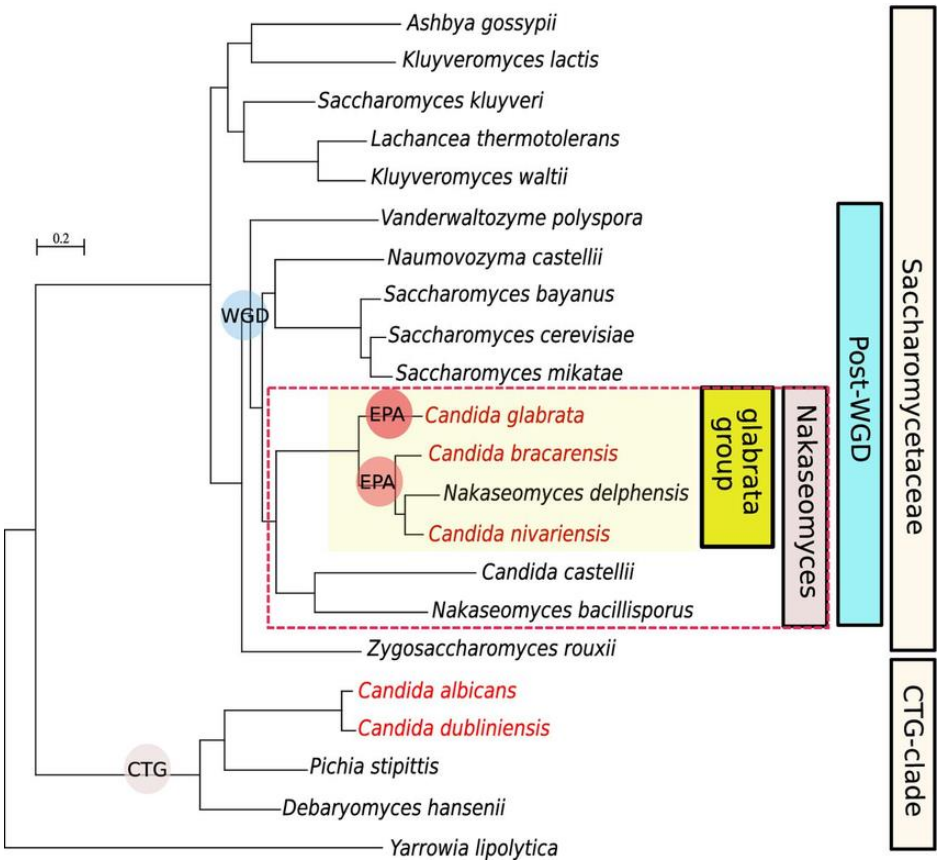

Fig 1.8: Phylogeny of *C. glabrata* (Adapted from *Gabaldón et al. 2015*)

1.3.2 General feature and Genomic Architecture

C. glabrata is a nondimorphic yeast that exists as small blastoconidia as a pathogen under every environmental condition (Almshawit 2015). *C. glabrata* blastoconidia (1 to 4 µm) are substantially smaller in size than *C. albicans* blastoconidia (4 to 6 µm) (Silva et al. 2012). General biology of *C. glabrata* and its distinctions with *C. albicans* are illustrated in table 3. *C. glabrata* is a petite positive yeast and crabtree positive yeast (Rodrigues et al. 2014). *C. glabrata* forms glistening, smooth, cream-colored colonies on sabouraud dextrose agar (SDA), and Chromagar, it appears as pink to purple color (Fig 1.9) (Gupta et al. 2019).

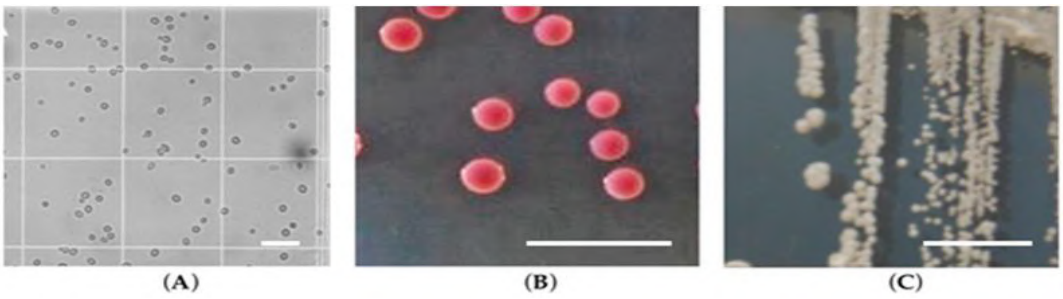

Fig 1.9: *C. glabrata* images a) Microscopic images b) on CHROMagar c) on SDA (Adapted from *Rodrigues et al. 2017*)

Clinically, *C. glabrata* can be identified via biochemical assay of carbon source utilization as it can't assimilate carbon sources other than glucose and trehalose or via culture-based assays and microscopic examination (Byadarahally Raju and Rajappa 2011; Dellière et al. 2016). There is no pseudohypha generation reported in *C. glabrata* at 37°C. Features of *C. glabrata* is represented in Table 1.3.

Table 1.3: Features of *C. glabrata* (Adapted from Kumar et al, 2019)

Features	***Candida glabrata***
Ploidy	Haploid
Cellular morphology	Yeast
Cell size	1–4 µm
Phylogeny	Non-CTG clade
Phenotypic switching	Present
Carbon assimilation	Glucose and trehalose
Auxotrophy	Niacin, thiamine, pyridoxine
Crab tree	Positive
Mitochondrial function	Petite positive
Mating genes	Present
Haem receptor	Absent
Haemoglobin and transferrin utilization	Absent
Innate azole resistance	Present
Secretory aspartyl proteases	Absent
Life style	Probably commensal, and pathogenic
Major sites of infection	Vaginal, oral, disseminated
Major adhesins	Lectins (Epa)
Biofilm	Present

Invasion	Not known
Damage to host cells	No significant damage

C. glabrata lost more genes than *S. cerevisiae* after WGD event, although its pathogenic lifestyle is considered to be due to the reductive genome evolution. Lost genes included genes for galactose, phosphate, nitrogen, sulfur metabolism, and pyridoxine biosynthesis (Dujon et al. 2004a). *C. glabrata* have natural auxotrophy to synthesize nicotinic acid, pyridoxine, and thiamine, and the inability to use galactose (Rodrigues et al. 2014).

Most typical *Candida* pathogens belong to the CTG clade, share a rare particularity in their codon usage such that the CUG codon encodes for serine instead of leucine (Gabaldón and Carreté 2016). In contrast, *C. glabrata* uses the standard genetic code. *C. glabrata* is a haploid yeast with a genome size of 12.3 Mb in size divided into 13 chromosomes, named from Chromosome A to M (Kumari et al. 2018). Only 238 (4.5%) ORFs are verified out of a total of 5293 open reading frames (ORFs) in the genome (http://www.candidagenome.org/). Only 446 genes representing 8.6% of the genome have no orthology with *S. cerevisiae* gene (Gabaldón and Carreté 2016).

C. glabrata possesses 20 kb circular mitochondrial genome coding for eleven ORFs. These include the three subunits of the cytochrome C oxidase, the apocytochrome b, and three subunits of the ATP synthase. The mitochondrial genome also codes for 23 tRNAs, 2 rRNAs, and a non-coding RNA (Kumar et al. 2019).

1.3.3 Case reports of *C. glabrata* epidemiology

Although *C. glabrata* is considered as human commensal but it has been isolated from various environmental sources such as from coffee beans, ragi, or oak tree (Gabaldón and Fairhead 2019).*C. glabrata* has inherent FLC resistant and in the last two decades, it emerged as an important nosocomial pathogen associated with high mortality among susceptible individuals (Fidel et al. 1999). Specific risk factors of infection include prolonged hospitalization, prior antibiotic use, prior FLC prophylaxis and hand carriage by hospital patients (Perlroth et al. 2007). The global distribution of *C. glabrata* infection is now 2nd to 4th according to the geographical location. *C. glabrata* increased from 16% to 27% of all isolates in Australia (Chapman et al. 2017). A similar rise has been observed in European countries also. By 2009, 26% of isolates from Denmark and 27% of infection in Belgium were due to *C. glabrata* (Arendrup et al. 2013). *C. glabrata* accounts for 21%,

13% and 15% of isolates in Scotland, Spain and Norway, respectively (Lamoth et al. 2018). In Asia, Taiwan reported 21.6% infection due to *C. glabrata* in 2012. In India and Pakistan *C. tropicalis* is the most prevalent species and *C. glabrata* ranks 4th with 7.1% and 16% infection (Chakrabarti et al. 2015; Lamoth et al. 2018).

C. glabrata is very notorious for causing infection in persons with diabetes mellitus (Chouhan et al. 2019). An 83-year old patient with diabetes mellitus was diagnosed with epidymo-orchitis due to *C. glabrata* (Jenks et al. 1995). A case of necrotizing urethritis caused by *C. glabrata* in a 56-year-old man with a past medical history of type 2 diabetes mellitus (Ibilibor and Cammack 2018). *C. glabrata* is very rare to cause fungal pneumonia and it was reported in 4 out of 140 patients (Yazici et al. 2016). Vulvovaginal candidiasis is very common among females and *C. glabrata* is the most prevalent organism to cause it (Bitew and Abebaw 2018; Makanjuola et al. 2018). A case of knee fungal arthritis by *C. glabrata* was observed in a patient who had undergone minimally invasive arthroscopic surgery (Chen et al. 2019). A rare case spondylodiscitis, an infection of the vertebral column, due to *C. glabrata* in a non-neutropenic diabetic patient, was reported (Gagliano et al. 2018).

1.3.4 Phenotypic and mating-type switching in *C. glabrata*

Phenotypic switching based on the graded different colored colony in the presence of 1mM $CuSO_4$ or phloxine B has been observed in *C. glabrata* (Lachke et al. 2000). The switching in colony color with 1mM $CuSO_4$ is spontaneous and reversible and referred to as ‘core switching’ from white (Wh) to light brown (LB) to dark brown (DB) and to very dark brown (vDB) (Lachke et al. 2002). These phenotypes switching has also been observed to occur at the sites of colonization in vaginitis patients (Brockert et al. 2003). In the presence of phloxine B, core switching has been shown to change from dark pink, medium pink, light pink, and white (Fig 1.10) (Lachke et al. 2002).

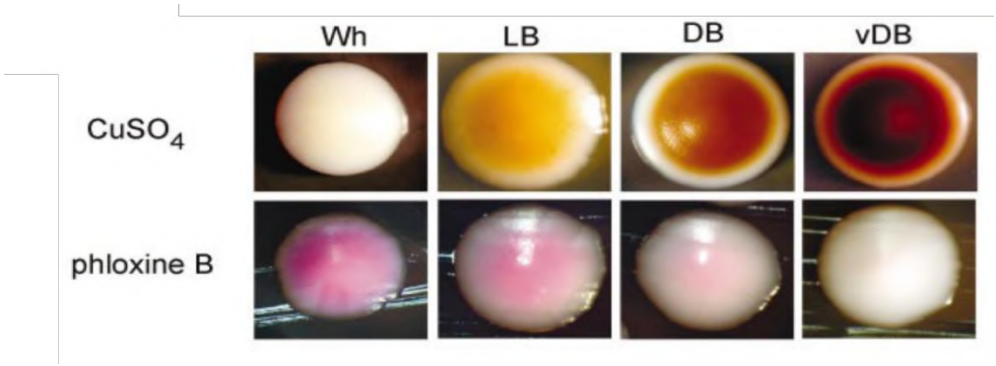

Fig 1.10: Phenotypic switching in *C. glabrata* in the presence of $CuSO_4$ and phloxine B. $CuSO_4$ and phloxine B treatment lead to switching from white (Wh) to light brown (LB) to dark brown (DB) and to very dark brown (vDB) (Adapted from *Lachke et al. 2002*)

Another spontaneous phenotypic switch from the core phenotype to an irregular wrinkle phenotype referred as 'irregular wrinkle switching' has been also reported (Srikantha et al. 2005). However, true hyphe formation is not observed in *C. glabrata,* but some stimuli such as nitrogen (N_2) starvation and carbon dioxide (CO_2) exposure induced pseudohypha formation has been reported (Csank and Haynes 2000; Sasani et al. 2016). Human fungal pathogen usually lacks an efficient sexual cycle. *C*. *glabrata* has never been shown to mate naturally, but haploid cells of both mating-types have regularly been isolated (Brisse et al. 2009). Evidence of recombination in mating genes has been detected, albeit very limited (Brisse et al. 2009). Moreover, genomic recombination between different clades and evidence for an active sexual cycle has recently been reported in *C. glabrata* (Carreté et al. 2018).

The genome of *C. glabrata* encodes two mating types at three different loci *CgMTL1* (MAT), *CgMTL2* (HMR), and *CgMTL3* (HML) and HO gene homolog encoding an endonuclease for mating-type switching (Boisnard et al. 2015). Fig 1.11 illustrates the organization of mating type locus in the genome. *CgMTL2* encodes for a-factor and *CgMTL3* encodes for α-factor, but these genes are close to telomeres. The *CgMTL1* locus encodes for either a or α, and this information determines the mating-type identity of the cell. Both *CgMTL1* and *CgMTL2* are transcriptionally active, but *CgMTL3* is subtelomerically silenced. Mating type switching has been reported to occur at the site of colonization in patients with vaginitis (Brockert et al. 2003).

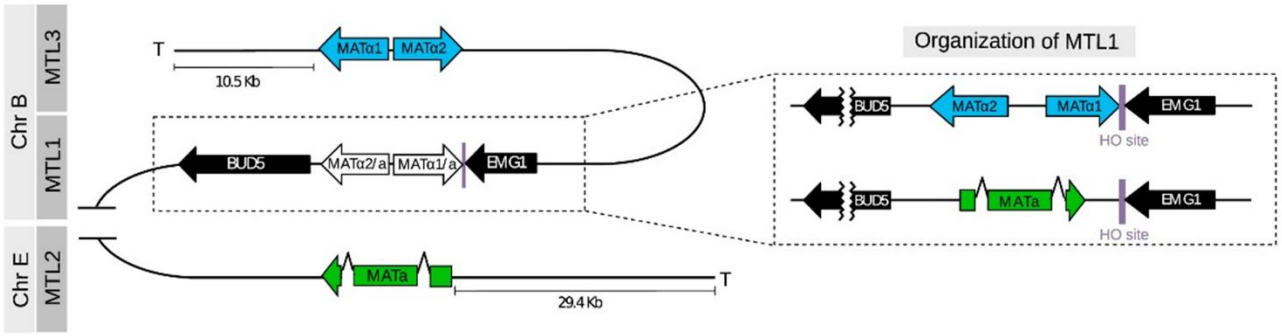

Fig 1.11: Organization of mating-type loci in *C. glabrata.* (Adapted from *Carrete et al. 2018*)

1.3.5 Virulence mechanism

C. glabrata can opportunistically become pathogenic in immunocompromised and elderly patients. The following are the known mechanisms of virulence listed below.

1.3.5.1 Adhesion

Adhesion allows yeast cells to colonize the mucosal surfaces to establish successful infections. The genome of *C. glabrata* encodes a large group of glycosylphosphatidylinositol (GPI)-anchored cell wall proteins, such as the adhesins from the *EPA* gene family, aspartic proteases (yapsins) family (Galocha et al. 2019). Adhesin genes have been classified into seven subfamilies based on their putative ligand-binding regions. *C. glabrata* reference strain CBS138 has 17 *EPA* genes, but a significant increase in the number of adhesin-encoding genes (101 and 107) have been observed in different clinical isolates (Timmermans et al. 2018). For example, *C. glabrata* BG2 strain has 23 putative *CgEPA* adhesins. CgEpa1p adhesin has been strongly related to adhesion of *C. glabrata* cells to mammalian epithelial cells and macrophages both in vitro and in vivo (Mendes-Giannini et al. 2005). CgEpa1p, a calcium-dependent lectin, has known to be regulated by transcription factor CgPdr1p (Vale-Silva et al. 2016). Two more adhesins, CgEpa6p and CgEpa7p, are known to be involved in adhesion to the epithelial and endothelial cells of the host (Valotteau et al. 2019).

1.3.5.2 Biofilm

Biofilm formation is an important determinant of virulence in *C. glabrata* (Kaur et al. 2014). Biofilms are complex multi-layered extracellular matrix formed at microbe-surface interactions. Clinical isolates of *C. glabrata* have the ability to form a biofilm with proteins, carbohydrates (e.g., β-1,3 glucans), and ergosterol in their matrixes (Rodrigues et al. 2017). The first step of *C. glabrata* biofilm development is adhesion on both biotic or abiotic surfaces (Timmermans et al. 2018). *C. glabrata* biofilms display antifungal resistance (Cavalheiro and Teixeira 2018). Differential expression of adhesin-encoding genes has been shown in biofilms under in vitro and in vivo conditions indicating adhesins are essential to forming biofilms (Kraneveld et al. 2011). Under high iron conditions, *C. glabrata* biofilms formation is also shown to be enhanced (d'Enfert and Janbon 2016). In addition, the capacity to form biofilms and to colonize murine organs in the systemic candidiasis model has been closely linked (Rasheed et al. 2018).

1.3.5.3 Aspartyl Proteases

Secreted aspartyl proteases are a vital factor contributing to *C. glabrata* virulence (Rasheed et al. 2018). Eleven putative GPI-anchored cell surface-associated aspartyl proteases are coded by its genome (Bairwa et al. 2014). These proteases are encoded by yapsins (*CgYPS1–11*) genes. A unique cluster on chromosome E encodes for eight *CgYPS* genes (*CgYPS3–6* and *CgYPS8–11*). With five *S. cerevisiae ScYPS* genes (*ScYPS1–3*, *ScYPS6*, and *ScYPS7*), *CgYPS* shows structural similarity (Rasheed et al. 2018). Unlike most aspartyl proteases, which have specificity for hydrophobic residues, yapsins cleave at basic amino acid residues (Bairwa and Kaur 2011).

Seven *CgYPS* genes (*CgYPS2*, *CgYPS4–5*, and *CgYPS8–11*) are observed to be up-regulated in response to internalization by macrophages. Accordingly, *CgYPS* have been associated with the survival of *C. glabrata* in macrophages, cell wall remodeling, activation of macrophages through nitric oxide generation, and virulence in both a systemic model of candidiasis (Rasheed et al. 2018). *CgYPS* are also shown to be involved in pH homeostasis, cell wall remodeling, and proper functioning of the vacuole (Bairwa and Kaur 2011).

1.3.6 *C. glabrata* interactions with host cells

C. glabrata live commensally in the mouth, esophagus, intestines, and vaginal mucosal surfaces, but less is explored about how it interacts with the host and its defense mechanisms (Rodrigues et al. 2014)? *C. glabrata* interacts with host cells during its commensal and pathogenic life (Brunke and Hube 2013). Host cells suppress the expression of pathogenic properties in *C. glabrata* and prevent its infection (Mendes-Giannini et al. 2005). Innate host immune system includes phagocytic cells (neutrophils, dendritic cells, and macrophages) against *Candida* infections (Drummond et al. 2015).

After the internalization of *Candida* cells, macrophages come as a primary defense mechanism that not only engulfs and kills the pathogen but also facilitates the recruitment of other immune cells through cytokine and chemokine production at the site of infection (Hernández-Chávez et al. 2017). Phagosome interacts with lysosomes to become phagolysosome for the clearance of infection (Pauwels et al. 2017). Phagocytic cells have various mechanisms to deal with the infection by means of low pH, hydrolytic enzymes, reactive oxygen species (ROS), and reactive nitrogen species (Uribe-Querol and Rosales 2017). *C. glabrata* genome has a single catalase gene (CTA1) to disrupt the oxidative burst of macrophage (Cuéllar-Cruz et al. 2008). *C. glabrata* seems to disrupt normal phagosomal maturation, ultimately inhibit the phagolysosome formation and phagosome acidification from reducing the radical oxidative species (Kasper et al. 2014). The macrophage environment has low availability of carbon source *C. glabrata* survive by activating autophagy of the self-cells to metabolize intracellular nutrients (Roetzer et al. 2010). The transcription of the *C. glabrata* copper-zinc superoxide dismutase (SOD) genes, *CgSOD1* and *CgSOD2*, are also induced during carbon source depletion (Kumar et al. 2019).

After engulfment by macrophages, there is no MAPK pathway activation has been observed (Galocha et al. 2019). Although GM-CSF production has been observed, there was no change in TNF-α, IL-6, IL-8, IL-12, and IFN- pro-inflammatory cytokines have observed (Seider et al. 2011; Kasper et al. 2015a). In human THP-1 macrophages upon *C. glabrata* infection Syk, a spleen tyrosine kinase become phosphorylated, which resulted in the production of inflammasome-dependent IL-1β (Rasheed et al. 2018).

Macrophage internalization leads to the upregulation of genes belonging to the glyoxylate cycle, oxidation of fatty acids, gluconeogenesis, methyl citrate cycle, and proteolysis, but

genes encoding glycolytic enzymes and ribosomal translational machinery components were downregulated. Microevolution due to macrophage contact led to a change in the morphology of *C. glabrata* cells from yeast to pseudohyphae by mutating chitin synthase-encoding gene *CgCHS2*. Macrophages are considered to be Trojan horses for *C. glabrata* due to the ability of the organism to subvert the immune response and replicate in macrophages *in vitro*.

C. glabrata adherence to the host epithelial tissue is mediated by a number of GPI-linked adhesin genes. 67 genes encoding putative adhesin-like GPI-modified cell wall proteins are present in *C. glabrata*. In-vitro adherence to epithelial cells is primarily mediated by the CgEpa1p adhesin, although CgEpa6p and CgEpa7p have also been shown to be pivotal to adherence under specific environmental conditions. *C. glabrata* strains carrying hyperactive transcription factor *CgPDR1,* which leads to the upregulation of Epa1 attributed to elevated adherence to Chinese Hamster Ovary derived-Lec2 cells (Fig 1.12). *C. glabrata* are shown to enhance the production of the granulocyte monocyte colony-stimulating factor (GM-CSF) in oral epithelial cells. Tryptophan-based pigment-producing *C. glabrata* strain has been reported to induce increased damage to human oral epithelial TR146 cells.

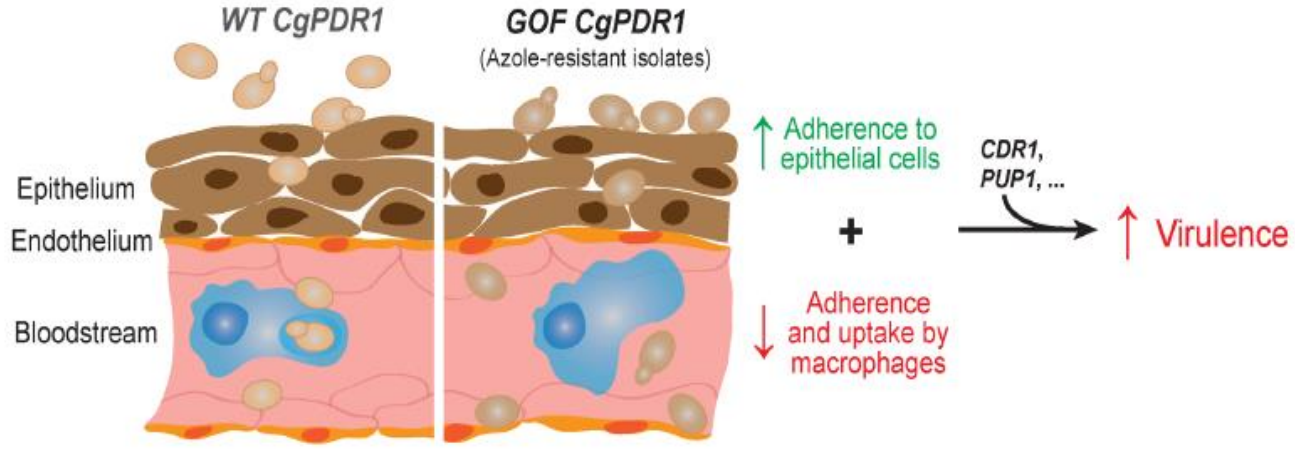

Fig 1.12: Transcription factor *CgPDR1* hyperactivity modulates host pathogen interaction (Adapted from *Vale-Silva and Sanglard et al. 2015*)

Dissemination and tissue invasion are prerequisites for systemic candidiasis. *C. glabrata* has been observed to cross the endothelial barrier in *in vitro* model of the human umbilical vein endothelial cells (HUVEC). CgPwp7p and CgAed1p are two GPI-anchored cell wall

proteins that are required for adherence to HUVEC (Desai et al. 2011). *C. glabrata* mutant lacking two enzymes of the N-linked glycosylation system has shown to be hyperadherent to the human microvascular endothelial cells HMEC-1 (West et al. 2013).

Neutrophils' roles are not well explored in *Candida* infection; however, these play a significant role. After engulfing *C. glabrata* cells, human neutrophils release neutrophil extracellular traps (Johnson et al. 2017). Monocytes preferentially engulf *C. glabrata* cells in the whole blood infection model. A recent study has shown the role of Natural Killer cells in combating *C. glabrata* infections (Vitenshtein et al. 2016). Besides, the murine dendritic cells have also been reported to modulate the host response to *C. glabrata* infection (Bourgeois et al. 2011). Further studies are required to dissect the proper host *C. glabrata* infection to combat the systemic candidiasis.

1.4 Drug resistance in *C. glabrata*

C. glabrata has inherent resistance to azole antifungal FLC. Continuous monitoring of antifungal susceptibility patterns and resistance mechanisms is important for clinically used antifungal agents to combat any outbreak.

1.4.1 Epidemiology of drug resistance *C. glabrata*

With the increasing use of FLC prophylaxis, *C. glabrata* resistant isolates have been increasing. *C. glabrata* cells are also shows cross- resistant to relatively newer azoles. In a study of 610 clinical isolates of *C. glabrata* from different parts of the world with invasive infections, 85.4%, 90.7%, and 92.8% percentages of strains were susceptible to posaconazole, ravuconazole, and VRC, respectively. Another study with 46 FLC-resistant isolates of *C. glabrata*, only 13% were susceptible to VRC, 4% were susceptible to posaconazole, and 8.7% were susceptible to ravuconazole (Nucci and Marr 2005).

SENTRY Antimicrobial Surveillance report that while none of the FLC-resistant *C. glabrata* isolates from 2001 to 2004 demonstrated echinocandins resistance but 11% of FLC-resistant isolates from 2006 to 2010 were also resistant to an echinocandin (Pfaller and Diekema 2012). Studies showed 1.5% resistance in a unit of 64 bloodstream isolates in two of the university hospitals in Austria and Germany (Klotz et al. 2016); none of the hospital in Itlay and Spain from 79 bloodstream isolates (Bassetti et al. 2013). From urine samples, about 2.1% of 94 invasive isolates obtained from Italy (Tortorano et al. 2013),

and about 1% of 193 isolates from France (Bourgeois et al. 2014) showed resistance. In USA, the prevalence was found between 2 to 4% to echinocandins from 1997 to 2000 (Castanheira et al. 2016).

Resistance may vary with region in the same country also. In a study of 1380 isolates of *C. glabrata* collected between 2008 and 2013 from four USA cities displayed 3.1%, to 3.6% resistance to ANF. Importantly, echinocandin resistance in *C. glabrata* is often associated with cross-resistance to azole antifungals yielding multidrug-resistant strains. In a recent study, nearly 36% of echinocandin-resistant isolates were also resistant to FLC. In many healthcare centers, the widespread use of echinocandin and azole prophylaxis has prompted an epidemiologic shift, with *C. glabrata* presenting as the dominant fungal bloodstream pathogen. With increasing use of azole antifungals for prophylaxis and therapy, the global azole resistance among *C. glabrata* isolates stands around 8%, while at some centers have rates exceed to about 20% of the isolates.

1.4.2 Clinical breakpoints of antifungal in *C. glabrata*

Failure to eliminate a fungal infection from a patient after administering antifungal drug in the same concentration in with in vitro activity against the fungus was known is called clinical resistance. In-vitro testing of the activity of an antifungal drug against a fungus is performed by microdilution methods. The CLSI has defined the standard breakpoints for the MIC to several antifungals. The CLSI breakpoints for Candida species is illustrated in table 1.4.

Table 1.4: CLSI breakpoints (Adapted from *Pristov and Ghannoun, 2019*)

Antifungal	***Candida spp.***	**MIC breakpoints (mg/L)**	
		S	R
Anidulafungin	*C. albicans*	0.3	1
	C. glabrata	0.1	0.5
	C. parapsilosis	2	8
	C. tropicalis	0.3	1
Caspofungin	*C. albicans*	0.3	1
	C. glabrata	0.1	0.5
	C. parapsilosis	2	8

	C. tropicalis	0.3	1
Micafungin	*C. albicans*	0.3	1
	C. glabrata	0.1	0.3
	C. parapsilosis	2	8
	C. tropicalis	0.3	1
Voriconazole	*C. albicans*	0.1	1
	C. glabrata	-	-
	C. parapsilosis	0.1	1
	C. tropicalis	0.1	1
Fluconazole	*C. albicans*	2	8
	C. glabrata	-	64
	C. parapsilosis	2	8
	C. tropicalis	2	8

1.4.3 Drug resistance mechanism

C. glabrata have C. glabrata acquires resistance more rapidly to different antifungal classes than other *Candida*. The ability of *C. glabrata* to survive antifungal pressure at high rates within individual patients highlights its astounding adaptive flexibility. This flexibility is likely due to a myriad of factors, including strong general cell stress responses (e.g., cell wall integrity pathway and regulation of associated genes) and multiple mechanisms of drug adaptation (e.g., HSP90/calcineurin, chitin synthesis, adhesion, genetic diversity). The combination of these cellular mechanisms (and other factors such as host immune status and drug penetration and pharmacokinetics) ultimately permit or enhance genetic escape (*CgPDR1* and *CgFKS* mutations) and stable resistance, which can result in clinical failure.

1.4.3.1 Azole resistance mechanism

Ever-increasing drug resistance in *C. glabrata* clinical isolates to various azoles, which makes it essential to monitor their resistant mechanism. *C. albicans* gain azole resistance by several mechanisms viz., upregulation, and mutation in target erg11 and overexpression of efflux pumps. Although, *C. glabrata* genome is haploid and point mutation can have a greater impact but studies suggested that mutations in *CgERG11*

have no effect in clinical azole resistance in this pathogen. Although recent reports have found a few mutations in *CgERG11* such as G944A, I166S, which links it to azole as well as cross-resistance to polyenes (Hull et al. 2012b; Teo et al. 2019). TF *CgPDR1* is a central player in the azole resistance acquired during antifungal therapy. Notable reports have shown that *C. glabrata* CgPdr1p directly binds to FLC, which resulted in the activation of drug efflux pumps, a mechanism similar to the regulation of multidrug resistance (MDR) by the pregnane X receptor (PXR), a nuclear receptor, in vertebrates (Thakur et al. 2008; Caudle et al. 2011). Moreover, single point mutations in the putative functional domains of *CgPDR1* (gain of function, GOF mutants) result in increased resistance to azoles and upregulated transcription of ABC transporters *CgCDR1, CgPDH1*, *and CgSNQ2* (Ferrari et al., 2009; Tsai, Krol, Sarti, & Bennett, 2006; Whaley et al., 2018). Also, TF *CgPDR1* controls major facilitator superfamily transporter *CgQDR2*, upregulation of which is involved in acquired azole resistance and enhanced virulence of this pathogen. Fig 1.13 represents the known mechanism of azole resistance in *C. glabrata*.

C. glabrata resistant clinical match paired isolates initially showed *CgCDR1* transcript increment, deletion of which made cell susceptible to azoles and reintroduction restored susceptibility (Sanglard et al. 1999a). *CgPDH1* was also first gained attention when its expression was found to be overexpressed in azole-resistant clinical isolates of *C. glabrata* (Miyazaki et al. 1998b). Further study showed that the deletion of Cg*PDH1* in the background of *CgCDR1* resulted in increased susceptibility to FLC (Sanglard et al. 2001a). Recently CgSnq2p was shown to contribute to azole resistance. Increased expression of *CgSNQ2* was found in two azole-resistant clinical isolates with normal expression of Cg*CDR1* or Cg*PDH1* (Sanguinetti et al. 2005a). Subsequently, it was shown to be required for the azole-resistant phenotype in one of the same isolates (Torelli et al. 2008a). An ABC transporter *CgAUS1* protects cells against azole antifungals in the presence of serum (Nagi et al., 2013; Nakayama H, et al., 2007). Cg*YOR1* and Cg*YBT1* were also found to be upregulated in azole-resistant lab mutant as well as in azole-resistant clinical isolates (Vermitsky et al. 2006a; Tsai et al. 2010a). A previous report also suggested the upregulation of Cg*YCF1*, Cg*YBT1, and* Cg*YOR1* in the azole resistant petite isolates (Ferrari et al. 2011a). Acquired azole resistance in *C. glabrata* populations

has also been associated with loss of mitochondrial function, thereby the upregulation of ABC transporter genes. It was also proposed that the calcium signaling be used as an important factor in azole resistance as loss of Ca2 + transforms the activity of FLC from

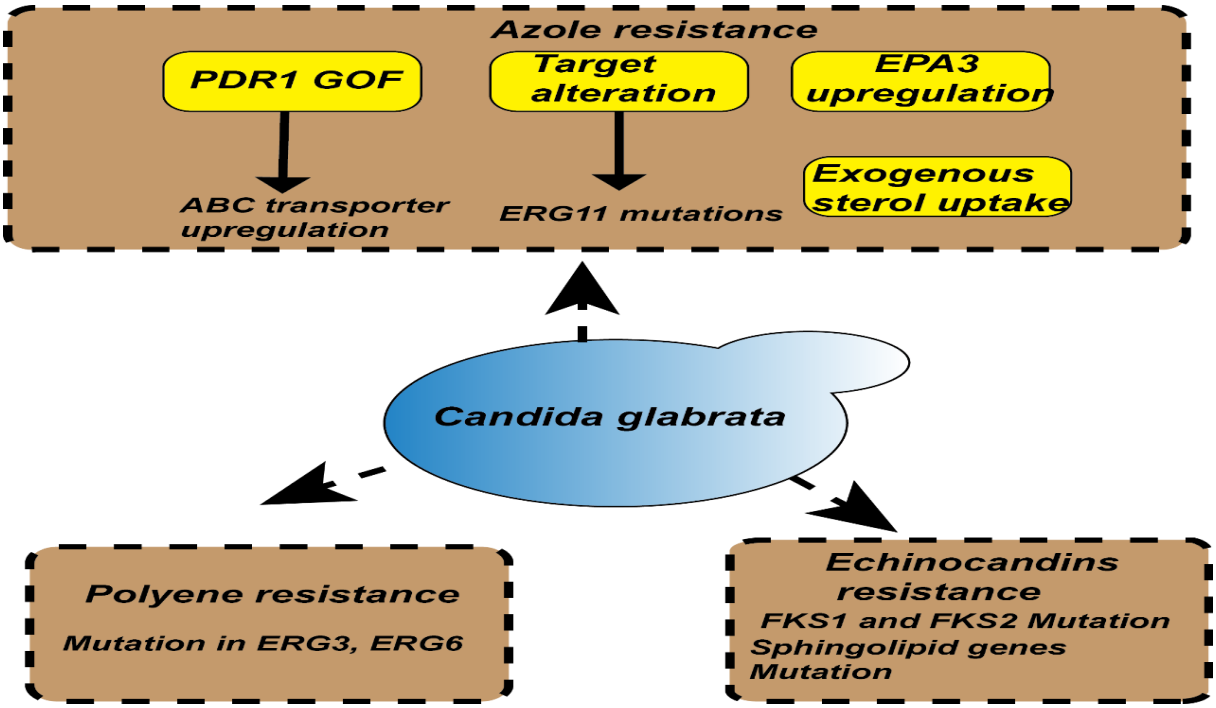

fungistatic to fungicidal.

Fig 1.13: Drug resistance (Azole, echinocandins and polyene) mechanism in *C. glabrata*.

Other studies have reported that *C. glabrata* subpopulations originating from a clonal population can develop heteroresistance to FLC through transient upregulation of efflux pumps. Active efflux of azoles is accomplished by membrane transporters, which belong to one of the two superfamilies in fungi: the ATP-binding-cassette superfamily (ABC) and the major facilitator superfamily (MFS). Several ABC transporters have been linked to drug resistance in *C. glabrata*, of which CgCdr1p and CgPdh1p have been extensively investigated. Previously published transcriptome data comparing young and 14-generation-old *C. glabrata* cells of the FLC-sensitive BG2 strain demonstrated increased expression of the genes *CgCDR1* (2-fold), *CgPDR16* (8-fold), and *CgYBT1* (10-fold). Enhanced efflux pump activity in old *C*. *glabrata* cells has also been observed mediated through enhanced efflux activity (Bhattacharya and Fries 2018).

1.4.3.2 Echinocandins resistance mechanism

Echinocandin therapy is highly efficacious, but emerging echinocandin drug resistance is a growing threat to successful clinical management. The primary factor of resistance developing towards echinocandin is its prior and prolonged exposure. *C. glabrata* develops echinocandin resistance through target mutation of the 1,3-beta-D-glucan synthase gene encoded by *CgFKS1* and *CgFKS2* genes (Alexander et al., 2013; Perlin, 2015). Drug adaptation is also a Key intermediate in leading to echinocandin resistance in *C. glabrata*. Drug adaptation has been illustrated in Fig. 1.4.

Another known factor responsible for emerging echinocandin resistance is amino acid substitution. The amino acid substitutions can decrease the sensitivity of glucan synthase by several log orders, resulting in elevated minimum inhibitory concentration (MIC) values. For *C. albicans*, amino acid changes at Ser641 and Ser645 are the most frequent and cause the most pronounced resistance phenotype, whereas in *C. glabrata*, amino acid modifications at Ser663 and Phe659 in CgFks2p andSer629 in CgFks1p, are the most prominent amino acid substitutions. *CgFKS* mutant strains of *C. albicans* and *C. glabrata* show poor drug response in pharmacodynamics studies of murine infection models.

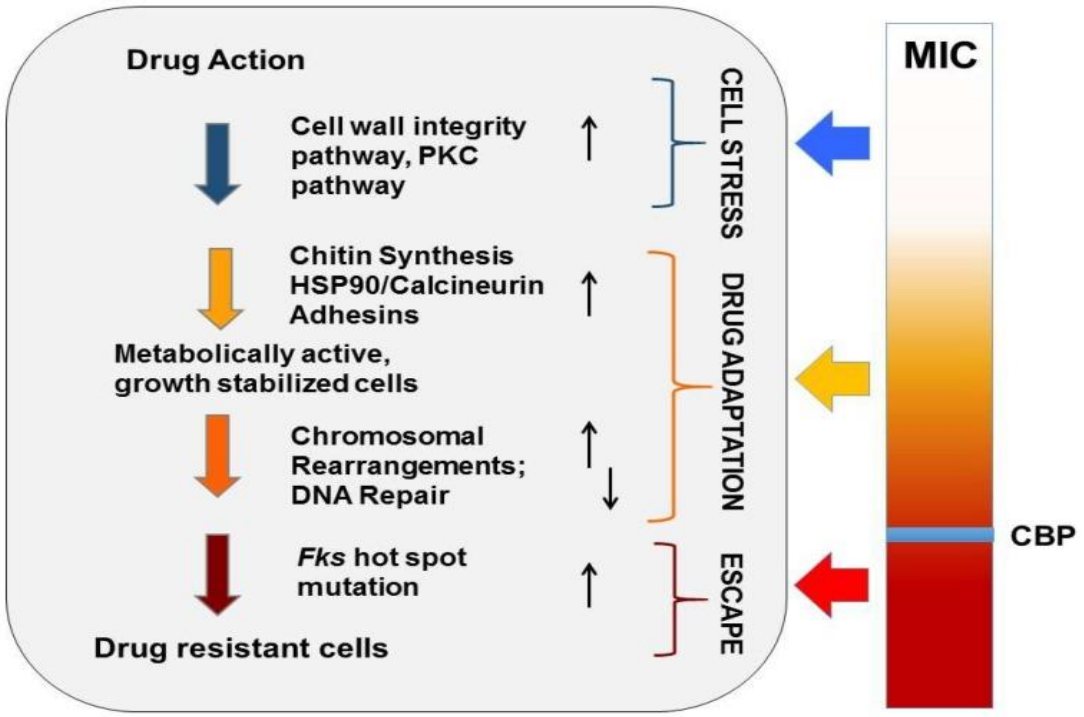

Fig 1.14: Evolution of echinocandins resistance in *C. glabrata* (Adapted from *Healey et al. 2018*)

1.4.3.3 Polyene antifungal resistance

Polyene antifungal is active against *C. glabrata* in such a way clinical isolate on polyenes is rarely identified (Ksiezopolska and Gabaldón 2018). AmB resistance in clinical isolates is caused by mutations in sterol biosynthetic pathway genes (Vale-Silva and Sanglard 2015). *CgERG2* and *CgERG6* mutations are associated with the polyene resistance in this organism (Hull et al. 2012a; Vale-Silva and Sanglard 2015). Mutation in these genes leads to loss of function mutations with the consequence of eliminating ergosterol from the mutant cells(Vandeputte et al. 2008).

1.5 ABC Transporters

ABC transporters are a family of membrane proteins that utilize cellular ATP hydrolysis to drive their transport of substrate across the biological membrane in all phyla (wilkins et al., 2015). These efflux pumps catalyze the transport of various substrates, such as the high-affinity uptake of micronutrients into prokaryotic cells and the export of cytotoxic compounds from eukaryotic cells (Kaspar P Locher, 2016). Eukaryotic ABC transporters are exporters whereas, in prokaryotes these are both importers and exporters (Wilkens 2015a). Fig 1.15 demonstrates the timeline of the ABC transporter work in yeast. ABC transporter was emerged from the nutrient uptake studies in prokaryotic cells (in *E. coli*) where ATP was required to translocate the nutrient (Theodoulou and Kerr 2015). In eukaryotes P-glycoprotein (Pgp) was one of the first members of the ABC superfamily to be studied comprehensively and is among proteins whose structure and function is well perceived (El-Awady et al. 2017). Both in prokaryotes and eukaryotes there is an additional large group of ABC proteins called soluble ABC proteins, are located in the cytosol and are employed mostly for maintenance and repair of DNA and for gene regulation (Jones et al., 2004). In eukaryotes ABC transporters are involved in the translocation of lipid molecule, antigen presentation, mitochondrial iron homeostasis, ATP dependent ion channel regulation and multi-drug resistance (Rees et al., 2009).

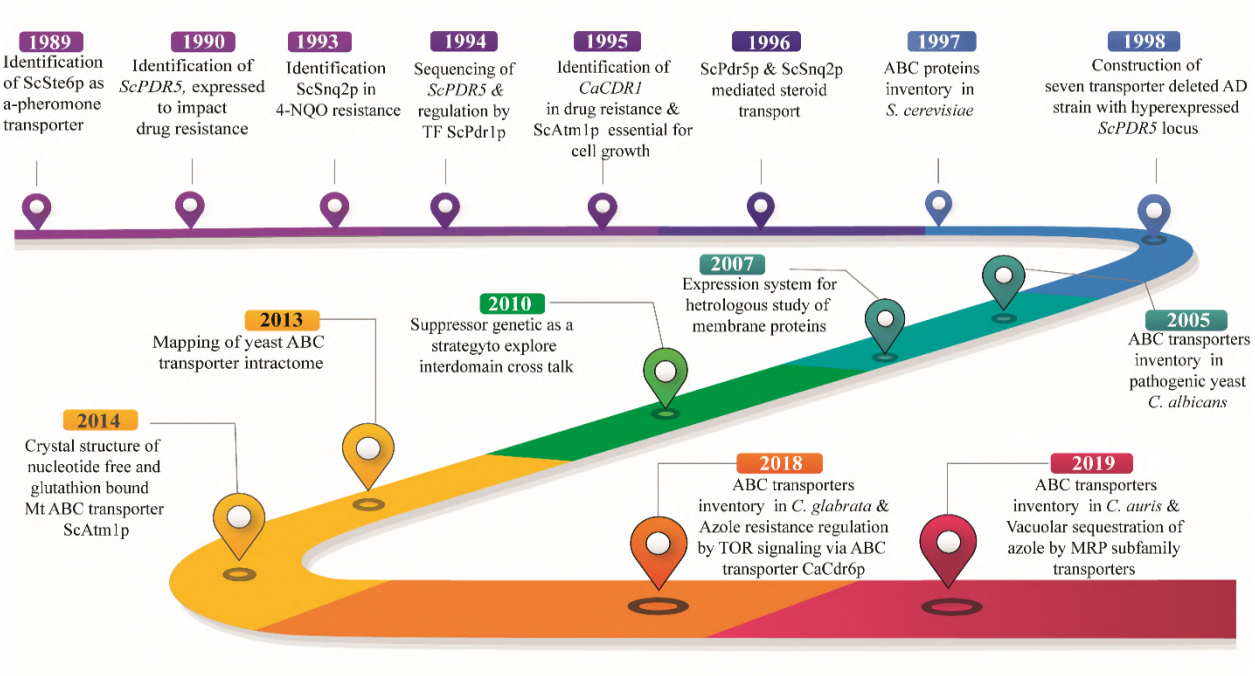

Fig 1.15: Timeline of ABC transporter work in yeast

1.5.1 Architecture of ABC transporter

ABC transporters typically share four architectural core domains: two hydrophobic transmembrane (TMD) and two hydrophilic nucleotide-binding domains (NBD) (Biemans-Oldehinkel et al. 2006). TMDs are membrane-embedded, and NBDs are cytosolic (ter Beek et al. 2014a). In eukaryotes, these domains are mostly encoded as a single peptide rather than as different peptide units in prokaryotes (Saurin et al. 1999; Jones and George 2002). To become a functional ABC transporter, all four core domains are required (Wilkens 2015a). Half-transporters have only one of each NBD and TMD and are assumed to function by forming either homo- or hetero-dimers (Rea 1999; Davidson and Chen 2004; Tarling et al. 2013). Some ABC proteins even possess accessory subunits that are either connected to TMD or NBD, such as additional TM helixes or elongated NBDs that can regulate transporter activity or can enhance substrate-binding affinity (Higgins 2001; Biemans-Oldehinkel et al. 2006). Both full and half transporters are arranged in either of two topologies: forward or reverse topology (Rutledge et al. 2011).

1.5.1.1 ABC subunits.

ABC subunit is the most important characteristic subunit for a protein to become an ABC protein (Jones and George 1999). NBDs are located at the cytoplasmic periphery and couple energy of ATP hydrolysis to power substrate export across the membrane in ABC transporters (Prasad et al. 2006; Wilkens 2015a). NBD is comprised of two subdomains, a large catalytic subdomain and a small α -helical subdomain (signaling subdomain). The catalytic subdomain has α/β structure that contains well-conserved sequence stretches such as P-loop or Walker A motif (GXXGXGK(S/T)), Walker B motif (ϕϕϕϕD, of which ϕ is a hydrophobic residue), the D-loop, and the H-motif (the switch region) (Walker et al. 1982; Schmitt and Tampé 2002; Rutledge et al. 2011). The second α-helical subdomain (signaling subdomain) is composed of α-helices and contains characteristic ABC signature sequence (C-loop, LSGGQ) and the Q-loop (Wilkens, 2015). Signature sequence is placed in between the two conserved motifs walker A and Walker B (Falcón-Pérez et al. 2001; Gaur et al. 2005a).

Structural elements of NBDs are arranged in a head-to-tail fashion in such a way that the Walker A of first NBD is orientated towards the signature sequence motif of the second NBD (Jones and George 1999; Rees et al. 2009). The first ATP binding site is made up of Walker A and B from the first and the signature and D-loop from the second NBD. Similarly, the second ATP binding site is comprised of Walker A and B from the second NBD and the signature and D-loop from the first NBD (Jones and George 1999; Higgins 2001; Davidson and Chen 2004; Rees et al. 2009) (Fig 1.16). Signature sequence functions as a link to communicate hydrolysis of ATP to the TMDs by interacting with cytoplasmic extensions of the transmembrane helices (TMHs) (Prasad et al., 2015; Rai et al., 2006)

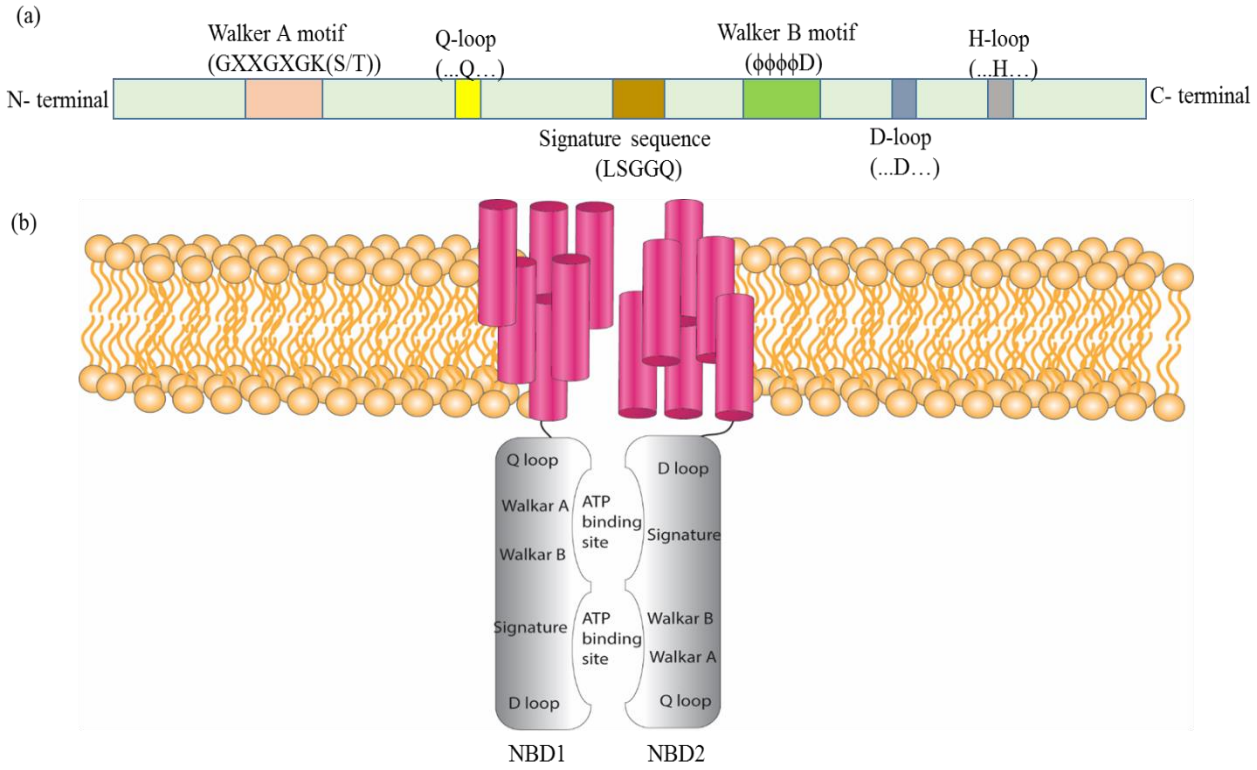

Fig1.16: NBD domain structure and formation of ATP binding sites (a) Conserved motifs present in NBD domain of ABC transporters includes Walker A, Walker B, signature sequences Q, D and H- loops (b) Formation of ATP binding subunits by these conserved motifs.

1.5.1.2 TM domains.

TMDs are hydrophobic substrate binding sites and form a substrate pathway for translocation across the membrane (Jones and George 1999; Wilkens 2015a). Each TMD is composed of six or more transmembrane-spanning α-helices depending on the ABC transporter class (Higgins, 2001). Two TMDs are organized in such a way that it forms a transmembrane pore accessible from the cytoplasm in ABC exporters or outside the cells in the ABC importers (Wilkens 2015a). In contrast to NBDs, TMHs of the TMDs display no significant sequence conservation which imparts poly-specificity to these transporters (Prasad Dr & Rawal, 2014); however, they share a similar topology within the same subfamily of transporters and high similarity between two TMDs of the same polypeptide (Wilkens 2015a). The diverse substrate profile of each transporter can be one of the reasons for this non-conservancy in the primary structure of TMDs.

1.5.2 Molecular Mechanism of action

Non availability of crystal structure of any of the yeast ABC transporters makes the study of structure and mechanism difficult, but the similarity in the ABC structures supports a common mechanism by which ABC transporters works. Based on the available structural and biochemical data from human and other ABC transporters and extensive studies of P-gp drug affinity, an 'ATP-switch model' has been proposed to explain the mechanism of transport (Linton & Higgins, 2007; Szöllősi et al., 2018). The model proposed to switch between low and high-affinity states of substrate binding coupled with the ATP catalysis in order to explain the transport mechanism. There are four steps required for the completion of the transport cycle, and these include substrate binding, ATP binding and substrate translocation, ATP hydrolysis, and return to the substrate-binding conformation (Linton & Higgins, 2007). In the ATP unbound state, the transporter possesses an open conformation with a high affinity for the substrate. In this inward-facing configuration, both the two TMDs are opened towards the cytosol with a hydrophilic binding pocket for substrates (Linton & Higgins, 2007; Zoghbi et al., 2017). Binding of the substrate at the TMD domain generates an induction for change in the conformation at the NBD domain, leading to a higher affinity for ATP binding (Arai et al., 2017). Binding of ATP resulted in the formation of a closed dimer, sufficient to generate a conformational change at TMDs to reverse their arrangement from inward to outward-facing. This change in arrangement causes a decrease in substrate affinity at TMD, which resulted in the translocation of the substrate outside the cell (Locher, 2016). This closed conformation is a transient state and destabilized by hydrolysis of ATP into ADP and Pi, which releases sufficient energy to again generate a conformational change in the TMDs to make them return to an open confirmation state (Wilkens, 2015) (Fig 1.17).

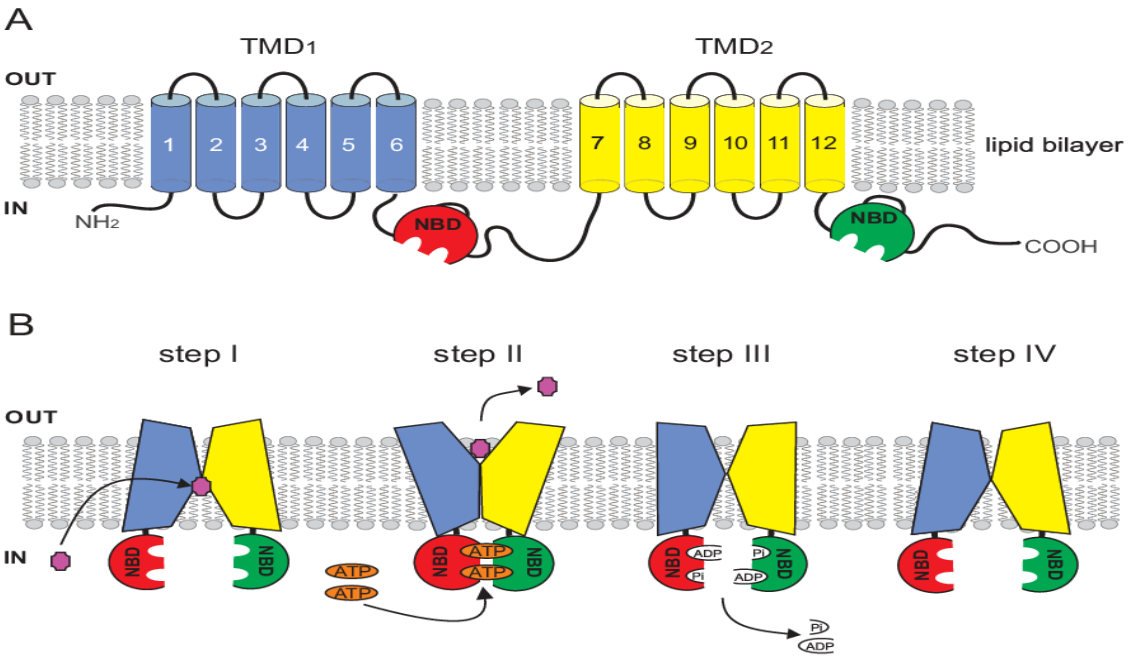

Fig1.17: Architecture and mechanism of action of ABC transporter (Adapted from *Dermauw et al. 2014*).

1.5.3 Subfamilies of ABC transporters

According to the adopted nomenclature by HUGO (Human Genome Organization) scheme the eukaryotic ABC protein superfamily is classified into nine subfamilies (ABCA to ABCI) (Dean et al., 2001). ABCA subfamily is absent in from yeast genome but presents in plants and several protists (Kovalchuk and Driessen 2010a). ABCB or multidrug resistance (MDR) subfamily proteins share a forward topology (TMD-NBD-TMD-NBD or TMD-NBD). The first characterized MDR member was ABCB1 for its ability to confer MDR in mammalian cells (Glavinas et al. 2004a). The further subdivision is proposed in this transporter with full transporters (involved in MDR), half transporters (involved in the peptide transport) and mitochondrial half membrane transporters (Anjard and Loomis 2002).

ABCC or multidrug resistance associated protein (MRP) subfamily members of eukaryotes are known to extrude a diverse array of toxic substrates, including xenobiotics outside the cell or sequestration into the vacuole (Klein et al. 2006). The distinctive feature of this subfamily is to recognize glutathione (GSH)-, glucuronate- and sulfate- conjugated organic anions (Jeong et al. 2017). MRPs also act synergistically with numerous enzymes such as GSH-S-transferase, UDP- glycosyltransferase to translocate substrates

(Dermauw and Van Leeuwen 2014). All members of this subfamily are full transporters with topology TMD_0TMD-NBD-TMD-NBD for long MRPs and TMD-NBD-TMD-NBD as short MRPs (Borst et al. 2000).

ABCD/ Adrenoleukodystrophy protein (ALDp) subfamily proteins found in all eukaryotes as half transporter with topology TMD-NBD with few exceptions to some plants where members exist as full transporter (Theodoulou et al. 2006). Half ALDp members function by homogenous or heterogeneous dimerization (Morita and Imanaka 2012).

The ABCE/ RNase L Inhibitor (RL1) subfamily proteins comprised of a characteristic pair of linked NBDs without TMDs. These soluble proteins are involved in several biological processes rather than in membrane transport (Dong et al. 2004; Tian et al. 2017). The members of ABCF/ Elongation Factor 3 (EF3) subfamily are topologically similar to RLI subfamily proteins with paired NBDs without TMDs. These soluble proteins perform many functions in human and yeast species, for example, ribosomal biogenesis, translational gene expression control, the export of mRNA to a cytoplasm, as well as translation elongation (Kovalchuk and Driessen 2010b).

ABCG/Pleiotropic drug resistance (PDR) subfamily is ubiquitous in all eukaryotes but absent in prokaryotes. PDR subfamily members in humans are found only as half transporters with reverse topology NBD-TMD, however, in yeast these represent both full and half transporters (NBD-TMD-NBD-TMD or NBD-TMD). Two possible reasons for the reverse orientation of domains can be first by fusion of independent NBD and TMD, or second by origination from the central portion of a member of the other ABC transporter (ABCA, ABCB, or ABCC) subfamilies (Anjard and Loomis 2002). Notably, this subfamily members perform important roles in extruding a variety of unrelated compounds, including agricultural fungicides, mycotoxins, herbicides, and antifungal drugs (Kolaczkowski et al. 1996a; Prasad and Goffeau 2012)

The genomes of arthropods and zebrafish contain ABCH subfamily transporters but not in most of the plants, animals and fungal genomes (Dermauw and Van Leeuwen 2014). The newly added ABC subfamily ABCI (the prokaryotic type ABC protein subfamily) contains ABC proteins without NBD and is confined to plant taxa (Kovalchuk and Driessen 2010b). Topology of the ABC transporter subfamilies is illustrated in Fig 1.18.

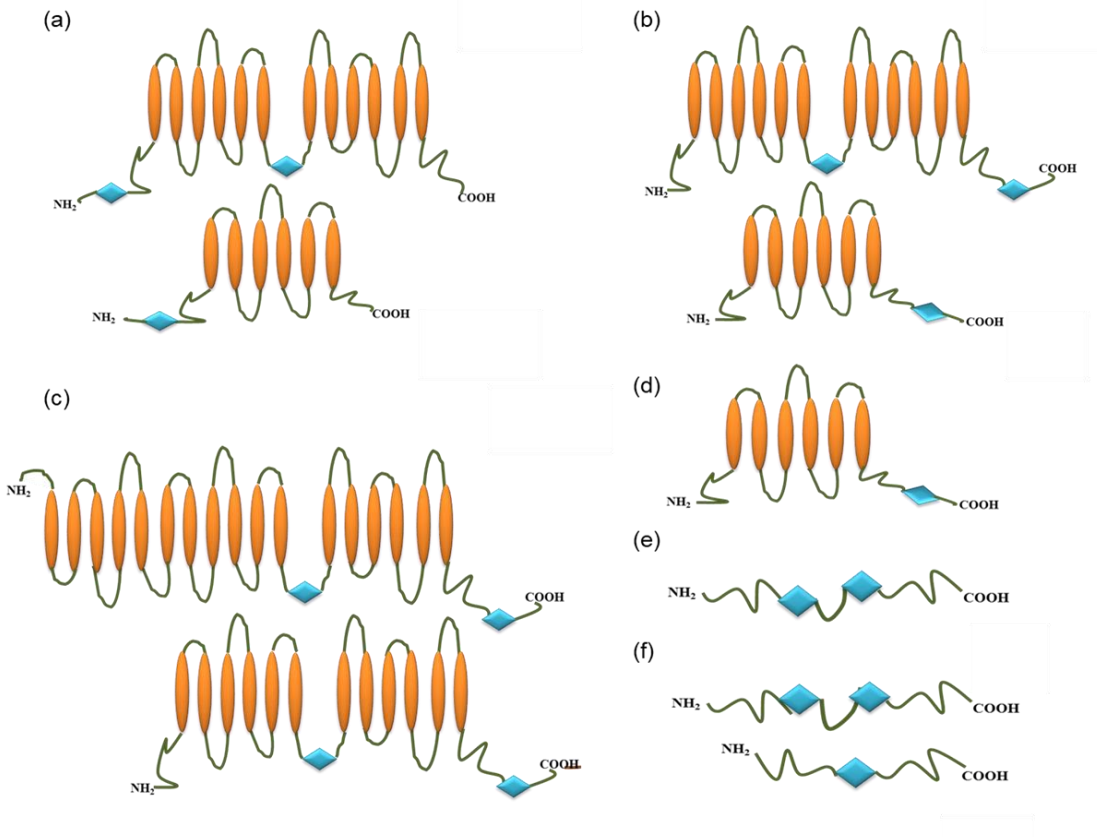

Fig 1.18: ABC proteins subfamilies and their topology. (a) PDR/ABCG subfamily, (b) MDR/ABCB subfamily (c) MRP/ABCC subfamily (d) ALDp/ABCD subfamily (e) RLI/ABCE and EF3/ABCE subfamily (f) others

1.5.4 Functions of ABC transporters

ABC transporters are generally considered as drug efflux pumps and their overexpression is commonly associated with multidrug resistance in yeasts. ABCG/PDR efflux pumps, for example, ScPdr5p and ScSnq2p in *S. cerevisiae* CaCdr1p in *C. albicans*, CgCDR1p, and CgPdh1p in *C. glabrata* are the most common cause of azole resistance. Transporters such as ScSnq2p in *S. cerevisiae* and CgSnq2p in *C. glabrata* have a role in the transport of mutagen 4-NQO, azoles (Decottignies et al. 1995; Torelli et al. 2008a). Not only the PDR transporters, members of MRP subfamily transporters also contribute to drug resistance. ScVmr1p, a vacuolar membrane-localized transporter in *S. cerevisiae* is drug transporters, deletion of which is associated with sensitivity to at least 11 amphiphilic drugs (Wawrzycka et al. 2010). The transporters belonging to ALDp, MDR

and some of MRP and PDR transporters functional relevance and their role in drug resistance are not yet established.

ABC transporters, apart from drug transport, perform several physiological functions, including metabolite export, peptide secretion and transport, ion transport, lipid transport and translocations. Few examples include ScPdr12p of *S. cerevisiae* in protection against weak organic acid toxicity (Casal et al. 2008; Gregori et al. 2008). Overexpression of this transporter enhances tolerance to longer chain length acids and obliteration improves tolerance to the shorter acetic and formic acid (Nygård et al. 2014). ScPdr5p functions as a detoxification determinant during exponential growth conditions and its level decreases rapidly when cells exit the log phase, growth on non-fermentable carbon sources, or by limitation of nutrients such as glucose or nitrogen (Mamnun et al. 2004).

Vacuolar sequestration of metal ions is one of the common mechanisms to cope up with the metal toxicity. In *S. cerevisiae* five vacuolar transporters is present at the vacuolar membrane (VM) out of which four are involved in vacuolar sequestration. Most studied transporter is ScYcf1p, which sequester GSH-conjugated metals and xenobiotics, bilirubin and free GSH for degradation within the vacuole deletion of which results in high sensitivity to Cd(II), Hg(II), Pb(II) and Sb(III). (Nagy et al. 2006; Lazard et al. 2011; Sousa et al. 2015). Its homologs ScYbt1p, ScBpt1p and Scvmr1p also mediate metal detoxification, the transport of glutathione conjugates, as well as free glutathione (Klein et al. 2002, 2006).

The peptide secretory systems are involved in various signaling processes in microorganisms, including sporulation, gene regulation in the proteolytic system, and virulence (Detmers et al. 2001). Unlike the typical secretory pathway, few peptides adopt an alternate mechanism of secretion. A well-studied example is a- pheromone transporter ScSte6p. It exports 12 residues long hydrophilic a-factor to the extracellular medium (21,131, 132). *Scste6* deletion makes cells unable to mate, which confirms its dedicated role in the yeast cells. SpMam1p and CaHst6p perform similar functions in *S. pombe* and *C. albicans* (Raymond et al. 1998). Unlike *S. cerevisiae* cells, different morphological forms of diploid *C. albicans* show constitutive expression of *CaHST6*, pointing to its basic biological function. *CaHST6,* when expressed in *S. cerevisiae* strain lacking *Scste6*, complemented the a- factor transport, suggesting a possibility of secretary function

performed by this transporter in *C. albicans* (Raymond et al. 1998; Hull and Johnson 1999).

Lipids are important biomolecule for cellular structure and function. The asymmetric distribution of membrane lipids, which is very typical to a membrane type, is functionally critical. Loss of membrane lipid asymmetry results in abrogated membrane protein functions leading to various pathological consequences in microorganisms. In this aspect, explored ABC transporters include *S. cerevisiae* ScPdr5p and ScYor1p and *C. albicans* CaCdr1p, CaCdr2p and CaCdr3p control the asymmetric distribution of phospholipids across the PM (Khakhina et al. 2015).

These are also implicated in biofilm formation and pathogenesis in pathogenic yeast strains. In a study of *C. glabrata* infection with neutropenic mice sterol scavenger transporter, *CgAUS1* expression was three times higher in cells recovered from kidneys than that in cells grown in vitro. The deletion of *CgAUS1* results in attenuated virulence in a mouse model of disseminated infection (Nagi et al. 2013b). Similarly, mitochondria dynamically regulate fungal virulence by affecting the transport of Fe/S cluster as one of the mechanisms (Verma et al. 2018). Mitochondrial ABC transporter Atm1p functions as a transporter of Fe/S cluster is conserved in yeast that has an impact on virulence. A report from highly pathogenic encapsulated yeast *C. neoformans* displayed the role of CnAtm1p in the virulence, which after deletion makes cell avirulent in a murine model of cryptococcosis (Do et al. 2018).

ABC transporters have a profound role in industries. For instance, overexpression of ScPDR12p enhances the production of short branched-chain fatty acids (Yu et al. 2016). Overexpression of the ScSnq2p, ScPdr5p and ScPdr15p transporters enhance tolerance against alkanes (Ling et al. 2013). In the presence of fermentation inhibitors, several ABC genes are upregulated, including ABCG/PDR members. Overexpression of these transporters can be performed for the construction of strain with high resistance to fermentation inhibitors and high product yields. Fig 1.18 depicts the divergent roles performed by ABC transporters.

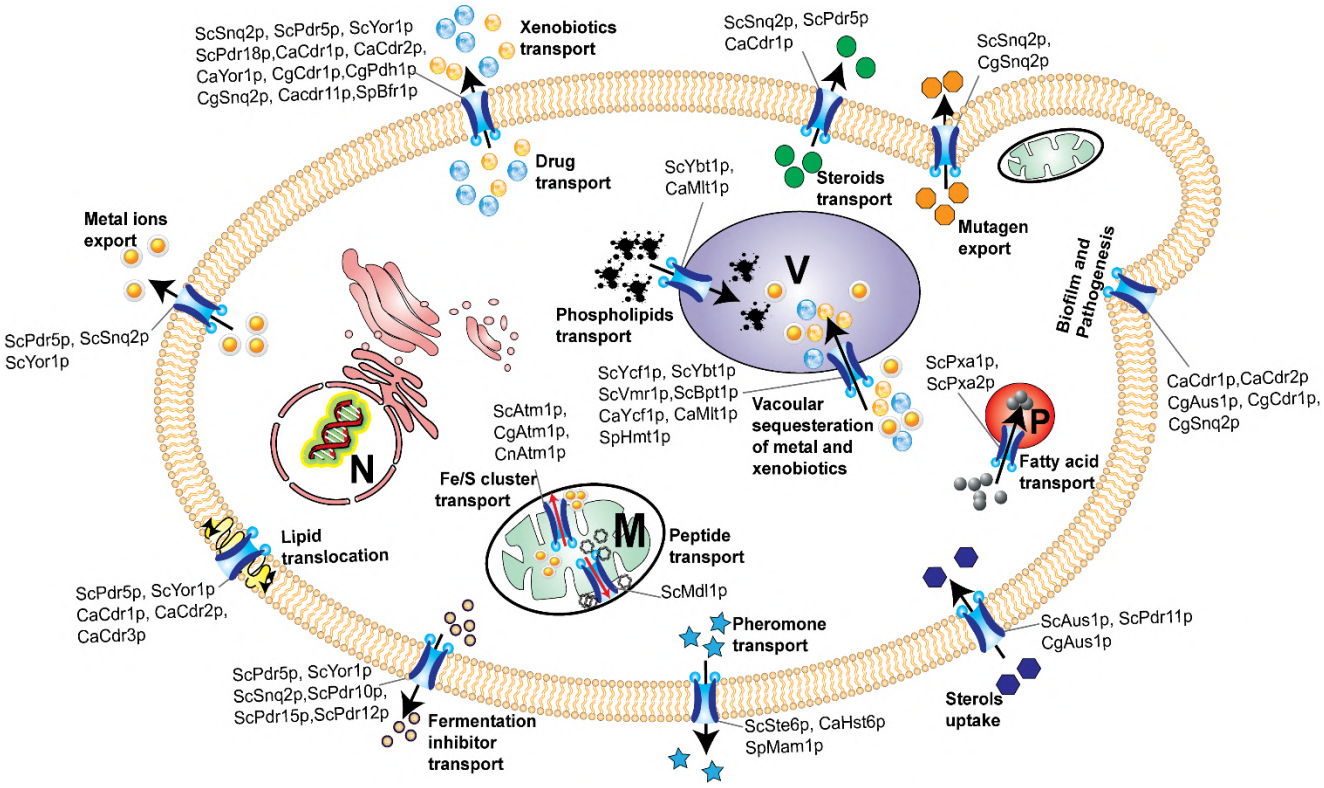

Fig 1.18: Diverse roles of ABC transporters in yeast.

1.6 Objectives and scope of this study

C. glabrata is a 2nd most common opportunistic human fungal pathogen with intrinsic resistance to azoles and can easily acquire resistance to echinocandins. The role of ABC transporters in clinical drug resistance in *C. glabrata* is well documented. The drug-resistant clinical match paired isolates of *C. glabrata* show *CgCDR1* transcript increment, deletion of which sensitizes cells to azoles and its reintroduction restores susceptibility (Sanglard et al. 1999a). *CgPDH1* another important ABC transporter that is recognized as an important determinant of azole resistance in clinical isolates of *C. glabrata* (Miyazaki et al. 1998b). Another transporter *CgSNQ2* encoding gene transcript was also raised in azole-resistant clinical isolates, where prominent transporters *CgCDR1* or *CgPDH1* expression remained unchanged (Sanguinetti et al. 2005a; Torelli et al. 2008a). A sterol scavenger ABC transporter CgAus1p protects cells against azole antifungals in the presence of serum and can also modulate virulence in this organism (Nagi et al., 2013; Nakayama H, et al., 2007). Likewise, the role of other members of ABC superfamily such as Cg*YCF1,* Cg*YOR1* and Cg*YBT1* in azole resistance is also recognized and confirmed by several studies (Vermitsky et al. 2006a; Tsai et al. 2010a; Ferrari et al. 2011a).
Realizing the importance of ABC transporters in clinical drug resistance in *C. glabrata* cells and the existence of a number of ABC members in this yeast, my study is focused on having a closer look to this superfamily. For this, my thesis work is divided into three chapters under the following major headings:

1. In- silico analysis of ABC proteins in *C. glabrata*.
2. Deletion library construction of ABC transporter.
3. Functional analysis of ABC transporter.

The first chapter of my thesis addresses the ABC protein superfamily inventorization by employing bioinformatics tools followed by clustering into respective subfamilies. Further confirmation of these putative proteins coding genes in the genome and their transcriptional response to transient drug treatment conditions in *C. glabrata* has been performed. This q-PCR analysis provided evidence for their possible role in drug resistance, which I have explored by creating a deletion library of all ABC transporters coding genes, covered in the second chapter of my thesis. The course of work led to not

only in the construction of a single knock out of each gene encoding ABC proteins but also in engineering a homologous expression system in *C. glabrata* in a background strain MSY8 with 7 key ABC transporter deletion and a gain of function mutation in transcription factor (TF) *CgPDR1.* While the role of some of the ABC members in drug resistance was apparent in this study, the lack of correlation with the resistance of many members also signified their other physiological roles in *C. glabrata*. In the third chapter, a detailed account of CgYor1p is presented, which is hitherto known for oligomycin resistance. However, in this organism, CgYor1p instead governs azole resistance while ignores oligomycin as a substrate.

MATERIALS

AND

METHODS

2. Materials and methods

2.1 Materials

2.1.1 Culture media, chemicals, antifungal drugs

All media components and chemicals were of molecular biology grade and were purchased from commercial sources. Growth media yeast extract peptone dextrose (YEPD) media, luria bertani (LB) broth, LB agar, yeast nitrogen base (YNB) media without amino acid and YNB media without ammonium sulfate and amino acids were purchased from Becton, Dickinson and Company (BD, USA) and Difco, Switzerland. 2',7'-dichlorofluorescein diacetate (DCFDA), Tris, dimethyl sulphoxide (DMSO) were purchased from Sigma, India. Agar, phenol, Sodium acetate, MOPS buffer sodium chloride, sodium hydroxide, sodium carbonate, sodium dodecyl sulphate (SDS), ethylenediaminetetraacetic acid (EDTA), glycerol, diethylpyrocarbonate (DEPC), lithium acetate, polyethylene glycol (PEG), isopropanol, tween-20, hydrochloric acid (HCl), acetic acid, di-thiothreitol (DTT), ethanol and hydrogen peroxide were procured form Sigma, India, TCI chemicals and Himedia chemicals. Antibiotics ampicillin (AMP), hygromycin B (HphB), nourseothricin (NTC) were purchased from Amresco, USA, TCI-chemicals, India and Clon Nat, Germany respectively. Fluconazole (FLC), ketoconazole (KTC), itraconazole (ITZ), rhodamine 6G (R6G), amphotericin B (AmB), nystatin (NYS), ketoconazole (KTC), voriconazole (VRC), miconazole (MCZ), myriocin (MYR), 4-Nitroquinoline 1-oxide (4-NQO), caspofungin (CSF), FK520, cyclohexenamide (CHX), beauvericin (BEA), oligomycin (OMY) and Rapamycin (RAPA) were procured from Sigma Chemical, India. All amino acids, adenine, and Uracil were purchased from Sigma.

2.1.2 Kits and enzymes

Gibson assembly kit was purchased from New England Biolabs (NEB), UK. RNA isolation kit, PCR product purification kit, and DNA gel extraction kit were procured from QIAGEN. Kits used for first strand c-DNA synthesis, quantitative real time-PCR were purchased from Invitrogen and Bio-Rad, India respectively. Enzymes used for PCR amplifications viz., Phusion polymerase and Taq polymerase were purchased from thermos scientific, Lithuania and G-biosciences, India respectively. Molecular cloning enzymes eg.

Restriction endonucleases, T4 –DNA ligase were purchased from NEB, UK and thermo scientific, Lithuania. DNase1 was purchased from thermos scientific, India.

2.1.3 Yeast strains and Plasmids

C. glabrata and *S. cerevisiae* based yeast strains were used and modified as per the need in the following studies. Both cloning plasmids and expression plasmid were employed according to their need. List of yeast strains and plasmids are listed in Table 7.2 and Table 7.3, respectively.

2.1.4 Growth media, buffers and solutions

All the media components and chemicals were sterilized by autoclaving at 121 °C at 15 psi for 15 min. Agar was added before autoclaving in the media for solid plate formation. The component that can't be autoclaved or was heat-labile were sterilized by filtration with filters having pore size 0.22 µM.

2.1.4.1 Culture media for Bacteria

Luria Bertani (LB) media

0.5% Yeast Extract

1% Tryptone

1% NaCl

Super Optimal Broth (SOB)

0.5% Yeast Extract

2% Tryptone

0.5% NaCl

2.5 mM KCl

10 mM MgCl2

10 mM MgSO4

Super Optimal broth with Catabolite repression (SOC) media

0.5% Yeast Extract

2% Tryptone

0.5% NaCl

2.5 mM KCl

10 mM MgCl2

10 mM MgSO4

20Mm Dextrose

2.1.4.2 Culture media for Yeast

Yeast Extract Peptone Dextrose (YPD) Media

1% Yeast Extract

2% Peptone

2% Dextrose

Synthetically defined (SD) media

0.67% Yeast Nitrogen Base (YNB)

2% Dextrose

For making nitrogen deprive and limiting conditions YNB without ammonium sulfate and the amino acid was used. For glucose limiting condition, glucose was used as low as 0.1-0.01%. For alternate carbon source utilization experiments, dextrose was replaced with other carbon sources *viz.,* ethanol, glycerol and sodium acetate. Ethanol and sodium acetate were used at a final concentration of 2% and glycerol was used at a final concentration of 3%.

Synthetically complete media (SC)

0.67% Yeast Nitrogen Base

2% Dextrose

0.6% Casamino acid

2.1.4.3 Buffers and solutions

Phosphate Buffered Saline (PBS)

PBS was prepared as a 10X stock solution and diluted to 1X concentration before autoclaving.

10 mM Na2HPO4

2 mM KH2PO4

137 mM NaCl

2.7 mM KCl

Final pH was adjusted to 7.0 with 11.6 N HCl and autoclaved for sterilization.

Tris-HCl buffer

1 M Tris-base

Final pH of buffer was adjusted to 7.5 needed using 11.6 N HCl.

EDTA

0.5 M EDTA

Final pH of buffer was adjusted to 8 by using 10 N NaOH.

Tris-EDTA buffer (TE)

Buffer was prepared as 10X concentrate and diluted to 1X concentration before use.

10 mM Tris-HCl (pH 8.0)

1 mM EDTA

Tris Acetic acid EDTA (TAE) buffer

Buffer was prepared as 50 X concentrate and diluted to 1X before use.

40 mM Tris Base

0.5 M EDTA

TAE buffer pH was adjusted to 8.5 with glacial acetic acid.

2.1.4.4 Bacterial transformation reagents

INOUE buffer

10 mM PIPES

15 mM $CaCl_2.2H_2O$

250 mM KCl

55 mM $MnCl_2.4H_2O$

These solutes were dissolved in 800 ml of H_2O, then 20 ml of 0.5 M PIPES (piperazine-1,2-bis[2-ethanesulphonic acid]) with pH 6.7 was added, final volume was adjusted to 1 liter with H_2O and filter sterilized by using a 0.22 µM membrane filtration unit and stored at -20°C.

PIPES Stock solution was prepared separately by dissolving 15.1 gm of PIPES in 80 ml of water. pH was then adjusted to 6.7 using 5 M KOH and final volume was adjusted to 100 ml.

2.1.4.5 Yeast transformation reagents

Lithium acetate

Lithium acetate was prepared at 1 M concentration and sterilized by either autoclaving or filter sterilizing.

Polyethylene glycol (PEG)

50 % PEG was prepared in milli Q water.

Single stranded carrier DNA

5ul of 10 mg/ml concentration of single stranded DNA was used for each yeast transformation

2.1.4.6 Yeast colony PCR buffer

Zymolyase buffer

2.5 mg/ml Zymolyase (MP Biomedicals)

1.2 M Sorbitol

The solution was prepared in1X PBS.

2.1.4.7 Yeast DNA extraction buffers

Buffer A

50 mM Tris-HCl

10 mM EDTA

150 mM NaCl

1% Triton-X

1% SDS

Buffer B

50 mM Tris-HCl (pH 7.5)

10 mM EDTA

1.1 M Sorbitol

50 mM β-mercaptoethanol (Added fresh before use)

Buffer C

100 mM Tris-HCl (pH 7.5)

10 mM EDTA

10% SDS

Phenol:Chloroform:Isoamyl alcohol (PCI, 25:24:1) solution

25 ml Phenol (pH 8.0)

24 ml Chloroform

1 ml Isoamyl alcohol

DNA sample loading buffer

0.25% Bromophenol blue

0.25% Xylene cyanol

15% glycerol

6X stock solution of the loading buffer was prepared in water was used at the final concentration of 1X.

2.1.4.8 RNA isolation buffer

RNA isolation buffer was either prepared in RNase free water or DEPC- treated water

Diethyl pyrocarbonate (DEPC)- treated Water

1 ml DEPC was added to 1L of water and kept overnight on a magnetic stirrer. The solution was then autoclaved.

AE buffer

3 M sodium acetate

0.5 M EDTA (pH 8.0)

Acid phenol solution

RNase-free water was added until phenol saturated. Briefly phenol (500g) was heated to 65^{o}C, then 100 ml of RNase-free water was added, mixed and cooled. After cooling about 100 ml water was added until a layer of water developed on top of phenol which made it water saturated. Solution was aliquoted into 50 ml tubes and frozen at -20.

TES Buffer

10 mM Tris pH 7.5

10 mM EDTA

0.5% SDS

2.1.4.9 Bacterial Plasmid isolation buffer

Solution I

50 mM glucose

25 mM Tris-Cl (pH 8.0)

10 mM EDTA (pH 8.0)

Solution II

0.2 N NaOH

1% (w/v) SDS

Solution III

5 M potassium acetate, glacial acetic acid

2.2 Methods

2.2.1 Microbiological methods

2.2.1.1 Culture conditions

Yeasts *C. glabrata* and *S. cerevisiae* strains were usually grown in YPD media or SD media, or SC media, unless specified. Yeast strains used were grown at 30°C with 200 rpm shaking. For selection of transformants was performed on YPD media containing NTC (200µg/ml) or HphB (500µg/ml) or SD without uracil media wherever needed. Yeast stocks for storage were prepared in 15% glycerol and stored at -80° C. frozen stocks were revived on YPD media or SD media with appropriate antibiotic or without uracil by streaking tipfull of frozen culture. Streaked culture were allowed to grow for 24-48 h and were stored at 4°C for a maximum period of two weeks.

For nitrogen starvation and limiting condition generation, cells were grown in media containing YNB (0.67%) without ammonium sulfate and amino acid. Proline was added at 30 µg/ml and 0.1 µg/ml as the sole nitrogen source for nitrogen limiting and starved conditions, respectively.

Plasmids were maintained for construction and propagation in *Escherichia coli DH5α* strain. *E. coli* strains were maintained in LB media with AMP (100µg/ml). Bacterial culturing was done at 37°C for 14-16 h with a continuous shaking of 150 rpm. 15% glycerol was used for long term storage of bacterial culture.

2.2.1.2 Ultra-competent *E. coli* cell preparation

Escherichia coli DH5α strain was revived from -80°C on LB-agar plate for 16-20 h. Single colony from plate was inoculated in 25 ml of SOB medium in a 250 ml flask and incubated for 6-8 h at 37°C with vigorous shaking at 250 rpm. 2-10 ml of starter culture was inoculated in 1 L flask each containing 250 ml of SOB media. Culture was then incubated overnight at 18°C with moderate shaking at 150 rpm. After overnight incubation, OD_{600} of the cultures was monitored till it reached 0.55. Then cells were kept on ice for 10 min. After incubation cells were then harvested by centrifugation at 2,500g for 10 min at 4°C. Supernatant was discarded completely by inverting on paper towel and pelleted cells were gently resuspended in 80 ml of ice-cold Inoue transformation buffer. Cells were then harvested by centrifugation at 2,500g for 10 min at 4°C and the decanted. The cell pellet was then resuspended in 20 ml of ice-cold Inoue transformation buffer gently. 1.5 ml of DMSO was added to the cells and incubated on ice for 10 min. Aliquots of cell suspension were made in pre-chilled 1.5 ml microfuge tubes. Cells were then snap-frozen in liquid nitrogen and stored in -80°C freezer till further use.

2.2.1.3 Bacterial transformation

Ultra-competent cells of *E. coli* DH5α were used for all bacterial transformations. Frozen competent cells were taken out from -80 °C freezer and thawed on ice for 15 min. Plasmid or ligation product (5-10 µl and 100-500 ng of DNA) to be transformed was added and incubated on ice for 30 min. Heat shock was given for 60- 90 sec at 42°C and was immediately kept on ice for 2 min. 1 ml of sterile SOC media was then added into it and incubated at 37°C with 150 rpm for 45 min. Then cells were spun down and resuspended in 50 µl of LB/ SOC medium. Resuspended cells were then plated on SOB/LB-agar medium containing appropriate antibiotics and incubated for 12-16 h at 37°C. Transformants were verified by PCR and restriction digestion.

2.2.1.4 Transformation in yeast

Both chemical transformation (for plasmid transformation) and electroporation method (for linear DNA fragment transformation) of transformation were employed.

2.2.1.4.1 Chemical method

Transformation was performed as previously described method (Gietz et al. 1992) with few modifications. Briefly, *C. glabrata* primary culture was prepared by growing a single colony in YPD media overnight at 30°Cwith 200 rpm. Secondary culture was prepared by inoculating overnight grown culture in 10 ml YPD broth at an initial OD_{600}o of 0.1. Culture was then allowed to grow for 4-5 h in a shaker set at 30°C with 200 rpm. Culture was immediately kept on ice when $OD6_{00}$ reached 0.6-0.8. Cells from the cultre were then harvested by centrifugation at 4000 rpm and washed twice with 10 ml of sterile water. Cells obtained were then resuspended in 1 ml of sterile water and were transferred to a 1.7 ml microfuge tube. Cells were harvested at 4,000 rpm for 5 min, resuspended in 50 µl of100 mM lithium acetate solution. A mixture of 240 µl PEG (50%), 36 µl of lithium acetate (1 M), 5 µl of heat denatured single stranded DNA (10 mg/ml) was added, mixed gently and incubated for 5 min at room temperature. 500 ng-1 µg of transforming DNA was added and final volume was maintained to 360 µl with sterile water. The tube was then incubated at 30°C for 45 min. 43 µl of sterile DMSO was added into this and heat shock was given at 42°C for 15 min. After 15 min tube was immediately kept on ice for 1 min and then centrifuged at 4,000 rpm. Supernatant was completely removed by pipetting and resuspended in 50 µl sterile water. Cells were then spread-plated on appropriate selection media and were incubated at 30°C for 24-48 h.

2.2.1.4.2 Electroporation method

Transformation by electroporation in yeast cells was performed by previously described method (Istel et al. 2015) with slight variation. Briefly, *C. glabrata* strains were grown overnight in YPD media at 30 °C with shaking at 200 rpm for primary culture. Secondary culture was prepared by diluting the culture in fresh YPD media to an OD_{600} of about 0.1, and continued to culture until an OD_{600} of 1.0 was reached. Cells were then harvested in 50 ml tubes by centrifugation at 400 rpm for 5 min and washed with sterile water at room temperature twice. Cell pellets were then gently resuspended in 8 ml sterile water, 1 ml 10X TE buffer and 1 ml 1 M lithium acetate by slow pipetting. Incubate the cell suspension(s) for 30 min at 30 °C and 130 rpm. 250 µl of 1 M DTT was added and suspensions were incubated for 60 min at 30 °C and 130 rpm. After incubation 40 ml of sterile pre-cooled water was added and centrifuged at 400 rpm for 5 min and 4°C. Pellets

were carefully resuspended by slow pipetting in 25 ml of sterile pre-cooled water and repeated the centrifugation step. Pellets were then gently resuspended in 5 ml pre-cooled 1 M sorbitol and centrifugation step was repeated. Finally, pellets of electro-competent cells were resuspended in 550 µl of pre-cooled 1 M sorbitol. 40 µl aliquots of electro-competent cell suspensions were taken into sterile precooled tubes, 5 to 10 µl of purified transforming DNA (0.5-1 µg) was added and 100ul volume maintained by 1M sorbitol. Suspension was then incubated on ice for 10 min and then poured into electro-cuvette. Electro pulses (200 Ω, 1.5 kV, 25 µF), was applied with the time constant at about 4.6 mS and then immediately put on ice. 950 µl of YPD media was added and transferred in a tube and allowed to grow for 3-5 h at 30 °C with shaking at 200 rpm for revival. Cells were then centrifuged and spread plated on appropriate media.

2.2.1.5 Serial dilution spot assay

C. glabrata mutants were phenotypically characterized by serial dilution spot assay. Briefly, the overnight grown cells were normalized to $OD_{600}$of 0.1 and were further serially diluted 10-fold in 0.9% NaCl five times. 3 µl of serially diluted culture were then spotted on the required plates. Plates were then allowed to incubate at 30°C (unless mentioned otherwise) for 24-48 h and growth was recorded by capturing their images. For checking the ability of mutants to utilize non-fermentable carbon sources, growth was recorded after 6-7 days of incubation.

2.2.1.6 Minimum inhibitory concentration detection assay

Overnight grown cells were resuspended in 0.9% saline to an OD_{600} of 0.1. Then, 100 µl the cells were added in 10ml YEPD media with final OD_{600} of cell is 0.01 or 10^4 cell/ ml. Dilutions of drugs/chemicals were prepared by serial dilution in 96 well plate and after that 100 µl of 0.01 OD_{600} cells were inoculated in each well. Growth differences were recorded following incubation of the plates for 48 h at 30°C.

2.2.1.7 Time course growth analysis

Time course growth curve analysis of *C. glabrata* mutant cells were performed in 96 well plate format by employing a liquid handling system (Tecon, Austria). For growth curve generation, cells were first grown in appropriate media overnight, followed by sub-culturing cells in test medium with an initial OD_{600} of 0.2 and growth was monitored by

recording the absorbance at 600 nm at regular time-intervals of 30 min till 24 h. Absorbance values obtained were then plotted with respect to time. The generation time of yeast strains were then calculated from the time when cells were in logarithmic phase of growth using the following equation.

Generation time(G)=T_2-T_1 X$\log_2 \log N_f/N_i$

Where G = Generation time (h)

T1 = Initial time point taken for analysis

T2 = Final time point taken for analysis

Nf= Number of cells at time T2

Ni = Number of cells at time T1

1 OD_{600} of *C. glabrata* corresponds to 2 X 10^7cells

2.2.2 Methods used in molecular biology techniques

2.2.2.1 Cloning

2.2.2.1.1 PCR reaction

Taq polymerase and Phusion polymerase were used in the PCR reaction according to their need.

2.2.2.1.2 Gel extraction, PCR purification

QIAquick® gel extraction kit (QIAGEN, 28706), QIAquick® PCR purification kit (QIAGEN, 28106) were used for gel extraction and PCR purification of DNA fragments respectively. All the extractions and purifications were performed as per manufacturer's instructions.

2.2.2.1.3 Restriction digestion and ligation

Restriction enzymes were procured from NEB and Thermo scientific. Restriction digestion of plasmid DNA (5-10µg) and PCR-amplified DNA (1-5µg) products were set in 50 µl reaction volume with appropriate buffer. Digested fragments were the gel extracted and concentrations were measured by NanoDrop™ 2000/2000c spectrophotometer, Thermo scientific. T4 DNA Ligase enzyme (NEB, M0202M) was used for ligation of digested

fragments. All ligation reactions were set in 20 µl reaction volume containing 1X ligase buffer, 3-10 units of DNA ligase enzyme and vector to insert molar ratio of 1:3. The ligation mixture was either incubated at 16°C for 16h or at room temperature for 2-3 h. Post incubation, ligation reaction was inhibited by heat in tubes at 65°C for 15-20 min. 5-10µl of ligation mixture was used to transform ultra-competent *E. coli* DH5α cells.

2.2.2.1.4 Gibson assembly

Gibson assembly was procured from NEB (E5510S) and used for cloning purpose. Procedure was followed as per the manufacturer's protocol.

2.2.2.1.5 Complementation plasmid construction

For complementation studies, modified plasmid pGRB2.3_hph was used with HphB as selection marker. Parent plasmid was procured from Addgene pGRB2.3 (Addgene #45343). Ura3 selection marker of the plasmid pGRB2.3 was replaced with HphMX gene that codes for hygromycin B phosphotransferase to make it pGRB2.3_hph by using gibson assembly. HphMX gene sequence was amplified from plasmid pSH69 (Euroscarf, P30675). This plasmid was then used as parent plasmid for further cloning of ABC transporters orf for complementation by us in Gibson assembly.

All 20 *C. glabrata* ABC ORFs, were PCR amplified from wild-type genomic DNA with 1kb promoter region using Phusion high-fidelity DNA polymerase. pGRB2.3_hph was also PCR amplified to linearize it. PCR fragments were then gibson assembled upstream of YeGFP. Final plasmids were confirmed by PCR and restriction digestion.

2.2.2.1.6 Transcription factor *CgPDR1* gain of function mutated plasmid construction

Initial plasmid was pBluescript II KS (+) from the lab stock. Yeast dominant selection marker NAT1 with FRT sites was PCR amplified from plasmid pRK625 (From lab of fungal pathogenesis, CDFD), cloned in pBluescript II KS (+) at EcoRV blunt end site and the plasmid was named as pMS1. PDR1terminator (755bp) was amplified and cloned at ClaI/KpnI site to facilitate homologous recombination (plasmid pMS2). Also, PDR1 orf with its 741bp promoter and 587bp terminator region was amplified from strain DSY565, which contains GOF mutation in the PDR1 gene (G840C) and then cloned into the

plasmid pMS2 at SacI/SacII site (plasmid pMS3). Plasmid pMS3 was linearized with SacI/KpnI digestion for transformation in yeast.

2.2.2.1.7 Expression plasmid construction for integration in MSY8 strain

To study the role of particular transporter we have constructed an integration plasmid which can be used to integrate GOI at *CgCDR1* locus. For constructing this plasmid, *CgCDR1* terminator (791bp) and promoter (719bp) were amplified from the genome of *C. glabrata* and cloned at KpnI/ClaI and SacI/SacII site respectively in plasmid pMS1 (plasmid pMS4 and pMS5 respectively). YeGFP-HISt (1135bp) was amplified from plasmid pGRB2.3 (Addgene #45343) and cloned at XmaI/ SpeI site (plasmid pMS6). The resulted plasmid pMS6 contained four unique restriction site (NotI/SpeI/SacII/PacI) for cloning the GOI to study the role.

2.2.2.1.8 Cloning in plasmid pMS6

C. glabrata CgYor1, *CgCDR1*, *CgPDH1*, *CgFLR1, S. cerevisiae YOR1* and *C. albicans YOR1* were PCR amplified from their respective genomes and cloned at SacI/SacII or NotI/PacI site. Positive plasmids were confirmed by PCR and restriction digestion. Final plasmids were linearized by SacI/ KpnI or the whole cassettes were amplified by using primers 5'CACTATAGGGCGAATTGGAGCTC3' and 5'CTAAAGGGAACAAAAGCTGGGTACC3' for integration in MSY8 strain.

2.2.2.1.9 *CgYOR1* complementation Plasmid construction for *S. cerevisiae*

CgYOR1 ORF was amplified from *C. glabrata* genome and was gel eluted for purification. Purified fragment were then blunt end ligated at SmaI site in a yeast expression plasmid pGPD2. Constructed plasmid was then transformed in *S. cerevisiae* for complementation study.

2.2.2.2 Plasmid and Nucleic acid isolation

2.2.2.2.1 Plasmid isolation

Bacterial plasmid DNA was isolated by employing alkaline lysis method. Briefly, 10 ml of LB medium supplemented with appropriate antibiotics was inoculated with a single bacterial colony and then incubated at 37°C for 16 h. Cultures were spun down at 8,000 rpm for 5 min, supernatant was discarded. In 150 µl solution I the cell pellet was

resuspended by vortexing allowed to rest for 2 minutes. Then 200 µl of solution II was added in the suspension to lyse the cells and gently mixed by inverting the tube 4-6 times til the mixture becomes viscous. 300 µl of solution III was added to neutralize and contents were mixed by inverting the tube 4-6 times. Suspension was spun down at 14,000 rpm for 5 min and supernatant was transferred to a new 1.7 ml microfuge tube. 500 µL of chloroform was added, mixed and centrifuged at 14,000 rpm for 5 min. Upper aqueous layer was taken, 2-2.5 volume of ethanol was added into it and incubated at -80°C for 30 min. After incubation, tube was centrifuge at 4°C with 14,000 rpm for 5 min and supernatant was removed. Pellet was then washed with 600 µL of 70% ethanol and centrifuged at 14,000 for 5 min. Thereafter, Pellet was air dried and dissolved in 50 µl RNase-water.

2.2.2.2.2 Yeast genomic DNA isolation

Glass bead lysis method

Yeast genomic DNA was isolated by mechanically lysing the yeast cells. Briefly, 10 ml of overnight grown yeast cultures were spun down at 4,000 rpm for 5 min. Media was decanted and pellet were washed with 10 ml sterile water. Washed cells were resuspended in 500 µl of Buffer A and transferred to a 1.7 ml microfuge tube. Tubes were allowed to incubat at 65°C for 15 min. Post incubation, 500 µl of PCI (25:24:1) solution was added along with 0.5 g of 0.5 mm glass beads. Cells were then lysed mechanically in a bead-beating homogenizer (MP Biomedicals, FastPrep®-24) thrice, 45 secs each, with intermittent cooling on ice. Tubes were then spun at 12,000 rpm for 5 min and the aqueous layer was transferred to a new 1.7 ml microfuge tube. 500 µl of PCI solution was then added and mixed gently by inverting the tubes. Tubes were centrifuged again at 12,000 rpm for 5 min and aqueous layer was transferred to another 1.7 ml microfuge tube. 2.5 volume of absolute ethanol was added to the aqueous layer, mixed well and incubated at -80°C for 30 min. Supernatant was decanted and the DNA pellet obtained was washed with 70% ethanol and centrifuged at 13,000 rpm for 10min. Washed DNA pellet was air-dried and dissolved in 100 µl sterile water by gently tapping the tubes.

Spheroplast lysis method

10 ml overnight grown *C. glabrata* cultures were harvested and washed with 10 ml sterile water twice. Cell pellet were resuspended in 500 µl of buffer A and incubated at 42°C for a period of 10 min. Post incubation, cells were centrifuged at 4,000 rpm for 5 min and resuspended in freshly prepared buffer B and one tip-full of lyticase (Sigma, L4025) was then added and incubated at 37°C for 1 h. After incubation, spheroplasts were collected by centrifuging tubes at 6,000 rpm for 5 min. Cell pelletw were then resuspended in 500 µl of buffer C and 500 µl of PCI (25:24:1) solution was added and centrifuged. The aqueous layer was transferred to a new1.7 ml microfuge tube and 2.5 volume of absolute ethanol (100%) and 1/10th volume of 3 M sodium acetate (pH 5.3) were added to it. Microfuge tubes were centrifuged at 13,000 rpm for a period of 10 min. Supernatant was then discarded and DNA pellet was washed once with 70% ethanol, centrifuged at 13,000 rpm for 10 min, air-dried at room temperature and was resuspended in 100-200 µl of 1X TE buffer or sterile water by gently tapping the tube. DNA was stored at -20°C till further use.

2.2.2.2.3 Total RNA isolation

Both manual method and kit were used to isolate RNA. Appropriate conditions for cultures were provided wherever it was necessary.

RNA isolation by kit

Total RNA isolation from yeast cells was performed by using RNeasy Mini Kit (QIAGEN, Germany). Briefly, overnight grown cultures of yeast *C. glabrata* were diluted to 0.1 OD_{600} and grown at 30 ºC for 4 h in YPD media. Cells were washed with PBS and then total RNA was extracted as per the manufacturer's protocol.

Hot phenol method

Yeast cells were grown under appropriate conditions and at suitable time points, cells were spun down at 4,000 rpm for 5 min. Yeast cell pellet was washed twice with ice-cold DEPC-treated water. Pellet was resuspended in 400 µl of TES buffer, then 400 µl acid phenol was added, vortexed and incubated for ~60min at 65^{o} with occasional vortexing. Suspension was then spun down for 5 min at 4ºC. Transfer aqueous layer to new 1.7 ml tube, then 400ml acid phenol was added, vortexed and centrifuged for 5 min at 4ºC. Upper aqueous layer was taken, 400 µl chloroform was added into it, vortexed

and spun down for 5 min at 4ºC twice. Upper layer was taken out, 10% volume of 3M NaOAc, pH5.2, 2-2.5 volume of 100% ethanol to final aqueous layer and incubated on ice for at least 1 h. Suspension was centrifuged for 15min at 4ºC, supernatant decanted and washed with 500 µl 70% ethanol. Pellet obtained was then air dried and resuspended in 50ml of RNase-free water. RNA was quantitated by taking reading from nanodrop at RNA was stored at -80 ºC till further use.

2.2.2.3 cDNA synthesis

2.2.2.3.1 DNase1 treatment

Deoxy ribonuclease I (DNase I) enzyme (Thermo scientific) was used to remove the DNA contamination from RNA samples, if any. Briefly, 5 µg of RNA was subjected to DNase I digestion by using 1 U of DNase I in a 10 µl reaction mixture which contained 1X DNase I buffer and appropriate volume of water. This reaction mixture was incubated at 37ºC for 60 min. To inhibit DNase I enzyme activity, 0.5 µl of 25 mM EDTA was added to the reaction mixture and tubes were heated at 65°C for 10 min. DNase I-digested RNA samples were used as template to perform PCR for the amplification of *CgPGK1*gene and absence of amplification product was used as criterion to confirm proper DNase I digestion and lack of DNA contamination in the RNA sample.

2.2.2.3.2 Complementary DNA (cDNA) synthesis

cDNA synthesis was performed by using RevertAid H minus first strand cDNA synthesis kit (Thermo Scientific, Lithuania). Briefly, 1 µg of DNase I digested RNA was incubated with 50 µM oligo(dT) and 50 µM of random primers at 65°C for 5 min in a 12 µl reaction mixture. 8 µl of cDNA synthesis mixture was added which contained 4 µl of 5X RT buffer, 2 µl of 10 mM dNTPs, 1 µl of Riboloc enzyme and 1 µl of RT enzyme. Mixture were incubated for 5 min at 25 °C, 42 °C for 60 min and was terminated at 75°C for 5 min. The quality check of synthesized cDNA was performed by using it as a template in a PCR reaction to amplify the housekeeping gene *CgPGK1* or *CgTEF3*. Amplification of *CgPGK1*was indicative of proper cDNA synthesis.

2.2.2.3.3 Semi-quantitative PCR

To confirm the deletions and absence of genes inside the genome, semi quantitative RT-PCR was performed. PCR reaction mixture contained in a total of 50 µl, 1 µl cDNA, 5 µl 10X PCR buffer, 1 µl dNTPs, 0.2 µl Taq DNA polymerase, 1 µl of each primer of (30 pM/ml). Each cycle involved denaturation for 30 sec at 95 °C, annealing for 30 sec at 55 °C and extension was given for 1 min at 72 °C, with an additional 2 min pre-denaturation before the cycles and a further 10 min extension after the cycles.

After the PCR amplification, 10 µl aliquot of each PCR reaction sample together with 2 µl of loading dye was subjected to gel electrophoresis on a 2% agarose gel. The PCR products were visualized by ethidium bromide staining, and then scanned using a Chemidoc XRS plus gel documentation system (Bio-Rad, USA), The band intensities of the target gene and the internal control gene were quantified using densitometry as described earlier (ref). The mRNA expression levels were determined as the ratio of intensity of the target gene to the internal control gene (*CgPGK1*).

2.2.2.3.4 Quantitative real-time PCR

Primers for real-time qPCR experiments were designed by using the Primer quest software to obtain 120-200 bps amplification products. DyNAmo Flash SYBR Green qPCR kit (Thermo Scientific, Lithuania) or Bio-Rad SYBR Green were used to quantify the gene expression profile. *CgPGK1* was used for normalization and were analyzed in CFX96TM real time PCR system (Bio-Rad, USA). The expression level of tested genes was measured by comparing the Ct-value of the gene with *CgPGK1*. qRT-PCR analysis was performed in biological duplicate with technical triplicate.

Comparative expression profiles were analyzed by $2^{-\Delta\Delta Ct}$ method.

Fold change upon treatment=$2^{-\Delta\Delta CT}$

$\Delta\Delta CT=\Delta CT$ Treated- ΔCT Untreated

ΔCT Treated= CT value for gene of interest upon treatment- CT value of internal control (*CgACT1*) upon treatment

ΔCT Untreated= CT value for gene of interest without treatment- CT value of internal control (*CgPGK1* or *CgTDH3*) without treatment

The reaction cycling conditions were as follows

1) 95°C for 10 min (initial activation)

2) 95°C for 15 sec (denaturation)

3) 60°C for 1 min (annealing and extension)

4) Go to step 2 (40 cycles)

6) 72°C for 10 min (final extension)

2.2.2.4 *C. glabrata* mutants construction

2.2.2.4.1 Construction of *C. glabrata* knockout

A fusion PCR mediated homologous recombination based strategy was used to disrupt *C. glabrata* ORFs with a cassette containing dominant selection marker *NAT1*gene, which codes for nourseothricin acetyltransferase and confer resistance to nourseothricin. Briefly, Briefly, 5' and 3'UTR flanking region of the gene were PCR amplified from wild type genomic DNA. Selection marker NAT1 gene with FRT sites was also PCR amplified in two halves from plasmid pRK625. Both the UTRs were fused to one half of the NAT1 gene and these fused PCR products were co-transformed into the wild type strain. The two NAT1 half amplified fragments share about 300-350 bp complimentary region. The fused PCR products were co-transformed in to the WT strain by electroporation and allowed to grow for 4-6 h in YPD broth for homologous recombination. Cells were then harvested and plated on YPD agar containing 200 µg/ml nourseothricin. Plates were then incubated at 30°C for 24-48 h. Nourseothricin-resistant colonies were purified and verified for gene disruption *via* homologous recombination by PCR using appropriate set of primers.

2.2.2.4.2 Construction of *C. glabrata* multiple knockout

For more than one gene knockout generation starting strain was *C. glabrata* BG14, which lacked ura3 gene. Sequentially multiple deletions were done by using drug based recyclable (FRT-NAT1-FRT) cassette, described above, followed by selection of mutants on the selection plate containing nourseothricin. Dominant selection marker NAT1 gene was recycled by using plasmid pRK70, which contain ura3 selection marker and codes

for Flipase gene under constitutive EPA1 promoter. Then after removing selection marker and flipase plasmid the strain was ready for next round of deletion. Next deletion was done by using same strategy stated above.

2.2.2.4.3 Introduction of GOF mutation in TF PDR1 (MSY8 strain)

pMS3 plasmid that from contained GOF mutation in the TF PDR1 gene (G840C) taken from strain *C. glabrata DSY565*. Plasmid was then linearized with SacI/KpnI digestion, the obtained fragment was transformed in the *C. glabrata* MSY7 strain and selected on the YPD agar plate containing 200µg/ml nourseothricin. Final strain made was named as MSY8.

2.2.2.4.4 Yeast colony PCR for K/O confirmation

For Yeast colony PCR, yeast cells were digested with zymolyase (MP Biomedicals, 0832092) to obtain the spheroplast. A digestion cocktail in 1XPBS consisting of zymolyase (2.5mg/ml) and sorbitol (1.2 M) was prepared. The cocktail was dispensed in 0.2 ml PCR tubes in 10 µl aliquots and a tip-full of yeast cells were added into it. Tubes were then incubated for 3 h at 37 °C and post incubation 1 µl of digested mixture taken out and was used as a template in a PCR reaction.

2.2.3 Biochemical techniques

2.2.3.1 Assessment of efflux activity

To know the R6G/ Nile Red (NR) efflux assay was energy-dependent, spectrofluorimeter based R6G and NR efflux assays were performed (Keniya et al. 2015; Gbelska et al. 2017). Briefly, yeast strains were cultivated in YEPD liquid medium at 200 rpm (30 °C) for 16 hours. The obtained cells were washed thrice with ice-cold glucose-free PBS. Cells were suspended in ice-cold glucose-free phosphate-buffered saline (PBS) and incubated at 200 rpm (30 °C) for 4 hours under starvation conditions to reduce ABC pump activity. Cells were then washed twice and diluted to 10^8 cells/ml in ice-cold glucose-free PBS. All samples were incubated for another 2 hours at 200 rpm (30 °C). Then, 10 µM (final concentration) R6G or 7mM NR was added, and cells were incubated for further 2 hours at 200 rpm (30 °C). The external R6G or NR was then removed by washing with glucose-free PBS. Glucose at final concentration of 2 mM was then added to the samples to

reactivate the ABC efflux pumps, with PBS as the negative control. Cell samples (1 ml) were taken at designated time points, centrifuged and 100 ml of supernatant from each sample were then transferred into a 96-well microtiter plate with clear bottoms. For R6G efflux 527 nm excitation and 555 nm emission and for NR 552 nm excitation and 636 nm emission were used. A straight line for the relation between fluorescence and concentration was plotted for both the substrates and the concentration in the supernatant was determine by plotting the fluorescence to this graph.

2.2.3.2 Substrate competition assay

Two substrates will compete with each other if both are the substrate of that particular transporter. To study substrate competition of a substrate for ABC transporters, R6G efflux assay was employed. Briefly, log phase growing cells were harvested washed with 1X PBS. Pellet were then dissolved in 1X PBS, 10 µM R6G was added, then 2X MIC of desired competitor (FLC, BEA or OMY) was added and allowed to grow for 2 h. Cells only with PBS was taken as the negative control.

2.2.3.3 Measurement of ROS level

The oxidant-sensitive probe DCFDA was used to measure endogenous ROS. Cells were set to a OD600 of 0.1 in YEPD medium and incubated for 4 h at 30 °C with shaking at 200 rev./min. Then, a 4 mM final concentration of H2O2 was added, and the culture was grown for 2 h. Cells were wahed thrice with PBS and then a final volume of 3µM DCFDA was added to the sample followed by incubation at 30 °C for 30 min. After three wash the cells were dissolved in PBC and then analyzed with a FACSCalibur flow cytometer at 495 nm excitation and 529 nm emission (filter FL1). A total of 10000 events were considered. The remaining cells were used to prepare slides and were observed under confocal microscopy with a FITC filter

2.2.4 Bioinformatical analysis

NCBI genome database were employed to download *C. glabrata* genome sequences with assembly no. ASM254v2. Identification of ABC proteins were performed by using the model ABC-tran (accession PF00005) of the Pfam database (http://pfam.sanger.ac.uk/) and the HMM search program from the HMMER package (http://hmmer.org/) using the default settings. Amino acid sequences were downloaded from UniProt

(www.uniprot.org/). ITS sequences of yeast species were taken from free online database SILVA (https://www.arb-silva.de/). Alignment of sequences were performed by ClustalW with default parameters. The phylogenetic trees of proteins were generated by MEGA6.06 using maximum likelihood (ML) method using the poisson amino acid substitution model and 1000 bootstrap replications. The sequence identities of ABC proteins with ABC proteins of same or different species were recorded by employing BLASTp (https://blast.ncbi.nlm.nih.gov/Blast.cgi?PAGE=Proteins) with default parameters. The topology of *C. glabrata* ABC proteins were predicted by online available softwares Topocons (http://topcons.cbr.su.se/) and Scan Prosite (http://prosite.expasy.org/scanprosite/). The size of ABC proteins and their chromosomal location were retrieved from Candida Genome Database (http://www.candidagenome.org/). The circular ideogram was constructed by using a software Circos (http://circos.ca/software/). The sofwares WoLF PSORT (https://www.genscript.com/wolf-psort.html) and LocTree3 (https://rostlab.org/services/loctree2/) software were employed for the subcellular localization prediction.

2.2.5 Animal model experiments

2.2.5.1 Mice wound infection

To test virulence of the mutants, wound infection experiment was performed in mice model. K/O were constructed in *C. glabrata* ATCC 2001 strain constitutively expressing luciferase. Briefly, Balb/c mice were given two doses of cyclophosphamide on day -4 (150 mg/kg) and -1 (100 mg/kg) to make them neutropenic followed by wound infection on day 0. Infected mice were segregated into three groups (n = 3/group) where group 1 mice were treated with WT cells, group 2 mice were treated with K/O (*Cgyor1*Δ*)* cells and group 3 with complemented strain (*CgYOR1* complemented strain). CFU was quantified from the wound after 4th day post infection in YPD media.

2.2.6 Other methods

2.2.6.1 Ethics statement

Experiments involving mice were performed at the RCB-THSTI animal facility, Gurugram, India strictly in accordance with the Committee for the Purpose of Control and Supervision

of Experiments on Animals (CPCSEA), committee guidelines. The procedures used in the studies were designed to minimize animal suffering.

CHAPTER I

3. Inventory of ABC proteins in human pathogenic yeast *Candida glabrata*

3.1 Background

ABC superfamily also known as 'Traffic ATPases' is very diverse and well-studied family of proteins known to exist from prokaryotes to higher eukaryotes (Glavinas et al. 2004b). These proteins are well known for their role as high affinity nutrient importers in bacterial cells and rose to prominence as exporters in higher eukaryotes. These proteins are known to perform diverse functions and their ability to confer MDR brought them to eminence. Typically, a full ABC transporter consists of four distinct domains: two TMDs consisting of six TMHs and two nucleotide binding domains (NBD), located on the cytosolic side of the membrane (Wilkens 2015b). The NBDs, which couple energy of ATP hydrolysis to power drug and transport export are highly conserved structure (Linton and Higgins 2007). Each NBD contains three characteristic motifs: Walker A and Walker B motifs, which form the nucleotide-binding site, and an ABC signature sequence, or C motif, for which several functions have been proposed, including communication between the TMDs and NBDs during the transport cycle (Rai et al. 2006; Prasad et al. 2015). TMDs on the other hand with its homo- or heteromeric repeats of unrelated TMHs provide three dimensional structures for substrate binding and help in transport process (ter Beek et al. 2014b). In contrast to NBDs which consist of conserved sub-domains, TMHs of two TMDs are of variable structure which imparts poly specificity to these transporters (Prasad Dr and Rawal 2014). While two NBDs and two TMDs are required to become a full functional ABC transporter, half ABC transporters also known to exist with one each of NBD and TMD and presumably function as homo-dimers (Wilkens 2015c).

C. glabrata is a human fungal pathogen notorious to cause infection in immunocompromised and immunocompetent individuals. *C. glabrata* genome is 12.3 Kb in size which is divided into 13 chromosomes. It also contains a 20 kb circular mitochondrial genome. The genome of the organism consists of 5054 open reading frames (ORFs) out of which only about 4.52% (239 ORFs) of the genome is characterized leaving a scope for a good study in the organism (Fig 3.1).

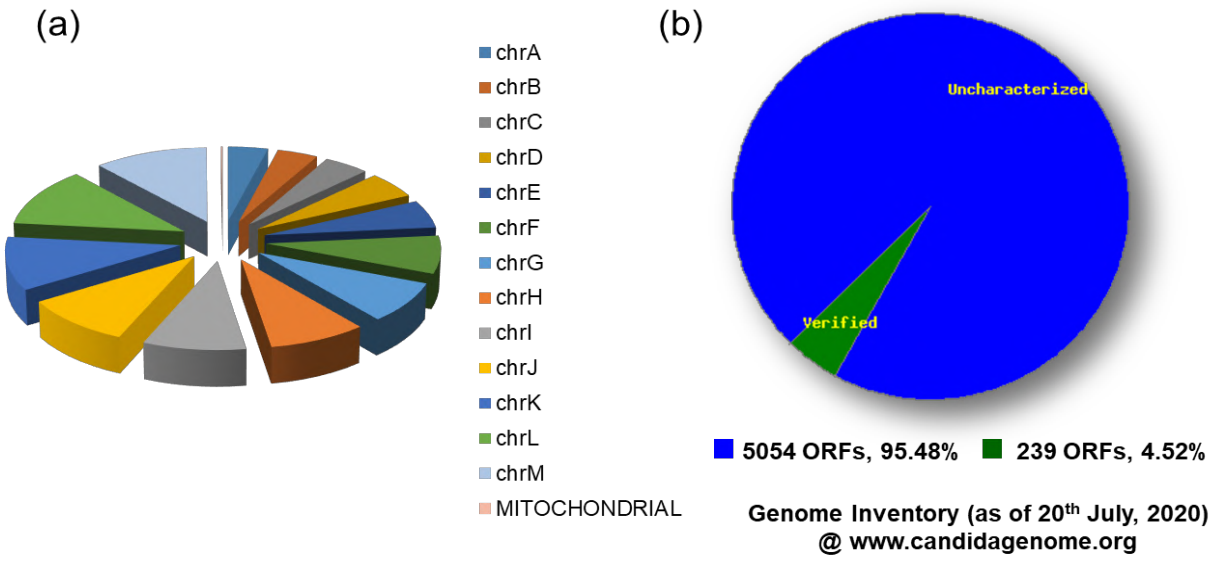

Fig 3.1: Genome snapshot of yeast *C. glabrata*. (a) Division of genomes on chromosome (b) snapshot of verified portion of genome in *C. glabrata.*

S. cerevisiae and *C. albicans* possess a battery of ABC proteins, which are reasonably well characterized for their role in MDR (Decottignies and Goffeau 1997; Gaur et al. 2005b). However, such information is lacking for an emerging pathogenic haploid yeast *C. glabrata*. Recent epidemiological data revealed that *C. glabrata* is the second most frequently isolated nosocomial species among fungal infections (Pfaller and Diekema 2007a), and exist as a commensal of normal microbiota of oral cavity, gastrointestinal and genital tract in humans (Kaur et al. 2005). Notably, *C. glabrata* is phylogenetically distant from pathogenic *C. albicans* and closer to nonpathogenic yeast *S. cerevisiae* (Dujon et al. 2004b). The clinical isolates of *C. glabrata* show high level of resistance towards commonly used antifungal such as azoles (Oxman et al. 2010). The acquisition of MDR towards various classes of antifungals is a serious clinical challenge for candidiasis treatment. Recently, high attention was derived by ABC proteins of *C. glabrata* due to the fact that some of the efflux pumps encoding genes such as *CAGL0M01760g* (*CgCDR1*), *CAGL0F02717g* (*CgPDH1*) and *CAGL0I04862g* (*CgSNQ2*) are highly expressed in clinical isolates of *C. glabrata* and contribute to the development of azole resistance (Sanglard et al. 1999b, 2001b; Sanguinetti et al. 2005b; Torelli et al. 2008b; Whaley et al. 2017). Earlier, *CAGL0M01760g* (*CgCDR1*) and *CAGL0F02717g*

(*CgPDH1*) upregulation independent of *CgPDR1* mutation in FLC heteroresistant *C. glabrata* clinical isolates has been also reported (Ben-Ami et al. 2016). Therefore, an in depth analysis of large members of ABC superfamily of *C. glabrata* is required to dissect their physiological relevance in MDR and other cellular processes.

3.2 Identification of *C. glabrata* ABC protein and their sequence retrieval

C. glabrata genome sequences with protein coding ORFs were downloaded from the NCBI genome database (ftp.ncbi.nlm.nih.gov/genomes) with assembly no. ASM254v2. ABC proteins were identified by using the model ABC-tran (accession PF00005) of the Pfam database (https://pfam.xfam.org/) and the HMM search program from the HMMER package (http://hmmer.org/) using the default settings. Positive hits above the default threshold were further filtered by a cutoff, defined from the plot of scores and e-values. Hits with domain scores greater than 56.4 and e-value less than 1.2e-20 were considered true positives containing the NBD domain and extracted as potential ABC sequences for further analysis. To investigate putative ABC proteins, the HMM profile of the ABC transporter domain (accession PF00005) was utilized as the queries to search against 5054 protein coding ORFs in *C. glabrata* genome. Initially, a total of 54 proteins consisting of NBD domain in the range of 150±20 amino acids were found. Since NBD is a member of the Rossman fold superfamily of nucleotide binding proteins, and to ensure that only NBD containing proteins are detected, a threshold was determined from the plot of domain scores and e-values, and a large inflection at a score of 56.4 and e-value of 1.2 e-20 was observed. Further, examination of sequences below this score and with a higher e-value showed that canonical motifs associated with NBD were absent in 29, out of these 54 proteins. Hence, only 25 proteins with higher score and lower e-value than the set threshold were considered for further study (Fig 3.2).

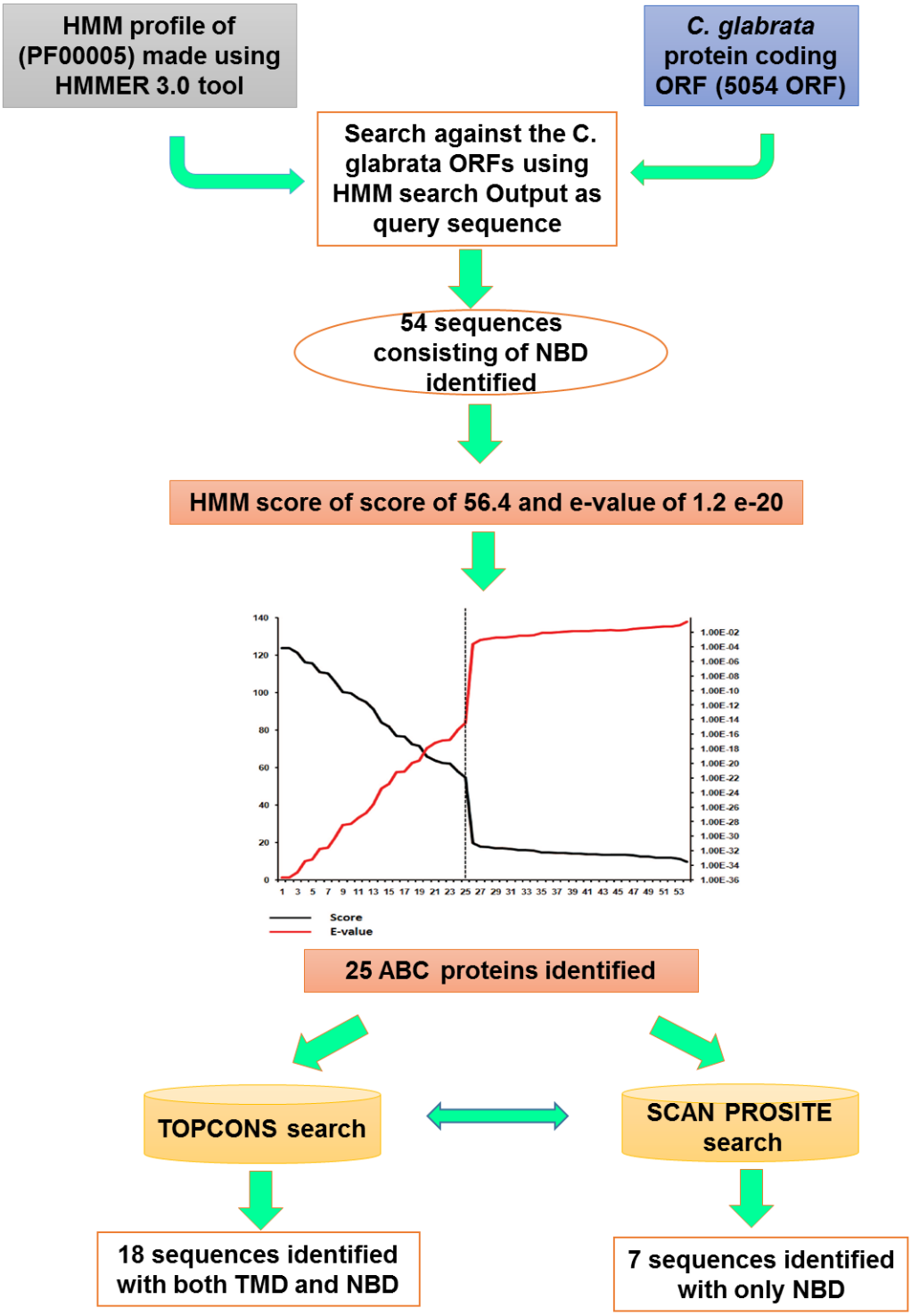

Fig 3.2: Methodology of identification of ABC proteins used in *C. glabrata*

Identified putative ABC proteins and their amino acid length is listed in Table 3.1.

Table 3.1: Predicted ABC proteins in *C. glabrata*

RefSeq ID	ORF Name	Gene names*	Length#	UniProt Entry
XP_448240.1	*CAGL0K00363g*		1227	Q6FNF4
XP_444820.1	*CAGL0A01133g*		801	Q6FXW2
XP_449941.1	*CAGL0M13739g*	*ATM1*	727	Q6FIK3
XP_445704.1	*CAGL0E00385g*		608	Q6FVP0
XP_445860.1	*CAGL0E03982g*		1659	Q6FV84
XP_445319.1	*CAGL0C03289g*	*YBT1*	1648	Q6FWS5
XP_445834.1	*CAGL0E03355g*		1535	Q6FVB0
XP_449053.1	*CAGL0L06402g*	*YCF1*	1535	Q6FL41
XP_446375.1	*CAGL0G00242g*	*YOR1*	1477	Q6FTR9
XP_445428.1	*CAGL0D00352g*		861	Q6FWG6
XP_449450.1	*CAGL0M02387g*		856	Q6FJZ4
XP_446712.1	*CAGL0G08041g*		607	Q6FST2
XP_445278.2	*CAGL0C02343g*	*ARB1*	720	Q6FWW6
XP_445575.1	*CAGL0D03674g*		1186	Q6FW19
XP_448674.1	*CAGL0K10472g*		752	Q6FM70
XP_445123.1	*CAGL0B03487g*	*TEF3*	1045	O93796
XP_447598.1	*CAGL0I08019g*		1285	Q6FQ96
XP_449421.1	*CAGL0M01760g*	*CDR1*	1499	Q6FK23
XP_447461.1	*CAGL0I04862g*	*SNQ2*	1507	Q6FQN3
XP_446088.1	*CAGL0F02717g*	*PDH1/CGR1*	1542	O74208
XP_449665.1	*CAGL0M07293g*		1515	Q6FJC9
XP_446033.1	*CAGL0F01419g*	*AUS1*	1398	Q6FUR1
XP_449114.1	*CAGL0L07744g*		1055	Q6FKY0
XP_446582.1	*CAGL0G05093g*		544	Q6FT62
XP_448758.1	*CAGL0K12474g*		294	Q6FLY6

* Name of genes given in the NCBI database # Length of proteins in amino acids

3.3 Phylogenetic analysis, domain organization and subfamily prediction

The complete genome sequence and phylogenetic analysis of *S. cerevisiae* and *C. albicans* identified 30 and 26 distinct ABC protein encoding genes, respectively (Prasad et al. 2016a). Considering close phylogenetic similarity of *C. glabrata* with *S. cerevisiae* and to predict subfamilies, an unrooted phylogenetic tree was constructed by aligning NBDs of *C. glabrata* and *S. cerevisiae* ABC proteins as described in methods. Based on resemblance in domain organization with *S. cerevisiae*, putative ABC proteins of *C. glabrata* were segregated into six major clusters and were assigned to MDR/ABCB, MRP/ABCC, ALDp/ABCD, RLI/ABCE, EF3/ABCF and PDR/ABCG subfamilies (Fig. 3.3). The domain organization of *C. glabrata* ABC proteins was consistent with that of *S. cerevisiae* in ML tree, wherein N- and C- terminal NBDs are segregated separately; indicating that full transporters could be the outcome of duplication of half transporters.

Amino acid sequences of *C. glabrata* NBDs (accession PF00005) were extracted as per their locations in the ABC proteins and *S. cerevisiae* NBD sequences of ABC proteins were retrieved by UniProt (www.uniprot.org/). The complete amino acid sequences of ABC proteins of *S. cerevisiae, C. albicans, Cryptococcus neoformans, Kleyvuromyces lactis* and *Schizosaccharomyces pombe* were taken from previously published report (Kovalchuk and Driessen 2010b). ITS sequences were taken from online database SILVA (https://www.arb-silva.de/). Sequences were aligned by ClustalW with default parameters and phylogenetic trees were generated by MEGA6.06 using maximum likelihood (ML) method and poisson amino acid substitution model with 1000 bootstrap replications. Sequence identities of ABC proteins among different species were analyzed by using BLASTp (https://blast.ncbi.nlm.nih.gov/Blast.cgi?PAGE=Proteins) with default parameters.

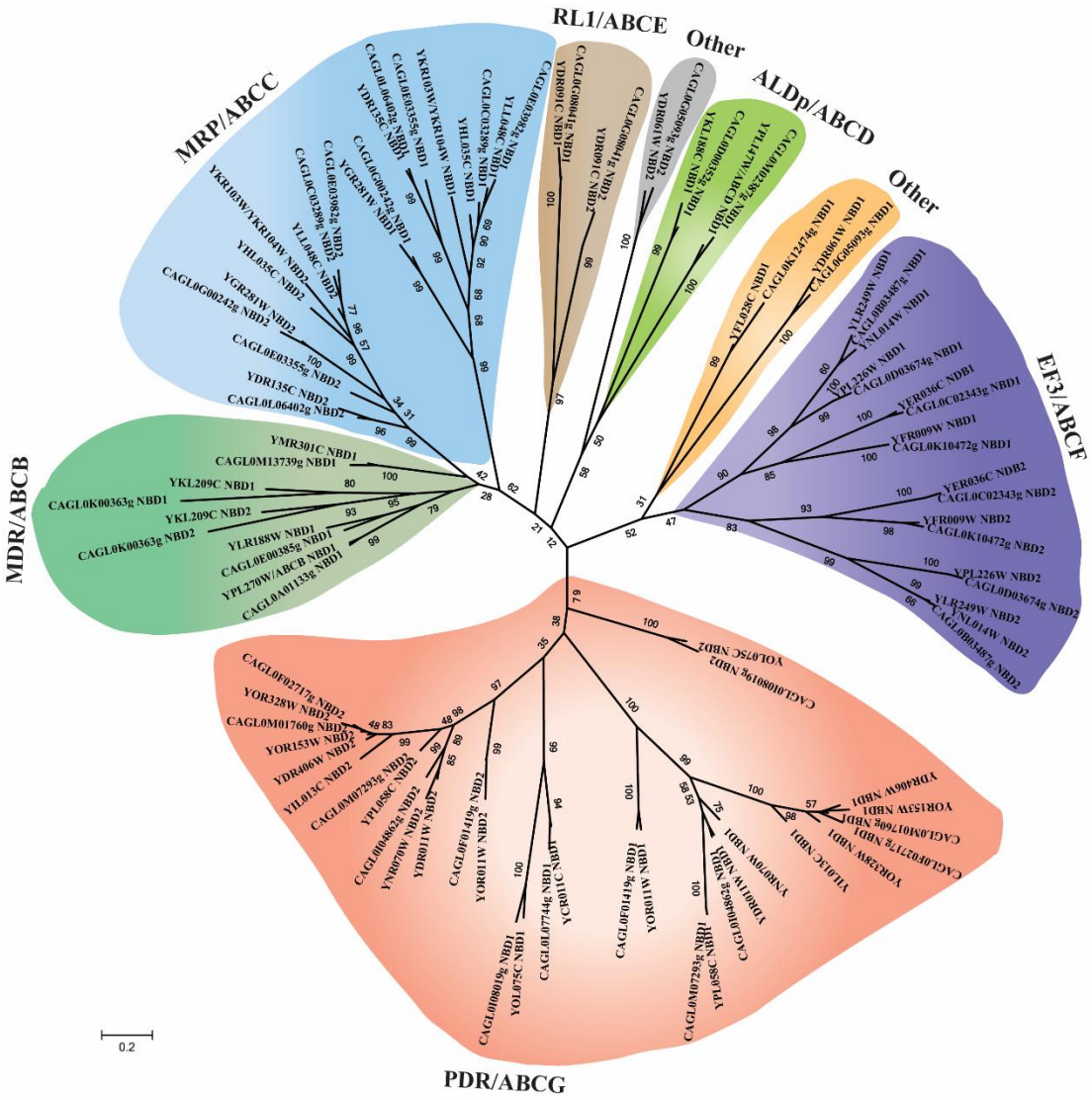

Fig 3.3: A schematic tree depicting the phylogenetic relationship among ABC subfamilies: NBDs of *C. glabrata* and *S. cerevisiae* ABC proteins were used in ML analysis. Clustering of *C. glabrata* NBDs is consistent with NBDs of *S. cerevisiae* ABC proteins. C-terminal NBDs of ABCC/MRP subfamily members clustered with ABCB/MDR subfamily NBDs. Phylogenetic tree is represented in radial form.

To attain a better understanding of evolutionary relationship in ABC proteins among yeast species another phylogenetic tree was constructed by using complete ABC proteins of six representative yeast species (*S. cerevisiae, C. albicans, C. neoformans, K. lactis* and *S. pombe*) including *C. glabrata* (Fig 3.4a). Among them, *S. pombe* possess the least member of ABC proteins (19 ABC proteins) while *C. neoformans* has maximum (33 ABC proteins) ABC protein members (Fig. 3.4b). Notably, *S. pombe* was distinct with regard

to a number of subfamilies since it does not have any member protein belonging to ABCD/ALDp subfamily. Our analysis further revealed that phylogenetically *C. glabrata* ABC subfamily proteins are closer to *S. cerevisiae* and *K. lactis* ABC proteins. Interestingly, in addition to the NBD, members of each family also have conserved amino acid sequences, which could help in providing a comparative evolutionary orthologous relationship among various yeast species. Considering almost similar size of *C. glabrata* (12.3Mb) and *S. cerevisiae* (12.1Mb) genome, it is notable that the former possess lesser number of ABC proteins, which could suggest loss of some of the genes during whole genome duplication (WGD) event (Birchler and Veitia 2010). In *S. cerevisiae* and *C. glabrata* ABCG/PDR family forms the largest subfamily, although it has significantly lower number in *C. glabrata*. Among subfamilies, preferentially MDR/ABCB, ALDp/ABCD and RLI/ABCE family members were retained during duplication event, indicating their significance in cell physiology.

(a)

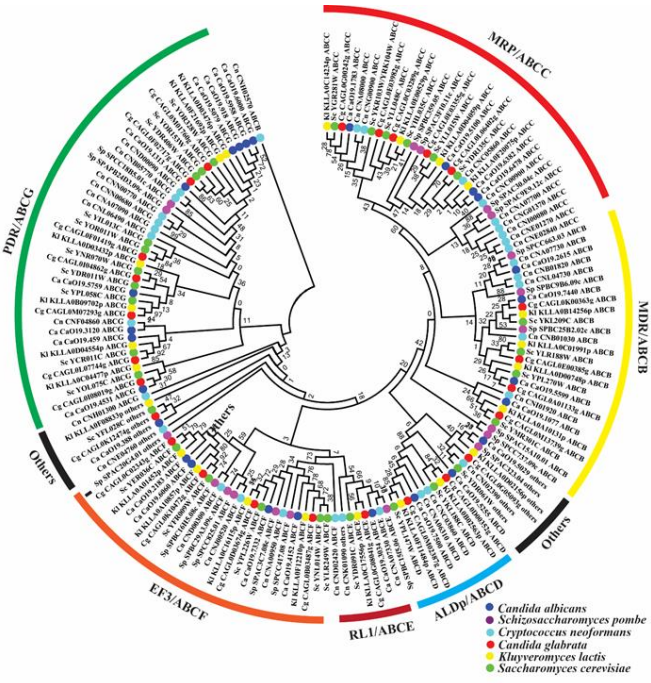

(b)

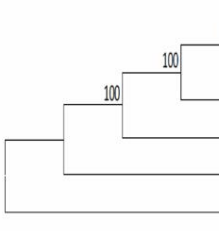

	MDR		MRP	ALDP	RL1	YEF3	PDR		Others	Total	
	Full	Half					Full	Half			
	1	3	4	2	1	4	4	2	2	23	*Kluyveromyces lactis*
	1	3	6	2	1	5	8	2	2	30	*Saccharomyces cerevisiae*
	1	3	5	2	1	4	6	1	2	25	*Candida glabrata*
	1	3	4	2	1	4	6	2	2	26	*Candida albicans*
	2	3	4	0	1	5	2	0	2	19	*Schizosaccharomyces pombe*
	2	4	9	2	1	4	6	2	3	33	*Cryptococcus neoformans*

Fig. 3.4: Comparison of ABC proteins in different yeast species. (**a)** Phylogenetic tree of the ABC proteins of six yeast species: The analysis was performed with putative *C. glabrata* ABC protein sequences with *S. cerevisiae, C. albicans, C. neoformans, K. lactis* and *S. pombe*. The numbers on the branches indicate the percentage of bootstrap support from 1000 replicates. The ABC subfamilies are identified based on known subfamilies in fungal species. (**b)** Distribution of ABC proteins among fungal species: *C. glabrata* harbors less number of ABC proteins as compared to *S. cerevisiae, C. neoformans* and *C. albicans* but more in number as compared to *K. lactis* and *S. pombe.* Organism phylogeny presented based on their ITS sequences.

3.3.1 Multi Drug Resistance (MDR)/ABCB Subfamily

The ABCB/MDR subfamily members comprise of both full and half transporters with forward topology, $(TMD\text{-}NBD)_2$ or (TMD-NBD). ABCB1 was the first characterized member of MDR subfamily for its ability to confer MDR in mammalian cells (Glavinas et al. 2004b). This subfamily is further divided into three subtypes: full transporters (involved in MDR), half transporters (involved in the transportation of peptides) and mitochondrial half membrane transporters (Anjard et al. 2002). Four ABC proteins of *C. glabrata CAGL0K00363g*, *CAGL0E00385g*, *CAGL0M13739g* (*CgATM1*), and *CAGL0A01133g* belong to MDR subfamily but are remain to be characterized. Among these *CAGL0K00363g*, the only member of MDR/ABCB full transporter in *C. glabrata*, was clustered with similar full transporters in other yeasts. It showed 42% sequence identity with *S. cerevisiae* haploid-specific ABC transporter *ScSTE6*, the a-factor pheromone transporter (Kuchler et al. 1989a). The three half transporters *CAGL0M13739g* (*CgATM1*), *CAGL0A01133g*, and *CAGL0E00385g* showed an orthologous relationship with *S. cerevisiae* mitochondrial half transporters. *CAGL0M13739g* (*CgATM1*) is ortholog of an inner mitochondrial membrane-localized transporters of *S. cerevisiae* (*ScATM1*), which translocate iron-sulfur (Fe/S) clusters into the cytosol (Kispal et al. 1997) and has a well-defined mitochondrial targeting signal sequence. Biogenesis of Fe/S clusters as a function of *ATM1* is highly conserved among various fungal species (Kovalchuk and Driessen 2010b). In *C. glabrata, CAGL0M13739g* (*CgATM1*) is involved in osmosensitivity and echinocandin sensitivity (Schwarzmuller et al. 2014). *CAGL0E00385g* and *CAGL0A01133g* are orthologs of peptide transporter coding genes *ScMDL1* and *ScMDL2*, respectively, of *S. cerevisiae* localized in the mitochondrial inner membrane (Dean et al. 1994).

3.3.2 Multi drug resistance associated proteins (MRP)/ABCC subfamily

None of the ABC proteins of this subfamily are characterized in *C. glabrata*. ABCC/MRP subfamily members belonging to mammalian cells and other major groups of eukaryotes are known to efflux diverse array of toxic substrates including drugs and xenobiotics compounds outside the cell or sequester into the vacuole (Klein et al. 2006). The unique feature of this family is to recognize glutathione (GSH)-, glucuronate- and sulfate-conjugated organic anions and are involved in detoxification processes (Jeong et al. 2017). It has also been observed that MRPs synergistically act with a large number of enzymes viz, GSH-S-transferase, UDP- glycosyltransferase to contribute resistance towards various substrates (Dermauw and Van Leeuwen 2014). Notably, unlike ABCB/MDR or ABCG/PDR subfamilies, all the MRP members exist as full transporters. Five putative ABC proteins of *C. glabrata* were clustered into this group, among them *CAGL0E03982g*, *CAGL0C03289g* (*CgYBT1*), *CAGL0E03355g*, and *CAGL0L06402g* (*CgYCF1*) have an extra transmembrane region $TMD_0(TMD\text{- }NBD)_2$ and were considered as long MRPs, and *CAGL0G00242g* (*CgYOR1*) has topology of $(TMD\text{- }NBD)_2$, considered to be short MRP. *C. glabrata* MRP members showed phylogenetic similarity with *K. lactis* and *S. cerevisiae* ABC proteins. However, *CAGL0G00242g* (*CgYOR1*) have 71% sequence identity with *S. cerevisiae ScYOR1*, a well-studied PM localized transporter involved in transport of various organic anions including oligomycin and phospholipids (Cui et al. 1996). *CAGL0G00242g* (*CgYOR1*) also exhibited 31% sequence identity with the only known channel human *CFTR/ABCC7* in the ABC transporter superfamily protein, where mutations in its encoding gene sequence were linked to cystic fibrosis (Vernon et al. 2017). *CAGL0C03289g* (Cg*YBT1*) has a sequence identity of 53% with *S. cerevisiae ScYBT1*. *CAGL0G00242g* (Cg*YOR1*) and *CAGL0C03289g* (Cg*YBT1*), both were found to be upregulated in azole resistant lab mutant as well as in azole resistant clinical isolates (Vermitsky et al. 2006b; Tsai et al. 2010b). 42% sequence identity of *CAGL0L06402g* (Cg*YCF1*) was observed with human *MRP1* which is involved in endobiotics and xenobiotics extrusion (Johnson and Chen 2017). Previous report also suggested the upregulation of *CAGL0L06402g* (Cg*YCF1*), *CAGL0C03289g* (Cg*YBT1*) *and CAGL0G00242g* (Cg*YOR1*) in the petite strain isolates (Ferrari et al. 2011b).

3.3.3 Adrenoleukodystrophy protein (ALDp)/ABCD)

ABCD/ALDp subfamily proteins found in all eukaryotic organisms with an exception to some plants predominantly exist as half transporters (Theodoulou et al. 2006). Half ABCD/ALDp members homogenously or heterogeneously dimerize to become functional (Morita and Imanaka 2012). In *C. glabrata CAGL0M02387g* and *CAGL0D00352g* belong to this subfamily which showed orthology with *S. cerevisiae ScPXA1* and *ScPXA2*, respectively. ALDps are peroxisomal membrane localized proteins in *S. cerevisiae,* involved in long and branched chain fatty acids import or their conjugate fatty acyl-CoA derivatives transport to peroxisome (van Roermund et al. 2011). Interestingly, mutations in either *ScPXA1* or *ScPXA2* make cells incompetent to grow on oleic acid, suggesting that probably they function as a heterodimer (Shani and Valle 1996). Moreover, both ABCD/ALDps of *C. glabrata* such as *CAGL0M02387g* and *CAGL0D00352g,* showed 32% and 33% sequence identity with human ABCD2 and 31% and 32% identity with *ABCD1*. The human *ABCD1* and *ABCD2* are involved in translocation of polyunsaturated VLCFA-CoA and mutation in these genes result in a human disease, X-linked Adrenoleukodystrophy (X-ALD) (Pujol et al. 2004). The clear evolutionary orthologous relationship between this family members in various species strongly point to their conserved functions.

3.3.4 RNase L Inhibitor (RLI)/ABCE Subfamily

The ABCE/RLI subfamily proteins have a characteristic pair of linked NBDs with no TMDs. These soluble proteins are predicted to have a role in biological processes rather than in membrane transport (Tian et al. 2017). In human *ABCE1*, an ABCE/RLI protein is associated with polyribosomes and functions to inhibit RNase L to initiate translation (Dong et al. 2004). *CAGL0G08041g*, the only member of this family in *C. glabrata*, displayed NBD-NBD topology and has a characteristic ferredoxin iron-sulfur type binding domain (4Fe-4S) with the consensus sequence of C-X-{P}-C-X(2)-C-{CP}-X(2)-C-[PEG], (pfam00037, where four C's are the 4Fe-4S center) which is a typical motif found in nucleic acid binding proteins. *CAGL0G08041g* showed high sequence identity with *S. cerevisiae ScRLI1* (89%) and *K. lactis KLLA0C17556p* (88%). *ScRLI1* of *S. cerevisiae*, an iron-sulfur (4Fe-4S) protein, is involved in maturation of ribosomal subunit, translation initiation through interaction with eIF3 complex and also have a role in translational

termination (Khoshnevis et al. 2010), however, this protein remains uncharacterized in *C. glabrata*.

3.3.5 Elongation Factor 3 (EF3)/ABCF subfamilies

The members of this subfamily are topologically similar to ABCE/RLI subfamily proteins with paired NBDs without TMDs. In human and yeast species, *EF3* is involved in several aspects of translation such as ribosome biogenesis, translational control of gene expression, exporting mRNA into cytoplasm, or act as a translational elongation factor (Kovalchuk and Driessen 2010b). A total of four members namely, *CAGL0K10472g*, *CAGL0C02343g*, *CAGL0D03674g*, and *CAGL0B03487g* (*CgTEF3*) of ABC proteins in *C. glabrata* belonged to this subfamily. *CAGL0B03487g* (*CgTEF3*) and *CAGL0C02343g* showed 88% and 90% sequence identity with *S. cerevisiae ScTEF3* and *ScARB1*, respectively. In *C. glabrata, CAGL0B03487g* (*CgTEF3*) is an essential gene for growth and at protein level, it has been reported to be down regulated at alkaline pH (Nakayama et al. 1998; Schmidt et al. 2008). The best characterized member of this subfamily in *S. cerevisiae* is *ScGCN20*, which mediates the activation of eIF-2α kinase (Vazquez de Aldana et al. 1995) and showed 89% sequence identity with *CAGL0K10472g*. All members of this family are remain uncharacterized in *C. glabrata*.

3.3.6 Pleiotropic Drug Resistance (PDR)/ABCG subfamily

ABCG/PDR subfamily is ubiquitous throughout the plants, fungi and animal kingdom but absent in bacteria. In animals, ABCG/PDR subfamily members exist as half transporters and are homologous to the white-brown-complex (WBC) family transporter of *Drosophila*. In previous report, it is suggested that there could be two possibilities of generation of PDR/ABCG subfamily, 1) by fusion of independent NBD and TMD, because it is the only subfamily in which NBD precedes the TMD (reverse topology) or 2) by direct origin from the central portion of a member of the ABCA, ABCB, or ABCC subfamilies (Anjard and Loomis 2002). Notably, ABCG/PDR subfamily members play important roles in extruding a variety of xenobiotics including agricultural fungicides, azoles, mycotoxins, herbicides, and antifungal drugs (Kolaczkowski et al. 1996b). Similar to *S. cerevisiae* and *C. albicans*, PDR/ABCG subfamily with 7 members; *CAGL0F02717g* (*CgPDH1*), *CAGL0F01419g* (*CgAUS1*), *CAGL0M01760g* (*CgCDR1*), *CAGL0I04862g* (*CgSNQ2*), *CAGL0I08019g*, *CAGL0M07293g*, and *CAGL0L07744g* represents the largest group in *C. glabrata*

wherein, all the members except *CAGL0L07744g* are full transporters. Importantly, *CAGL0M01760g* (*CgCDR1*), *CAGL0I04862g* (*CgSNQ2*) and *CAGL0F02717g* (*CgPDH1*) have been shown to play major role in the development of MDR phenotypes in clinical isolates and petite mutants of *C. glabrata* (Miyazaki et al. 1998a; Izumikawa et al. 2003a; Brun et al. 2004; Whaley and Rogers 2016). These three transporters are regulated by transcription factor PDR1 and their upregulation is linked to the azole resistance (Torelli et al. 2008b). *CAGL0F01419g* (*CgAUS1*) is a sterol transporter and protects cells against azole antifungals in the presence of serum (Nakayama et al. 2007; Nagi et al. 2013a). These *C. glabrata* genes showed sequence similarity with human ABCG members involved in exporting anti-cancerous drugs and cholesterol transport. Other members of ABCG/PDR subfamily are poorly characterized in *C. glabrata*. However, their functions can be predicted based on sequence identity with PDR/ABCG members of other yeast species. For instance, *CAGL0M07293g* is an ortholog of *S. cerevisiae ScPDR12* with 85% sequence identity, which is involved in organic acid transport (Piper et al. 1998), while *CAGL0I08019g* with 36% sequence identity to Ca*CDR6/CaROA1* of *C. albicans* governs resistance to azoles (Khandelwal et al. 2017). The half transporter *CAGL0L07744g* shows 67% sequence identity with *S. cerevisiae ScADP1,* the first identified half transporter belongs to the WBC family of *Drosophila* (Rogers et al. 2001).

3.3.7 Others

Soluble ABC proteins that do not cluster into any specified subfamily has been kept under the category of others. In *C. glabrata* two proteins, *CAGL0G05093g* and *CAGL0K12474g* come into this category with two NBD and one NBD, respectively. *CAGL0G05093g* showed an orthologous relationship with uncharacterized protein in *S. cerevisiae* (*YDR061W*) and have 32% sequence identity with *C. albicans MODF*. *CAGL0K12474g* gene has orthologous relationship with *ScCAF16* of *S. cerevisiae* which is known to be a part of CCR4-NOT regulatory complex involved in transcriptional control of gene regulation (Liu et al. 2001).

3.4 Topology Prediction of ABC transporters

The topology of *C. glabrata* ABC proteins was predicted by online softwares Scan Prosite (http://prosite.expasy.org/scanprosite/) and Topocons (http://topcons.cbr.su.se/). Scan Prosite was used to recognize the NBD location and Topocons was utilized for TMH

identification. Size and chromosomal location of the ABC proteins were retrieved from the Candida Genome Database (http://www.candidagenome.org/) and a circular ideogram was generated by using Circos software (http://circos.ca/software/). To predict subcellular localization of ABC proteins, LocTree3 (https://rostlab.org/services/loctree2/) and WoLF PSORT (https://www.genscript.com/wolf-psort.html) were employed with input of putative ABC proteins amino acid sequences.

ABC proteins have two characteristic topological structures: TMD and NBD. The presence of hydrophobic TMD in the protein makes it an eligible candidate of membrane-localized proteins, while presence of only NBD makes it a putative soluble protein. To investigate whether *C. glabrata* ABC proteins follow the same domain organization as reported in other organisms, the position of NBDs and TMDs were determined in each of the ABC protein sequences by using Topocons and Scan Prosite (Fig 3.5). Based on the order of NBDs and TMDs, the ABC proteins belonging to the subfamilies ABCB/MDR, ABCC/MRP, ABCD/ALDp were predicted to possess forward topology, wherein TMD precedes the NBD (TMD-NBD), while the members of ABCG/PDR subfamily have reverse orientation, where TMD follows NBD (NBD-TMD**)** (Xiong et al. 2015).

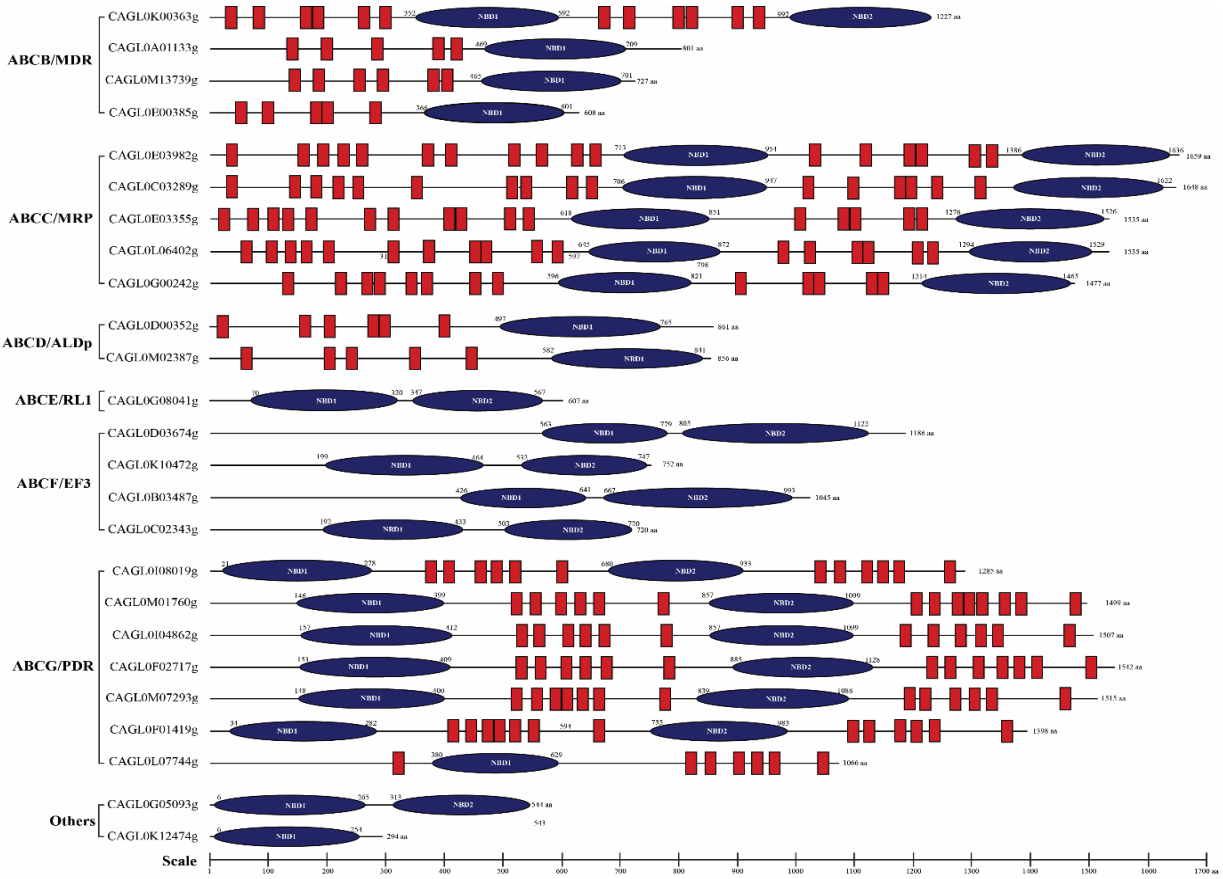

Fig 3.5: Pictorial depiction of ABC protein topology in *C. glabrata*. Topology prediction was performed by online softwares Scan Prosite and Topocons: All the subfamily members of ABC proteins harbor either one or two NBD. The ABCB/MDR subfamily displayed forward topology and consist of both full and half transporters, while members of the ABCG/PDR subfamily displayed reverse topology. One of the MRP/ABCC family members *CAGL0G00242g* (*CgYOR1*) does not contain extra set of transmembrane domains. ABCD/ALDp member proteins are half transporter with same topology as ABCB/MDR half transporters. Members of the ABCE/RLI, ABCF/EF3 and other soluble ABC proteins do not contain transmembrane domains. The scale indicates the number of amino acids.

A typical TMD is comprised of 6 to 10 TMHs (Khunweeraphong et al. 2017), however the prediction with different topology predicting softwares indicated the presence of a variable number of TMH in ABC proteins containing TMDs in Table 3.2. All the proteins with only NBDs in primary structure belong to ABCE/RLI and ABCF/EF3 subfamilies and were predicted as soluble proteins.

Table 3.2: Number of transmembrane domain prediction in all ABC proteins using different online tools.

ABC genes	TOPOCONS	OCTOPUS	PHILIUS	SCAMPI	TMHMM	UNIPROT
CAGL0K00363g	12	12	12	12	12	12
CAGL0A01133g	6	6	3	6	3	3
CAGL0M13739g	6	6	5	5	5	5
CAGL0E00385g	6	6	6	6	5	4
CAGL0E03982g	17	19	17	17	16	16
CAGL0C03289g	17	20	17	17	14	13
CAGL0E03355g	18	18	17	16	17	17
CAGL0L06402g	17	17	14	16	14	13
CAGL0G00242g	14	14	11	14	10	10
CAGL0D00352g	6	6	2	5	4	4
CAGL0M02387g	5	6	3	5	1	1
CAGL0G08041g	0	0	0	0	0	0
CAGL0C02343g	0	0	0	0	0	0
CAGL0D03674g	0	0	0	0	0	0
CAGL0K10472g	0	0	0	0	0	0
CAGL0B03487g	0	0	0	0	0	0
CAGL0I08019g	12	12	13	12	12	11
CAGL0M01760g	14	13	12	12	12	12
CAGL0I04862g	12	12	13	12	11	11
CAGL0F02717g	13	13	12	12	10	12
CAGL0M07293g	13	13	12	12	10	10
CAGL0F01419g	13	13	12	12	12	12
CAGL0L07744g	7	7	8	8	8	8
CAGL0G05093g	0	0	0	0	0	0
CAGL0K12474g	0	0	0	0	0	0

3.5 Chromosomal location, and localization prediction of ABC proteins

C. glabrata have a haploid genome consists of 13 chromosomes (Chr A to Chr M) (Dujon et al. 2004b). Chr M harbors maximum number of ABC protein encoding genes (4 genes) followed by Chr E, Chr G and Chr K, each possess 3 genes. Each of Chr C, Chr D, Chr

F, Chr I and Chr L accommodate 2 genes. Each Chr A and Chr B reside only 1 gene, however, Chr H and Chr J do not contain any ABC protein coding gene (Fig 3.6).

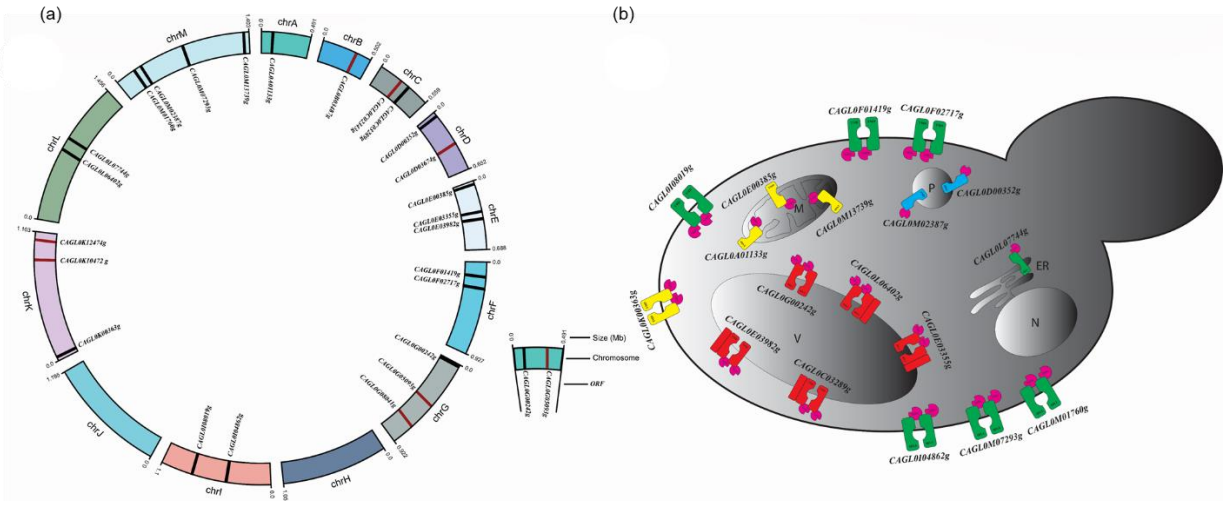

Fig. 3.6: Chromosomal location and subcellular localization of ABC proteins in *C. glabrata*. **(a)** *C. glabrata* chromosomes (chrA - chrM) are displayed in circular ideogram. Black color indicates location of ABC transporter and dark maroon indicates soluble ABC proteins location. Chromosome M harbors maximum number of ABC genes and Chromosome H and J do not contain ABC genes. (**b**) Subcellular localization of the ABC transporters were predicted by LocTree3 and WoLF PSORT: Only membrane proteins are depicted.

Subcellular localization (SCL) of a protein is important to elucidate the potential function in various cellular processes. It is anticipated that proteins localized in the same cellular compartment of different organisms could perform similar type of function. SCLs of ABC proteins of *C. glabrata* were analysed by using online software LocTree3. The results obtained suggested that most of the *C. glabrata* MDR/ABCB members are localized at MM and ABCC/MRP members are localized in VM. As expected, ABCD/ALDp members were predicted to be localized on peroxisomal membrane. ABC proteins of ABCG/ PDR subfamily were predicted in PM except *CAGL0L07744g*, which was found to be localized on endoplasmic reticulum (ER). Previous reports supported our localization prediction as two of the known ABCG/PDR members, *CAGL0M01760g* (*CgCDR1*) and *CAGL0F02717g* (*CgPDH1*) were shown to be PM localized (Lamping et al. 2007a). Notably, localization prediction varies by the use of different softwares. ABC proteins, *CAGL0I08019g* and *CAGL0K00363g* belonging to PDR/ABCG and MDR/ABCB subfamilies, respectively, were predicted to be localized at the nucleus by LocTree3

software, however, WoLF PSORT predicted these proteins localization at PM. WoLF PSORT predicted *CAGL0G00242g* (*CgYOR1*) and *CAGL0L07744g* localization to PM, while LocTree3 predicted in VM and ER membranes, respectively. The predicted localizations of 18 ABC membrane proteins are depicted in Fig 3.6b, while soluble ABC proteins are predicted to be confined to the cytosol or nucleus are listed in Table 3.3.

Table 3.3: Subcellular localization prediction of all ABC proteins of *C. glabrata*

ABC protein coding genes	LocTree3	WoLF PSORT
CAGL0K00363g	Nucleus	Plasma membrane
CAGL0A01133g	Mitochondrial membrane	Mitochondrial membrane
CAGL0M13739g	Mitochondrial membrane	Plasma membrane
CAGL0E00385g	Mitochondrial membrane	Mitochondrial membrane
CAGL0E03982g	Vacuolar membrane	Plasma membrane
CAGL0C03289g	Vacuolar membrane	Plasma membrane
CAGL0E03355g	Vacuolar membrane	Plasma membrane
CAGL0L06402g	Vacuolar membrane	Plasma membrane
CAGL0G00242g	Vacuolar membrane	Plasma membrane
CAGL0D00352g	Peroxisomal membrane	Mitochondrial membrane
CAGL0M02387g	Peroxisomal membrane	Nucleus
CAGL0G08041g	Nucleus	Plasma membrane
CAGL0C02343g	Cytoplasm	Mitochondria
CAGL0D03674g	Cytoplasm	Nucleus
CAGL0K10472g	Cytoplasm	Nucleus
CAGL0B03487g	Cytoplasm	Cytoplasm
CAGL0I08019g	Nucleus	Plasma membrane
CAGL0M01760g	Plasma membrane	Plasma membrane
CAGL0I04862g	Plasma membrane	Plasma membrane
CAGL0F02717g	Plasma membrane	Plasma membrane
CAGL0M07293g	Plasma membrane	Plasma membrane
CAGL0F01419g	Plasma membrane	Plasma membrane
CAGL0L07744g	ER membrane	Plasma membrane
CAGL0G05093g	Mitochondria	Mitochondria

CAGL0K12474g	Cytoplasm	Cytoplasm

3.6 Confirmation of the presence of ABC transporter coding gene in the genome

The goal of the work was to unravel the role of membrane localized efflux pumps in development of MDR. Hence for expression analysis, only 18 potential membrane localized members of the ABC superfamily were selected. It is expected that expression level of genes may vary among strains with different genetic background and source of isolation. Therefore, in this study we evaluated the expression level of ABC transporter genes between the two strains of *C. glabrata*: a reference strain CBS138/ATCC2001 and a widely used clinical isolate BG2.

Initially, basal expression level of these ABC gene were performed under laboratory growth conditions. qRT-PCR analysis of the mid-log phage grown cells in YPD media at 30°C confirmed that all selected ABC transporter were transcribed under normal growth condition in both the strains. However, the degree of basal expression showed considerable variation in these strains. Since strain BG2 was an isolate from a patient with initial exposure to FLC treatment, expectedly, in comparison to CBS138/ATCC2001, its encoding transporter genes were upregulated at basal level (Fig. 3.7).

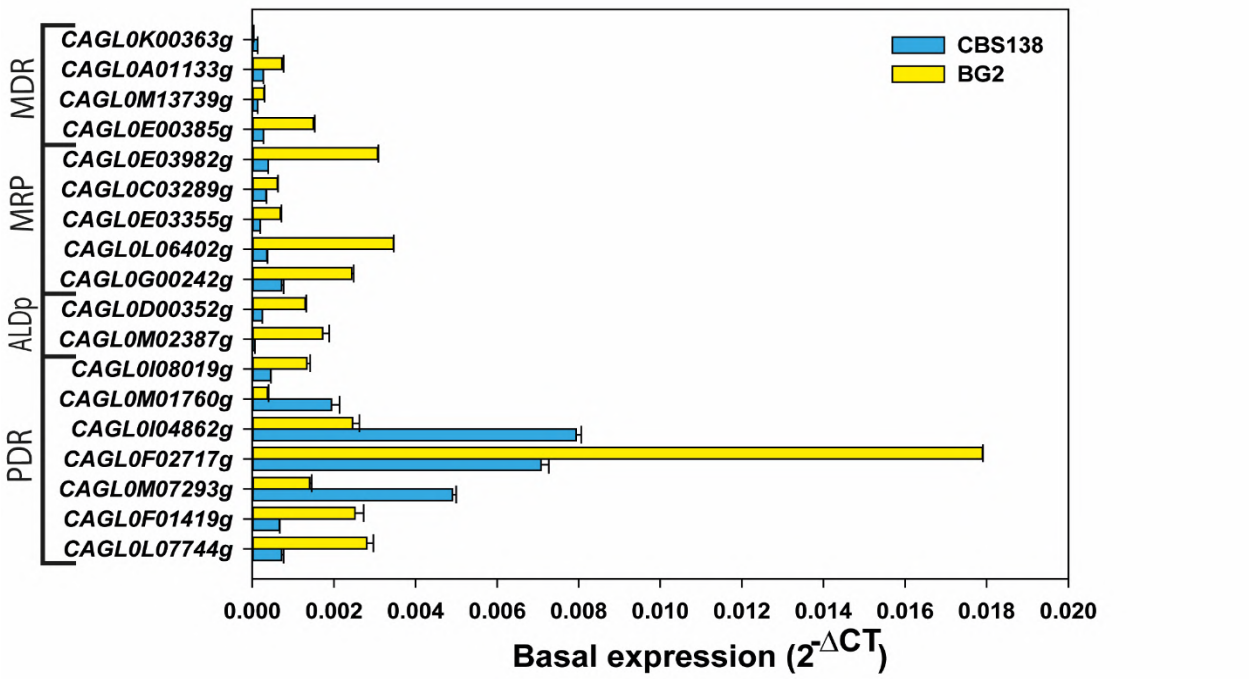

Fig 3.7 Comparative basal expression of ABC transporters in CBS138/ATCC2001 and BG2 strains. The basal level expressions of ABC transporters were tested by qRT-PCR in log phase grown cell under laboratory conditions (YPD, 30ºC) and data was measured in $2^{-\Delta CT}$ by normalizing with housekeeping gene *CgTDH3*. Among all ABC transporters *CAGL0K00363g* exhibited minimum expression level in both the strains.

3.7 Membrane localized ABC subfamily genes displayed variable response to drug exposure

Our long term goal is to unravel the role of membrane localized efflux pumps in development of MDR. Hence, for expression analysis, we selected 18 potential membrane localized members of the ABC superfamily. It is expected that expression level of genes may vary among strains with different genetic background and source of isolation. Therefore, after transient drug exposure, the ABC transporter genes of BG2 show lesser changes in their expression. But in CBS138/ATCC2001 strain, the transient drug induction yielded stronger response and comparatively showed higher changes in expression pattern of ABC genes in all tested condition (Fig 3.8).

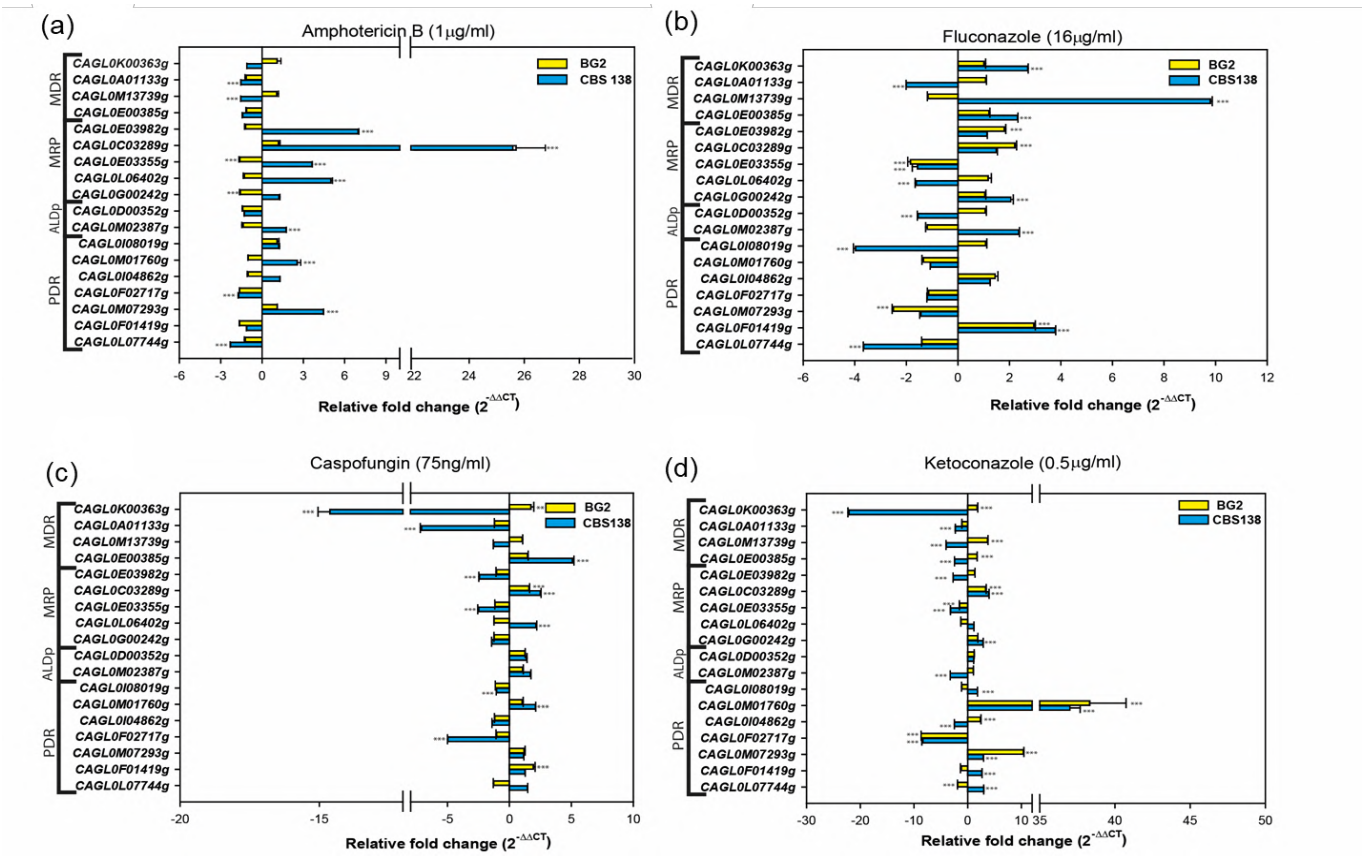

Fig 3.8. Comparative expression of ABC transporters encoding genes after transient drug exposure of CBS138/ATCC2001 and BG2 strains. The expression level was tested by qRT-PCR and data was measured by $2^{-\Delta\Delta CT}$ method in the presence of AmB (a), FLC (b), CSF (c), and KTC (d). Transporters behaved differently in these four conditions. Expression data were assessed by two-way ANOVA and statistical significant differences relative to untreated condition (YPD) were determined by Sidak's multiple comparisons test and are indicated as stars with p value <0.0001.

Frequently, enhanced expression of several ABC superfamily genes was directly linked to the acquisition of drug resistance among different yeast species. Earlier, several reports demonstrated that in clinical MDR isolates of *C. glabrata*, ABC transporters such as *CAGL0M01760g* (*CgCDR1*), *CAGL0I04862g* (*CgSNQ2*) and *CAGL0F02717g* (*CgPDH1*) were highly expressed and their expression varied in laboratory strains during transient drug induction and environmental conditions (Samaranayake et al. 2013; Vale-Silva et al. 2013a). For evaluating the role of ABC membrane proteins coding genes, we further tested expression of all selected ABC transporters followed by 60 min exposure to azoles (FLC and KTC), echinocandin (CSF) and polyene (AmB) drugs. The data obtained by qRT-PCR provided an interesting insight on to the expression pattern of ABC transporters under stress conditions. For instance, all the tested drugs exhibited differential expression pattern of membrane ABC superfamily genes, implying their role in the development of drug resistance phenotypes.

Among ABCB/MDR members, basal expression of *CAGL0K00363g* was lowest, in both the strains. Notably, *CAGL0K00363g* ortholog in *S. cerevisiae* (Sc*STE6*) is a dedicated pheromone transporter and its human homolog (*ABCB1*) mediated MDR in various chemotherapy resistant tumors by effluxing toxic compounds (Wu et al. 2008). Although *CAGL0K00363g* was 1.7 fold upregulated in presence of both CSF and KTC in BG2 strain, but in CBS138/ATCC2001 strain it was down regulated to 14.6 and 22.1 fold in presence these drugs. Most of the MDR genes in CBS138/ATCC2001 strain displayed down regulation following AmB, CSF, and KTC treatment but were up regulated in FLC exposed cells. Interestingly, in BG2 strain the expression level of other MDR members remained unchanged during FLC, AmB and CSF inductions except for *CAGL0E00385g* and *CAGL0M13739g* (*CgATM1*), wherein expression level was significantly higher followed by KTC exposure.

Among ABCC/MRP subfamily members, basal expression level of *CAGL0E03355g* was low in both the strains. *CAGL0G00242g* (*CgYOR1*) was upregulated by azoles in CBS138//ATCC2001, while, in BG2 strain the expression level was down regulated by 1.5 fold following AmB treatment. However, in case of KTC exposed cells, it was 1.8 fold upregulated. *CAGL0G00242g* (*CgYOR1*) ortholog in *S. cerevisiae* (Sc*YOR1*) has a well demonstrated role in pleiotropic drug resistance (Klein et al. 2011). *CAGL0C03289g* (*CgYBT1*) displayed higher expression following drug treatment in both strains. While, *CAGL0E03982g* transcript level was significantly upregulated only in FLC treated BG2 cells, whereas in CBS138/ATCC2001 strain, it was upregulated by AmB treatment only. *CAGL0E03355g* transcript level was significantly down regulated in both tested strains, followed by most of the inducing conditions. Notably, human MRP family member *ABCC1* is involved in multidrug resistance, especially during cancer and leukemia chemotherapy treatments (Slomka et al. 2015). However, its ortholog *CAGL0L06402g* (*CgYCF1*) in *C. glabrata* does not respond to the tested drug in BG2 strain but were significantly upregulated in the case of AmB and CSF exposed CBS138/ATCC2001 strain. Together, qRT-PCR analysis of MRP subfamily genes in *C. glabrata* similar to other yeast species do point to their involvement in drug detoxification.

Both ABCD/ALDp members exhibited significantly higher expression at the basal level in BG2 than in CBS138/ATCC2001. The expression level of ALDp members remained unresponsive to drug treatment in BG2. However, in CBS138/ATCC2001 strain, *CAGL0M02387g* was significantly down regulated in KTC and upregulated with other tested inducing conditions while *CAGL0D00352g* showed significant down regulation in FLC treatment.

Together, ABBCG/PDR subfamily member genes revealed constitutive expression, and they are the best responders to transient drug treatments. *CAGL0M01760g* (*CgCDR1*) and *CAGL0F02717g* (*CgPDH1*) have similar behavior with KTC treatment in both the strains. The expression of *CAGL0M07293g,* an ortholog of *S. cerevisiae PDR12* (weak acid transporter) was higher following KTC treatment in both the strains. The low level of expression of *CAGL0M07293g* in FLC resistant isolates of *C. glabrata* was earlier recorded by Vermitsky *et. al.* (Vermitsky et al. 2006b), which could be consistent with the low expression in BG2 strain. In BG2 strain *CAGL0M07293g* gene behaved differently in

different azoles, where an imidazole and a triazole yielded opposite response. *CAGL0F02717g* (*CgPDH1*) was down regulated in most of the treatment condition in both the strain. Based on homology with *CaCDR1* and *CaCDR2*, it is reasonable to expect that *CAGL0F02717g* (*CgPDH1*) could be involved in phospholipid translocation and membrane lipid asymmetry maintenance (Smriti et al. 2002). As expected, FLC treatment induced *CAGL0F01419g* (*CgAUS1*) expression in both the strains. ABCG/PDR members displayed varying degree of changes in expression, which strongly indicate their role in multi drug resistance.

3.8 Discussion and Conclusion

The presented study is the first comprehensive transportome analysis of ABC proteins in *C. glabrata*, which led to the identification of 25 ABC proteins, representing 0.479% of protein coding genes, distributed on 11 out of 13 chromosomes. The phylogenetic comparison with other fungal species clustered these ABC members into six major subfamilies: MDR/ABCB, MRP/ABCC, ALD/ABCD, RLI/ABCE, EF3/ABCF and PDR/ABCG. The constitutive expression of all the genes encoding putative membrane localized ABC members not only confirmed their genomic presence but also reflected their biological relevance. The exposure to drugs presented variable transcriptional response among ABC membrane proteins, nonetheless, it provided sufficient clue for their potential contribution in emerging clinical drug resistance in *C. glabrata* isolates. Of note, majority of members of subfamilies remain unexplored. The sequence identity of *C. glabrata* ABC proteins with other organism could provide a basis for functional characterization of these unexplored important proteins; however, our analysis could only predict their localization and expression profile. On the basis of their similarities with ABC proteins of S. cerevisiae and *C. glabrata* the predicted function of the ABC transporter is listed in (Table 3.4).

Table 3.4: Predicted function of ABC transporters in *C. glabrata*

ABC transporter genes	ABC transporter common names	Description	Function/Putative Function
CAGL0K00363g	CgSte6p	Uncharacterized	Role in oligopeptide transport.
CAGL0A01133g	CgMdl2p	Uncharacterized	role in cellular response to hydrogen peroxide .
CAGL0M13739g	CgAtm1p	Uncharacterized	Role in cellular iron ion homeostasis and osmoregulation
CAGL0E00385g	CgMdl1p	Uncharacterized	Role in oligopeptide export from mitochondria.
CAGL0E03982g	CgVmr1p	Uncharacterized	Role in drug transport and response to metal ion.
CAGL0C03289g	CgYbt1p	Uncharacterized	Role in bile acid transport. Gene is upregulated in azole-resistant strain.
CAGL0E03355g	CgBpt1p	Uncharacterized	Role in bilirubin and glutathione S- conjugate transport.
CAGL0L06402g	CgYcf1p	Uncharacterized	Role cadmium, bilirubin and glutathione S-conjugate transport.
CAGL0G00242g	CgYor1p	Uncharacterized	Involved in multidrug resistance, gene is upregulated in azole-resistant strain.
CAGL0D00352g	CgPxa2p	Uncharacterized	Role in fatty acid transport.
CAGL0M02387g	CgPxa1p	Uncharacterized	Role in fatty acid transport
CAGL0I08019g	CgRoa1p	Uncharacterized	Role in drug transport

CAGL0M01760g	CgCdr1p	Characterized	Involved in resistance to azoles regulated by TF CgPdr1p. Overexpressed in azole resistant strains and petite strains.
CAGL0I04862g	CgSnq2p	Characterized	Role in multidrug resistance and TF CgPdr1pmediated azole resistance.
CAGL0F02717g	CgPdh1p	Characterized	Role in azole resistance, regulated by TF CgPdr1p. Overexpressed in azole resistant clinical isolate.
CAGL0M07293g	CgPdr12	Uncharacterized	Putative ABC transporter of weak organic acids; gene is downregulated in azole-resistant strain
CAGL0F01419g	CgAus1p	Characterized	Role in exogenous sterol uptake and virulence
CAGL0L07744g	Cgadp1p	Uncharacterized	unknown

Based on the information available in *S. cerevisiae* and other yeasts, most of the ABC transporter genes are non-essential and hence construction of homozygous knockouts (KOs) should be realtively easy. The analysis of KOs of each member is a way forward in dissecting their role in MDR, pathogenicity and virulence. The studies so far do suggest that some of the ABC members, particularly those belonging to PDR family (*CgCDR1*, *CgPDH1* and *CgSNQ2*) have demonstrable role in developing drug resistance but considering the vast information about the role of ABC members in *C. albicans* and in other organisms, it is a long way before their physiological relevance of these ABC proteins could be unraveled.

CHAPTER II

4. Construction of ABC transporter disruptome

4.1 Deletent library and their phenotypic characterization

4.1.1 Background

Clinical isolates of *C. glabrata* have high innate resistance towards azoles and can acquire cross-resistance to various subgroups of antimycotic drugs. Overexpression of ABC transporters is one of the most frequent known mechanisms for the acquisition of multiple drug resistance (MDR). There are 25 ABC proteins in the genome of *C. glabrata,* and based on the topology, only 18 proteins are ABC transporters, and the remaining seven are soluble ABC proteins. As discussed in the previous chapter, their transcription responses with transient exposure with different antifungals prompted to explore the contribution of these ABC transporters in the development of drug resistance and for any physiological relevance.

The functional characterization of a gene in yeast can be performed either by gene knockout, gene silencing, or by gene overexpression. Gene silencing is only present in some yeast, including fission yeast *S. pombe* and in some budding yeast. These transcription silencing related genes have lost from *S. cerevisiae* genome during the course of evolution (Drinnenberg et al. 2009). Since *C. glabrata* is phylogenetically closer to *S. cerevisiae* than other pathogenic yeast of *Candida* genus, there might be a possibility of the absence of this pathway in its genome. With this background, the present ABC gene characterization in *C. glabrata* is explored by two methods: gene deletion and gene overexpression.

4.1.2 Construction of Knockout library

Two strains BG2 and BG14 strain were used to as wild type (WT) strain for the construction of ABC transporter K/O. Strain BG14 is the *ura3* auxotroph of BG2, so wherever more than single deletion was required, BG14 strain was used as WT. Fusion PCR based method utilizing intrinsic homologous recombination capacity of the *C. glabrata* cells was used to delete the ABC transporter genes. Dominant selection marker *NAT1* with FRT sites was used to delete each of the coding sequences of the gene. The

method of cassette construction, their integration in the genome to replace the open reading frame (ORF) is represented in Fig 4.1.

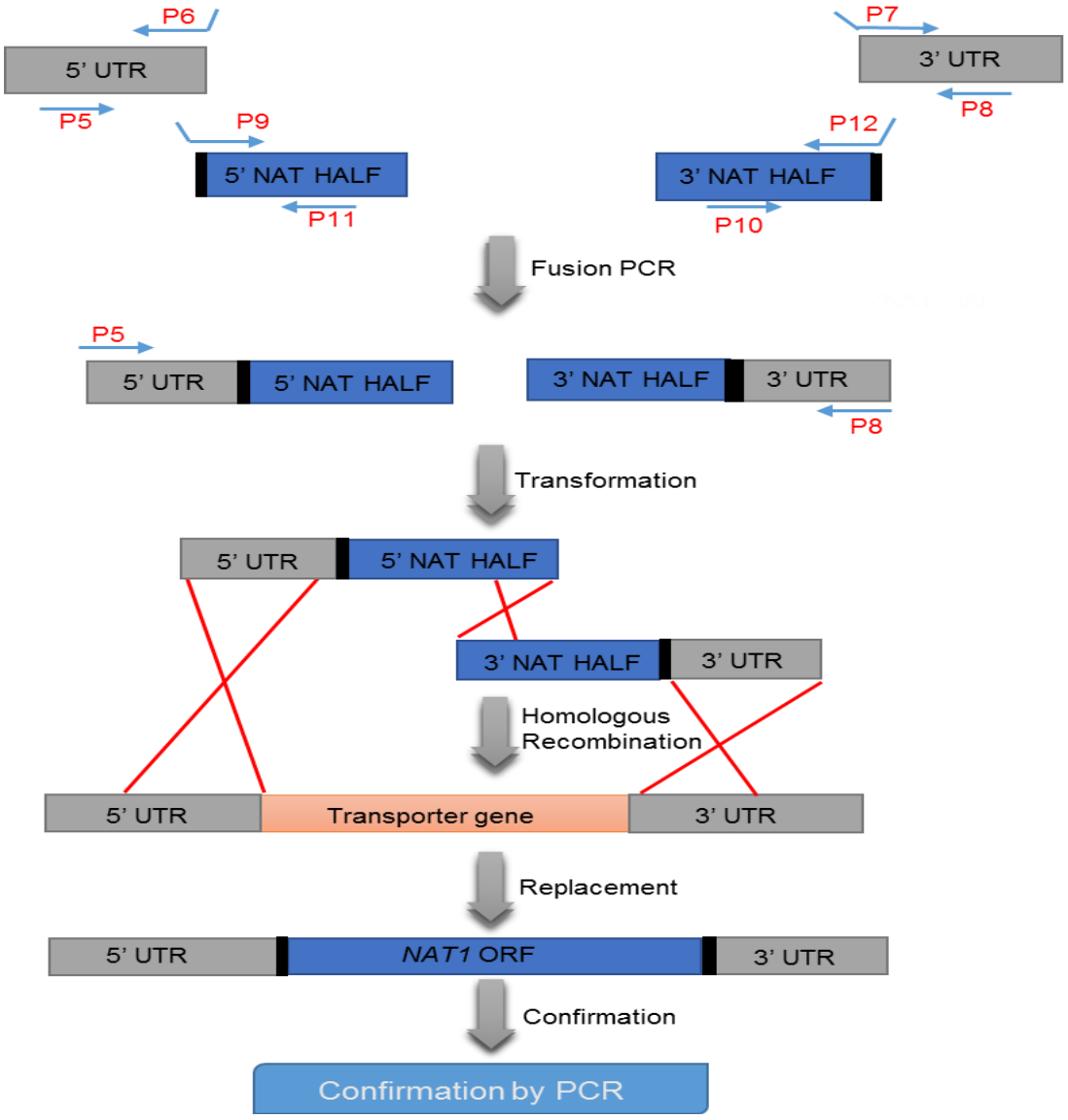

Fig 4.1: Strategy for gene deletion in *C. glabrata*: Knockout generation in C. glabrata includes three step. In the first step, PCR amplification of UTRs and NAT- half and their fusion takes place. Second step include the transformation of these fusion product in the WT cells and require three homologous recombination to occur for proper integration of the cassette. The final step involves the confirmation of the gene deletion by genomic DNA PCR.

Replacement of the ORF with deletion cassette was confirmed by PCR. Four sets of primers were used in the confirmation illustrated in Fig 4.2. The first set of primers (P1 and P2) is to confirm the proper integration of 5' NAT half with 5' UTR. The second set of primers used to check proper integration of 3' UTR-3' NAT half. The third set of primers was from the internal region of the deleted ORF. The fourth set of primers was to assess full cassette amplification.

By utilizing the mentioned startegy, viable single deletions of each of 18 transporters were performed. The deletion confirmations of all ABC transporters are demonstrated in Table 4.1.

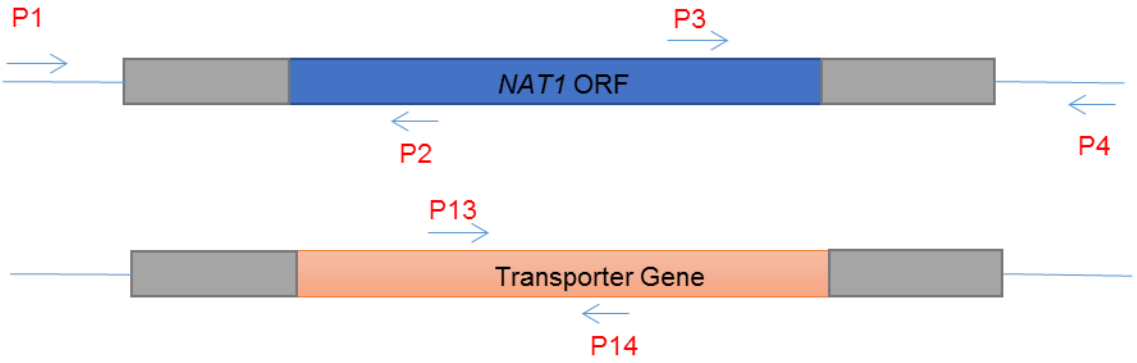

PCR type	Primers	Purpose	WT	K/O
5'- check	P1 and P2	Integration of 5'UTR +5' NAT half	-	+
3'- Check	P3 and P4	Integration of 3'UTR + 3'NAT half	-	+
Full gene - check	P1 and P4	Full cassette integration at the same site	-	+
Internal – check	P13 and P14	Absence of ORF	+	-

Fig 4.2: Gene deletion confirmation: Confirmation of the gene knockout was performed at four levels by using genomic DNA PCR

Table 4.1: Deletion and confirmation of *C. glabrata* ABC transporters genes

S. N.	Deletions	Deletion confirmation	Band Size (Bp)*
1	*Cgcdr1*Δ	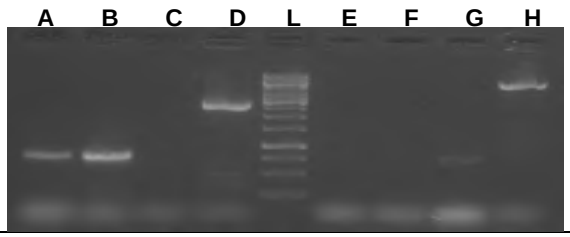	A – 767 E- N/A B – 779 F- N/A C - N/A G- 697 -2575 H- 5775
2	*Cgsnq2*Δ	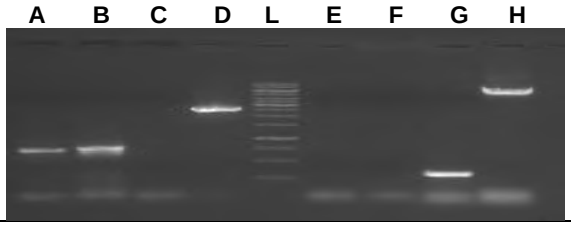	A – 684 E- N/A B – 783 F- N/A C- N/a G- 321 D-2460 H- 5684
3	*Cgpdh1*Δ	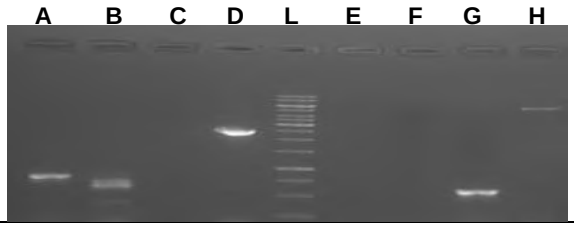	A – 734 E- N/A B – 617 F- N/A C- N/a G- 534 D-2380 H- 5709
4	*Cgaus1*Δ	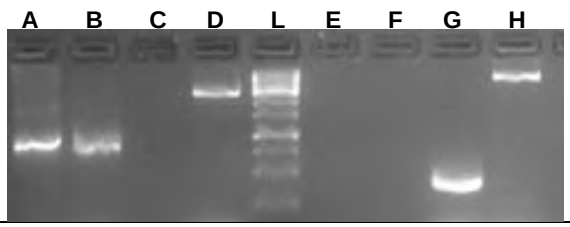	A – 826 E- N/A B – 779 F- N/A C- N/A G- 391 D-2734 H- 5684
5	*Cgroa1*Δ	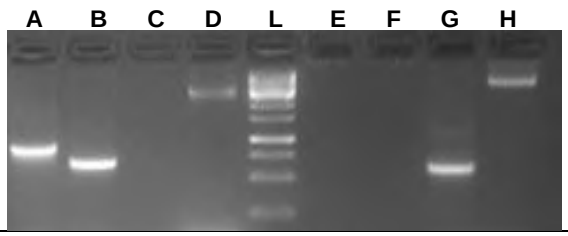	A – 867 E- N/A B – 676 F- N/A C- N/a G- 598 D-3067 H- 6063

6	*Cgpdr12*Δ	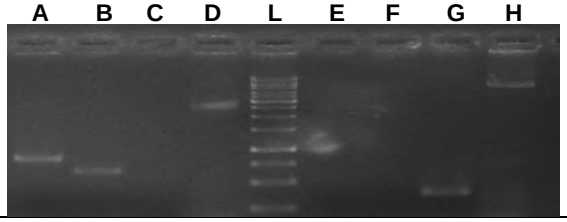	A – 770 E- N/A B – 679 F- N/A C- N/A G- 397 D-2564 H- 5069
7	*Cgadp1*Δ	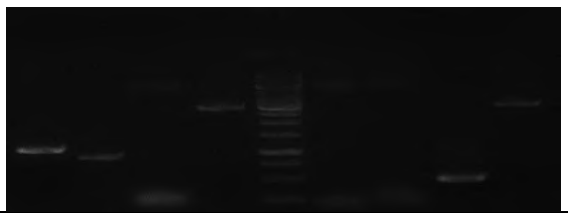	A – 1021 E- N/A B – 899 F- N/A C- N/A G- 521 D-3046 H- 3284
8	*Cgyor1*Δ	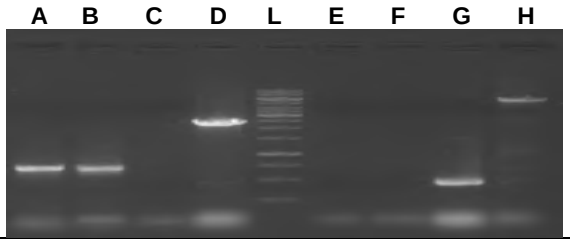	A – 730 E- N/A B – 738 F- N/A C- N/A G- 477 D-2507 H- 5641
9	*Cgycf1*Δ	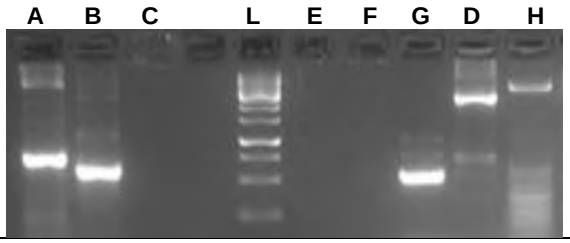	A – 904 E- N/A B – 773 F- N/A C- N/A G- 359 D-2607 H- 5987
10	*Cgybt1*Δ	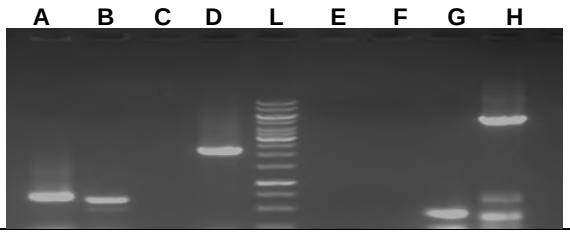	A – 865 E- N/A B – 773 F- N/A C- N/A G- 452 D-2444 H- 6091
11	*Cgvmr1*Δ	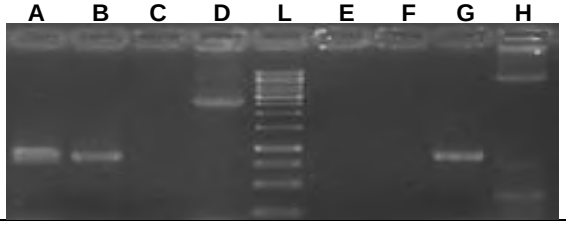	A – 768 E – N/A B – 763 F – N/A C – N/A G – 321 D–2660 H–5984
12	*Cgbpt1*Δ	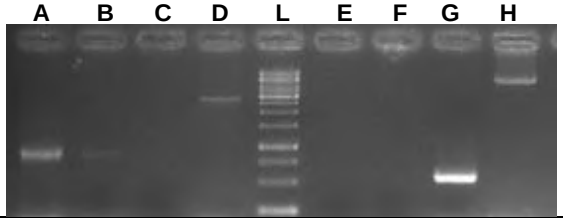	A – 899 E – N/A B – 873 F – N/A C – N/A G – 608 D–2678 H–6064

13	*Cgatm1*Δ	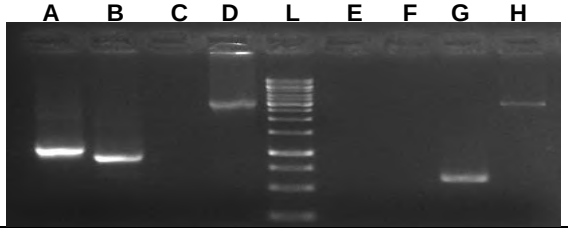	A – 1031 E- N/A B – 893 F- N/A C - N/A G- 658 D-2697 H- 3151
14	*Cgmdl1*Δ	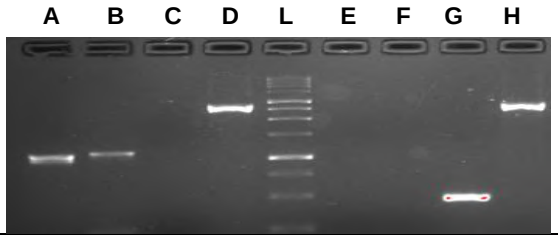	A – 997 E- N/A B – 898 F- N/A C - N/A G- 569 D-2903 H- 3709
15	*Cgmdl2*Δ	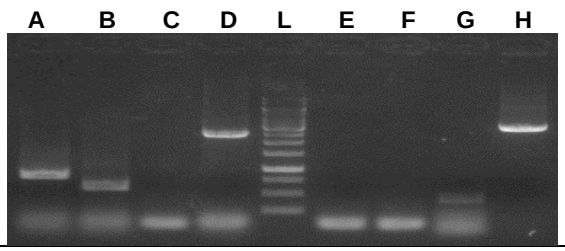	A – 984 E- N/A B – 643 F- N/A C - N/A G- 321 D -2760 H- 3275
16	*Cgste6*Δ	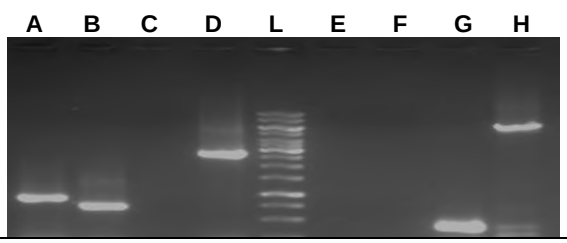	A – 989 E- N/A B – 873 F- N/A C- N/A G- 321 D-2677 H- 5061
17	*Cgpxa1*Δ	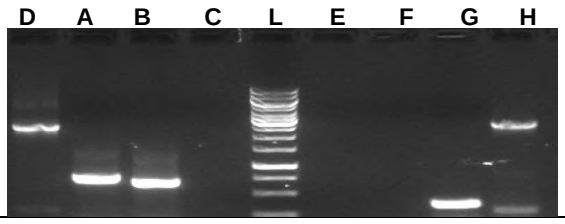	A – 787 E- N/A B – 700 F- N/A C- N/A G- 345 D-3019 H- 3268
18	*Cgpxa2*Δ	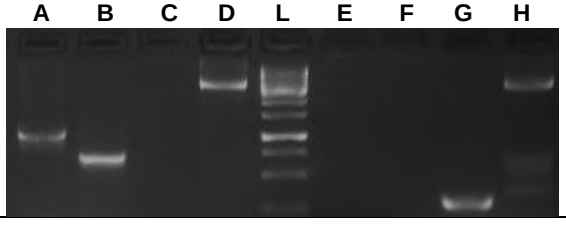	A – 1004 E- N/A B – 680 F- N/A C- N/A G- 301 D-3060 H- 3284

***** A: 5' integration check in K/O, B: 3' integration check in K/O, C: Internal check in K/O, D: Full gene Check in K/O, L: 1 Kb Ladder, E: 5' integration check in WT, G: 3' integration check in WT, G: Internal check in WT and H: Full gene check in WT.

4.1.3 Construction of complemented strains

Working with *C. glabrata* has a benefit that it can retain plasmid. So for complementation studies we have taken advantage of *C. glabrata* CEN/ARS based expression plasmid pPGRB2.3. This plasmid contains *Ura3* selection maker as yeast selection maker. Our ABC mutants are both in the BG2 and BG14 strains. BG2 is WT strain that contain no *Ura3* auxotrophy so it this plasmid cannot be used with the strain. We have modified this plasmid by replacing its *Ura3* maker with *HphB* marker that cause resistance to hygromycin B resistance (pGRB2.3_HphB). The replacement of the marker is performed by utilizing gibson assembly, represented in Fig 4.3.

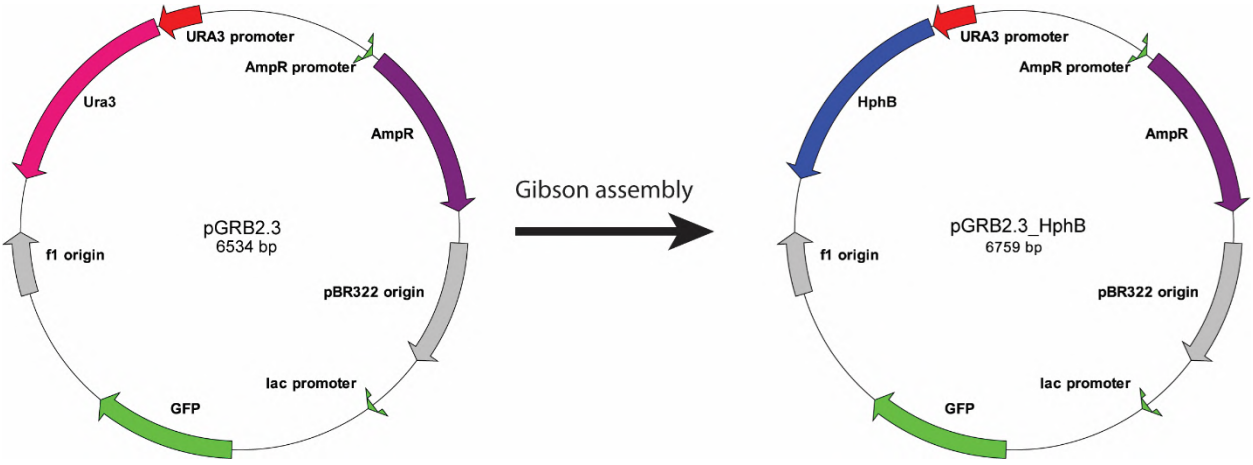

Fig 4.3: Construction of pGRB2.3_HphB. The plasmid was then used as the parent plasmid for further cloning and expression.

For complementation studies *C. glabrata* ORFs were PCR amplified along with their promoter sequences from wild-type genomic DNA using Phusion high-fidelity DNA polymerase. These amplified products were then cloned up-stream of the GFP by employing gibson assembly. The confirmation of the plasmids after gene cloning was performed by restriction digestion and PCR. The method of construction is illustrated in Fig 4.4. By employing this all complementation constructs were constructed (plasmids listed in supplementary File 3) and the strains constructed are listed as supplementary File 2. The complemented strains are employed with the mutants showing altered phenotype than WT.

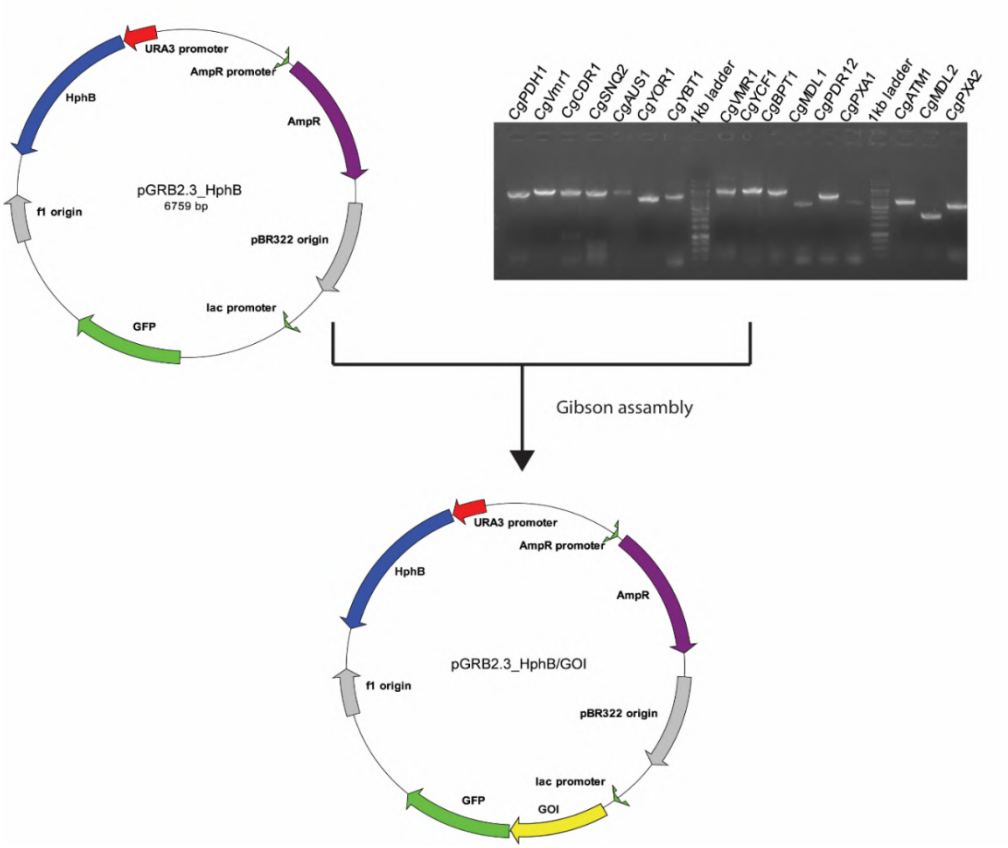

Fig 4.4: Construction of plasmids by gibson assembly for *C. glabrata* complementation studies.

4.1.4 Growth phenotypes of K/O mutants

The impact of gene deletions on *C. glabrata* was assessed to rule out any impact on its growth that could influence the efficiency to replicate within the host cell or against drug-treated conditions. For this, the growth curve assay of each deletant was monitored at 30°C in YPD by a micro-cultivation method using a 96-well plate in a liquid handling system (Tecan, Austria). Briefly, overnight grown cells were inoculated at a dilution of 0.1 OD_{600} in a 96-well plate and then allowed to grow at 30 °C. OD_{600} was measured every 30 min for an interval to up to 24 h. Doubling times of strain were calculated by measuring the time taken in doubling of logarithms values of the OD_{600} of the exponential phase. The doubling time of the mutants is listed in Table 4.2.

ABCG/PDR subfamily transporters, ABCC/MRP subfamily transporters, ABCD/ALDp subfamily transporters show similar growth as of WT with doubling time (~60 min).

However, an ABCB/MDR subfamily transporters *Cgatm1*Δ showed reduced growth in YPD with doubling time 80 min. Growth profiles of the mutants are illustrated in Fig 4.5.

Table 4.2: Doubling time of all ABC transporter mutants

S. N.	Strains	Subfamily	Doubling Time ± SD (in min)
1	WT (BG2)		60.23 ± 0.45
2	*Cgcdr1*Δ	PDR	60.35 ± 0.96
3	*Cgsnq2*Δ		60.54 ± 0.67
4	*Cgpdh1*Δ		60.29 ± 0.19
5	*Cgaus1*Δ		60.69 ± 0.64
6	*Cgroa1*Δ		61.45 ± 1.09
7	*Cgpdr12*Δ		61.09 ± 0.99
8	*Cgadp1*Δ		60.34 ± 0.76
9	*Cgatm1*Δ	MDR	80.02 ± 0.28
10	*Cgmdl1*Δ		60.98 ± 0.94
11	*Cgmdl2*Δ		60.45 ± 0.67
12	*Cgste6*Δ		61.98 ± 0.97
13	*Cgyor1*Δ	MRP	60.45 ± 0.70
14	*Cgycf1*Δ		61.34 ± 0.87
15	*Cgybt1*Δ		60.37 ± 0.82
16	*Cgvmr1*Δ		60.56 ± 0.19
17	*Cgbpt1*Δ		61.98 ± 0.54
18	*Cgpxa1*Δ	ALDp	60.50 ± 0.85
19	*Cgpxa2*Δ		61.06 ± 0.93

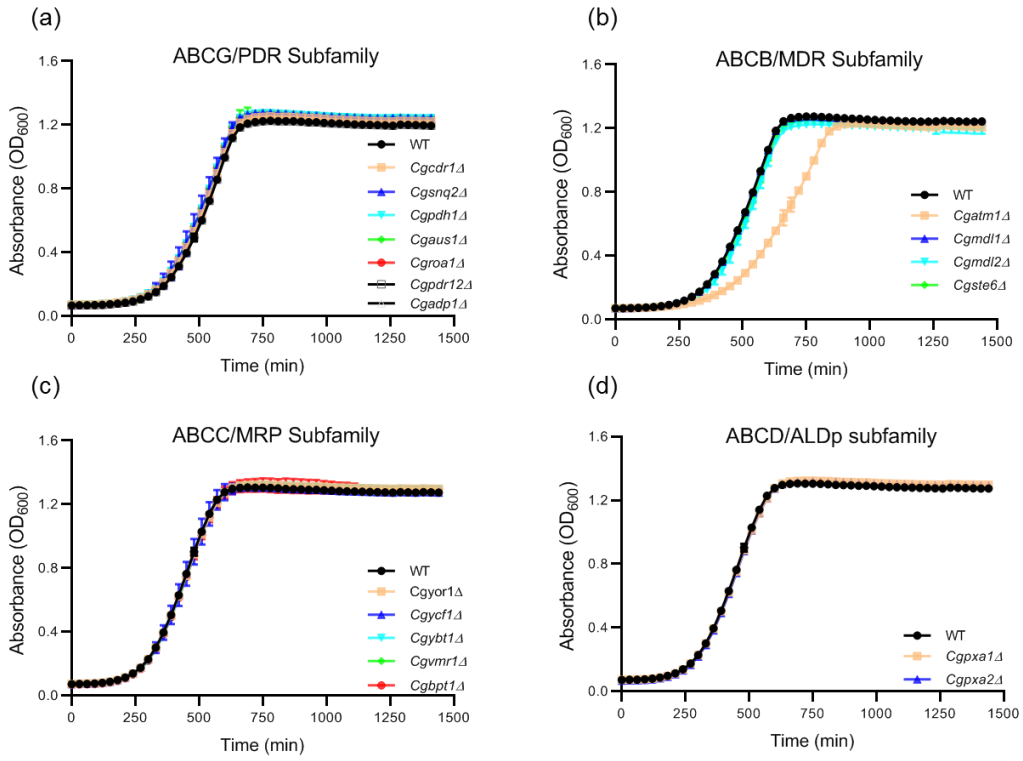

Fig 4.5: Growth curves of all 18 ABC transporter mutants: (a) ABCB/MDR transporters (b) ABCC/MRP transporters (c) ABCD/ALDp transporters (d) ABCG/PDR transporters growth curves. Only *Cgatm1*Δ, ABCB/MDR subfamily transporter, showed reduced growth in laboratory growth condition.

4.1.5 Drug susceptibility of knockouts

ABC transporters are generally considered as drug efflux pumps. In chapter 1, Fig 3.8, the observed upregulation of almost every transporter encoding gene following brief exposure of *C. glabrata* cells to different drugs also supported the notion. The availability of 18 single deletion of each transporter provided an opportunity to explore their role as drug transporters. For this, all the transporter mutants were subjected for susceptibility tests by exposing mutant cells to numerous drugs and antifungals that included azoles (FLC, KTC, VCR, ITZ and MCZ), echinocandins (CSF), polyene (AmB), allylamine (TER), protein synthesis inhibitors (ANY and CHX), and mutagen (4-NQO). The drug susceptibility was measured by broth micro-dilution assays, as described earlier (Shah et al. 2017). The MIC_{80} was defined at the lowest concentration inhibiting growth by at least 80% relative to the drug-free YPD control after incubation (Table 4.3). The

growth curves analysis of these mutants was also performed by using micro-cultivation method in 96- well plates. The following are the results described in subfamily wise.

Table 4.3: MIC_{80} of all ABC transporter mutant strains.

Deletion	MIC80										
	FLC	**KTC**	**ITZ**	**MCZ**	**VRC**	**4-NQO**	**AmB**	**ANY**	**CSF**	**TER**	**CHX**
WT (BG2)	16	0.5	8	0.062	4	4	1	0.6	0.075	16	2
ABCG/PDR Subfamily mutants											
*Cgcdr1*Δ	1	0.015	0.125	0.003	0.125	4	1	0.018	0.075	0.5	0.062
Cgsnq2Δ	16	0.5	8	0.062	4	0.5	1	0.6	0.075	16	2
*Cgpdh1*Δ	16	0.5	8	0.062	4	4	1	0.6	0.075	16	2
*Cgaus1*Δ	16	0.5	8	0.062	4	4	1	0.6	0.075	16	2
*Cgroa1*Δ	16	0.5	8	0.062	4	4	1	0.6	0.075	16	2
*Cgpdr12*Δ	16	0.5	8	0.062	4	4	1	0.6	0.075	16	2
*Cgadp1*Δ	16	0.5	8	0.062	4	4	1	0.6	0.075	16	2
ABCB/MDR Subfamily mutants											
*Cgatm1*Δ	4	0.125	1	0.015	2	4	1	0.3	0.018	16	2
*Cgmdl1*Δ	16	0.5	8	0.062	4	4	1	0.6	0.075	16	2
*Cgmdl2*Δ	16	0.5	8	0.062	4	4	1	0.6	0.075	16	2
*Cgste6*Δ	16	0.5	8	0.062	4	4	1	0.6	0.075	16	2
ABCC/MRP Subfamily mutants											
*Cgyor1*Δ	16	0.5	8	0.062	4	4	1	0.6	0.075	16	2
*Cgycf1*Δ	16	0.5	8	0.062	4	4	1	0.6	0.075	16	2
*Cgybt1*Δ	16	0.5	8	0.062	4	4	1	0.6	0.075	16	2
*Cgvmr1*Δ	16	0.5	8	0.062	4	4	1	0.6	0.075	16	2
*Cgbpt1*Δ	16	0.5	8	0.062	4	4	1	0.6	0.075	16	2
ABCD/ALDp Subfamily mutants											
*Cgpxa1*Δ	16	0.5	8	0.062	4	4	1	0.6	0.075	16	2
*Cgpxa2*Δ	16	0.5	8	0.062	4	4	1	0.6	0.075	16	2

4.1.5.1 PDR transporter mutants

Sufficient studies with ABCG/PDR transporters have implicated their role in drug resistance such as ScPdr5p in *S. cerevisiae,* CaCdr1p and CaCdr2p in *C. albicans* and CauCdr1p in *C. auris* (Miyazaki et al. 1998b; Sanglard et al. 1999a; Shukla et al. 2003; Torelli et al. 2008a; Rybak et al. 2019; Kim et al. 2019a). PDR subfamily transporters are considered as first line of defense against antifungals. In *C. glabrata* four of the members of these families have been implicated in drug transport. The transcription of these transporter genes is usually high in azole resistant clinical and petite isolates. Apart from conventional antifungals, ABCG/PDR members also efflux various unrelated xenobiotic compounds for example, CgSnq2p in *S. cerevisiae* and *C. glabrata* transports mutagen 4-NQO, and ScPdr15p confers resistance to chloramphenicol (Decottignies et al. 1995; Wolfger et al. 2004; Torelli et al. 2008a). Besides MIC_{80} determination, the susceptibility of all the deletents was also confirmed by performing spot and growth curve assays (Fig 4.6 and 4.7).

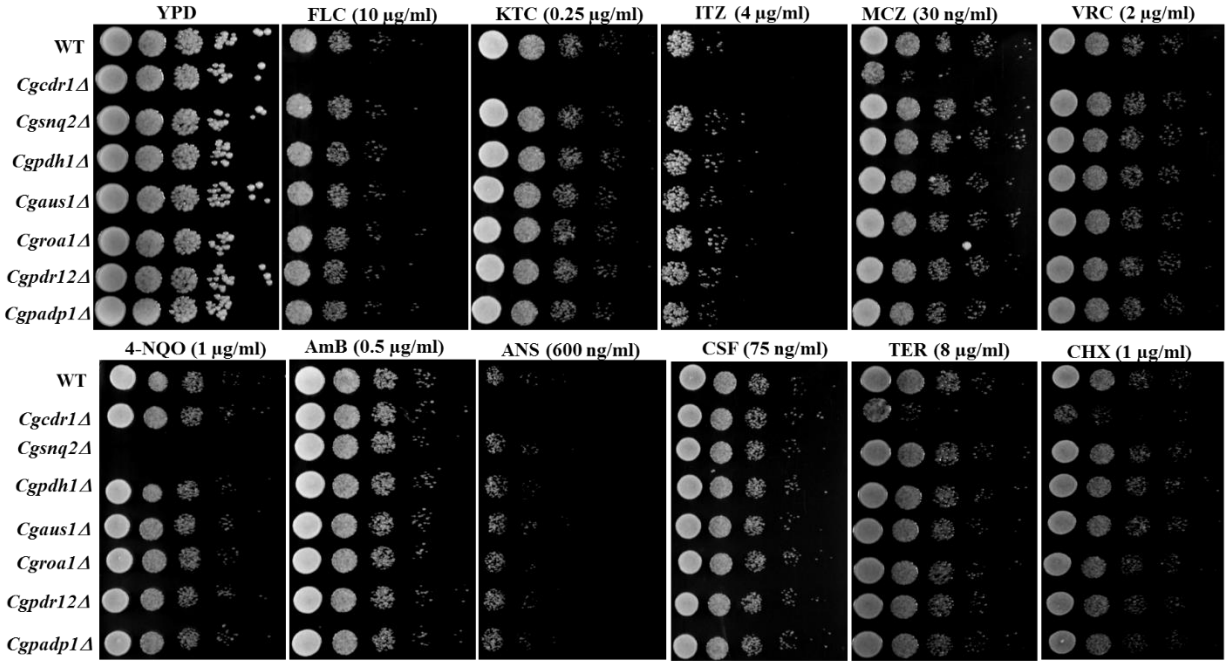

Fig 4.6: Spot assay of ABCG/PDR mutants in the presence of antifungal agents: *Cgcdr1*Δ mutant is sensitive to all tested azoles, protein synthesis inhibitors and allylamine. *Cgsnq2*Δ mutant shows sensitivity to mutagen 4-NQO.

The drug profiling of this subfamily mutant display susceptible phenotype of *Cgcdr1*Δ and *Cgsnq2*Δ towards tested antifungals. While *Cgcdr1*Δ mutant was susceptible to azoles, allylamine, protein synthesis inhibitors, *Cgsnq2*Δ mutant was only susceptible on its known substrate 4-NQO. Rest of the transpters' mutants were unresponsive to all the used antifungals. Additioanlly, the susceptibility of the transporters of this subfamily towards polyene and echinocandin remained unchanged upon their deletion. Although the role of CgPdh1p, CgAus1p and CgSnq2p is established in clinical azole resistance, however, the deletion of *Cgpdh1, Cgsnq2* and *Cgaus1* did not give any phenotype in the presence of azole antifungal agents. In the liquid growth curve analysis, the result obtained with spot assay and MIC_{80} are replicated (Fig 4.7).

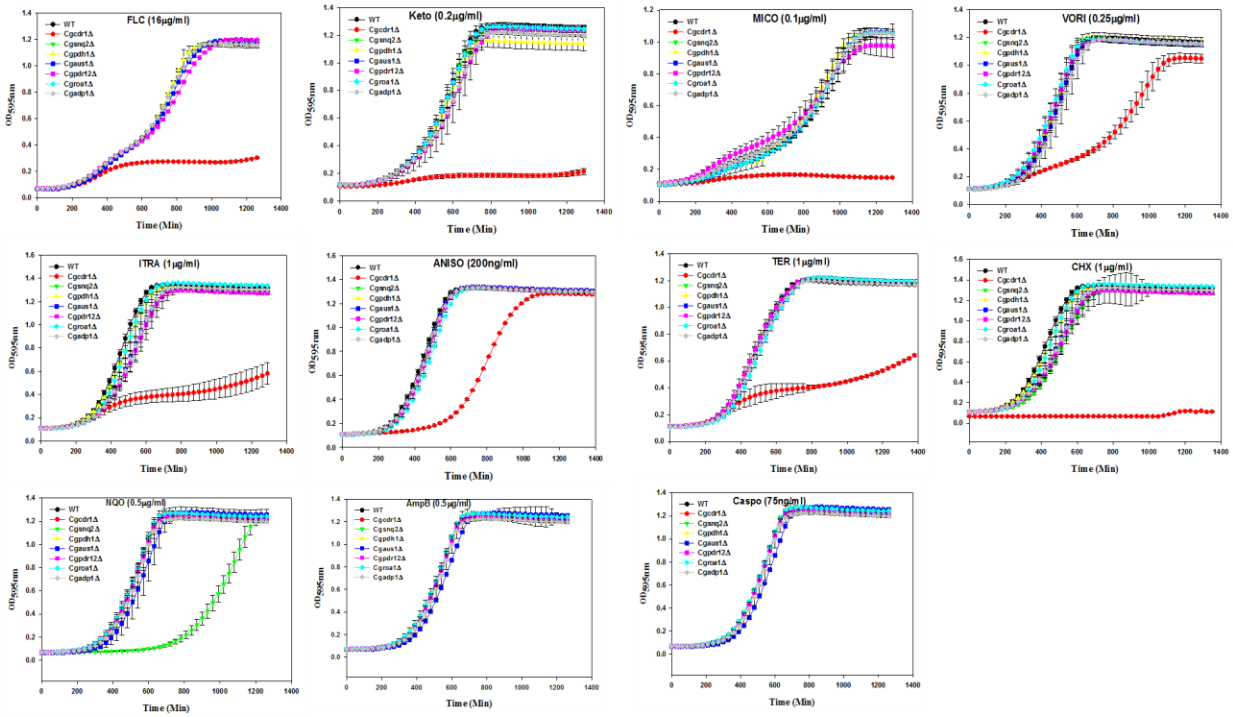

Fig 4.7: Growth curve of ABCG/PDR mutants in the presence of antifungal agents.

4.1.5.2 ABCB/MDR transporters

ABCB/MDR subfamily typically include both half and full transporters perform several functions. In human (Mdr1p) is a major transporter in extruding anti-cancerous drugs (Flanagan and Huber 2007). In yeast, these perform a-pheromone transport to peptide transports and also involved in the maintenance of iron homeostasis (Kuchler et al.

1989b; Berkower and Michaelis 1991, p. 6; Chloupková et al. 2004; Srinivasan et al. 2014, p. 1). The four mutants of ABCB/MDR subfamily transporters were screened for antifungals in both liquid media and solid plates with antifungal agents. MIC_{80} of the strains are listed in Table 4.3. The spot assay of these mutants also matched the MIC_{80} data as illustrated in Fig 4.8.

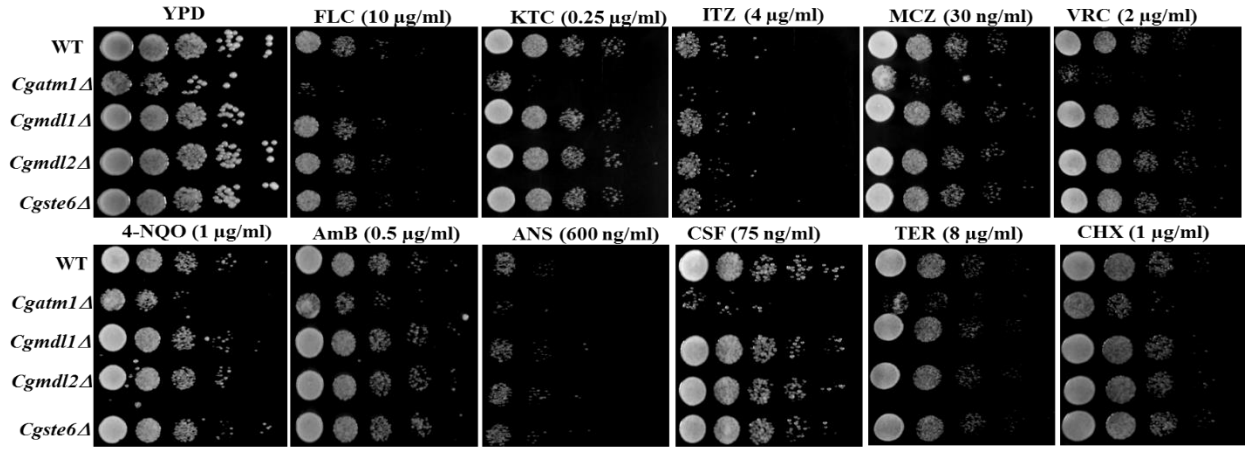

Fig 4.8: Susceptibility testing of ABCB/ MDR subfamily transporters in the presence of antifungals. *Cgatm1*Δ mutant was susceptible on azoles and echinocandin CSF.

In the presence of azoles, one of the ABCB/MDR mutant, *Cgatm1*Δ, an inner-mitochondrial localized transporter showed increased susceptiblity to azoles. Interestingly the mutant is also susceptible to echinocandin CSF. However, the other three mutant members of the subfamily showed no change in susceptibility towards tested drugs. Further analysis of mutants with growth curve corroborated the spot tests observations. (Fig 4.9).

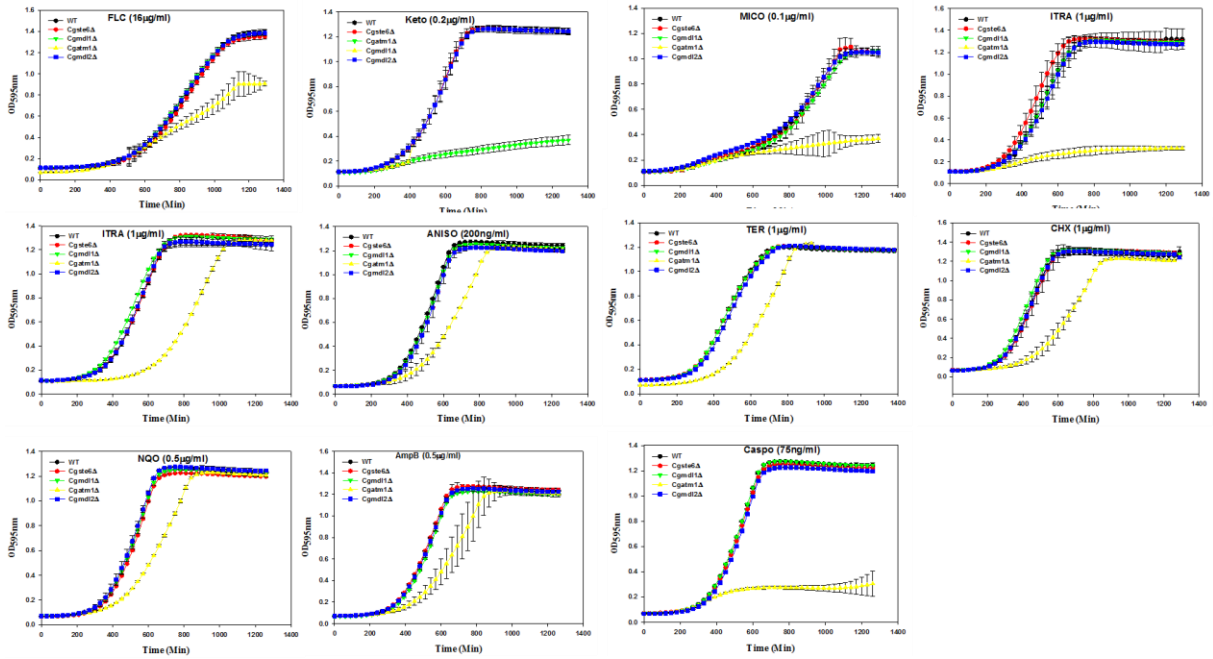

Fig 4.9: Growth curve analysis of all MDR subfamily mutants in the presence of antifungal agents.

4.1.5.3 ABCC/MRP transporters

ABCC/MRP subfamily transporters are known to efflux various kinds of xenobiotics, heavy metals, and metalloids. There are five members of this family transporter present in *C. glabrata*,however, the deletion of none of these members showed any change in either the MIC_{80} values or displayed in spot or growth assays (Table 4.3, Fig 4.10 and 4.11).

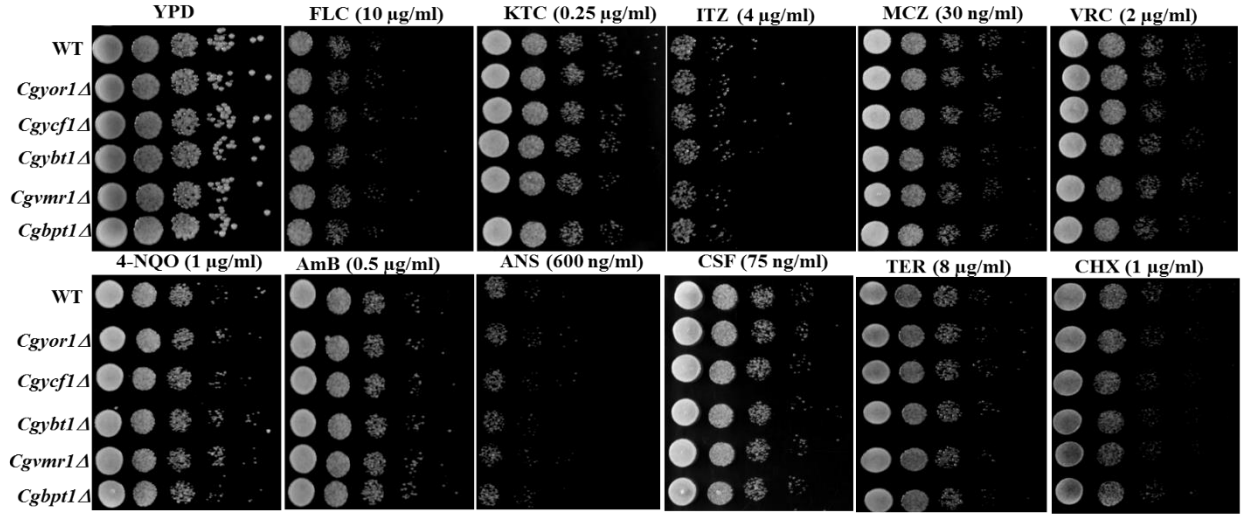

Fig 4.10: Spot assay of ABCC/MRP family transporters of *C. glabrata* on antifungals. None of the transporters displayed sensitivity to any tested conditions.

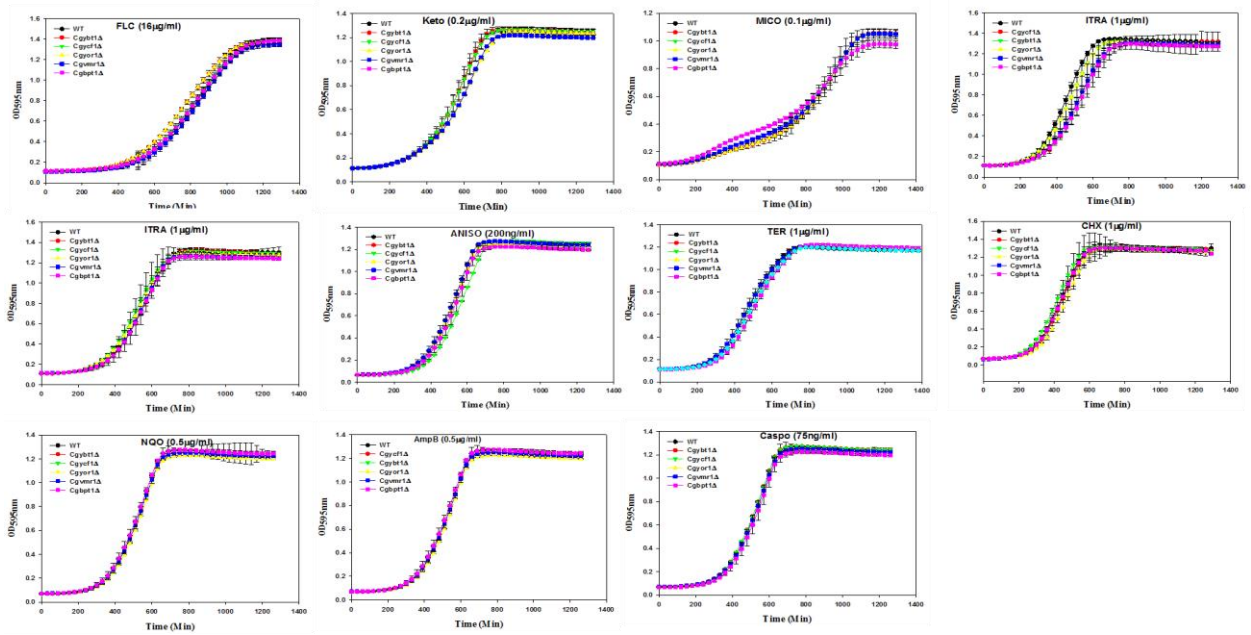

Fig 4.11: Growth curve of ABCC/MRP subfamily transporter mutant in the presence of antifungals.

4.1.5.4 ALDP transporters

The members of ALDP subfamily are peroxisomal membrane-localized transporters and are implicated in fatty acid transport and none so far in drug transport (Shani et al. 1995, p. 1; Chuang et al. 2014, p. 1). To better understand if ALDP members of *C. glabrata* have any role in drug resistance, drug susceptibility of these mutants on both liquid media and solid plate was performed. No change in MIC_{80}, or in spot or growth assays was recorded (Fig 4.12). Notably, the transient drug exposure of antifungal did induce the expression of these transporters as discussed in previous chapter (Fig 3.8).

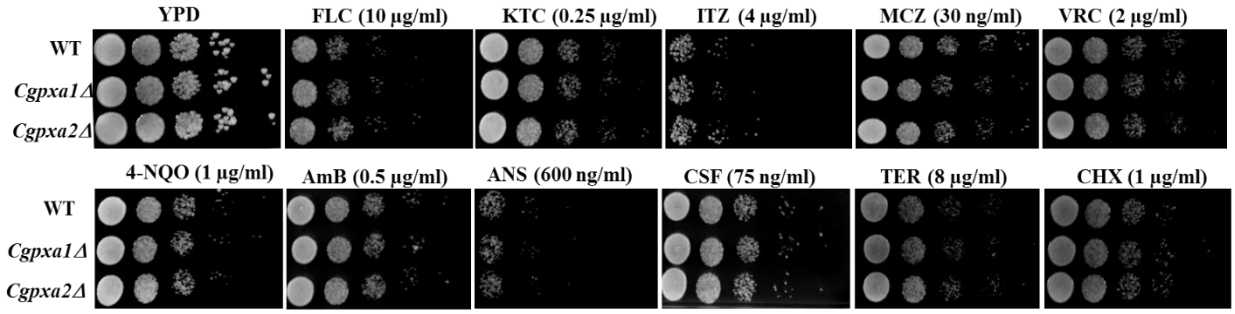

Fig 4.12: Spot assay of ABCD/ALDp mutants with antifungal agents: Spot assay performed in YPD supplemented with particular concentration of antifungal agents.

The growth curve analysis of these mutants also reflected the same effect. The growth curves of the ABCD/ALDp mutants on antifungal agents are represented in Fig 4.13.

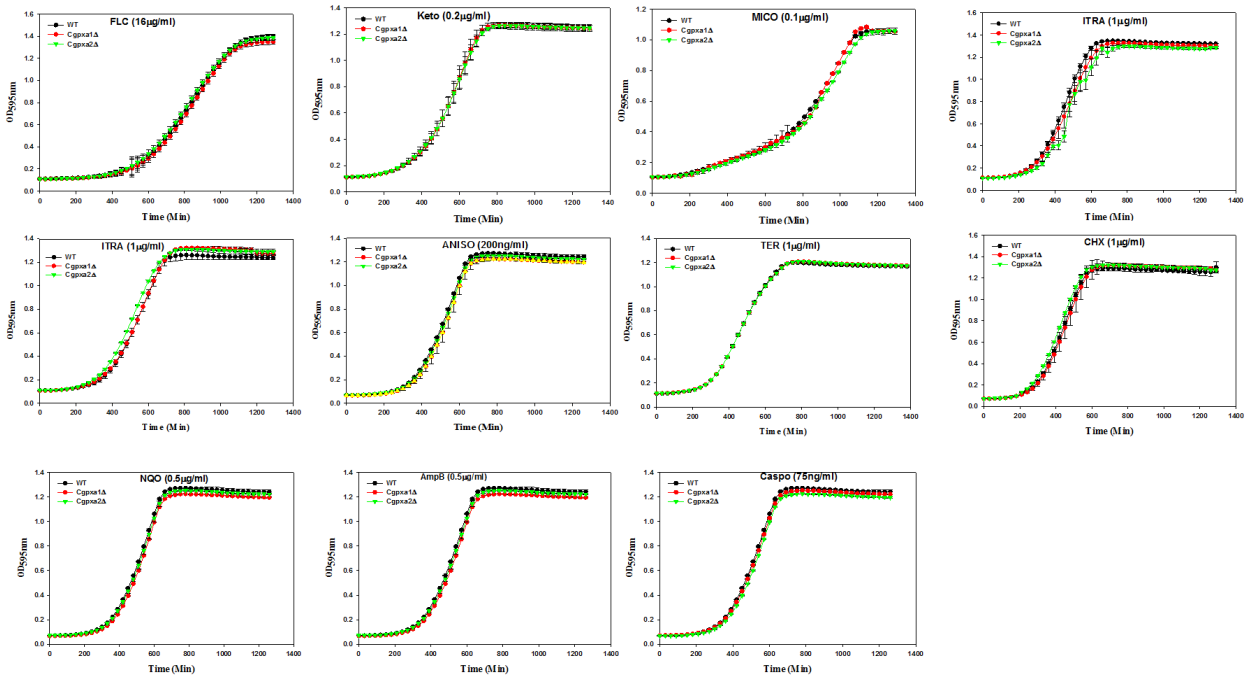

Fig: 4.13: Growth curves of ABCD/ALDp transporter mutants in the presence of antimycotics.

4.1.6 Reversal of phenotype by introducing WT copy of the gene

Only three mutants of ABC transporters displayed susceptible phenotypes on antifungal drugs. To know whether the deletion is responsible for the obtained phenotype, WT copy of the genes were introduced as described in Fig 4.3. After getting the correct transformants screening on antifungals were tested by using spot assay. The reversal of sensitivity on azoles was observed in case of *CgCDR1* revertant and *CgATM*1 revertant and similarly, reversal of 4-NQO and OP sensitivity was observed with *CgSNQ2* revertant (Fig 4.14).

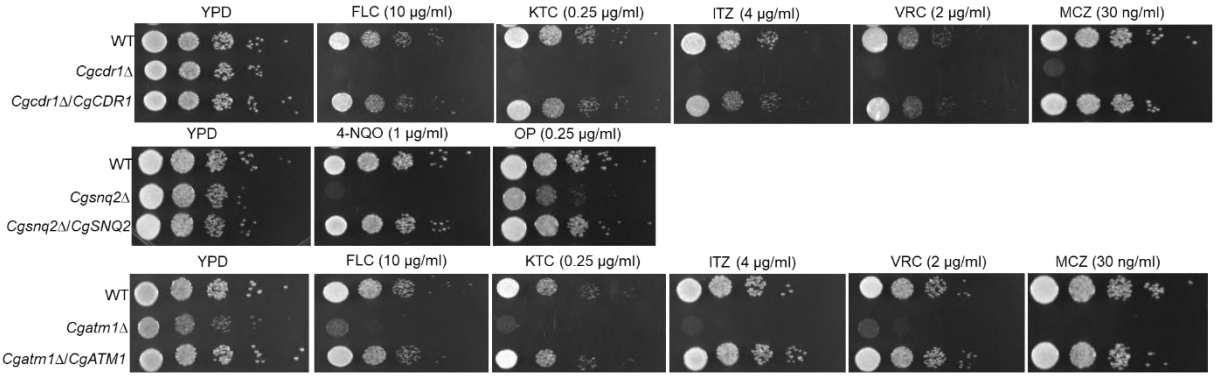

Fig 4.14: Phenotypes reversal after introducing WT copy of genes of the deletions: Introduction of WT copy of CgCDR1, CgSNQ2 and CgATM1 in their respective deletions reversed their deletion phenotypes.

4.1.7 Discussion and Summary

The genome of *C. glabrata* harbours 18 membrane localized ABC transporters. The deletion of each of the gene in haploid *C. glabrata* resulted in viable strains. All the mutants except *Cgatm1*, the growth was similar to the WT. In contrast, the mitochondrial membrane localized *Cgatm1* mutant growth was severely hampered which can be due to mitochondrial genome loss or unregulated iron homeostasis. Notwithstanding the transcriptional response of these ABC transporter genes in response to drug treatment, the deletion of most members did not impact drug susceptibility of these mutants. In the presence of antifungals, only a few transporters such as *Cgcdr1*, *Cgsnq2,* and *Cgatm1* mutants displayed influence on their growth. These results are summarized and depicted in Fig 4.15.

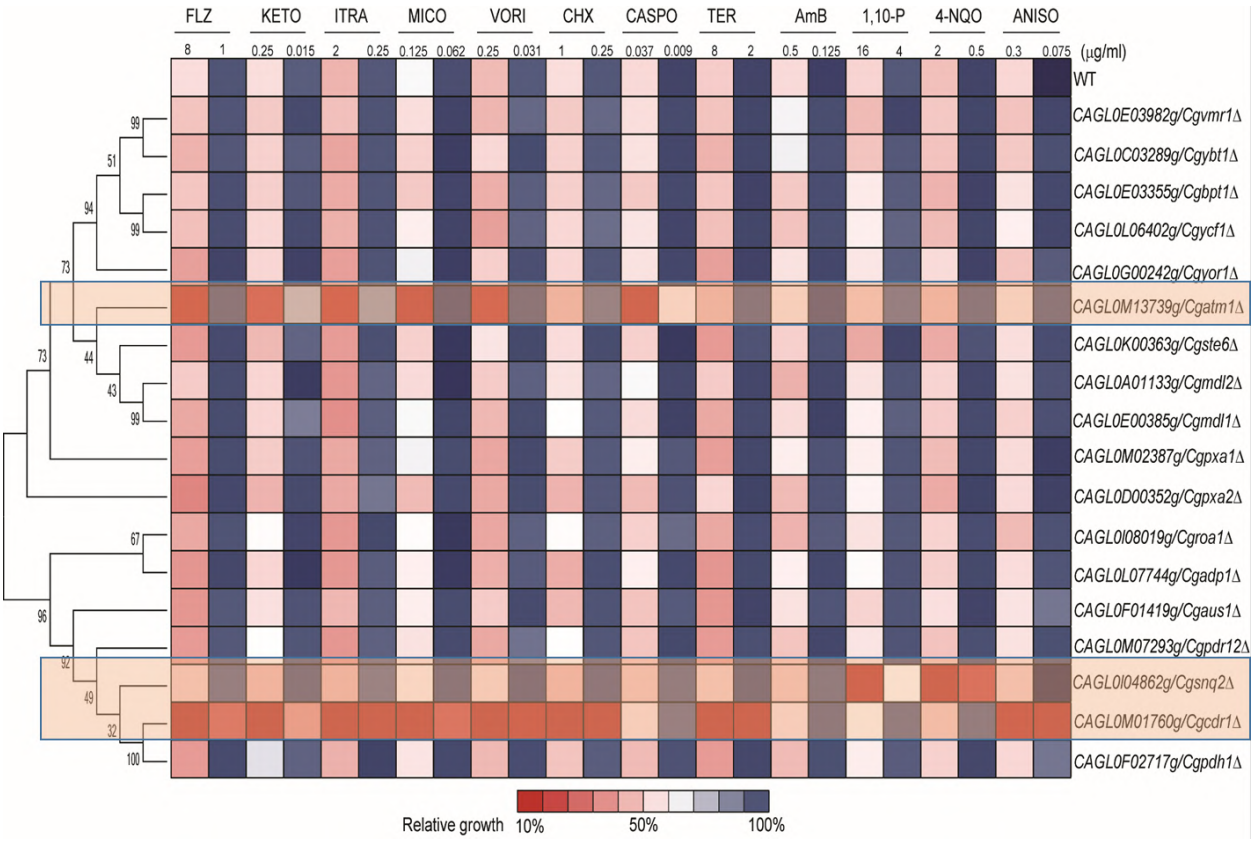

Fig 4.15: A summary figure of antifungal susceptibility testing of all the mutants. Highlighted mutants show sensitivity to different antifungals.

In the presence of azoles, the deletion of only two transporters *Cgcdr1*Δ and *Cgatm1*Δ from PDR and MDR, respectively, resulted in increase susceptibility towards tested drugs. Intrestingly, other transporters such as *Cgpdh1*Δ and *Cgsnq2*Δ mutants also show susceptible phenotype on azoles if deleted in some clinical isolates. The genetic background of the strains might be a reason for the different behavior of these transporters. For example, in a hospital survey, out of 20 resistant *C. glabrata* clinical isolates, 18 showed overexpression of *CgCDR1, CgPDH1*, or of both. The remaining two resistant isolates showed overexpression of only *CgSNQ2* (Sanguinetti et al. 2005a). However, only one of the strains displayed susceptible phenotypes to azoles after the deletion of *Cgsnq2* (Torelli et al. 2008a). This explains that the phenotype varies from strain to strain and the presence of other major transporters could impact their responses. Notably, a mitochondrial transporter *Cgatm1*Δ mutant displayed sensitivity to echinocandin CSF, which is a unique feature of this superfamily transporter, as

echinocandins are not known substrate for this transporter. The echinocandin drugs target the cell wall (CW) of yeast cells, so, deletion of *Cgatm1* could impact CW integrity.. Other transporters' transcript (*CgYOR1, CgYCF1, CgYBT1, CgSNQ2, CgPDH1*), displayed upregulation upon drug exposure (Fig 3.8, chapter 1) , but the deletion of these transporter genes did not affect drug susceptibility. The possibility of the masking effect of major transporters that would shield the functional relevance of other transporters cannot be ruled out. The deletion of an ABC transporter and its effect can be compensated by the overexpression of related ABC transporters of the same subfamily or other subfamilies. Single deletion of *Scsnq2*∆ and *Scyor1*∆ in *S. cerevisiae* led to the increased tolerance to KTC and the effect was found even more pronounced in their double deletion. The increased tolerance to the azoles was proposed to be due to the increased transcript of *ScPDR5*, possibly through shifting of the transcriptional pool of TF ScPdr1p (Kolaczkowska et al. 2008). In another report with CaMlt1p, a VM transporter, when deleted in a background of PM-localized major transporter devoid strain, highlighted its role in governing azoles susceptibility by way of sequestration of the drug into the vacuole (Khandelwal et al. 2019). Similarly, in *C. glabrata CgPDH1* and C*gSNQ2* mutants show susceptibility to azoles only in the absence of dominant transporter *CgCDR1* (Whaley et al. 2018, p. 2). Suffice to speculate that if the impact of shielding of these transporters is removed, the effect of other transporters could be higlighted. While discovering the role of *CgYOR1* in the present work, the shielding effect of major transporters became very visible (Chapter III).

4.2 A homologous overexpression system to study roles of drug transporters in *Candida glabrata*

4.2.1 Background

The continuous use of antimycotic drugs, especially azoles, has led to an emergence of drug-resistant clinical strains (Ksiezopolska and Gabaldón 2018). *C. glabrata* exhibits intrinsically low susceptibility to azoles (Whaley et al. 2016). This clinically rising drug resistance in *C. glabrata* is a culmination of several mechanisms which also includes overexpression of drug efflux pumps belonging to ATP Binding Cassette (ABC) superfamily and Major Facilitator Superfamily (MFS) of transporters, which help cells to rapidly extrude antimycotic drugs to circumvent their lethality (Holmes et al. 2016). The

existence of a large number of ABC transporters in *C. glabrata* genome makes it difficult to dissect the functional relevance of individual transporters (Kumari et al. 2018). Presently, a widely used *Saccharomyces cerevisiae* based heterologous expression system that lacks several ABC transporters has been extensively used to study membrane proteins from different yeasts (Lamping et al. 2007b). These studies helped in unraveling details of drug efflux, protein localization, and directed mutagenesis to dissect the molecular basis of the promiscuity towards substrate recognition (Redhu et al. 2018). Notwithstanding the immense importance of *S. cerevisiae* that has contributed immensely to the study of ABC transporters, questions are always raised concerning the differences among different species and non-pathogenic host strain's cellular environment, the lipid content of membrane and protein sorting behavior.

To circumvent these issues, we have developed a system in *C. glabrata* devoid of any masking effects by dominant drug transporters and an integrative plasmid for the expression of the gene of interest (GOI). For this, a strain of *C. glabrata* MSY8 was constructed by disrupting seven clinically relevant membrane-localized ABC drug transporter genes that included *CgSNQ2, CgAUS1, CgCDR1, CgPDH1, CgYCF1, CgYBT1,* and *CgYOR1* and introduced a gain of function (GOF) mutation in the *CgPDR1* transcription factor (TF) resulting in a hyper-activation of *CgCDR1* locus. The integration of GOI by employing an engineered expression plasmid allowed overexpression of fully functional ABC and MFS transporters.

4.2.2 Construction of multiple ABC transporters deleted strain of *C. glabrata*

ABC transporters extrude a wide variety of physiological compounds. Among ABC subfamilies, there is a greater similarity in the sequence and structure, which could make them share partial overlapping substrate profiles (Kolaczkowski et al. 1998). Due to the similarity in the substrate profile, some transporters may function as dominant transporters by masking the function of other transporters. The dominance of ABC transporters such as CaCdr1p and CgCdr1p, and CgPdh1p in *C. albicans* and *C. glabrata,* respectively, or ScPdr5p in *S. cerevisiae,* are few examples which are well reported. Therefore, functional analysis of a transporter in the absence of dominant transporters is very important to evaluate its true potential for drug efflux and the development of multiple drug resistance. To generate such a host strain, we selected

seven transporters genes (*CgSNQ2, CgAUS1, CgCDR1, CgPDH1, CgYCF1, CgYBT1,* and *CgYOR1*) which were earlier shown to be upregulated in azole-resistant clinical isolates of *C. glabrata* or involved in drug resistance (Sanguinetti et al. 2005a; Vermitsky et al. 2006a; Torelli et al. 2008a; Ferrari et al. 2011a). For these deletions, a recyclable FRT based dominant selection marker *NAT1* was used by employing fusion PCR based homologous recombination (Borah et al. 2011; Srivastava et al. 2015). Thus, we sequentially deleted these transporters coding sequences, and resulting strains were designated as MSY1 - MSY7. These deletions were not in a particular order. Each deletant was designated as MSY1 (*Cgsnq2*Δ), MSY2 (MSY1 + *Cgaus1*Δ), MSY3 (MSY2 + *Cgcdr1*Δ), MSY4 (MSY3 + *Cgpdh1*Δ), MSY5 (MSY4 + *Cgycf1*Δ), MSY6 (MSY5 + *Cgybt1*Δ), MSY7 (MSY6 + *Cgyor1*Δ).

4.2.3 Growth kinetics of MSY1 - MSY7 strains

To determine the effect of each transporter deletion on growth, we performed growth kinetics by micro-cultivation method. The cells were grown in YPD broth at 30°C and OD_{600} was recorded for 24 h and the growth curves of WT and deletion mutants MSY1 - MSY7 are depicted in Fig 4.15. Notably, the doubling time of MSY1 to MSY6 was similar to WT strain (60 min), however, deletion of *Cgyor1*Δ (MSY7) resulted in a slightly slower growth rate with a doubling time of 68.04 min. To further confirm if the slow growth phenotype of the MSY7 is due to *Cgyor1* deletion and not due to any other changes, we complemented the *CgYOR1* gene by episomal expression in plasmid pGRB2.2. While the episomal complementation reversed the drug sensitivity phenotype in MSY7 to a level up to MSY6, it could not restore the growth defect of MSY7. This growth defect is probably due to the cumulative effect of deletions. The growth curve of the mutant is given in Fig 4.16.

4.2.4 Drug susceptibility profiling of MSY1 - MSY7 mutants

The drug susceptibility profile of each deletion mutant was determined by spot assays, MIC_{80} determination by micro-dilution method and growth kinetics using FLC, KTC, VRC, MCZ and ITZ, CSF, echinocandins AmB and NYS, allylamine TER, protein synthesis inhibitors cycloheximide CHX and ANY, DNA damaging agents 4-NQO and metal chelator OP at indicated concentrations. The initial two deletions, MSY1 (*Cgsnq2*Δ) and MSY2 (*Cgsnq2*Δ*, Cgaus1*Δ), did not show any alteration in MIC_{80} with respect to WT on

all the tested drugs except for 4-NQO and OP, which was supported by spot assays as well. However, when *Cgcdr1*Δ was deleted, in MSY3 strain, as expected, the mutant MIC_{80} were dropped dramatically for tested azoles, including FLC MIC_{80} drop from 64 µg/ml to 4 µg/ml. The MIC_{80} was two doubling dilution lower (1 µg/ml) for FLC when *Cgpdh1*Δ was deleted to make MSY4 strain. The subsequent deletion of *Cgycf1*Δ, in MSY5, and *Cgybt1*Δ in MSY6, did not yield any further change in MIC_{80} of FLC as well as of other tested drugs (except for KTC). The subsequent last deletion of *Cgyor1*Δ, MSY7, led to another 4-fold drop in MIC of FLC (0.25 µg/ml) in comparison to MSY6 strain. A similar reduction of MIC_{80} of MSY7 was also observed with other azoles, protein synthesis inhibitors and allylamine. As expected, the deletion of *Cgsnq2*Δ, MSY1 displayed dramatic susceptibility towards 4-NQO and OP, which are the known substrates of ScSnq2p; however, no further change in susceptibility towards 4-NQO and OP was noticed in subsequent deletions MSY2 - MSY7. This indicated that changes in drug susceptibility are transporter dependent.

Table 4.4: MIC_{80} of constructed strains MSY1-MSY7

Drugs	MIC_{80} (µg/ml)							
	WT	MSY1	MSY2	MSY3	MSY4	MSY5	MSY6	MSY7
FLC	64	64	64	4	1	1	1	0.25
ITZ	16	16	16	0.125	0.031	0.031	0.031	<0.031
VRC	8	8	8	0.125	0.062	>0.031	0.062	0.015
KTC	1	1	1	0.5	0.12	0.031	0.031	0.002
MCZ	0.25	0.25	0.25	0.002	<0.002	<0.002	<0.002	<0.002
CSF	0.075	0.075	0.075	0.075	0.075	0.075	0.075	0.075
AmB	0.5	0.5	0.5	0.5	0.5	0.5	0.5	0.5
NYS	1	1	1	1	1	1	1	1
CHX	2	2	2	0.0625	0.0312	0.0312	0.0312	0.007
ANS	0.6	0.6	0.6	0.018	0.009	0.009	0.009	0.002
4-NQO	4	0.5	0.5	0.5	0.5	0.5	0.5	0.5
TER	16	16	16	0.5	0.25	0.25	0.25	0.031

OP	32	16	16	16	16	16	16	16

We further confirmed the drug susceptibility profile of each deletion mutant by growth curve analysis in the presence of tested drugs (Fig 4.16). The MIC_{80} to tested echinocandin and polyenes remained unchanged in all the deletion strains even after the deletion of all the seven transporters. Together, these results suggested that the deletion of seven ABC transporters, which generated the MSY7 strain, displayed supersensitive phenotype to a wide range of tested drugs.

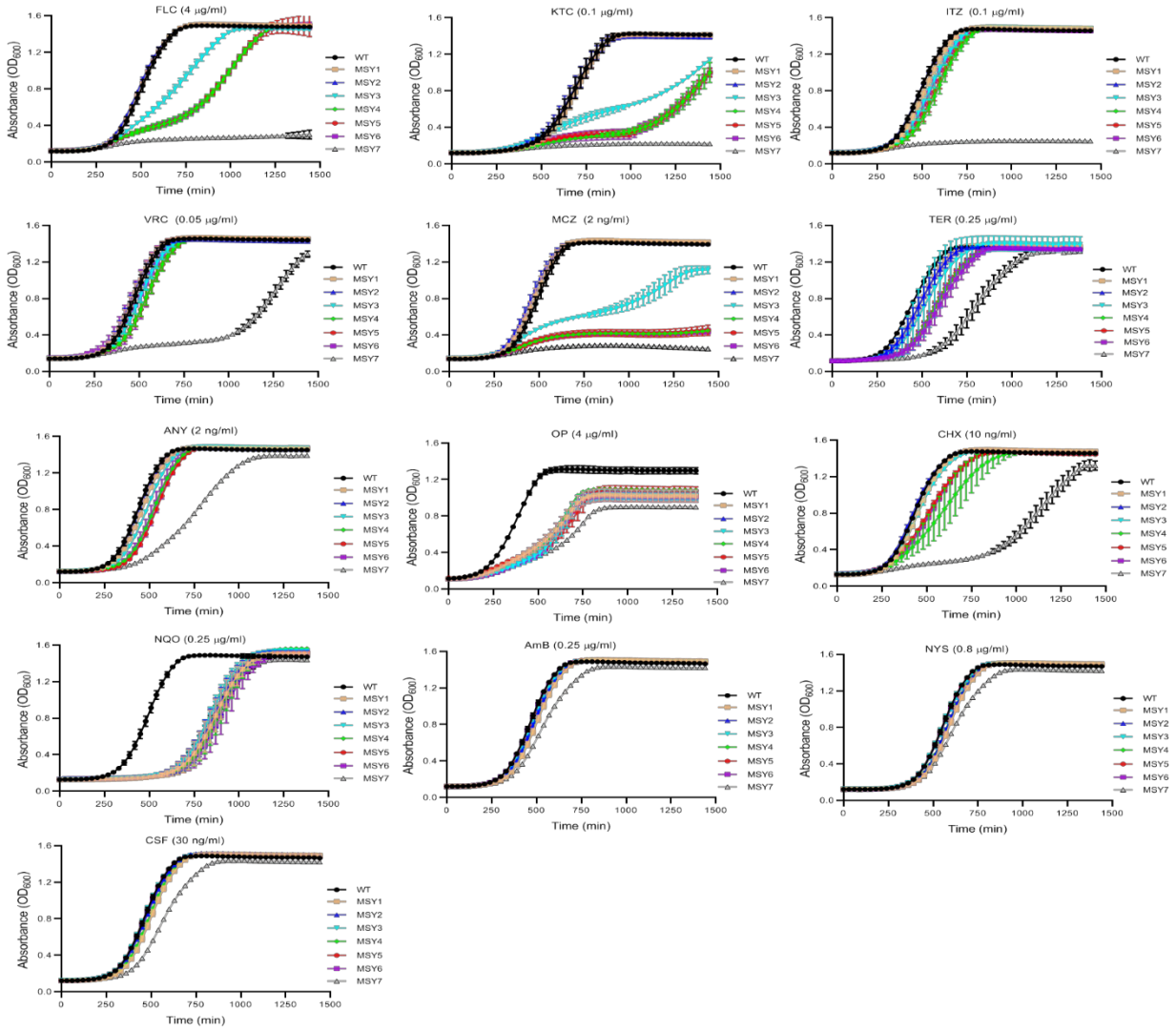

Fig 4.16: Growth curve analysis of strains MSY1-MSY7 in the presence of antifungals.

4.2.5 Assessment of efflux capacity of MSY1 - MSY7 mutants

Fluorescent compounds R6G and NR are the known substrates of some of the ABC transporters and have been commonly used to evaluate the efflux activity. Therefore, we tested the R6G and NR efflux by MSY1 - MSY7 deletion mutants to confirm the transport defect in these mutants. Indicated cells were pre-incubated with R6G or NR for 4 h in the absence of energy source to accumulate the dyes inside the cells. The energy-starved cells were then supplemented with 2% glucose to initiate the efflux of fluorescent substrates. After 45 min, the fluorescence was recorded in the supernatant and quantified. As expected, there was no reduction in R6G efflux in MSY1 - MSY2 mutant strains. Surprisingly, MSY3 strain (*Cgcdr1*Δ) showed only ~10% reduction in R6G efflux and an almost 48% reduction in NR efflux as compared to WT cells. The subsequent *Cgpdh1*Δ in MSY4 resulted in 33 and 44 % reduction of R6G and NR efflux, respectively, which coincided well with a recorded drop in MIC_{80} of FLC. Subsequent deletions (MSY5

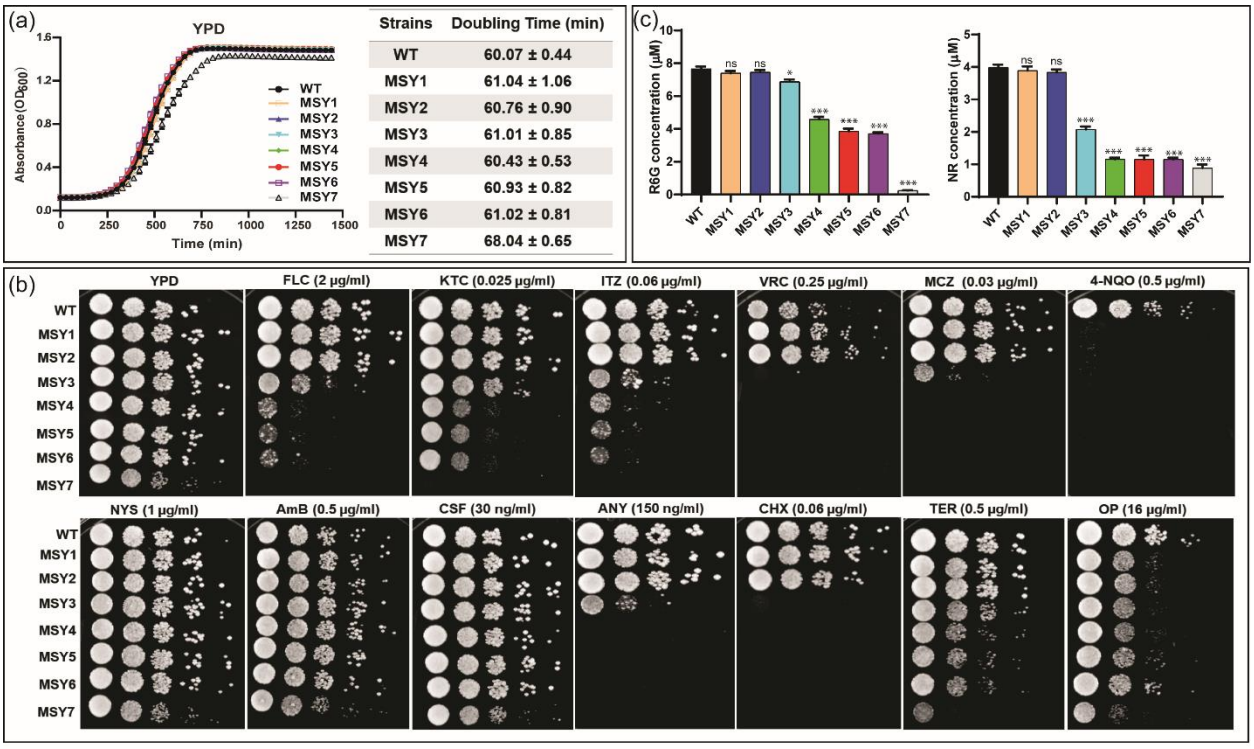

Strains	Doubling Time (min)
WT	60.07 ± 0.44
MSY1	61.04 ± 1.06
MSY2	60.76 ± 0.90
MSY3	61.01 ± 0.85
MSY4	60.43 ± 0.53
MSY5	60.93 ± 0.82
MSY6	61.02 ± 0.81
MSY7	68.04 ± 0.65

- MSY6) did not show any significant changes in R6G and NR efflux. However, the deletion of *Cgyor1*Δ (MSY7 strain) further decreased R6G efflux by ~93% and NR efflux by ~23% as compared to MSY4 (Fig 4.17).

Fig 4.17: Phenotypic characterization of strains MSY1 - MSY7. (a) Growth kinetics study of MSY1 - MSY7 strains was performed by a micro-cultivation method in a 96-well plate using Liquid Handling System (Tecan, Austria) in YPD broth at 30 °C. Doubling time for the strains was calculated by quantifying the time taken in doubling of logarithms values of the log phase. Experiments were conducted in triplicates (n=3), and values are expressed in mean ± standard deviation. (b) Spot assays were performed by serial dilution spot assay to check the effect of deletion on the antifungals tested. (c) R6G and NR efflux in MSY1 - MSY7 cells. The experiment was performed in biological triplicates with technical replicates. Significance was determined by calculating the *p*-value for all the strains with respect to WT by employing the student's t-test. *p*-values ≤0.05 = *, ≤0.0005 = *** and ns = not significant.

4.2.6 GOF mutation in WT enhances azole resistance by <100 fold

In *C. glabrata,* the upregulation of ABC transporters is linked to alterations in zinc-clustered TF *CgPDR1*. This TF recognizes PDRE present at promoters of several ABC transporters genes including *CgCDR1, CgPDH1, CgSNQ2, CgYOR1, CgYCF1* and *CgYBT1*. Several GOF mutations in *CgPDR1* coding region have been linked to increase in the expression of transporters and resistance towards azoles (Ferrari et al. 2009a). A *CgPDR1* GOF mutation (*CgPDR1*^{G840C}) in *C. glabrata* DSY565 strain showed MIC_{80} of FLC 128 µg/ml along with approximately 64-fold upregulation of *CgCDR1* transcript (Ferrari et al. 2009a). We introduced this mutation (*CgPDR1*^{G840C}) in WT, and the

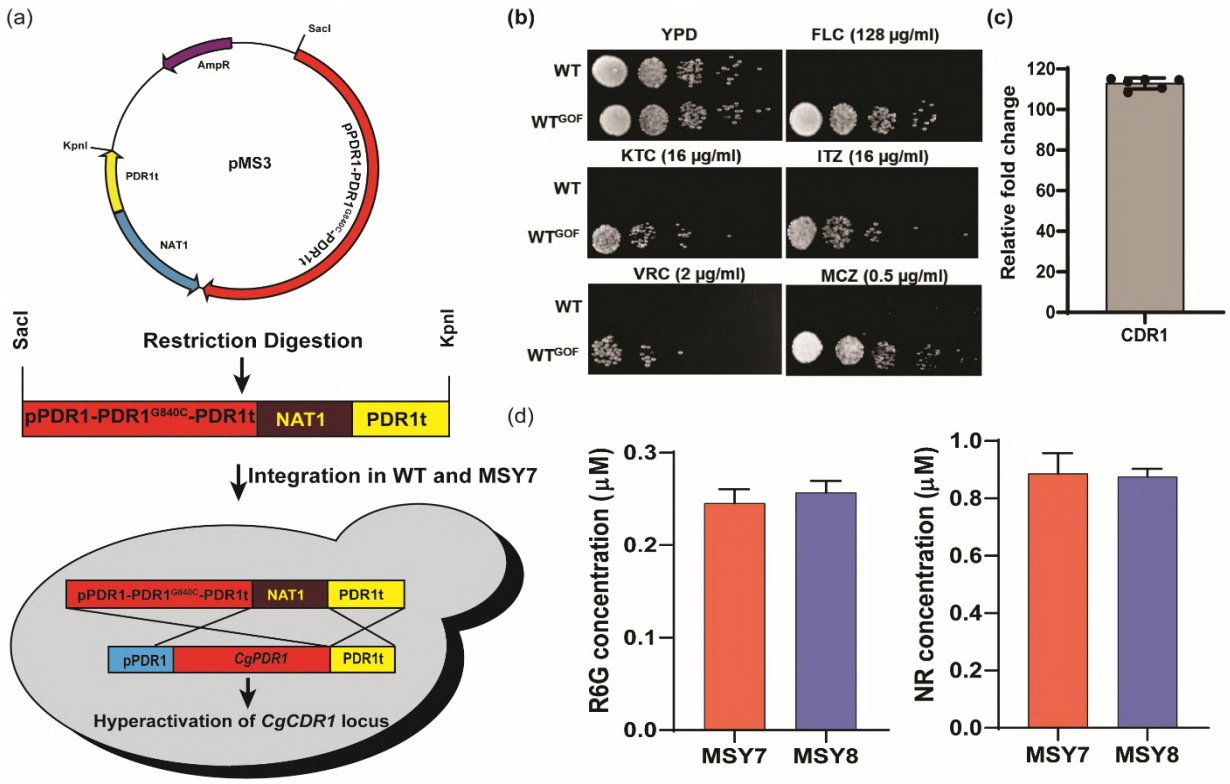

resulting mutant was designated as WT^{GOF} (*Cgpdr1::CgPDR1*^{G840C}). For this, pMS3 plasmid was linearized with SacI/ KpnI and transformed by electroporation, which replaced the native *CgPDR1* coding sequence. The drug susceptibility of WT^{GOF} was tested for azoles and expectedly we observed increased resistance to FLC along with ~114-fold upregulated transcript of *CgCDR1* gene (Fig 4.18).

Fig 4.18: Introduction of GOF mutation (*CgPDR1*^{G840C}) in MSY7 and phenotypes tested with of MSY8 strain: (a) Integration plasmid for GOF TF *CgPDR1* was constructed by cloning mutated C*gPDR1* ORF (*CgPDR1*^{G840C}) from *C. glabrata* strain DSY565 (Ferrari et al. 2009a). The resulting plasmid pMS3 was then digested with KpnI/ SacI and transformed in WT and MSY7 strain to introduce the GOF in the genome to construct WT^{GOF} and MSY8, respectively. (b) Serial dilution spot assay to depicts drug susceptibility of WT^{GOF} cells. (c) Expression analysis of *CgCDR1* in WT^{GOF} cells as compared with WT cells. (d) Substrate transport assay (R6G and NR) with MSY7 and MSY8 strains.

4.2.7 GOF mutation in MSY8 does not impact growth, susceptibility to antifungals and substrate transport

To construct a supersensitive *C. glabrata* strain where GOI could be overexpressed without the interference of dominant transporters for functional analysis, we constructed MSY8 strain, with seven transporter deletions and hyperactive *CgCDR1* locus in its genome. For this, the above-constructed cassette from digested pMS3 plasmid was transformed in the above-constructed MSY7 strain to generate MSY8 strain. The constructed MSY8 strain has a GOF *CgPDR1* (*CgPDR1*^{G840C}) and a hyperactive *CgCDR1* promoter (Fig 4.19). Since TF *CgPDR1* regulon includes several other genes apart from ABC transporters, we checked the possibility of altered growth and azole susceptibility in MSY8 strain. Interestingly MSY8 did not show further change in susceptibility towards antifungals and efflux of substrates to MSY7 strain.

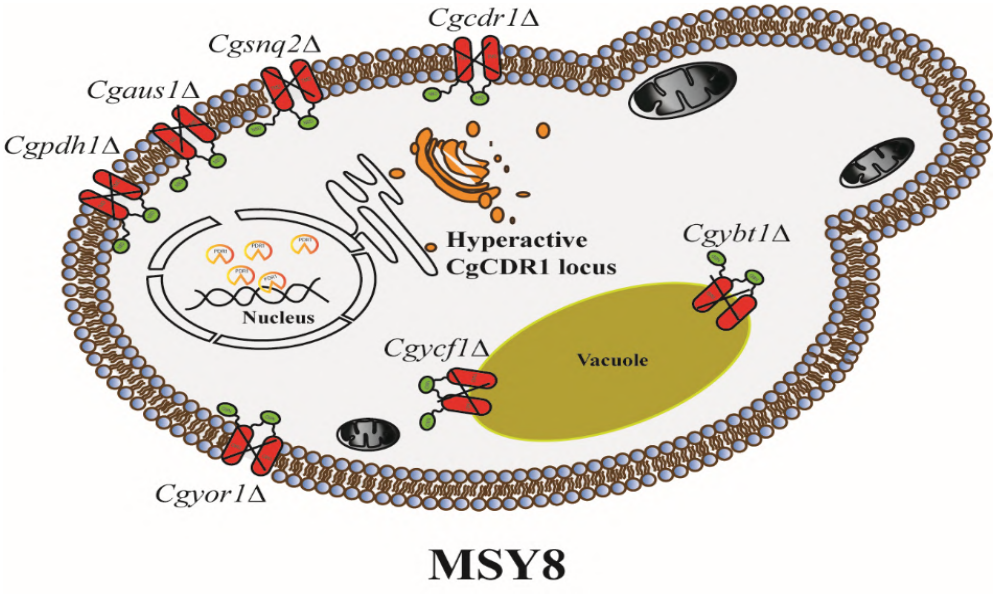

Fig 4.19: MSY8 graphical representation.

4.2.8 Overexpression of ABC transporters validated the appropriateness of MSY8 as an expression system

To validate the expression system, we expressed well known ABC transporters of *C. glabrata* (*CgCDR1* and *CgPDH1*), *C. albicans* (*CaCDR1*) and *S. cerevisiae* (*ScPDR5*) in MSY8 strain. These transporters were cloned in pMS6 plasmid upstream of the *YeGFP* at either SacI/ SacII or NotI/ PacI sites. The whole cassette containing GOI-GFP chimeric

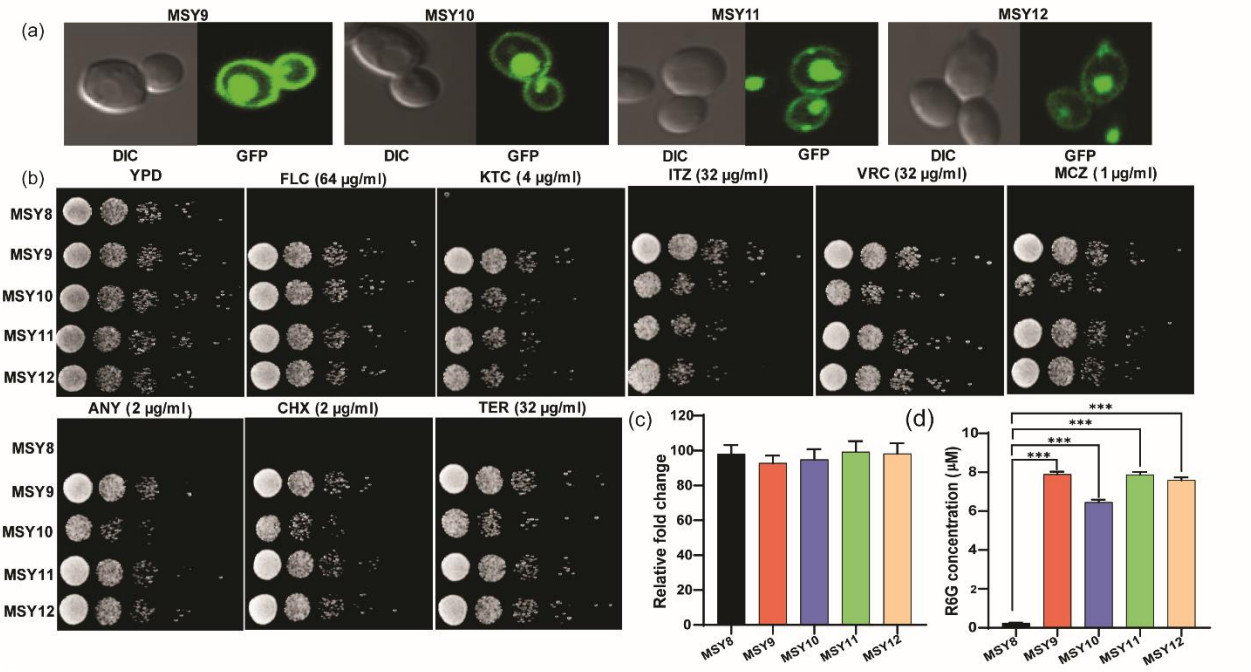

construct was then digested with SacI/ KpnI and integrated into MSY8 strain at *CgCDR1* locus. The constructed strains MSY9 (MSY8/*CgCDR1*), MSY10 (MSY8/*CgPDH1*), MSY11 (MSY8/*CaCDR1*), and MSY12 (MSY8/*ScPDR5*) were tested for the expression and localization. As evident from confocal images, all the GFP-chimeric transporters CgCdr1-GFP, CgPdh1-GFP, CaCdr1-GFP and ScPdr5-GFP showed clear plasma membrane localization. The transcripts levels of each transporter *CgCDR1, CgPDH1, CaCDR1 and ScPDR5* in MSY9, MSY10, MSY11, and MSY12 cells were confirmed by RT-PCR, which also displayed the overexpression of these transporters at the locus (Fig 4.20).

Fig 4.20: Overexpression of ABC transporters and their characterization: (a) Integration of ABC transporters *CgCDR1, CgPDH1, CaCDR1,* and *ScPDR5* was performed as described in Methods and resulting strains designated as MSY9 - MSY12. Confocal images of MSY9 - MSY12 show the localization at the plasma membrane. Confocal images were taken by using the FITC filter. (b) Drug susceptibility tests were performed by spot assays at indicated concentrations. (c) Transcript levels of integrated transporters into MSY8 was determined by RT-PCR. (d) R6G substrate transport assay with the overexpressed transporters. *p*-value was determined by the student's t-test and *p*-value ≤0.0005 represented as (***).

4.2.9 Functional analysis of CgCdr1-GFP, CgPdh1-GFP, CaCdr1-GFP, and ScPdr5-GFP

The functionality of the recombinantly expressed ABC transporters in MSY9 - MSY12 strains was analyzed by testing their susceptibility towards azoles, allylamines, and protein synthesis inhibitors in comparison to parental strain MSY8. We rationalized that the overexpressing transporter proteins should be able to reverse the higher susceptibility of MSY8 cells. Expectedly, the expression of all four transporters drastically decreased the susceptibility of MSY8 cells, albeit to variable levels (Table 4.5). R6G is a known substrate of ABC transporters, and these four transporters are known to efflux R6G (Lamping et al. 2007b). Spectrophotometric based efflux assay showed a 25 to 32-fold increased efflux of R6G as compared to MSY8 cells (Fig 4.19). Results indicated that ABC transporters from different fungal species could be expressed and functional in MSY8 strain.

Table 4.5: MIC_{80} of overexpressed strains MSY9-13 as compared to MSY8

Drugs	MIC_{80} (µg/ml)

	MSY8	MSY9	MSY10	MSY11	MSY12	MSY13
FLC	0.25	256	128	256	256	8
ITZ	<0.031	>64	64	64	64	2
VRC	0.015	64	64	64	64	4
KTC	0.002	8	4	8	8	1
MCZ	<0.002	2	1	1	1	0.25
CSF	0.075	0.075	0.075	0.075	0.075	0.075
AmB	0.5	0.5	0.5	0.5	0.5	0.5
NYS	1	1	1	1	1	1
CHX	0.007	4	4	4	4	0.0312
ANS	0.002	>2.4	2.4	2.4	2.4	0.009
4-NQO	0.5	0.5	0.5	0.5	0.5	0.5
TER	0.031	64	>32	>32	>32	0.031
OP	16	16	16	16	16	16

4.2.10 MSY8 expression system is suitable to study non-ABC transporters

We explored the suitability of our expression system for functional analysis of non-ABC membrane transporters. For this, we transformed and integrated a GFP-chimeric-*CgFLR1* transporter belonging to MFS superfamily in MSY8 strain to generate MSY13

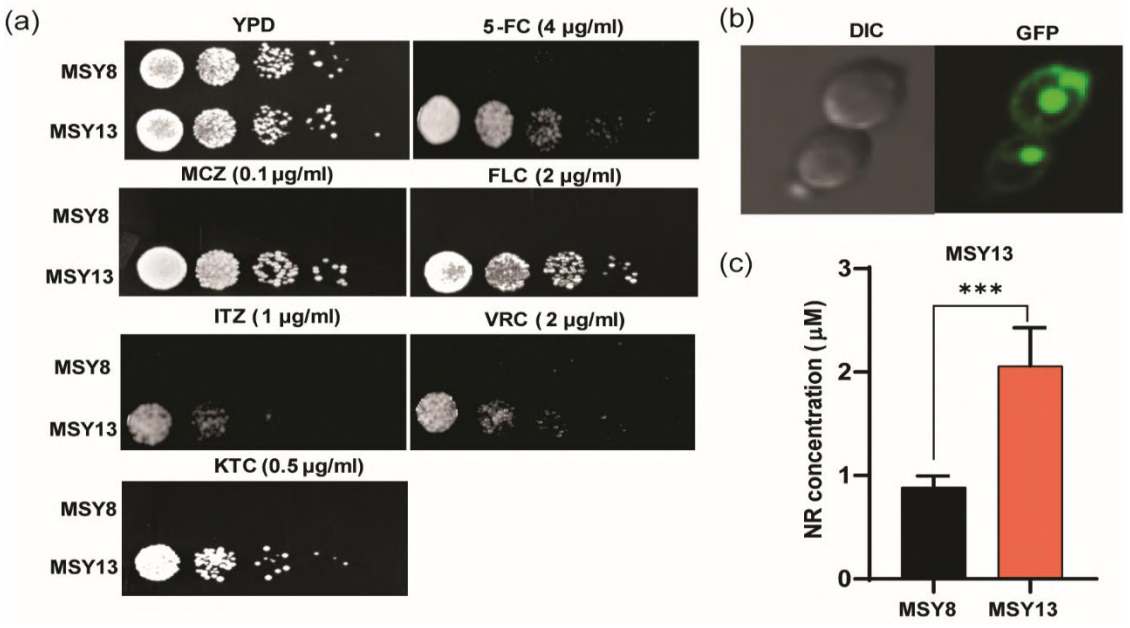

strain. Drug: H^+ antiporter CgFlr1p is a well-known drug transporter that confers 5-flucytosine (5-FC) antifungal resistance in *C. glabrata* (Pais et al. 2016). While the homolog CgFlr2p confers resistance to both azoles and 5-FC, the *Cgflr1*Δ deletant imparts susceptibility to 5-FC, but not to azoles (Chen et al. 2007). As expected, MSY13 strain became resistant to 5-FC and, interestingly, also demonstrated increased resistance to azoles (Table 4.5, Fig 4.20). The increased azole resistance could be attributed to the masking effect of *CgFLR2* on azole resistance phenotype of *CgFLR1*. MSY13 overexpressing CgFlr1-GFP showed proper localization at the plasma membrane, as was evident from confocal images, and 2-fold increased efflux of NR, a well-known MFS transporters substrate (Fig 4.21).

Fig 4.21: Expression of MFS transporter and its phenotypic characterization. (a) Drug spot assays of MSY13 by serial dilution at indicated concentrations. (b) Confocal images of localization of CgFlr-GFP taken from the FITC filter of the confocal microscope. (c) NR efflux in MSY13 cells. Each experiment was performed in biological triplicates with three technical replicates. *p*-value was determined by paired student t-test, and *p*-value ≤0.0005 was represented as (***).

4.2.11 Discussion and conclusion:

Several independent studies have called attention to the relevance of drug transporters belonging to ABC and MFS superfamilies in drug resistance and their posing of a serious hindrance to successful antifungal therapy. Such a situation demands an in-depth structure and function analysis of clinically relevant drug transporters. For this, there is always an unmet need for an overexpression system that can act as a platform to facilitate the functional characterization of these transporters to analyse the basis of their substrate poly-specificity, structural analysis and to develop inhibitors/modulators. Over the years, this requirement has been successfully met by the *S. cerevisiae* overexpression system established by Goffeau's and Cannon's groups (Decottignies et al. 1998; Lamping et al. 2007b). Using this approach, efflux pumps not only from *S. cerevisiae* but from different fungal pathogens as well could be structurally and functionally analyzed (Shukla et al. 2003; Lamping et al. 2007b; Panapruksachat et al. 2016). Notwithstanding, the extensive use of the *S. cerevisiae* system by several laboratories for nearly two decades, concerns have been raised pertaining to its artefactual environment posed by heterologous system, particularly applicable to the functionality of drug transporters of pathogenic *Candida* species. The differences in regulatory circuitry governing drug resistance and subtle

differences in membrane lipid environment influencing the functionality of drug transporter proteins are some of the concerns faced by such studies. In this context, it is worth mentioning that membrane lipids do impact drug transporter protein insertion, integrity, and overall functioning (Opekarová and Tanner 2003; Pasrija et al. 2008).

Our present study focused to resolve challenges imposed by the heterologous system for the overexpression of drug transporter proteins of *C. glabrata.* We took advantage of a GOF mutation of TF *CgPDR1* azole-resistant clinical isolate of *C. glabrata* and introduced it into an engineered hyper-susceptible MSY7 mutant strain, which was deleted for seven dominant ABC transporters. Thus the resulting strain MSY8 apart from major transporters deleted background also possessed hyper-activated *CgCDR1* locus. This followed by the construction of an integration-based plasmid for cloning GOI at the activated *CgCDR1* locus. The suitability of the expression system was well demonstrated by overexpressing fully functional clinically relevant ABC drug transporters of *C. glabrata* (*CgCDR1* and *CgPDH1*), *C. albicans* (*CaCDR1*), *S. cerevisiae* (*ScPDR5*) and *C. glabrata* MFS transporter *CgFLR1*. This MSY8 system thus presents a good platform for detailed substrate profiling and functional analysis of transporter proteins with minimum interference by major drug transporters of *C. glabrata*.

CHAPTER III

5. Characterization of MRP subfamily ABC transporter *CgYOR1*

5.1 Background

The most remarkable human fungal pathogen belongs to genus *Candida*. *Candida glabrata,* being a commensal in the human microbiota, are also known for superficial to serious life-threatening bloodstream infections (Kasper et al. 2015b). Azoles are the first-line antifungal to prevent superficial to bloodstream fungal growth by interfering with the ergosterol biosynthesis (Sheehan, Hitchcock, & Sibley, 1999). Fluconazole (FLC), the most common azole, targets active site of 14-α-sterol-demethylase (ERG11), a cytochrome P-450 enzyme by inhibiting lanosterol conversion to ergosterol (Cowen et al. 2015). The efficacy of the azoles in the treatment of invasive candidiasis is severely hampered by azole resistance in *C. glabrata* (Fidel, Vazquez, & Sobel, 1999). In order to overcome azole resistance in *C. glabrata*, it is first important to comprehensively understand the mechanisms by which it exhibits resistance to the azoles. There are a multitude of mechanism to cope up with incoming azole drug in *C. glabrata vis.*, mutations in target genes, gain of function (GOF) mutation in transcription factor (TF) *CgPDR1,* efflux pumps overexpression, and mutation in DNA repair pathway genes (Healey et al. 2016; Whaley et al. 2018).

Recently a mutation in *ERG11* such as G944A, I166S causing the alteration in target has been reported, henceforth contributed cross-resistance for both azole and polyenes (Hull et al., 2012; Teo et al., 2019). TF CgPDR1 is a central player in the azole resistance acquired during antifungal therapy. Notable reports have shown that *C. glabrata* Pdr1 directly binds to fluconazole, which resulted in the activation of drug efflux pumps, a mechanism similar to the regulation of multidrug resistance (MDR) by the pregnane X receptor (PXR), a nuclear receptor, in vertebrates (Thakur et al. 2008; Caudle et al. 2011). Moreover, single point mutations in the putative functional domains of CgPDR1 result in increased resistance to azoles and upregulated transcription of ABC transporters *CgCDR1, CgPDH1*, *and CgSNQ2* (Ferrari et al., 2009; Tsai, Krol, Sarti, & Bennett, 2006; Whaley et al., 2018).

C. glabrata resistant clinical match paired isolates originally showed *CgCDR1* transcript increment, deletion of which made cell susceptible to azoles and reintroduction restored

susceptibility (Sanglard et al. 1999a). *CgPDH1* was also first gained attention when its expression was found to be overexpressed in azole-resistant clinical isolates of *C. glabrata* (Miyazaki et al. 1998b). Further study showed that the deletion of Cg*PDH1* in the background of *CgCDR1* resulted in increased susceptibility to fluconazole (Sanglard et al. 2001a). Recently CgSnq2p was shown to contribute to azole resistance. Increased expression of *CgSNQ2* was found in two azole-resistant clinical isolates with normal expression of Cg*CDR1* or Cg*PDH1* (Sanguinetti et al. 2005a). Subsequently, it was shown to be required for the azole-resistant phenotype in one of the same isolates (Torelli et al. 2008a). An ABC transporter *CgAUS1* protects cells against azole antifungals in the presence of serum (Nagi et al., 2013; Nakayama H, et al., 2007). Cg*YOR1* and Cg*YBT1* were also found to be upregulated in azole-resistant lab mutant as well as in azole-resistant clinical isolates (Vermitsky et al. 2006a). A previous report also suggested the upregulation of Cg*YCF1*, Cg*YBT1 and* Cg*YOR1* in the azole resistant petite isolates (Ferrari et al. 2011a).

ABC transporters impart drug resistance by effluxing out drug outside and rendering cells to survive. A recent study indicated hyper-activation of TOR signaling could be a major contributor to azole resistance in the absence of ABC transporter CaCDR6 (Khandelwal et al. 2018). Noteworthy reports also revealed the elegant role of TOR cascade, molecular chaperone Hsp90, its downstream target and calcineurin stabilization in enabling cellular stress responses crucial for the emergence and maintenance of drug resistance in *Aspergillus* and *Candida* species (Robbins et al. 2010; Singh-Babak et al. 2012). Suppression of TOR1 causes suppression of HSP90, which destabilizes the protein phosphatase calcineurin, allowing for its deactivation (Cowen 2005; Cowen et al. 2006).

In *S. cerevisiae* and *C. albicans YOR1* are employed in the extrusion of oligomycin (OMY) and natural product beauvericin (BEA) (Katzmann et al. 1995a; Ramírez-Zavala et al. 2018). Knockout of *Cgyor1*∆ in *C. glabrata* has no effect on common antifungals but also ineffective on OMY, which made it an interesting candidate for the present study. Further, Yor1p transports BEA, which was recently known to potentiate azole activity against diverse fungal pathogens and renders antifungal resistant pathogens responsive to treatment in mammalian infection models (Shekhar-Guturja et al. 2016a). BEA has been shown to act in part through inhibition of TOR signaling in both *S. cerevisiae* and *C. albicans* (Shekhar-Guturja et al. 2016c).

5.2 The dominant *CgCDR1* transporter shields function of other transporters.

ABC transporters share quite a high sequence homology, domain organizations and have overlapping substrates profile. For example, *CgCDR1* shares a sequence identity of 72.49% with *CgPDH1* and 48.19% with *CgSNQ2*. This close similarity among ABC members' demands more intense analysis to determine the contribution of each transporter towards the export of a substrate. The substrates specificity of *S. cerevisiae PDR5*, *SNQ2*, *YOR1* are mostly overlapping (Kolaczkowski et al. 1998; Kolaczkowska et al. 2008), which strongly suggest a possibility of masking the effect of their transport function. Notwithstanding the reported dominant impact of *CgCDR1* on *CgPDH1 and CgSNQ2* in *C. glabrata* (Sanglard et al. 2001a; Whaley et al. 2018), the fact remains that there are studies pointing role of many other ABC transporters (*CgYOR1*, *CgYCF1* and *CgYBT1*) in clinical azole resistance (Ferrari et al., 2011; Nagi et al., 2013; *Nakayama H, et al. (2007)*; Vermitsky et al., 2006). In this study, we addressed this issue and explored the dominance of *CgCDR1*, by constructing double deletant of those transporters whose transcripts have been earlier reported to be upregulated in drug resistant clinical isolates of *C. glabrata*. Thus, each of the such transporter encoding genes was deleted in the *Cgcdr1Δ* background. These, double deletents; *CgCdr1Δ/Cgpdh1Δ*, *CgCdr1Δ/Cgsnq2Δ*, *CgCdr1Δ/Cgaus1Δ*, *CgCdr1Δ/Cgyor1Δ*, *CgCdr1Δ/Cgycf1Δ* and *CgCdr1Δ/Cgybt1Δ* were then subjected to drug susceptibility profiling. The mutants *CgCdr1Δ/Cgsnq2Δ*, *CgCdr1Δ/Cgaus1Δ*, *CgCdr1Δ/Cgycf1Δ,* and *CgCdr1Δ/Cgybt1Δ* even in the absence of *CgCdr1Δ* exhibited no change in susceptibility to azoles, implying their other cellular roles. Interestingly, *CgCdr1Δ/Cgyor1Δ* and *CgCdr1Δ/Cgpdh1Δ* showed increased susceptibility to azoles which was noticeably absent when these were deleted individually. The growth defect of *CgCdr1Δ/Cgpdh1Δ*, *CgCdr1Δ/Cgyor1Δ* cells in presence of azoles was evident on spot as well as in liquid growth assays (Fig. 5.1). While *CgPDH1* role in azole resistance is fairly well established, we focused this study to uncover the role of *CgYOR1* in azole susceptibility which otherwise remained masked by *CgCDR1.*

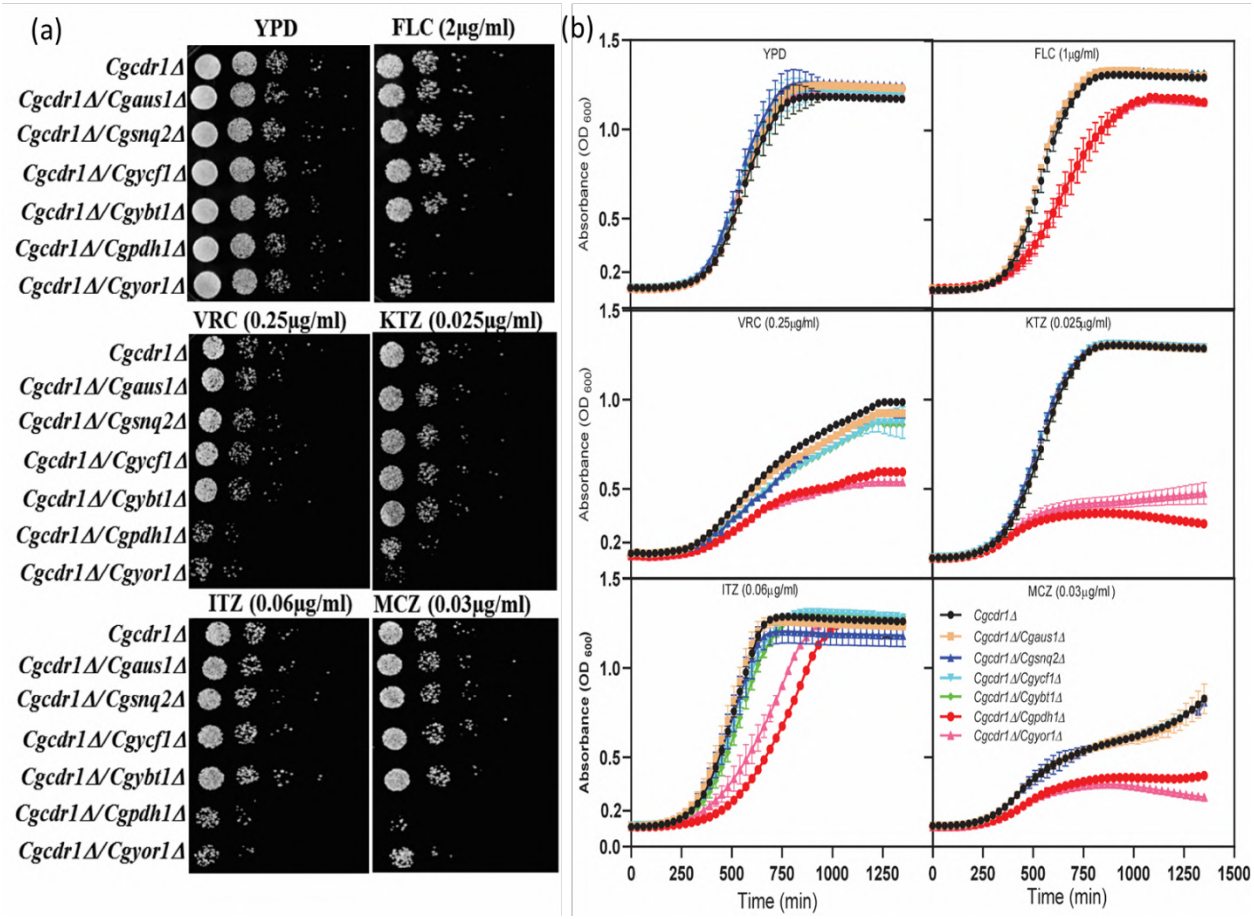

Fig 5.1: Susceptibility of ABC protein mutants in the background of *Cgcdr1*Δ: (a) Drug susceptibility of all the mutants were tested by spot assays on solid agar media and (b) growth curves were made by micro-cultivation method in 96-well plate in YPD media.

5.3 Only *CgCDR1* masks *CgYOR1* transporter function

Although *CgCDR1* is a major contributor to azole resistance in *C. glabrata, CgPDH1* has also been implicated in azole resistance (Izumikawa et al. 2003b, p. 1; Vermitsky and Edlind 2004). *CgPDH1* overexpression in *Cgcdr1*Δ strain could restore resistance to azoles. An overexpression of *CgPDH1* in pdr5Δ strain of *S. cerevisiae* also reverted its susceptibility to azoles (Izumikawa et al., 2003). However, none of the other transporters (*CgSNQ2, CgPDH1, CgYCF1, CgYBT1* and *CgAUS1*) whose transcript is reported to be overexpressed in azole resistant clinical isolates, their single deletion did not change azole sensitivity. The noticeable manifestation of azole resistance in *CgCdr1Δ/Cgyor1Δ* prompted us to explore if any other transporter could also conceal *CgYOR1* influence on azole susceptibility. To address this issue, we constructed double KOs in the background

of *Cgyor1Δ* such as *Cgyor1Δ/Cgpdh1Δ*, *Cgyor1Δ/Cgsnq2Δ*, *Cgyor1Δ/Cgaus1Δ*, *Cgyor1Δ/Cgycf1Δ, Cgyor1Δ/Cgybt1Δ*. We subjected each of these double KOs to drug susceptibility tests which also included *Cgyor1Δ/Cgcdr1Δ* mutant. Importantly, none of the double KO mutants except *Cgcdr1Δ/Cgyor1Δ* could impact azole susceptibility. The data points that either these transporters do not contribute in shielding of *CgYOR1* function. The efflux of R6G confirmed drug susceptibility data. In all the double KO mutants R6G efflux remained unchanged except in *Cgcdr1Δ/Cgyor1Δ* where it was reduced. Notwithstanding, increase efflux of R6G reported in earlier studies in *CgCDR1* overexpressing cells (Lamping et al. 2007b), its deletion (*Cgcdr1Δ)* resulted in only marginal reduction in R6G efflux (Fig 5.2). This led us to conclude that azoles could be the preferred efflux substrate of *Cg*Yor1p.

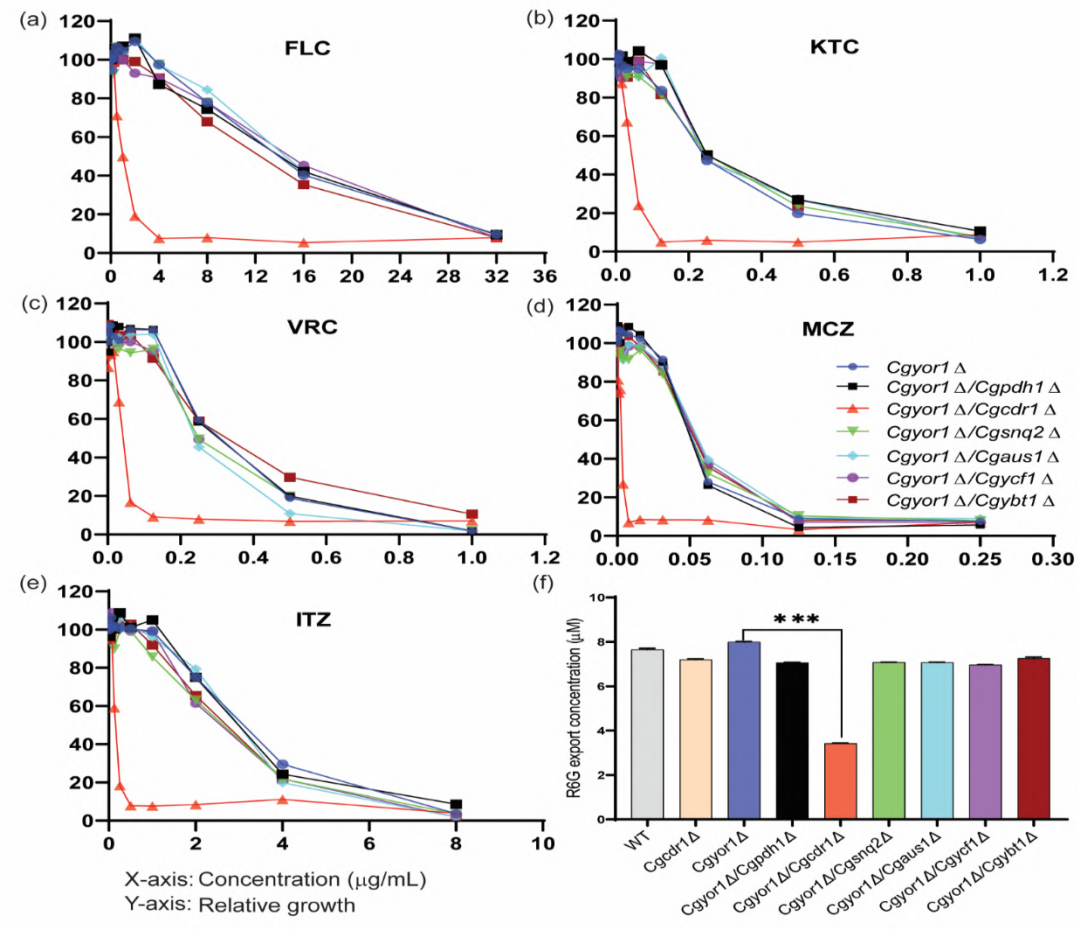

Fig 5.2: Growth kinetics and R6G efflux in *Cgyor1Δ/Cgpdh1Δ*, *Cgyor1Δ/Cgsnq2Δ*, *Cgyor1Δ/Cgaus1Δ*, *Cgyor1Δ/Cgycf1Δ, Cgyor1Δ/Cgybt1Δ* and *Cgyor1Δ/cdr1Δ*. (a) MIC_{80} of only

*Cgyor1*Δ/*Cgcdr1*Δ indicates sensitivity on azoles but rest of double KO were non-sensitive to tested azoles (b) R6G efflux assay of double KO mutants. Only *Cgyor1*Δ/*Cgcdr1*Δ showed reduction in R6G efflux.

5.4 *CgYOR1* deletion does not impart susceptibility to oligomycin

S. cerevisiae ScYOR1 is well known to transport organic anions especially, OMY, a macrolide that is influenced by gain of function (GOF) mutations in transcription factor pdr1/pdr3 (Katzmann et al. 1995b). OMY is also a substrate of *C. albicans CaYOR1* (Ramírez-Zavala et al. 2018). A cyclic hexadepsipeptide natural product BEA is another reported substrate of Sc*YOR1*. Although BEA is not an antifungal but by blocking efflux pumps and inhibiting TOR kinase and protein kinase CK2, acts as a potent enhancer of FLC efficiency and turned it into a fungicidal (Shekhar-Guturja et al. 2016b, c). Surprisingly, while *Cgyor1Δ* cells showed susceptibility to BEA, the susceptibility to OMY remained unchanged (Fig 5.4a). We also tested the probability of enhanced combined efficacy of FLC and BEA after *Cgyor1* deletion by employing dose-response matrix. The FLC susceptible *Cgyor1*Δ cells showed enhanced synergy in presence of BEA but the same was not evident in *Cgcdr1*Δ cells, which further supported that BEA is a substrate of CgYor1p (Fig 5.3). However, none of the mutants *Cgyor1*Δ and *Cgcdr1*Δ showed any synergy with OMY and FLC.

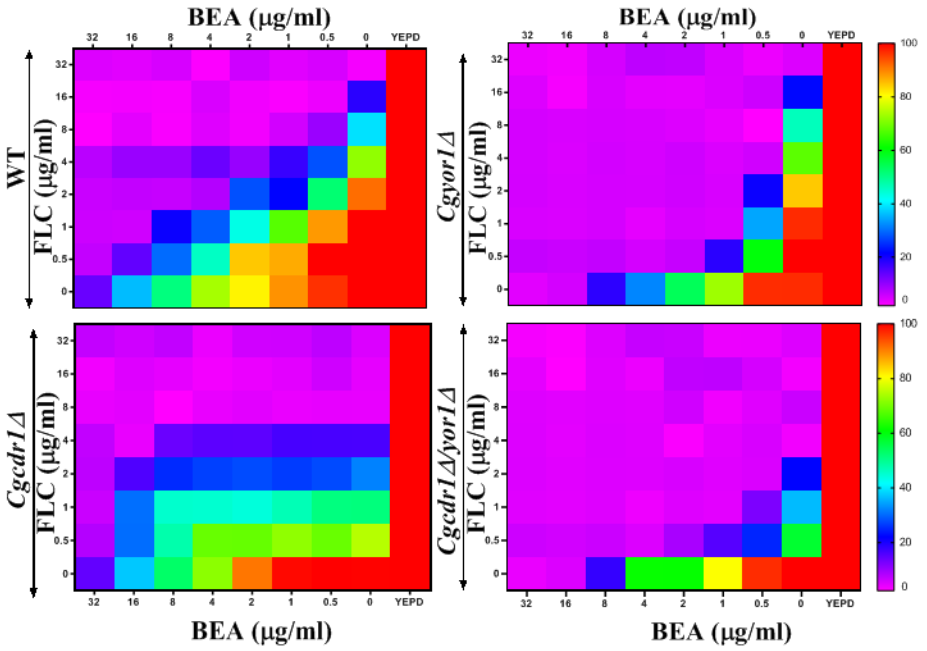

Strains	W/O BEA	With 0.5 µg/ml BEA	W/O FLC
	FLC MIC_{80}	FLC MIC_{80}	BEA MIC_{80}
WT	16	4	32
Cgyor1Δ	16	2	8
Cgcdr1Δ	4	4	32
Cgcdr1Δ/Cgyor1Δ	2	1	8

Fig 5.3: Synergism of FLC and BEA with the mutants: indicates enhanced synergism after *Cgyor1*Δ**.**

To order to further confirm that OMY is not a substrate, we have overexpressed *CgYOR1* in the MSY8 strain, which lacks 7 ABC transporters and possesses GOF in TF Pdr1, rendering hyperactive *CgCDR1* locus. However, MSY8/*CgYOR1* didn't revert the OMY sensitivity but reverted the BEA sensitivity.

Notably, the complementation of *CgYOR1* in *Scyor1Δ* strain also did not change sensitivity to OMY but could reverse the susceptibility of BEA, which again supported our results that OMY may not be a substrate of *CgYOR1* (Fig 5.4b). In order to further confirm it, we overexpressed *CgYOR1* in a well-recognized heterologous expression system in *S. cerevisiae* which was used earlier by us and others for overexpressing ABC proteins (Khandelwal et al., 2016; Lamping et al., 2007; Shukla et al., 2003). Multideletent *S. cerevisiae* strain (AD1-8U^-) lacks 7 ABC transporters with hyperactive *PDR5* locus. The overexpression of desired ABC protein is achieved in AD1-8U^- strain where the possibility of interference of major ABC transporters is largely excluded. We integrated *CgYOR1* at hyperactive *PDR5* locus. Notably the strain AD1-8U^-/*CgYOR1* overexpressing *CgYOR1* could not revert OMY susceptibility while it could fully reverse sensitivity of BEA (Fig 5.4). Moreover, substrate competition efflux assays of R6G in presence of 10x concentration of both OMY and BEA in the *CgYOR1* overexpressed strain (MSY8/*CgYOR1*) further provided credence to our observation. The efflux of R6G was reduced by half in the presence of BEA but remained unchanged in presence of OMY (Fig 5.4). Together, OMY does not appear to be the substrate of CgYor1p.

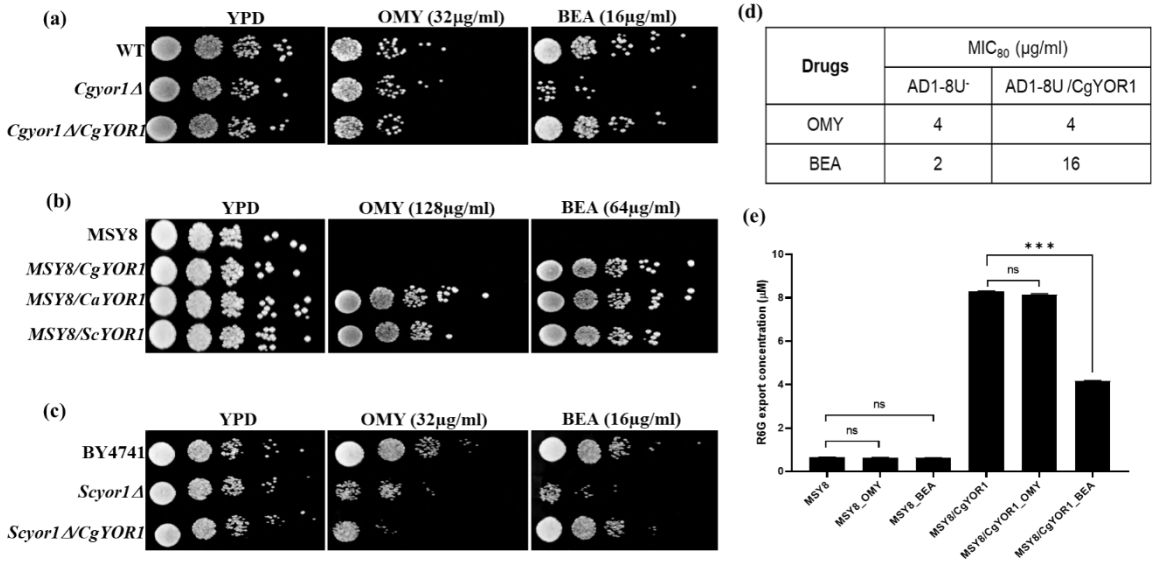

Drugs	MIC_{80} (µg/ml)	
	AD1-8U⁻	AD1-8U /CgYOR1
OMY	4	4
BEA	2	16

Fig 5.4: Substrate specificity of *CgYOR1*: Drug susceptibility of all the mutants were tested by spot assays on solid agar media in presence of OMY or BEA; (a) *Cgyor1*Δ strain was susceptible to BEA but not to OMY (b) overexpression of CgYOR1 in MSY8 could not reverse OMY susceptibility but were reversed by CaYOR1 and ScYOR1, however all the overexpressed strains reversed BEA susceptibility at a similar extant (c) Complementation of CgYOR1 in *S. cerevisiae* (*Scyor1*Δ*)* background experienced no reversal of OMY sensitivity. (d) An overexpression of *CgYOR1* in heterologous expression system AD1-8U⁻ did not restore OMY sensitivity (e) Substrate competition of BEA and OMY with the efflux of R6G in MSY8/*CgYOR1* overexpressing strain in presence of 10x concentration of BEA or OMY indicated efflux reduction by BEA but no change was recorded with OMY.

5.5 Azoles are substrates of CgYor1p

ABC transporters belonging to subfamily PDR are the major transporters known to transport azoles from yeast cells. Notably, vacuolar ABC transporter *CaMLT1* belonging to MRP subfamily in shown to sequester azoles into vacuoles only in the absence of dominant PDR transporters (Khandelwal et al. 2019). Based on the fact that *Cgcdr1Δ*/*Cgyor1Δ* cells become susceptible to azoles, we posit that azoles are substrates of *Cg*Yor1p. Also, while screening the phenotypes of MSY1- MSY7 strains, we observed a drastic increment in susceptibility to azoles after the last deletion *Cgyor1Δ* (Fig 4.17). To explore the *CgYOR1* role in azole resistance, we overexpressed MSY8/*CgYOR1* on azoles and observed resistant phenotype. Substrate competition with FLC and R6G in MSY8/*CgYOR1* demonstrated a reduction in R6G efflux by more than half which was in agreement with the above results. We noticed the reversal of sensitivity to all the tested

azoles. To further explore, we tested azoles susceptibility by hetrologously overexpressing *CgYOR1* in AD1-8U$^-$ strain (AD1-8U$^-$/*CgYOR1*), which also dislayed azole resistance phenotype (Fig 5.5). All of these results gave a confirmation of azoles as a substrate og CgYor1p in *C. glabrata*.

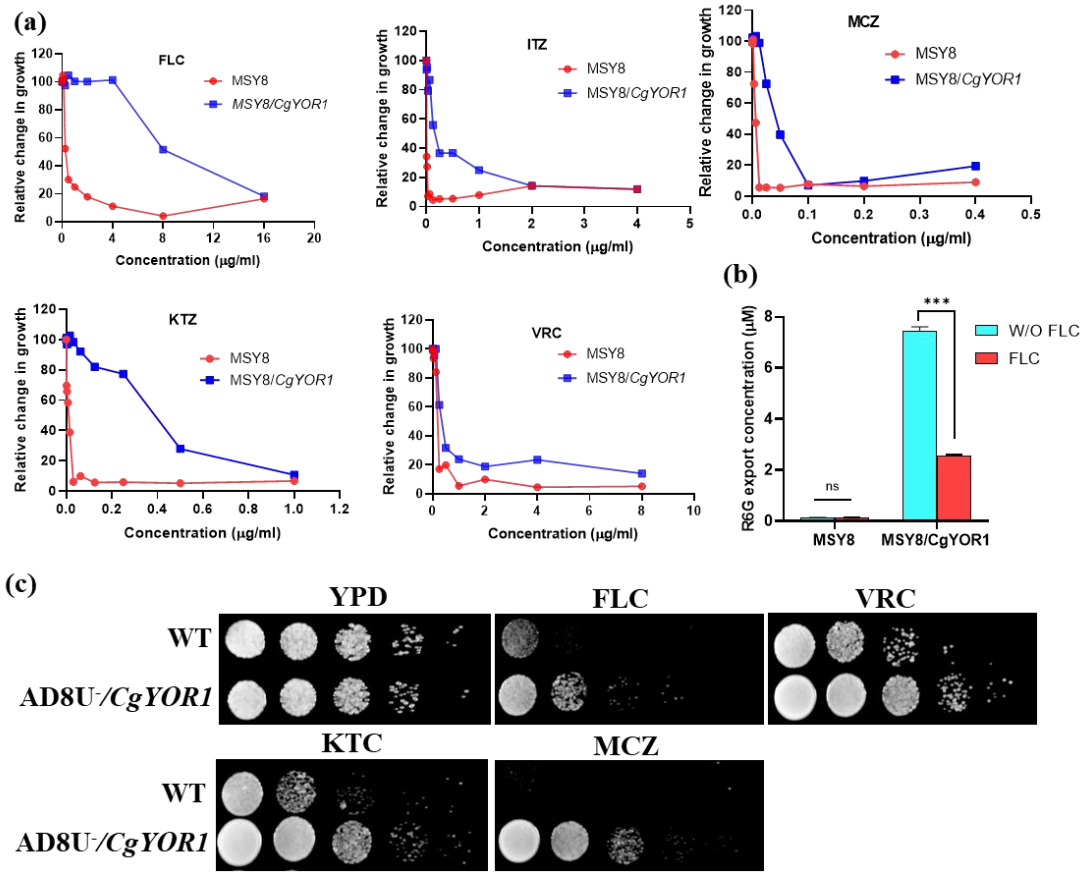

Fig 5.5 : Azoles as substrate of *CgYOR1*: (a) Overexpressing strain MSY8$^-$/*CgYOR1* showed reversal of FLC susceptibility (b) Efflux of R6G was determined in overexpressing strain in presence of 10x concentration of FLC reduced the export of R6G (c) Heterologous overexpression of *CgYOR1* further confirmed azole resistance.

5.6 *CgYOR1*Δ leads to ER stress and enhanced ROS generation

Azoles targets ER localized ERG11p by blocking the production of ergosterol that leads to its depletion from the membrane and increment in the accumulation of toxic sterol intermediate in the cell (Li et al. 2018). Recent independent studies in several pathogenic fungi do point a role of ER stress in influencing the antifungal resistance and pathogenesis (Miyazaki and Kohno 2014). ER stressors are shown to enhance the effect of azoles and show synergy with the antifungals that lead to defect in protein folding, Ca2+ homeostasis

and ROS generation (Chaillot et al. 2015) T. Miyazaki & Kohno, 2014). Azoles do increase ROS generation in *Candida* cells, albeit to different magnitudes. (Delattin et al. 2013).

In the following experiments, we explored these possibilities towards involvement in FLC sensitivity in *Cgyor1*∆ cells. We tested whether the target of azoles is being affected in Cgyor1∆ cells. In this context, the transcript levels of *ERG11, ERG3, ERG6, ERG4* and *ERG2* in Cgyor1∆ cells were assessed by qPCR. As evident from Supplementary Fig 3, there was no change in the expression levels of tested *ERG* genes, thus ruling out the possibility of any major change in the target or accumulation of toxic ergosterol in the membrane. The impact of *CgYOR1* deletion on ER stress was examined by exposing Cgyor1∆ cells to a well-known ER stress inducer, tunicamycin (TM). *Cgyor1Δ* mutant displayed enhanced susceptibility on TM, which was rescued in *Cgyor1∆/CgYOR1* revertant cells (Fig 6a). This pointed to an increased ER stress in *Cgyor1*∆ cells as was also observed in *Scyor1*∆ cells (Hernández-Elvira et al. 2019). The deletion of *Cgyor1Δ* also resulted in an increased sensitivity to H_2O_2, indicating defective oxidative stress management (Fig 5.6a). We checked the status of endogenous ROS production in the mutant *Cgyor1Δ* cells. ROS was quantitated by employing an oxidant sensitive fluorescent probe 2',7' –dichlorofluorescin diacetate (DCFDA) wherein its fluorescence intensity is directly proportional to ROS levels (Rastogi et al. 2010). By employing FACS analysis, we observed 30% raised fluorescence intensity of DCFDA dye in *Cgyor1*∆ cells as compared to WT cells and *Cgyor1*∆/*CgYOR1* revertant cells (Fig 5.6b). The confocal images well supported the FACS data (Fig 6c). Together, observed ER stress and ROS generation in the *Cgyor1*∆ cells prompted us to explore if these multiple effects can influence the target of rapamycin **(**TOR) and calcineurin signaling that can affect azole susceptibility.

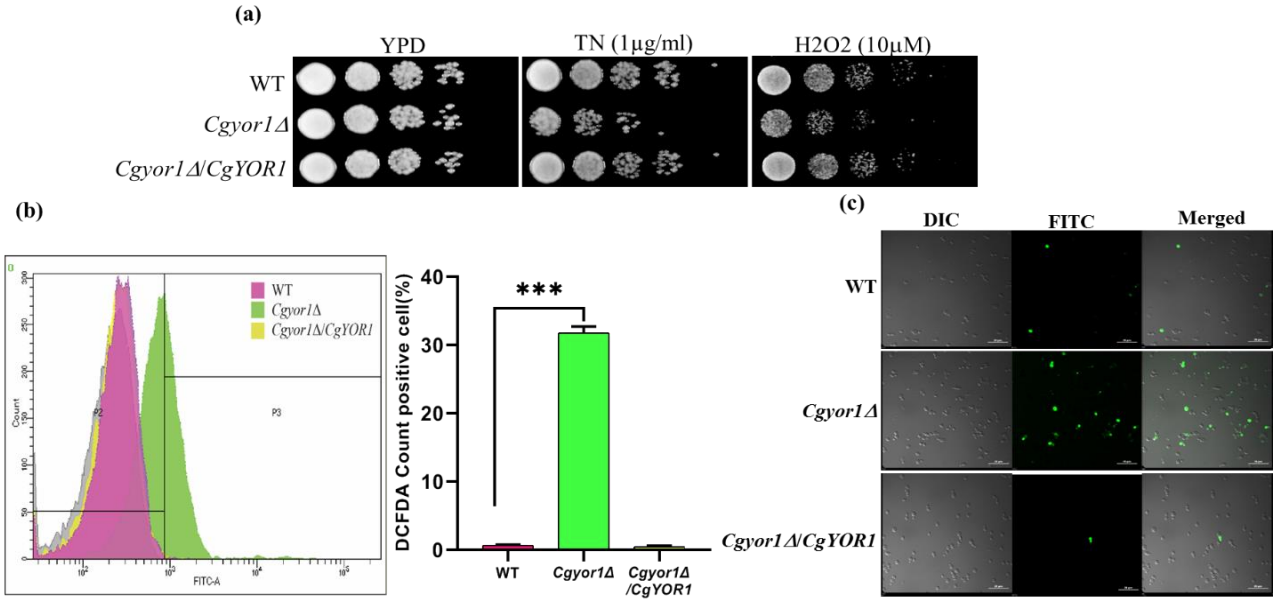

Fig 5.6: *Cgyor1*Δ leads to enhanced ER stress and ROS generation: The susceptibility of *Cgyor1*Δ and its revertant *Cgyor1*Δ/*CgYOR1* towards TM and H2O2 was tested by spot assays on solid agar media (a) *Cgyor1*Δ susceptibility to TM and H_2O_2 displayed increased ER stress and endogenous ROS generation (b) ROS measurement by DCFDA in WT, *Cgyor1*Δ, *CgYOR1* complemented strains (c) The confocal images of *Cgyor1*Δ and its revertant *Cgyor1*Δ/*CgYOR1* cells in presence of DCFDA.

5.7 Lack of *CgYOR1* suppresses TOR signaling

The target of rapamycin (TOR) is a highly conserved serine/threonine kinases that control cell growth in response to nutrients (Wedaman et al., 2003; Wullschleger et al., 2006). *C. glabrata* harbors two paralogs of TOR kinase (TOR1 and TOR2), which form two structurally and functionally distinct complexes: TOR complex 1 (TORC1) and TOR complex 2 (TORC2) (Jandric et al. 2013). TOR1 is rapamycin sensitive kinase that controls cell growth in response to nutrients by promoting anabolic processes such as translation and ribosome biogenesis while TOR2 is mainly controlled in response to changes in sphingolipid metabolism (Shertz et al. 2010; Shimobayashi et al. 2013). In *C. albicans* and *S. cerevisiae,* suppression of TOR kinases potentiate the activity of antifungal agents (Shekhar-Guturja et al. 2016b).

In the following, the involvement of TOR pathway was checked by comparing the growth of WT, *Cgyor1*Δ and *Cgyor1*Δ/*CgYOR1* cells in the presence of rapamycin (RAPA) using spot assays. The *Cgyor1*Δ mutant displayed increased susceptibility on RAPA, which

could be rescued by the revertant (*Cgyor1Δ/ CgYOR1*) cells (Fig 5.7a). Noticeably, the transcript levels of *CgYOR1* was 4-fold downregulated when WT cells were exposed to RAPA (Fig 5.7b) while no change was observed in transcripts levels of other ABC transporters encoding genes. To exclude the possibility if CgYor1p could transport RAPA, we performed a substrate competition efflux assay with R6G in the presence of 10X concentration of RAPA in MSY8/*CgYOR1* strain. The R6G efflux activity remained unchanged in the presence of RAPA in MSY8/*CgYOR1* cells, thus ruling out the possibility of RAPA being a substrate of CgYor1p (Fig 5.7c).

The involvement of TOR kinase in suppressing the growth of *Cgyor1Δ* mutant was validated by, monitoring transcript levels of some of the downstream genes (*KNS1, YPK1, LCB1* and *LCB2*) involved in the signaling cascade. *KNS1* is negatively regulated by TOR1 kinase and interestingly, the transcript of *KNS1* was upregulated in *Cgyor1Δ* cells, further confirming the suppression of TOR1 in *Cgyor1Δ* mutant cells (Fig 5.7d). Moreover, downregulation of both serine palmitoyltransferase (SPT) enzymes coding genes *LCB1* and *LCB2* was observed in *Cgyor1Δ* deletion which also suggest interference of TOR2 kinase. Both the TOR1 and TOR2 functions by their several downstream effector kinases such as ORM1/2, YPK1 and NPR1. TOR1 suppression further deactivate the NPR1 kinase and TOR2 inactivation activates YPK1 which can also be seen through the transcript expression. The upregulation of *YPK1* and 2-fold down regulation of NPR1 in *Cgyor1Δ* well supported TOR kinases involvement (Fig 5.7d).

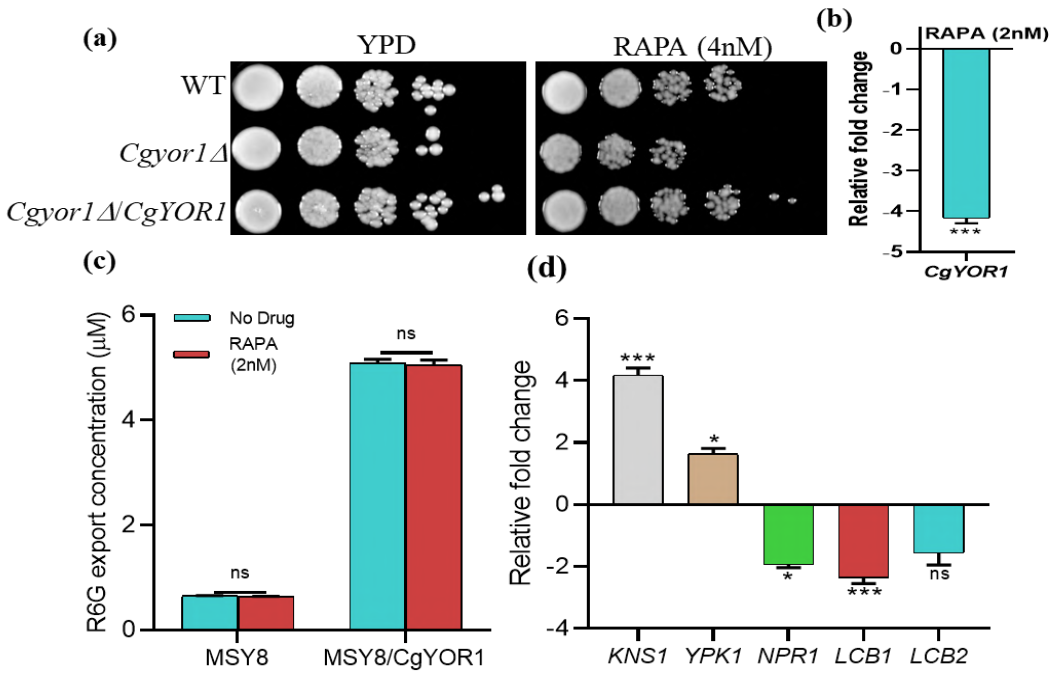

Fig 5.7: *Cgyor1*Δ deletion leads to TOR1 suppression: (a) The susceptibility of *Cgyor1*Δ and its revertant *Cgyor1*Δ*/ CgYOR1* towards RAPA was tested by spot assays on solid agar media. *Cgyor1*Δ mutant was susceptible on RAPA. The left panel of spot assays show an expression of *CgYOR1* transcript in the presence of RAPA (b) MSY8/*CgYOR1* shows a synergy between FLC and RARA (c) No reduction in R6G efflux was observed in substrate competition with RAPA (d) Transcriptional level expression of downstream TOR pathway genes *KNS1, YPK1, NPR1 LCB1* and *LCB2*.

5.8 Nitrogen depletion mimics TOR suppression and display enhanced susceptibility to azoles

Nitrogen (N_2) is an essential nutrient for yeast growth, and its availability or scarcity has numerous consequences on gene expression, signaling, and metabolism (Otsubo et al. 2017). N_2 source deficiency could have an impact on SNF1/AMP-activated protein kinase (AMPK), cAMP-dependent protein kinase (PKA), and target of rapamycin (TOR) signaling pathways that lead to substantial transcriptomic changes (Murai et al. 2009). It is established that N_2 starvation suppresses TOR kinases in several yeasts (Tesnière et al. 2017). To assess the impact of N_2 source, we grew *Cgyor1*Δ cells and its revertant *Cgyor1*Δ*/ CgYOR1* in N_2 replete (SD media with ammonium sulfate as a rich N_2 source) and N_2 deplete (SD media with 0.3µg/ml proline as a poor N_2 source) conditions as detailed in Methods. The drug susceptibility assays that followed after 5 h of growth in N_2

deplete conditions, revealed enhanced susceptibility of *Cgyor1*Δ cells to FLC that could be rescued partially in *Cgyor1*Δ*/CgYOR1* cells. In contrast, no change towards FLC susceptibility was noticed in mutant cells when grown under N_2 replete conditions (Fig 5.8a). Noticeably, no change in the FLC susceptibility in *Cgcdr1*Δ cells was observed in both N_2 deplete or replete conditions. In *Cgyor1*Δ cells grown under N_2 replete conditions, the transcript of *CgCDR1* was raised by 2.5 fold which might be a reason for no visible phenotype of the KO on azoles (Fig 5.8b). But in N_2 deplete condition, the transcripts of *CgCDR1* was downregulated by 4-fold in the *Cgyor1*Δ cells (Fig b). This data implies that *CgCDR1* is unable to mask the azole susceptibility phenotype of the *Cgyor1*Δ cells. Under N_2 depletion condition R6G efflux was reduced as compared to WT cells where it remained unchanged in N_2 replete condition again supporting the enhanced FLC susceptibility of *Cgyor1*Δ cells under N_2 depletion (Fig 5.8c). Together, data confirms the masking of *Cg*Yor1p by *Cg*Cdr1p and that azole susceptibility shown by *Cg*Yor1p is influenced by TOR kinases.

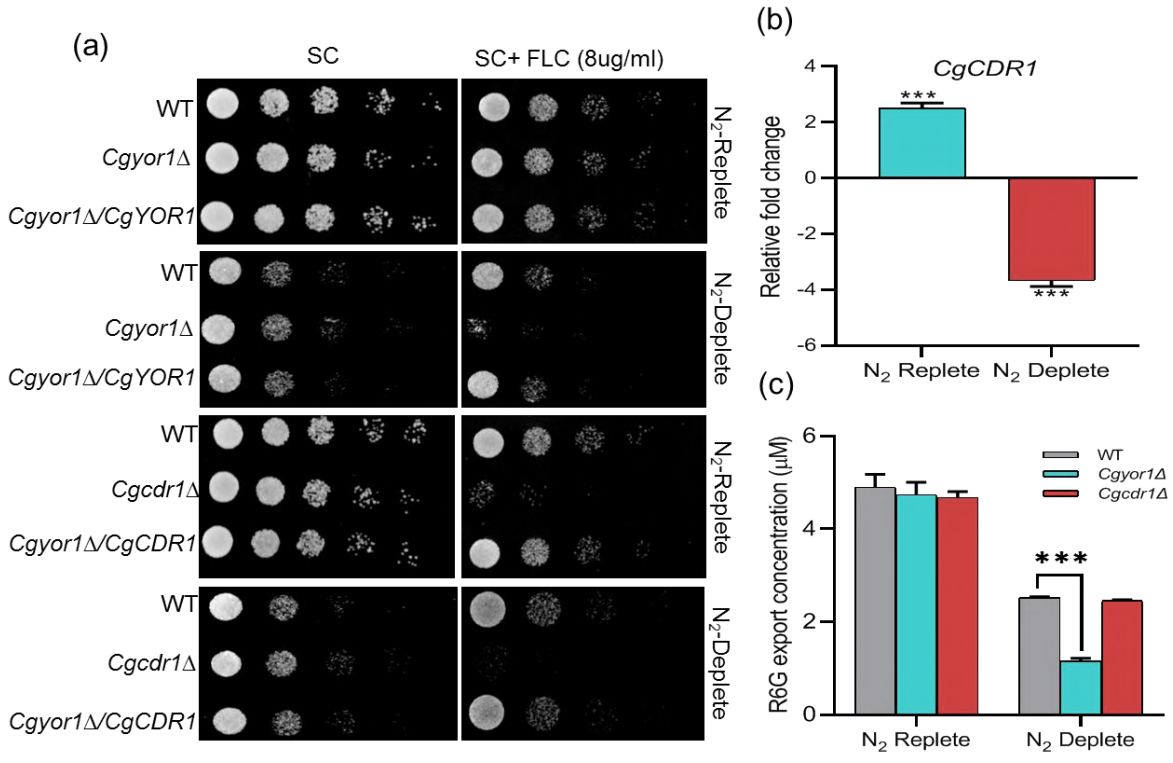

Fig 5.8: Nitrogen depletion condition reveal the function of Cgyor1p. To assess the impact of nitrogen source, *Cgyor1*Δ cells and its revertant *Cgyor1*Δ*/ CgYOR1* were in nitrogen replete condition (SD media with ammonium sulfate, rich nitrogen source) and nitrogen deplete condition (SD media with 0.3µg/ml

proline as a poor nitrogen source) as detailed in Methods.: (a) The susceptibility of *Cgyor1*Δ and its revertant *Cgyor1*Δ*/ CgYOR1* in N2 deplete condition as indicated was tested by spot assays on solid agar media. (b) Transcript level of *CgCDR1* and *CgPDH1* in *Cgyor1*Δ under N2 deplete and replete conditions (c) R6G efflux in N2 deplete and replete conditions.

5.9 Absence of *Cgyor1* suppresses calcineurin pathway

Calcineurin is a key downstream effector of TOR1 signaling is a mediator of various stress responses and plays a critical role in mediating drug resistance and virulence in various fungi including in *C. glabrata* (Steinbach et al., 2007; Miyazaki et al., 2010a). Calcineurin, a serine-threonine-specific protein phosphatase, is stabilized by molecular chaperon HSP90. A phosphorylated HSP90 by protein kinase CK2 destabilizes calcineurin. The KNS1 kinase phosphorylates regulatory subunit CKb2 of CK2, resulting in its activation. The active phosphorylated CKb2 in turn, phosphorylates HSP90 and suppresses the calcineurin which makes cells unable to combat various stresses. Previous independent reports have indicated that both of the regulatory and activation domain of protein kinase CK2 mutants are involved in azole resistance wherein the deletion of CKa1/2 and CKb1/2 make cells resistant to azoles implying higher activity of CK2 enhances azoles susceptibility. To check whether observed CK2 is activated in *Cgcdr1*Δ*/Cgyor1*Δ mutant has any effect on azole resistance, we constructed the regulatory subunit K/O strain in the background of *Cgcdr1*Δ*/Cgyor1*Δ (*Cgcdr1*Δ*/Cgyor1*Δ/*Cgckb1*Δ and *Cgcdr1*Δ*/Cgyor1*Δ/*Cgckb2*Δ). We observed that *Cgcdr1*Δ*/Cgyor1*Δ harboring any of the regulatory subunit mutation display reversal of azole susceptibility, implying the impact of protein kinase CK2 on *CgYOR1* mediated azole susceptibility (Fig 5.9a). The suppression of HSP90 by CK2 activation was also evident with its 2 fold down regulated transcript level in *Cgyor1*Δ cells along with downregulated calcineurin regulatory subunit transcript (cnb1) (Fig 5.9b). The suppressed calcineurin signaling cascade in *Cgyor1*Δ mutant was further confirmed when we tested calcineurin inhibitor FK520 susceptibility. We observed that *Cgyor1*Δ mutant cells showed increased susceptibility to FK520 (Fig 5.9c). The zinc-finger transcription factor Crz1, which regulates calcineurin function, its transcript was 6-fold downregulated in *Cgyor1*Δ mutant cells, which again implied a link between suppressed calcineurin and azole sensitivity.

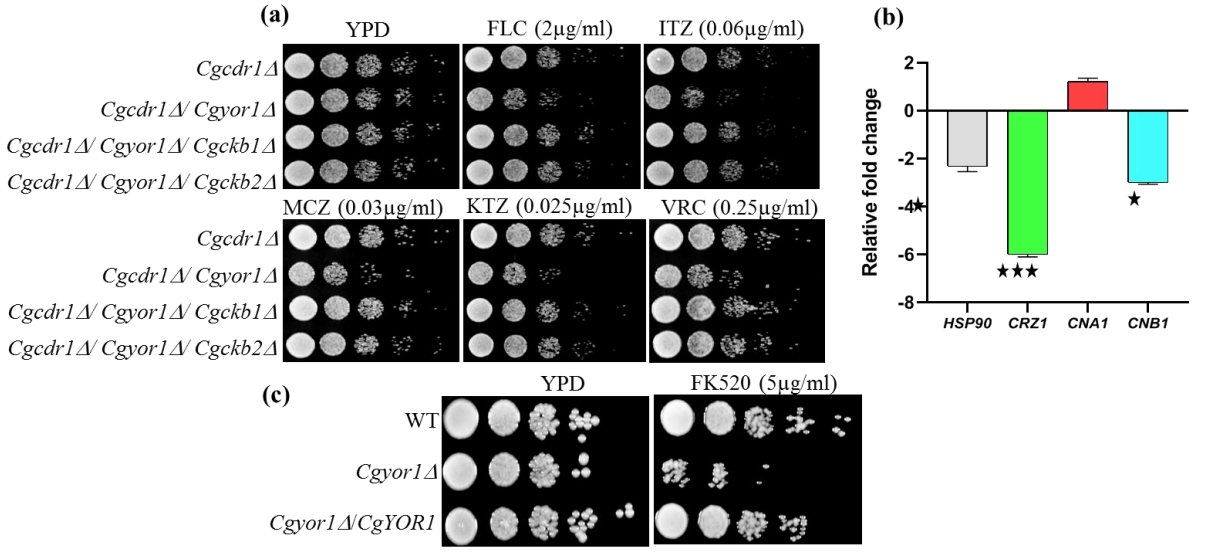

Fig 5.9: Calcineurin was suppressed in *Cgyor1*Δ: (a) Regulatory subunit (CKb1 and CKb2) of protein kinase CK2 deletion reverse the azole susceptible phenotype of *Cgcdr1*Δ*/Cgyor1*Δ (b) *Cgyor1*Δ was sensitive on calcineurin inhibitor FK520 (c) Transcript level expression indicates downregulation of HSP90 and transcription factor CRZ1, which regulates downstream calcineurin effectors.

5.10 Inhibition of sphingolipid biosynthesis in *Cgyor1* K/O mutant

Sphingolipids (SLs) which are important membrane biomolecules regulate various stress related singling pathways. Interestingly, *Cgyor1*Δ mutant cells were susceptible on myriocin (MYR) which blocks serine palmitoyltransferase (SPT), the initial step of sphingolipid formation and aureobasidin A (AbA) which inhibits inositol phosphorylceramide synthase (IPC), the key enzyme for complex sphingolipid formation (Fig 5.10a). Transcriptional level expression of most of sphingolipid pathway genes in *Cgyor1*Δ mutant was downregulated (Fig 5.10b). Together, the data suggest that TOR2 cascade is critical for *CgYOR1* mediated azole susceptibility.

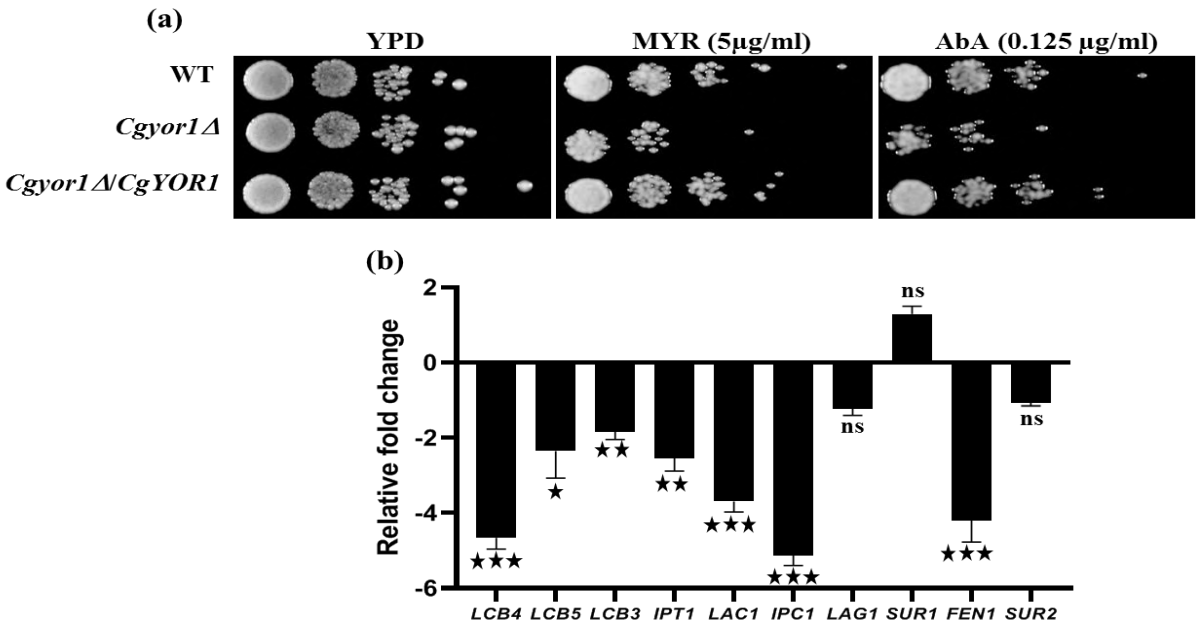

Fig 5.10: *Cgyor1* deletion affects sphingolipid homeostasis: (a) *Cgyor1*Δ mutant was susceptible on sphingolipid inhibitors MYR and AbA (b) RNA level expression indicated downregulation of sphingolipid synthesis pathway genes.

5.11 *Cgyor1*Δ deletion attenuates virulence in topical infection in neutropenic mice model.

ABC transporters are not only the mediators of azole resistance but also are involved in various physiological functions. For instance, upregulation of ABC transporters has been observed when cells are inside the macrophages in several fungi (Rosinha et al. 2002; Sanguinetti et al. 2006; Song et al. 2013). *C. neoformans yor1* mutant show attenuated nonlytic exocytosis during murine macrophage infection (Jung 2017). A report from *C. glabrata Cgyor1*Δ mutant also demonstrated reduced biofilm formation (Schwarzmüller et al. 2014). We explored the role of *Cgyor1*Δ impact on virulence in mouse model. For this, we employed a bioluminescent ATCC 2001 lucOPT 7/2/4 (strain WT BL) strain of *C. glabrata* strain, which has optimized the firefly luciferase gene under enolase promoter (p*ENO1*). (Persyn et al. 2019). This strain was earlier used in determining biofilms of *C. glabrata* on catheter implanted inside mice. We deleted Cgyor1 in this bioluminescent strain by using fusion PCR based method and designated it as *Cgyor1*Δ BL. For complementation studies, a WT copy of CgYOR1 was introduced as described in material and methods. These strains WT BL, *Cgyor1*Δ BL and *Cgyor1*Δ/CgYOR1 BL were used

to perform wound infection in mice model to assess the impact of *Cgyor1*Δ deletion. Balb/c mice were given two doses of cyclophosphamide on day -4 (150 mg/kg) and -1 (100 mg/kg) to make them neutropenic followed by wound infection on day 0. Infected mice were segregated into three groups (n = 5/group) where group 1 mice were treated with WT BL cells, group 2 mice were treated with *Cgyor1*Δ BL cells and group 3 with *Cgyor1*Δ*ICgYOR1* BL strain. The fungal load in the infections was quantified by CFU counts and by in vivo bioluminescence imaging. CFU quantification on day 4 with *Cgyor1*Δ BL cells recovered from the wound witnessed a significant reduction in fungal growth as compared to WT BL and *Cgyor1*Δ BL cells indicating attenuation of virulence by the *Cgyor1*Δ cells (Fig 11 a). Reduced bioluminescent signal in *Cgyor1*Δ infected wound confirmed *CgYOR1* contribution in the virulence (Fig 11b).

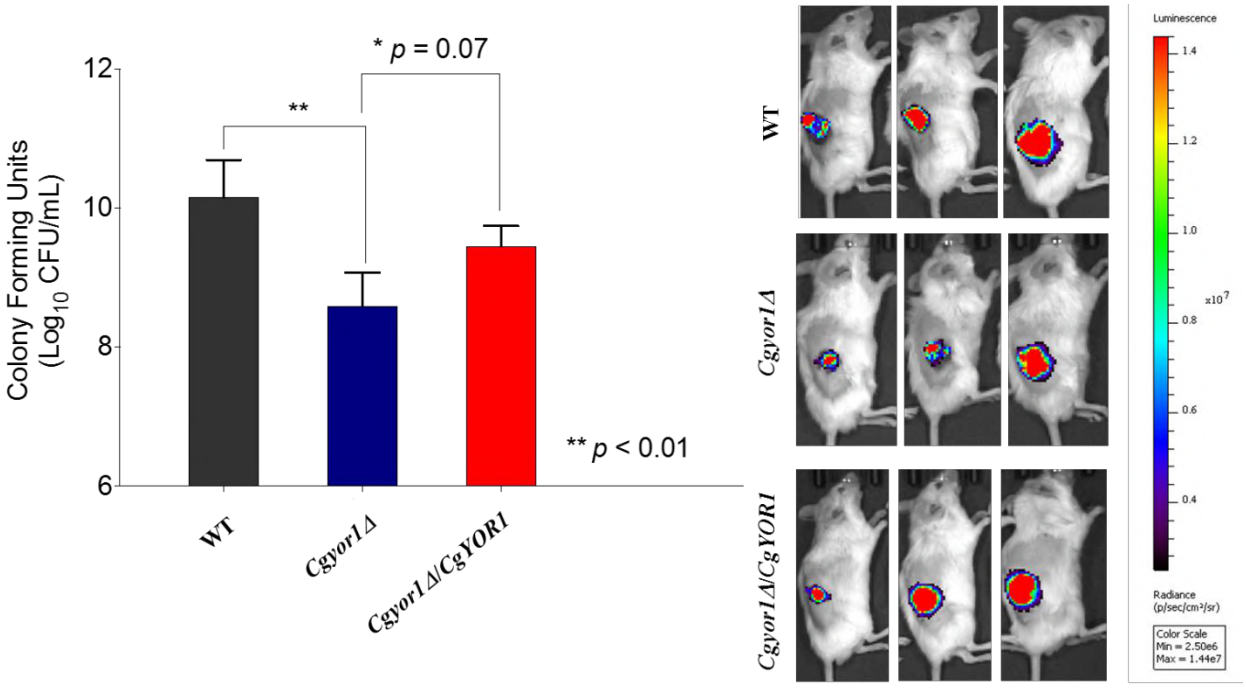

Fig 5.11: Attenuated virulence was observed in *Cgyor1*Δ: (a) CFU from skin tissue revealed reduced growth in mice infected with *Cgyor1*Δ mutant than WT and *CgYOR1* complemented strain (B) Luciferase expression after the infection by using luciferin as substrate. Increased luciferase displays higher infection.

5.12 Discussion and conclusion:

The redundancy of ABC transporters in Candida strongly hints at their multiple roles. This assertion is well supported by several independent reports. Thus ABC transporters, apart from being drug transporters, are also shown to govern membrane lipid translocation, endocytosis, maintenance of mitochondrial integrity and many virulence traits etc. (Prasad et al. 2016b; Rizzo et al. 2019). ABC transporters such as ScPDR5 CaCDR1, CaCDR2 and CaCDR3 are phospholipid translocators that maintain membrane asymmetry. MRP subfamily transporters (YOR1, YBT1, YCF1, MLT1 and BPT1) in diverse fungi are involved in transport of phosphatidylcholine (PC), phosphatidylethanolamine (PE), ions, bile salts and vacuolar detoxification (Decottignies et al. 1998; Jungwirth and Kuchler 2006; Paumi et al. 2009; Khandelwal et al. 2016). *CnAFR1* of *C. neoformans* and AbcB of *Aspergillus fumigatus* are required for pathogenesis (Orsi et al. 2009; Paul et al. 2013). Biofilms of genus Candida demonstrate an upregulation of ABC transporters indicating their potential role in biofilm formation and its resistance to antifungals (Chaturvedi et al. 2010; Fonseca et al. 2014; Jiang et al. 2016; Kean et al. 2018).

The abundance of ABC transporters also shown to mask functions of fellow member proteins. We attempted to look into the entire family of ABC membrane proteins of *C. glabrata,* wherein we created single null mutants of all 18 ABC proteins to assess their role as drug transporters. While our deletion library phenotypes confirmed the role of *CgCDR1* as major drug transporters of *C. glabrata*, we also discovered that *CgYOR1* contributes to azole resistance. However, this role of *CgYOR1* was only manifested in *Cgcdr1*Δ background. In order to examine masking affect by other member proteins, we created various combinations of single and double deletions of ABC proteins, but none could hide the function of *CgYOR1*. Interestingly, *CgYOR1* does not impact susceptibility to OMY and does not transport it; however, *Cgyor1*Δ cells turned susceptible to cyclic hexadepsipeptide natural product BEA which is also a well-known substrate of YOR1p. The functional complementation in *Scyor1*Δ with *CgYOR1* also could not restore OMY susceptibility while it could do so in the case of BEA. That OMY is not a substrate of *CgYOR1* was well supported by dose response matrix, which demonstrated that BEA and OMY could potentiate FLC activity but the same was not evident in *Cgcdr1*Δ cells. The

efflux studies wherein efflux of a test substrate R6G could be competed out by BEA and by OMY further supported our observation that *CgYOR1* unlike in other yeasts does not transport OMY. *CgYOR1*, however, does transport FLC as was evident by its ability to restore FLC and other tested azoles resistance in overexpressed MSY8/*CgYOR1* and AD1-8U^{-}/*CgYOR1* cells. This was further reinforced by the fact FLC could also compete with R6G efflux in the MSY8/*CgYOR1* cells.

The azole resistance imparted by major transporters *CgCDR1* and *CgPDH1* are well regulated by TF *CgPDR*1 (Caudle et al. 2011). CgPDR1 acts through binding to the PDRE site at the promoter region of genes and controls several genes. Some of the common drug transporters that have PDRE site includes PDR subfamily ABC transporters *CgCDR1, CgPDH1 and CgSNQ2,* MRP subfamily ABC transporters *CgYBT1and CgYOR1, and* Major Facilitator Superfamily transporter *CgQDR2 etc*. in *C. glabrata* (Vermitsky and Edlind 2004; Tsai et al. 2010a; Caudle et al. 2011). TF PDR1 regulon also indicated the upregulation of five ABC transporters (Tsai et al. 2010a). Multiple gain of function (GOF) mutations in TF CgPDR1 have been reported in different clinical isolates of *C. glabrata* which increases MICs of antifungals (Ferrari et al. 2009b; Vale-Silva et al. 2013b). Notably, a report in azole-resistant clinical isolate of *C. glabrata* demonstrated a drastic decrease in FLC MIC to as low as 2 µg/ml from 256 µg/ml after *CgPDR1* deletion, however, single deletion of *Cgcdr1*Δ in the same strain could lower FLC MIC only to 16 µg/ml and triple deletions of *Cgcdr1*Δ*, Cgpdh1*Δ and *Cgsnq2*Δ resulted FLC MIC_{80} to decrease to 8 µg/ml (Whaley et al. 2018). These observations strongly points that to additional undiscovered regulators influencing drug resistance in *C. glabrata*. A summary of the chapter's work is represented in Fig 5.12.

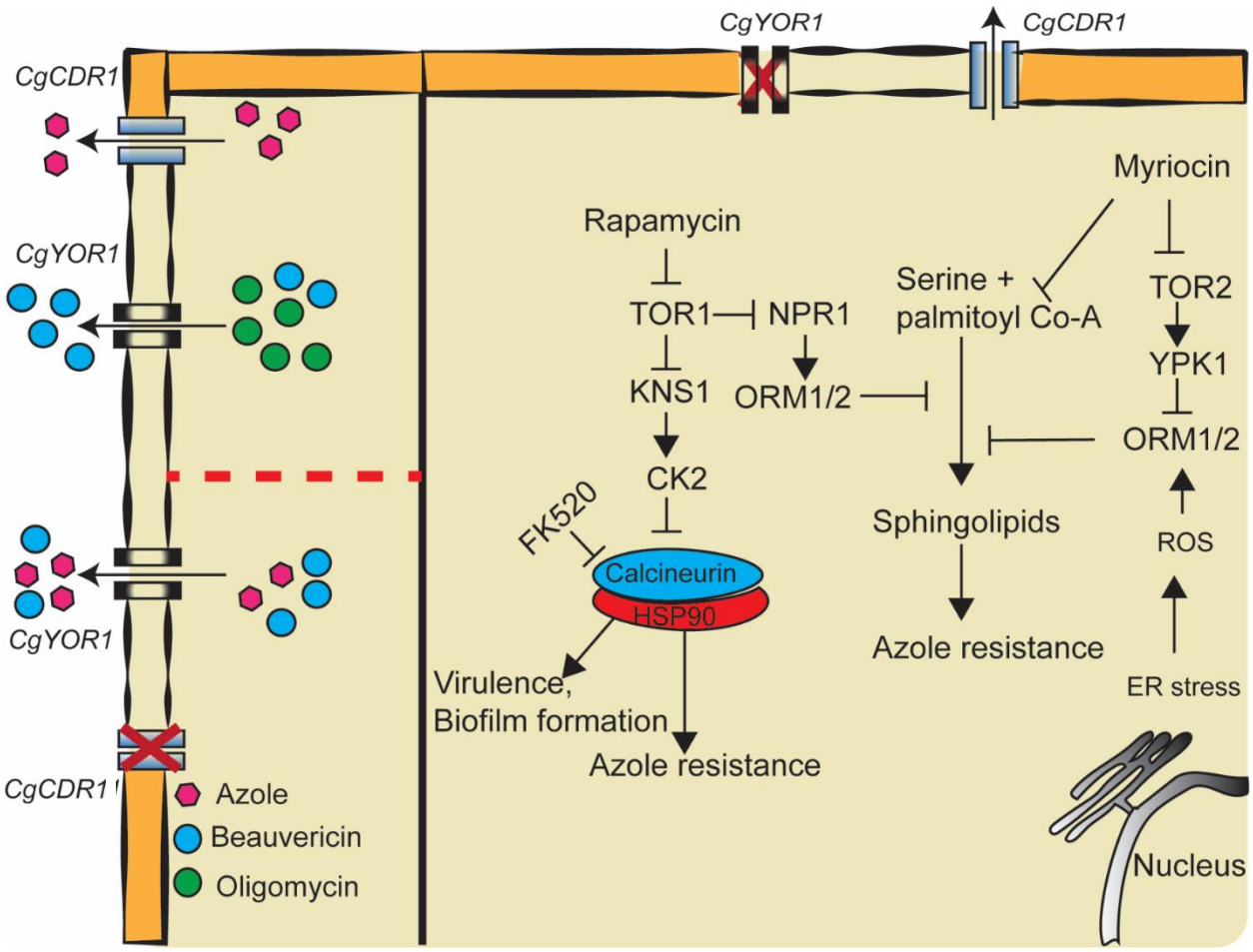

Fig 5.12: Model to explain the functional characterization of CgYOR1.

Similar to other yeasts, *CgPDR1* appear to regulate both ABC and MFS transporter genes in *C. glabrata*, however, there are several reports which hints to alternate strategies which yeasts adopt in bestowing drug resistance. Recently TOR kinases, Calcineurin and their downstream signaling is shown to influence azole resistance in *C. albicans* and *S. cerevisiae* (Shekhar-Guturja et al. 2016b, c). Our observations do show that both TOR1 and TOR2 kinases and its downstream signaling have important roles in manifesting *CgYOR1* mediated azole resistance. A direct link with TOR kinases was evident from the fact that while the deletion of *CgYOR1* and N_2 starvation independently suppresses TOR signaling resulting in increased susceptibility towards azoles, *CgCDR1* under similar conditions had no impact on azole susceptibility. Together, we show that *CgYOR1* function which remains masked by the presence of dominant transporters like *CgCDR1,* does not transport OMY but contributes to azole resistance via ROS generation, suppressed TOR and calcineurin signaling culminating in attenuated virulence.

SUMMARY

6. Summary

A large number of population has been identified to be affected by fungal infections worldwide. Most of the fungal infection remains superficial but some develop into invasive mycoses (Pfaller and Diekema 2007b). Leading cause of invasive mycoses include various species of *Candida, Aspergillus* and *Cryptococcus* infections among people showing any type of immunosuppression such as post-surgery and neutropenic patients (Badiee and Hashemizadeh 2014). The use of broad spectrum antifungal agents, use of chemotherapy, radiotherapy, immunosuppressive agents and disruption of the mucosal layer are the prevalent factor for invasive mycoses (Ramage et al. 2012). *Candida* is the fourth most common human pathogen (more than 90% of invasive infections) recovered from blood cultures in patients (Delaloye and Calandra 2014). Historically among *Candida* species isolated from human, *C. albicans* is the most prevalent species (Megri et al. 2020). Apart from *C. albicans*, recent epidemiological data reveals the emergence of other non-*albicans Candida* isolates such as *C. glabrata* in fungal Infection (Richardson and Lass-Flörl 2008). *C. glabrata* is an innoxious commensal of normal microbiota present in the oral cavity, gastrointestinal and genital tract in humans. *C. glabrata* can be responsible for various clinical manifestations like mucosal and bloodstream infections (Fidel et al. 1999). *C. glabrata* infection is higher in adults as compared to children (Steinbach 2016).

The genome of *C. glabrata* consists of 13 chromosomes (12.3Mb) (Dujon et al., 2004). Despite of having similarity in pathogenesis with *C. albicans*, it is phylogenetically distant from *C. albicans* and closer to *S. cerevisiae* (Barns et al. 1991, Dujon et al., 2004). *C. glabrata* is haploid despite showing similarities in mating genes with *S. cerevisiae* (Boisnard et al. 2015). During the course of evolution *C. glabrata* also lost some metabolic pathways completely (Dujon et al., 2004, Butler et al., 2009). Regardless of the fact that *C. glabrata* lacks various virulence factors, it shows a high resistance towards azoles among clinical isolates (Pfaller et al. 2014). In comparison to other *Candida* species, *C. glabrata* acquires resistance rather at a faster rate to echinocandins, which were introduced only recently (Dellière et al. 2016, p. 1). The acquisition of MDR towards various classes of antifungals poses a serious clinical threat to the treatment of candidiasis. There are two superfamilies of efflux proteins: Major facilitator family proteins

(MFS proteins) and ATP binding cassette proteins (ABC proteins). ABC proteins substrate range is broad, ranging from antifungal drugs to several unrelated chemicals (Lefèvre and Boutry 2018).

ABC superfamily is a well-studied family of transporter protein from prokaryotes to higher eukaryotes. ABC transporters are known to translocate a variety of substrates through biological membrane energizing by ATP hydrolysis (Wilkens 2015). Basic structure of ABC transporter consists of TMD and NBD. The NBD has some conserved idiotypic sequence motif, which are ABC signature sequence, walker A motif and walker B motif (Schmees et al., 1999, Rajendra et al., 2015). These two motifs are separated by about 120 amino acids residues (Walker et al., 1982; Manisha et al., 2005). NBDs, which are the source of energy of ABC transporter, are localized in the cytoplasmic face and utilized energy by hydrolyzing ATP for substrate translocation. Two NBDs and two TMDs are most prerequisite requirements to become a functional ABC transporter (Wilkens 2015). Half transporters with one NBD and one TMD need to form homodimers or heterodimers to become functional. (Hyde et al. 1990). These ABC genes can be divided into various subfamilies on the basis of the topology of TMD and NBD. There are 6 subfamilies of ABC proteins in yeast: ABCB (MDR), ABCC (MRP), ABCD (ALDp), ABCF (YEF3), ABCE (RL1) and ABCG (PDR). The proteins belonging to YEF3 and RL1 do not contain TMD, and are soluble ABC proteins other proteins belonging to PDR, MDR, MRP and ALDp subfamilies contain both TMD and NBD and are membrane transporters (Rajendra, et al., 2015).

Our inventory identified 25 putative ABC proteins in the genome of *C. glabrata*. Out of these 25 ABC proteins, only 18 contain TMD in their topological structure, making them candidates for membrane transporter. All the 18 ABC transporters encoding genes showed constitutive expression, which confirmed their genomic presence and also reflected their biological relevance. The exposure to antifungal drugs presented variable transcriptional response among ABC membrane proteins and also provided sufficient information for their potential contribution in emerging clinical drug resistance in *C. glabrata* isolates. Noteworthy is that majority of members of ABC subfamilies transporters in *C. glabrata* are unexplored for their function.

In order to study their potential role, we created a mini-library of knockouts of all membrane ABC transporters. The deletion of each of the genes in *C. glabrata* resulted in viable strains; however, *Cgatm1*Δ represented slow growth as compared to WT. The deletion of most of the ABC transporters displayed no visible change in drug susceptibility. Only *CgCDR1*, *CgSNQ2,* and *CgATM1* knockout mutants displayed influence on their growth in the presence of antifungals. The results indicated the masking effect of one transporter towards others.

Being its haploid nature, ABC transporter studies in *C. glabrata* offers some advantages. Also plasmid based study in this organism makes this system a good model organism for research. In order to study the ABC transporters in a homologous overexpression background, we developed a system an endogenous expression system in *C. glabrata* without the masking effect of major transporter MSY8. MSY8 was constructed by disrupting seven ABC transporters from the genome, which are localized either in the plasma membrane or in the vacuolar membrane and introduction of a GOF mutation in the TF *CgPDR1* factor in the genome, which ultimately causes overexpression of *CgCDR1* locus. This followed the construction of an integration-based plasmid for cloning GOI at the activated *CgCDR1* locus. The utilization of the expression system was well demonstrated by overexpressing fully functional clinically relevant ABC drug transporters of *C. glabrata* (*CgCDR1* and *CgPDH1*)*, C. albicans* (*CaCDR1*), *S. cerevisiae* (*ScPDR5*) and *C. glabrata* MFS transporter *CgFLR1*. This MSY8 system thus presents a good platform for detailed substrate profiling and functional analysis of membrane transporters with minimum interference by other drug transporters of *C. glabrata*.

CgYOR1 transcript has been earlier reported to be upregulated in various azole-resistant clinical isolates of *C. glabrata*, however, its single deletion did not change susceptibility to any of the tested azoles. While screening MSY1-MSY7 strains, the sudden drop in azoles MIC_{80} of the strains after *Cgyor1* deletion prompted us to study its role. Importantly, *Cgyor1*Δ showed no change in susceptibility towards oligomycin, which is otherwise a well-known substrate of *YOR1* in other yeasts. However, *CgYOR1* role in azole susceptibility only became evident when major transporter *CgCDR1* was deleted. Thus *Cgyor1*Δ/*Cgcdr1*Δ cells turned highly susceptible to azoles while still displaying no change in susceptibility towards oligomycin. Notably, *Cgyor1*Δ cells also showed

increased susceptibility to rapamycin and FK520, proposing involvement of TOR signaling and calcineurin pathways in impacting azole susceptibility. Additionally, in nitrogen depleted condition which suppresses TOR kinase, *Cgyor1*Δ demonstrated azole sensitive phenotype independent of CgCdr1p. The deletion of *Cgyor1* also displayed attenuated virulence in an immunosuppressed mouse model. Collectively, our findings showed that the TOR and calcineurin signaling govern *CgYOR1* mediated azole susceptibility and virulence in *C. glabrata*.

In conclusion, we inventoried putative ABC transporters in *C. glabrata* and showed their presence in the genome. Transcriptional responses by ABC transporters encoding genes displayed by transient induction of drugs indicated towards their involvement in drug transport, however, majority of single deletion mutants did not show any phenotype on antifungal. It suggested the interference of other transporter in the development of single deletion phenotype. The construction of MSY8 strain and its hyper-expression system relieved this constrain, where there is no making effect by major transporters in homologous background. We have also found an ABC transporter CgYor1p that actually, works after major transporter CgCdr1p and also it has functions independent of CgCdr1p. The study also opened a window to further characterization of lesser explored ABC transporters.

SUPPLEMENTARY MATERIALS

7. Supplementary files

7.1: Primers used in the study

Table 7.1: List of primers used in the study for gene deletion, plamid construction and RT-PCR.

Primers used in gene deletions		
Primer name	**Sequences (5'-3')**	**Description**
5'NAT HALF_F	CGTACGCTGCAGGTCGACGCCTTCC GCTGCTAGGCGCGCCGTG	5' NAT Half amplification forward primer
5'NAT HALF_R	TCTGTTCCAACCAGAATAAG	5' NAT Half amplification reverse primer
3'NAT HALF_F	GTCTACTACTTTGGATGATAC	3' NAT Half amplification forward primer
3'NAT HALF_R	CTACGAGACCGACACCGTCGGGCCG CTGACGAAGT	3' NAT Half amplification reverse primer
SNQ2_5' UTR_F	CTTCCAAGAAAATTGTCAGG	5' UTR amplification forward primer for *CgSNQ2* gene
SNQ2_5' UTR_R	GCGTCGACCTGCAGCGTACGTGTTTC ACTCGTTATTGCAG	5' UTR amplification reverse primer for *CgSNQ2* gene
SNQ2_3' UTR_F	CGACGGTGTCGGTCTCGTAGATGCA CTGTACTGCATTTTTACAAC	3' UTR amplification forward primer for *CgSNQ2* gene
SNQ2_3' UTR_R	GGTTATATTGGGTCTACCTGGTG	3' UTR amplification reverse primer for *CgSNQ2* gene
AUS1_5' UTR_F	CTCGTACTGGTGCTTATACCATTC	5' UTR amplification forward primer for *CgAUS1* gene
AUS1_5' UTR_R	GCGTCGACCTGCAGCGTACGGCCAA AGACATCTTATATTTCCC	5' UTR amplification reverse primer for *CgAUS1* gene
AUS1_3' UTR_F	CGACGGTGTCGGTCTCGTAGGACTA AGAGTGACTCCTACAAGC	3' UTR amplification forward primer for *CgAUS1* gene
AUS1_3' UTR_R	TTTGTGTAAGAACTGCGTAACGTC	3' UTR amplification reverse primer for *CgAUS1* gene
CDR1_5' UTR_F	GTACGTGCTGTCCTCTCAGATC	5' UTR amplification forward primer for *CgCDR1* gene
CDR1_5' UTR_R	GCGTCGACCTGCAGCGTACGTGTTA CTTTTCTTTACTTTG	5' UTR amplification reverse primer for *CgCDR1* gene
CDR1_3' UTR_F	CGACGGTGTCGGTCTCGTAGTTTATT TAGCCTGCGCTCAT	3' UTR amplification forward primer for *CgCDR1* gene
CDR1_3' UTR_R	CAAGACTATTACTGAATTCCTGC	3' UTR amplification reverse primer for *CgCDR1* gene
PDH1_5' UTR_F	CACTCTGCACTTTGCACTCTG	5' UTR amplification forward primer for *CgPDH1* gene
PDH1_5' UTR_R	GCGTCGACCTGCAGCGTACGGTCAT CGGGTGTGTTCATCAC	5' UTR amplification reverse primer for *CgPDH1* gene
PDH1_3' UTR_F	CGACGGTGTCGGTCTCGTAGACATCA GAATTCAGTGACG	3' UTR amplification forward primer for *CgPDH1* gene
PDH1_3' UTR_R	CTATAGAACCGGGATGTTATG	3' UTR amplification reverse primer for *CgPDH1* gene
YCF1_5' UTR_F	TCGAATGGGTGCGTAGTAGTTACC	5' UTR amplification forward primer for *CgYCF1* gene

YCF1_5' UTR_R	GCGTCGACCTGCAGCGTACGATTGTT AAAACCCAATAGGAATAT	5' UTR amplification reverse primer for *CgYCF1* gene
YCF1_3' UTR_F	CGACGGTGTCGGTCTCGTAGGAAAT GTGTATAATACCGCAAATG	3' UTR amplification forward primer for *CgYCF1* gene
YCF1_3' UTR_R	GCATTAGCCACGCAAAGGTACTAG	3' UTR amplification reverse primer for *CgYCF1* gene
YBT1_5' UTR_F	CCCCTTCCACGGGATCTATTATG	5' UTR amplification forward primer for *CgYBT1* gene
YBT1_5' UTR_R	GCGTCGACCTGCAGCGTACGACTGA ATTGTTTTATTGGTAGTG	5' UTR amplification reverse primer for *CgYBT1* gene
YBT1_3' UTR_F	CGACGGTGTCGGTCTCGTAGAAGAT CATTATCCTATTTCATTTG	3' UTR amplification forward primer for *CgYBT1* gene
YBT1_3' UTR_R	CAGATCGCTCATACAACTAGAGACTC	3' UTR amplification reverse primer for *CgYBT1* gene
YOR1_5' UTR_F	CGACGAAGCTACAGAATCC	5' UTR amplification forward primer for *CgYOR1* gene
YOR1_5' UTR_R	GCGTCGACCTGCAGCGTACGGGCTG AGTCTTTCCTGAGC	5' UTR amplification reverse primer for *CgYOR1* gene
YOR1_3' UTR_F	CGACGGTGTCGGTCTCGTAGGCATA ACTGTAGATGACTTTC	3' UTR amplification forward primer for *CgYOR1* gene
YOR1_3' UTR_R	ATTGATACTCCAGTTAGAG	3' UTR amplification reverse primer for *CgYOR1* gene
STE6_5' UTR_F	ATTCGTGTACTTTCTTAGTCAACTG	5' UTR amplification forward primer for *CgSTE6* gene
STE6_5' UTR_R	GCGTCGACCTGCAGCGTACGTTGTTT TGGTTGTCGAATAGTACG	5' UTR amplification reverse primer for *CgSTE6* gene
STE6_3' UTR_F	CGACGGTGTCGGTCTCGTAGAACATC GATAACTATTTTACG	3' UTR amplification forward primer for *CgSTE6* gene
STE6_3' UTR_R	CTGAAGAACCCCTCACACAACTTG	3' UTR amplification reverse primer for *CgSTE6* gene
PDR12_ 5'UTR_F	GTGGATCAGAAAGTGCCTACTC	5' UTR amplification forward primer for *CgPDR12* gene
PDR12_ 5'UTR_R	GCGTCGACCTGCAGCGTACGAGGCA TTCTAAGTCAGATTCTTTAC	5' UTR amplification reverse primer for *CgPDR12* gene
PDR12_ 3'UTR_F	CGACGGTGTCGGTCTCGTAGCTCTTT CTTTCACCTAACTAATGAC	3' UTR amplification forward primer for *CgPDR12* gene
PDR12_ 3'UTR_R	GAATAATACGTCCCAAAGTCACATG	3' UTR amplification reverse primer for *CgPDR12* gene
MDL2_5' UTR_F	GAAGGAGTTGCAGACGCCAGCTG	5' UTR amplification forward primer for *CgMDL2* gene
MDL2_5' UTR_R	GCGTCGACCTGCAGCGTACGGTCCT ATTCAGCAGCGGTTGTC	5' UTR amplification reverse primer for *CgMDL2* gene
MDL2_3' UTR_F	cgacggtgtcggtctcgtagCTAGAAGGAGTT CACATAATTAGTAC	3' UTR amplification forward primer for *CgMDL2* gene
MDL2_3' UTR_R	CACTCCAACACATCACAGAGGTC	3' UTR amplification reverse primer for *CgMDL2* gene
ATM1_5' UTR_F	TCAGATAGTTGCGAATAGTGGGAC	5' UTR amplification forward primer for *CgATM1* gene
ATM1_5' UTR_R	GCGTCGACCTGCAGCGTACGGCACC ACCTATAAGCATTGTTTG	5' UTR amplification reverse primer for *CgATM1*gene
ATM1_3' UTR_F	CGACGGTGTCGGTCTCGTAGGTCTAT CTAAAAATCTCAAATTCCC	3' UTR amplification forward primer for *CgATM1* gene
ATM1_3' UTR_R	GTCTTGGGTGATATCTTACGCAAC	3' UTR amplification reverse primer for *CgATM1* gene
MDL1_5' UTR_F	CCTATAGTCACGAACTCATTTGTAGT G	5' UTR amplification forward primer for *CgMDL1* gene

MDL1_5' UTR_R	GCGTCGACCTGCAGCGTACGCTTATA TCCAATCAAGTCCCATGTAAAC	5' UTR amplification reverse primer for *CgMDL1* gene
MDL1_3' UTR_F	CGACGGTGTCGGTCTCGTAGGTCTG GAACATCATAAATAGGATCC	3' UTR amplification forward primer for *CgMDL1* gene
MDL1_3' UTR_R	CCCCCAATATCTAGTTACCTCTC	3' UTR amplification reverse primer for *CgMDL1* gene
PXA2_5' UTR_F	CAGTAGAAGCCTTACAAATCCAC	5' UTR amplification forward primer for *CgPXA2* gene
PXA2_5' UTR_R	GCGTCGACCTGCAGCGTACGCTTGG TAGTAAGTATTGTACAGA	5' UTR amplification reverse primer for *CgPXA2* gene
PXA2_3' UTR_F	CGACGGTGTCGGTCTCGTAGCATAAC ATGATCTGCATCTG	3' UTR amplification forward primer for *CgPXA2* gene
PXA2_3' UTR_R	CAAAAGGTTTATTACATTCGGATC	3' UTR amplification reverse primer for *CgPXA2* gene
PXA1_5' UTR_F	GAATTTCCCAAAGAGGGACCAG	5' UTR amplification forward primer for *CgPXA1* gene
PXA1_5' UTR_R	GCGTCGACCTGCAGCGTACGCGTAT ACCATCCATCGTTTTGG	5' UTR amplification reverse primer for *CgPXA1* gene
PXA1_3' UTR_F	CGACGGTGTCGGTCTCGTAGGTTTAA GGAATAAGTCGACATGAG	3' UTR amplification forward primer for *CgPXA1* gene
PXA1_3' UTR_R	GAA AAG AGA CAT GAA GAG AAG GAC	3' UTR amplification reverse primer for *CgPXA1* gene
VMR1_5' UTR_F	GATACAGTAAGAATTCTCTTCAATACC	5' UTR amplification forward primer for *CgVMR1* gene
VMR1_5' UTR_R	GCGTCGACCTGCAGCGTACGGTTTC CTGATATTCCCTCTTTGTTC	5' UTR amplification reverse primer for *CgVMR1* gene
VMR1_3' UTR_F	CGACGGTGTCGGTCTCGTAGAATTGC TCACAGATTGAGGTCAG	3' UTR amplification forward primer for *CgVMR1* gene
VMR1_3' UTR_R	ATATGAGAGTATCTACTATGTATGATC C	3' UTR amplification reverse primer for *CgVMR1* gene
BPT1_5' UTR_F	GACTCCGGTAGTTCTTAAGGATAC	5' UTR amplification forward primer for *CgBPT1* gene
BPT1_5' UTR_R	GCGTCGACCTGCAGCGTACGGGTTG AAGCTTAGGAATTGTCAG	5' UTR amplification reverse primer for *CgBPT1* gene
BPT1_3' UTR_F	CGACGGTGTCGGTCTCGTAGAGACA GGACTATTTTGACAATTGC	3' UTR amplification forward primer for *CgBPT1* gene
BPT1_3' UTR_R	GGGTCGAACCCATAATCTTCTG	3' UTR amplification reverse primer for *CgBPT1* gene
ROA1_5' UTR_F	CATACTGGTGAATGCCAACGAAG	5' UTR amplification forward primer for *CgROA1* gene
ROA1_5' UTR_R	GCGTCGACCTGCAGCGTACGTATGTT CTGTCGAAATGGTCATC	5' UTR amplification reverse primer for *CgROA1* gene
ROA1_3' UTR_F	CGACGGTGTCGGTCTCGTAGCATAAC TGTCTAAATAAGTAATCAC	3' UTR amplification forward primer for *CgROA1* gene
ROA1_3' UTR_R	AGCGCTAGTGAAACCATGACTGTC	3' UTR amplification reverse primer for *CgROA1* gene
ADP1_5' UTR_F	CAATACGTGGTAGTCACATGTGTAC	5' UTR amplification forward primer for *CgADP1* gene
ADP1_5' UTR_R	GCGTCGACCTGCAGCGTACGGTATC GTCTTGTATCGTAGTATCGTC	5' UTR amplification reverse primer for *CgADP1* gene
ADP1_3' UTR_F	CGACGGTGTCGGTCTCGTAGCAGGA CTCTGCTCACAATAGAATTAC	3' UTR amplification forward primer for *CgADP1* gene
ADP1_3' UTR_R	TACGACCATAAGATACGAACCATACC	3' UTR amplification reverse primer for *CgADP1* gene
CKB1_5' UTR_F	CAACTCATTTTCTTCCTTGTTG	5' UTR amplification forward primer for *CgCKB1* gene

CKB1_5' UTR_R	GCGTCGACCTGCAGCGTACGCTAAG ATAGGGATATTAGAAC	5' UTR amplification reverse primer for *CgCKB1* gene
CKB1_3' UTR_F	CGACGGTGTCGGTCTCGTAGTAGTA GATGGTATGACAACTAG	3' UTR amplification forward primer for *CgCKB1* gene
CKB1_3' UTR_R	AGC CGG GAT GAA GTA AGA GAG	3' UTR amplification reverse primer for *CgCKB1* gene
CKB2_5' UTR_F	CGAAGCGTTGAATCCGTTAC	5' UTR amplification forward primer for *CgCKB1* gene
CKB2_5' UTR_R	GCGTCGACCTGCAGCGTACGGTCAT GGTATCACTTAATATC	5' UTR amplification reverse primer for *CgCKB2* gene
CKB2_3' UTR_F	CGACGGTGTCGGTCTCGTAGCTCCG TTAATAATATTTGCCG	3' UTR amplification forward primer for *CgCKB2* gene
CKB2_3' UTR_R	CAATTTAGGGCTGCTCTAGCTC	3' UTR amplification reverse primer for *CgCKB2* gene
Primers used in confirmation of gene deletion		
NAT_INT _F	TGCGCACGTCAAGACTGTCAAGG	5' integration confirmation common reverse primer
NAT_INT _R	TGTGAATGCTGGTCGCTATACTGC	3' intergation confirmation common forward primer
SNQ2_U PS_F	CTCTTCTAGGTAATAACTTC	5' integration confirmation forward primer for *CgSNQ2* gene
SNQ2_U PS_R	ACCTTTCGCTATACTAAGCAC	3' integration confirmation reverse primer for *CgSNQ2* gene
SNQ2_IN T_F	CTGGTGGTGTTGAAGGTGAAATC	Gene internal confirmation forward primer for *CgSNQ2* gene
SNQ2_IN T_R	CAGCAATGGAGACACGCTTACG	Gene internal confirmation reverse primer for *CgSNQ2* gene
AUS1_U PS_F	CCGTACAAGTGTCCTGCCATTCG	5' integration confirmation forward primer for *CgAUS1* gene
AUS1_U PS_R	CTGTTGTACGTAATGGGTCATGTG	3' integration confirmation reverse primer for *CgAUS1* gene
AUS1_IN T_F	TGGTAATCACATCAACCCAGAG	Gene internal confirmation forward primer for *CgAUS1* gene
AUS1_IN T_R	GACCACTAAGCAGAACTTGAAAC	Gene internal confirmation reverse primer for *CgAUS1* gene
CDR1_U PS_F	GATTAGCCTTCGTTTACATGTTGGC	5' integration confirmation forward primer for *CgCDR1* gene
CDR1_U PS_R	AACATTGCTCATGTCTGGTGGGC	3' integration confirmation reverse primer for *CgCDR1* gene
CDR1_IN T_F	CGATGACTACAACCCAAGATTG	Gene internal confirmation forward primer for *CgCDR1* gene
CDR1_IN T_R	GACACGCTTACGTTCACCAC	Gene internal confirmation reverse primer for *CgCDR1* gene
PDH1_U PS_F	TGCACAGCAGCAACGGAGTATCCC	5' integration confirmation forward primer for *CgPDH1* gene
PDH1_U PS_R	CAACCAATAGTGAGAGTACAGTGTG	3' integration confirmation reverse primer for *CgPDH1* gene
PDH1_IN T_F	CAACAGCGATGAGTTCTCCAG	Gene internal confirmation forward primer for *CgPDH1* gene
PDH1_IN T_R	CGACCTTTGTGTCCCTTGTG	Gene internal confirmation reverse primer for *CgPDH1* gene
YCF1_U PS_F	TGACTAAGCAGCGTGAGAGGTGC	5' integration confirmation forward primer for *CgYCF1* gene
YCF1_U PS_R	GGTGCAGAGAGAGAGTCACAACC	3' integration confirmation reverse primer for *CgYCF1* gene

YCF1_INT_F	GGTACCAGAGATCTGTGGAGAC	Gene internal confirmation forward primer for *CgYCF1* gene
YCF1_INT_R	TTGTGGCCTAGTTCCCAACCTCC	Gene internal confirmation reverse primer for *CgYCF1* gene
YBT1_UPS_F	GCTAGACCCATCCCAAATTTACTGC	5' integration confirmation forward primer for *CgYBT1* gene
YBT1_UPS_R	GATCAATACCGCGACCGTGGAGTC	3' integration confirmation reverse primer for *CgYBT1* gene
YBT1_INT_F	GCAATGGCCTGACAGTGGTAAG	Gene internal confirmation forward primer for *CgYBT1* gene
YBT1_INT_R	CAGTACTAACCAAATTGACACGC	Gene internal confirmation reverse primer for *CgYBT1* gene
YOR1_UPS_F	GGAATCAGTGGAGTCGCGCGGAAC	5' integration confirmation forward primer for *CgYOR1* gene
YOR1_UPS_R	CTCTACGGATTACTGTCGAATTCGG	3' integration confirmation reverse primer for *CgYOR1* gene
YOR1_INT_F	GTGAAGATAGGTTACAAGAGAAC	Gene internal confirmation forward primer for *CgYOR1* gene
YOR1_INT_R	GATCAGCACTGATCTCGCCTG	Gene internal confirmation reverse primer for *CgYOR1* gene
STE6_UPS_F	TCATGGAAGTCCTCATCTGTGATC	5' integration confirmation forward primer for *CgSTE6* gene
STE6_UPS_R	TACTGGGGACACACCAGCCATGG	3' integration confirmation reverse primer for *CgSTE6* gene
STE6_INT_F	CTATGGATTTAAACTCGTGCTGAC	Gene internal confirmation forward primer for *CgSTE6* gene
STE6_INT_R	TAGACCACTTGTTAATATCGCAGG	Gene internal confirmation reverse primer for *CgSTE6* gene
PDR12_UPS_F	TTCAATCTCGGCTGGTACCTTTTG	5' integration confirmation forward primer for *CgSTE6* gene
PDR12_UPS_R	CAAGATAGCTGTAACTCAACCTCAAC	3' integration confirmation reverse primer for *CgSTE6* gene
PDR12_INT_F	CAAGGTATCGAACCAGGTGACTC	Gene internal confirmation forward primer for *CgPDR12* gene
PDR12_INT_R	GTTCTGGACAGTAAATGACATAGCC	Gene internal confirmation reverse primer for *CgPDR12* gene
MDL2_UPS_F	GACTTCCTGCGAAAAGCTGGTGC	5' integration confirmation forward primer for *CgMDL2* gene
MDL2_UPS_R	GACTGGATACCTCGATCCCCGTAG	3' integration confirmation reverse primer for *CgMDL2* gene
MDL2_INT_F	GGTGATACTGAGTGCATCTGTC	Gene internal confirmation forward primer for *CgMDL2* gene
MDL2_INT_R	CAGTAAGGTCACCAATAGTCAGG	Gene internal confirmation reverse primer for *CgMDL2* gene
ATM1_UPS_F	CTTAGCACCGAAGAGCAATTTGCG	5' integration confirmation forward primer for *CgATM1* gene
ATM1_UPS_R	GCGATGGAGTCACCTTTGTGATTTC	3' integration confirmation reverse primer for *CgATM1* gene
ATM1_INT_F	GATGAAACTTGACTTAGGCTGGC	Gene internal confirmation forward primer for *CgATM1* gene
ATM1_INT_R	CAACCCATATACATCATTCCGG	Gene internal confirmation reverse primer for *CgATM1* gene
MDL1_UPS_F	ATGTAACTATTGGATGCGAAATGCCC	5' integration confirmation forward primer for *CgMDL1* gene
MDL1_UPS_R	GCCCTCTTCGGCAATACCAAAGC	3' integration confirmation reverse primer for *CgMDL1* gene

MDL1_INT_F	GAACTCCCTAAAAACTGTGCAAGCG	Gene internal confirmation forward primer for *CgMDL1* gene
MDL1_INT_R	GTTGAATGTGATAGGTAACCC	Gene internal confirmation reverse primer for *CgMDL1* gene
PXA2_UPS_F	TGGCCCTACAAAAGTAGCTTCC	5' integration confirmation forward primer for *CgPXA2* gene
PXA2_UPS_R	GCAAAGAAGTTCAAGACTCAACCT	3' integration confirmation reverse primer for *CgPXA2* gene
PXA2_INT_F	GGTCAATGGATGGTATTAGGTATACC	Gene internal confirmation forward primer for *CgPXA2* gene
PXA2_INT_R	GGATCGGAACCAACTTTCAAGAG	Gene internal confirmation reverse primer for *CgPXA2* gene
PXA1_UPS_F	CGACGTCGCACCCTACTCCAAGAAC	5' integration confirmation forward primer for *CgPXA1* gene
PXA1_UPS_R	CTACAGAGTCCACAGATGTTAC	3' integration confirmation reverse primer for *CgPXA1* gene
PXA1_INT_F	CCTACATCCTCTAAGAAGAATAAGAAG	Gene internal confirmation forward primer for *CgPXA1* gene
PXA1_INT_R	GCAAGAACCTCCTGCCACGGCCG	Gene internal confirmation reverse primer for *CgPXA1* gene
VMR1_UPS_F	TCAACTGTCCCCCCTTCCTGATCC	5' integration confirmation forward primer for *CgVMR1* gene
VMR1_UPS_R	GTTTTCCTATTGTTGGTTGCTGTCGG	3' integration confirmation reverse primer for *CgVMR1* gene
VMR1_INT_F	CCTGGTAACCTATGGTCTGTATCGTTC	Gene internal confirmation forward primer for *CgVMR1* gene
VMR1_INT_R	CAGCCATCAAATTGATAATAGCCCC	Gene internal confirmation reverse primer for *CgVMR1* gene
BPT1_UPS_F	GCAGGAACACATCAAGTTGTAAAAC	5' integration confirmation forward primer for *CgBPT1* gene
BPT1_UPS_R	GGCTAATTCAACCACAGATGCAG	3' integration confirmation reverse primer for *CgBPT1* gene
BPT1_INT_F	CCTCTTTCATTATCGAGTCCTTTAC	Gene internal confirmation forward primer for *CgBPT1* gene
BPT1_INT_R	AAGCTTCTAAGTAATAGTGGTTGC	Gene internal confirmation reverse primer for *CgBPT1* gene
ROA1_UPS_F	ATTCAGAAGTTACTCCTCAACC	5' integration confirmation forward primer for *CgROA1* gene
ROA1_UPS_R	GATCGAAGCAGTTTCATCTAGG	3' integration confirmation reverse primer for *CgROA1* gene
ROA1_INT_F	CGCATAGAGGACTTTCAGGAGGTG	Gene internal confirmation forward primer for *CgROA1* gene
ROA1_INT_R	CAACTATTGCACCCATCACCACG	Gene internal confirmation reverse primer for *CgROA1* gene
ADP1_UPS_F	TACTGTAGTGGCCTGCGCTTGTC	5' integration confirmation forward primer for *CgADP1* gene
ADP1_UPS_R	GTCCCTTTACATAGCAGGCTGGTG	3' integration confirmation reverse primer for *CgADP1* gene
ADP1_INT_F	GTGCTACCGCGGAGGTGCCC	Gene internal confirmation forward primer for *CgADP1* gene
ADP1_INT_R	CTTGAGGGTCATATCGGGACTCCTG	Gene internal confirmation reverse primer for *CgADP1* gene
CKB1_UPS_F	TGCGTAGTTATCCTGCGCAG	5' integration confirmation forward primer for *CgCKB1* gene
CKB1_UPS_R	CTAGGTCTCAACATATGATTCAG	3' integration confirmation reverse primer for *CgCKB1* gene

CKB1_INT_F	CGCAGGAAGTGCCACACTAC	Gene internal confirmation forward primer for *CgCKB1* gene
CKB1_INT_R	GTATCTCGGACAAGTACCG	Gene internal confirmation reverse primer for *CgCKB1* gene
CKB2_UPS_F	CTGTATATCTCCGCGACTCC	5' integration confirmation forward primer for *CgCKB2* gene
CKB2_UPS_R	CAGAATCGGTTACTGGATCTAGTC	3' integration confirmation reverse primer for *CgCKB2* gene
CKB2_INT_F	CTGTGACGTCGATCCAGAATAC	Gene internal confirmation forward primer for *CgCKB2* gene
CKB2_INT_R	CTGTGTCTAGATGACTTAGG	Gene internal confirmation reverse primer for *CgCKB2* gene
Primers used in revertants construction		
REV1	TTAGTTTTGCTGGCCGCATCTTCTTATTCCTTTGCCCTCGGACGAGTGC	HphB amplication forward primer
REV2	GGAAACGAAGATAAATCATGGGTAAAAAGCCTGAACTC	HphB amplication reverse primer
REV3	GTTCAGGCTTTTTACCCATGATTTATCTTCGTTTCC	pGRB2.3 vector amplification forward primer for marker replacement
REV4	GCACTCGTCCGAGGGCAAAGGAATAAGAAGATGCGGCCAGCAAAAC	pGRB2.3 vector amplification reverse primer for marker replacement
REV5	ATGGAGCTCCAGCTTTTGTTC	pGRB2.3_HphB vector amplification forward primer for revertant construction
REV6	ATGTCTAAAGGTGAAGAATTATTCAC	pGRB2.3_HphB vector amplification reverse primer for revertant construction
REV7	GAACAAAAGCTGGAGCTCCATCAAGAACCAGTAGTGGGTAGTG	YCF1 Forward primer
REV8	TAATTCTTCACCTTTAGACATATGCTGCAAACCAGCTTCTTTACTC	YCF1 Reverse primer
REV9	GAACAAAAGCTGGAGCTCCATGTGTCCCCAGAACCACCCGTAG	YOR1 Forward primer
REV10	TAATTCTTCACCTTTAGACATTGGAAAGTCATCTACAGTTATG	YOR1 Reverse primer
REV11	GAACAAAAGCTGGAGCTCCATGCGCATCAGAAAGACATTTCC	AUS1 Forward primer
REV12	TAATTCTTCACCTTTAGACATGTCCTTGGATGCTCTAGACTTG	AUS1 Reverse primer
REV13	GAACAAAAGCTGGAGCTCCATGTAGCCGCCTTTCCCGATAG	YBT1 Forward primer
REV14	TAATTCTTCACCTTTAGACATTTTCTTGGAATCAGAGTTC	YBT1 Reverse primer
REV15	GAACAAAAGCTGGAGCTCCATACAGAAAACAGTCTATGGGACCAC	PDH1 Forward primer
REV16	TAATTCTTCACCTTTAGACATGAAGGGAATTAACCTTCTAAT	PDH1 Reverse primer
REV17	GAACAAAAGCTGGAGCTCCATCAAAGTAGCGCATGGAAATCC	CDR1 Forward primer
REV18	TAATTCTTCACCTTTAGACATTTTCTTGGCAAGTTTACCAG	CDR1 Reverse primer
REV19	GAACAAAAGCTGGAGCTCCATGAACGGAGATTCTGTACGCCAG	SNQ2 Forward primer
REV20	TAATTCTTCACCTTTAGACATGTTGGACTTCTTCCCCCTC	SNQ2 Reverse primer
REV21	GAACAAAAGCTGGAGCTCCATGAACAATGGCTTAATCACTG	ATM1 Forward primer

REV22	TAATTCTTCACCTTTAGACATGATAGACTTGTTTAGCTTTTCTAG	ATM1 Reverse primer
REV23	GAACAAAAGCTGGAGCTCCATACCACTGACGATCCAAGTAGC	PDR12 Forward primer
REV24	TAATTCTTCACCTTTAGACATAAATTTTTGCTTCACTTTTTCTTC	PDR12 Reverse primer
REV27	GAACAAAAGCTGGAGCTCCATCTTAACGAATAGTGAATTGGTTC	STE6 Forward primer
REV28	TAATTCTTCACCTTTAGACATTAAGTTAAGAAGTTTTCGAAATTC	STE6 Reverse primer
REV29	GAACAAAAGCTGGAGCTCCATAGATGTTCCTGTCATGTACAG	MDL1 Forward primer
REV30	TAATTCTTCACCTTTAGACATTTTATGATGTTCCAGACCCTC	MDL1 Reverse primer
REV31	GAACAAAAGCTGGAGCTCCATTCTACCAAGACGCAGTCTCG	PXA2 Forward primer
REV32	TAATTCTTCACCTTTAGACATTGTTTTCTTTTTCTGCTTC	PXA2 Reverse primer
REV33	GAACAAAAGCTGGAGCTCCATCATGTAGAAGTTCAAAGGTC	MDL2 Forward primer
REV34	TAATTCTTCACCTTTAGACATGAGGTTTTCATCTTTTTGTAGC	MDL2 Reverse primer
REV35	GAACAAAAGCTGGAGCTCCATAGTCGCAAGGCCTCGTTATC	PXA1 Forward primer
REV36	TAATTCTTCACCTTTAGACATAACAACGGATAATTTTCTAATC	PXA1 Reverse primer
REV37	GAACAAAAGCTGGAGCTCCATAGGTTAATTACTGATCCCAGTTC	VMR1 Forward primer
REV38	TAATTCTTCACCTTTAGACATCTCCGCATTCATTTTTTTAAC	VMR1 Reverse primer
REV39	GAACAAAAGCTGGAGCTCCATAGAACTATTGCCTGCAGAAGAC	BPT1 Forward primer
REV40	TAATTCTTCACCTTTAGACATTGTTCTGTTCTTTAAATAGCCTCC	BPT1 Reverse primer
REV41	GAACAAAAGCTGGAGCTCCATACACAATGCCCTTGAAACTTAC	ROA1 Forward primer
REV42	TAATTCTTCACCTTTAGACATCCATTTCAGCCATTCAAGTTTTG	ROA1 Reverse primer
REV43	GAACAAAAGCTGGAGCTCCATACTCTGATGAAGACACGCTTGTC	ADP1 Forward primer
REV44	TAATTCTTCACCTTTAGACATTTGTTCTACTACTATTAATTTC	ADP1 Reverse primer
Primers used in overexpression plasmids construction		
OE 1	CGCGAATCGATCTGCGCTCATAATCTGGCTCTG	CgCDR1 terminator forward primer with ClaI site
OE 2	CGCGAGGTACCTGAATGCCTTGTTGTGAATAC	CgCDR1 terminator reverse primer with KpnI site
OE 3	CGCGAGAGCTCCACCGTGGGAGAAAGGGAC	CgCDR1 promoter forward primer with SacI site
OE 4	CGCGACCGCGGGCTTAATTAAGCTTTTCTTTACTTTGTATATATC	CgCDR1 promoter reverse primer with SacII site
OE 5	CGCGAACTAGTATGTCTAAAGGTGAAGAATTATTC	YeGFP forward primer with SpeI site
OE 6	CGCGACCCGGGCCTTTACCTCTATATCGTGTTCG	YeGFP reverse primer with XmaI site

OE 7	CGCGAATCGATAGACAGTGTGCATAGCCTG	CgPDR1 terminator forward primer with ClaI site
OE 8	CGCGAGGTACCCACTCATAGACATGGGTGCTG	CgPDR1 terminator reverse primer with KpnI site
OE 9	CGCGAGAGCTCTCCCGCAACCAGACAAAGAC	CgPDR1 ORF with promoter and terminator amplification forward primer with SacI site
OE 10	CGCGACCGCGGCACTTACAAGATAGTCAATC	CgPDR1 ORF with promoter and terminator amplification reverse primer with SacII site
OE 11	CGCGATTAATTAAATGCCCGAGGCCAAGCTTAAC	Forward primer for cloning ScPDR5 with PacI site
OE 12	CGCGAGCGGCCGCTTTCTTGGAGAGTTTACCGTTC	Reverse primer for cloning ScPDR5 with NotI site
OE 13	CGCGATTAATTAAATGTCAGATTCTAAGATGTCGTC	Forward primer for cloning CaCDR1 with PacI site
OE 14	CGCGAGCGGCCGCTTTCTTATTTTTTTTCTCTCTGTTAC	Reverse primer for cloning CaCDR1 with NotI site
OE 15	CGCGATTAATTAAATGTCTCTTGCAAGTGACAAG	Forward primer for cloning CgCDR1 with PacI site
OE 16	CGCGAGCGGCCGCTTTCTTGGCAAGTTTACCAGATTTC	Reverse primer for cloning CgCDR1 with NotI site
OE 17	CGCGATTAATTAAATGAACACACCCGATGACTC	Forward primer for cloning CgPDH1 with PacI site
OE 18	CGCGAGCGGCCGCGAAGGGAATTAACCTTCTAAT	Reverse primer for cloning CgPDH1 with NotI site
OE 19	CGCGATTAATTAAATGAATTATCTTCATAATTTTAAAG	Forward primer for cloning CgFLR1 with PacI site
OE 20	CGCGAGCGGCCGCCCTGTTGTATTTAGACATGGAAC	Reverse primer for cloning CgFLR1 with NotI site
OE 21	CGCGATTAATTAAATGACGATTACCGTGGGGGATG	Forward primer for cloning ScYOR1 with PacI site
OE 22	CGCGAGCGGCCGCAACTTCTGTTCTCGAAATCATTTTC	Reverse primer for cloning ScYOR1 with NotI site
OE 23	CGCGATTAATTAAATGCTCAGGAAAGACTCAGC	Forward primer for cloning CgYOR1 with PacI site
OE 24	CGCGAGCGGCCGCTTGGAAAGTCATCTACAGTTATG	Reverse primer for cloning CgYOR1 with NotI site
OE 25	CGCGATTAATTAAATGACACCCCCACCTAATTCAG	Forward primer for cloning CaYOR1 with PacI site
OE 26	CGCGAGCGGCCGCAAAACCCAGTAGCTTCTTGGAAAT	Reverse primer for cloning CaYOR1 with NotI site
OE 27	CACTATAGGGCGAATTGGAGCTC	Forward primer to amplifying whole cassette
OE 28	CTAAAGGGAACAAAAGCTGGGTACC	Reverse primer to amplifying whole cassette
Real time Primers		
RT1	CTTTATATGAGGCAAGACC	PDH1 Forward primer
RT2	GAAGTTCACCAGGAAATAG	PDH1 Reverse primer
RT3	GTCACCATACACTTACTTC	AUS1 Forward primer
RT4	CAACCATCCACCATATTC	AUS1 Reverse primer
RT5	CTGTACCTCTGAACTTCT	ATM1 Forward primer
RT6	CCATCACTCTTGCTTATAC	ATM1 Reverse primer
RT7	TCTTACGTGCTCTTACTC	YOR1 Forward primer
RT8	CCATTAGTAGGCCAATTATC	YOR1 Reverse primer
RT9	TGATGGCTGTAAGACTATG	CDR1 Forward primer

RT10	TCCATACTTCGTGGTAATC	CDR1 Reverse primer
RT11	GATCCAGGTGACTCTTATAC	SNQ2 Forward primer
RT12	GATCCAGGTGACTCTTATAC	SNQ2 Reverse primer
RT13	CCTCTTCTACTGGTGATATTG	YCF1 Forward primer
RT14	CCCACATAGAATGACCTAAA	YCF1 Reverse primer
RT15	GTCGACTATGACAAGATTC	YBT1 Forward primer
RT16	ATCCAACTCTCCACTATC	YBT1 Reverse primer
RT17	CTCTCACGTATGCTATTTC	VMR1 Forward primer
RT18	AGTAGTGATAGTACCTTCG	VMR1 Reverse primer
RT19	CTAAGAGTCCTAAGTGAAAG	MDL2 Forward primer
RT20	GAACGAGATACCACATAAG	MDL2 Reverse primer
RT21	CCAACACTATTCAACGATAC	STE6 Forward primer
RT22	TTCCACCAGAACCTATTC	STE6 Reverse primer
RT23	CTTTAATGGATCACCAGAG	ROA1 Forward primer
RT24	CTGGTCTTAGAGTGTATTTC	ROA1 Reverse primer
RT25	CACAGGAAGGAAACTATG	BPT1 Forward primer
RT26	GAGAGAGCATCTTCTAGT	BPT1 Reverse primer
RT27	CACGATAAGAAGGTTGTATG	PDR12 Forward primer
RT28	CACTATATGGGCAGTAGTT	PDR12 Reverse primer
RT29	GGGTTACCTATCACATTC	MDL1 Forward primer
RT30	GACCCAGTCCTATAATAAC	MDL1 Reverse primer
RT31	CCTCCCAGCTATTCTATTC	PXA1 Forward primer
RT32	CTAGTCTTGCGACAAATAAG	PXA1 Reverse primer
RT33	CGAAATTCCTGGGTATAAG	ADP1 Forward primer
RT34	GGTGATTGAGACACATAC	ADP1 Reverse primer
RT35	GGTGTTCAGCAAAGATTAG	PXA2 Forward primer
RT36	CAGACAGATATAACCGAGAT	PXA2 Reverse primer
RT37	TAACTTCGTCTTCCCTAAC	ERG11 Forward primer
RT38	GTGGAGTTCTTCATCAATTC	ERG11 Reverse primer
RT39	CCACGGTAGATACGCTGGTG	TDH3 Forward primer
RT40	CAG AAC CCC ATG GCA AGT TAG C	TDH3 Reverse primer
RT41	GAACTATCTTCAACCATCC	ERG3 Forward primer
RT42	AGTACAGCTTAGAGTATCC	ERG3 Reverse primer
RT43	GCTTTGCCAACCATCAAGTATG	PGK1 Forward primer
RT44	CAACTGGAGCCAAGGAGTATTT	PGK1 Reverse primer
RT45	GAACAGTACTTGGCATACAT	ERG6 Forward primer
RT46	TGGTAGTCGTTGTTGTTTAG	ERG6 Reverse primer
RT47	CAATGGTGTACTTGCCAAAC	ERG2 Forward primer
RT48	CATCTCTGGTGTACTCGTTAAT	ERG2 Reverse primer
RT49	ACTTGAAACCTGAGGAAATC	ERG4 Forward primer
RT50	CGCAATTCTACCACCATAAA	ERG4 Reverse primer
RT51	GAAGGTGGTGCTCAAGATAAG	HSP90 Forward primer

RT52	CTGGAAGCGAAAGAAGATGG	HSP90 Reverse primer
RT53	TACAAGGTAAGACACAAAC	KNS1 Forward primer
RT54	CTATCACAAGACTCCATTAC	KNS1 Reverse primer
RT55	TGGTAAAGTGATGCAGGTAAG	YPK1 Forward primer
RT56	AGGATTGTTCTCTCTGCTAATG	YPK1 Reverse primer
RT57	TCGAACAACGGTTCGAATAA	CRZ1 Forward primer
RT58	TTCCCACAAACTTCACATACA	CRZ1 Reverse primer
RT59	TTTGGATGCTGAGAGGTAATC	CNA1 Forward primer
RT60	TCAACGCAGCTAATGGTAAA	CNA1 Reverse primer
RT61	ATTCAGTGGAAGAGGTTCAAA	CNB1 Forward primer
RT62	GTTGCAATTGCTTGTCATCA	CNB1 Reverse primer
RT63	CCCGAAGAATCTCAGCATATAA	NPR1 Forward primer
RT64	TCGGTCCCACCTACATATT	NPR1 Reverse primer
RT65	AGCTAGCAAGCCAAACTTAT	LCB1 Forward primer
RT66	ACGAGTTTCAACACCAGAAT	LCB1 Reverse primer
RT67	TGCTGCTGTAAGAACATTCA	LCB2 Forward primer
RT68	AGGCAATCAGTTCAGGTAAAT	LCB2 Reverse primer

7.2: Strains used in the study

Table 7.2: List of strains used in the study

Strains	Genotype	Source/Reference
WT (BG14)	*ura3Δ::Tn903 Neo^R*	Lab strain
BY4741	MATa his3Δ1 leu2Δ0 met15Δ0 ura3Δ0	Lab stock
*Scyor1*Δ	BY4741/*Scyor1*Δ*::*KanMX	Lab stock
WT BL	ATCC 2001/ lucOPT 7/2/4 (WT in mice experiments)	Persyn et al., 2019
*Cgsnq2*Δ	Δ*Cgsnq2::NAT1*	This study
*Cgaus1*Δ	Δ*Cgaus1::NAT1*	This study
*Cgcdr1*Δ	Δ*Cgcdr1::NAT1*	This study
*Cgpdh1*Δ	Δ*Cgpdh1::NAT1*	This study
*Cgroa1*Δ	Δ*Cgroa1::NAT1*	This study
*Cgpdr12*Δ	Δ*Cgpdr12::NAT1*	This study
*Cgadp1*Δ	Δ*Cgadp1::NAT1*	This study
*Cgste6*Δ	Δ*Cgste6::NAT1*	This study
*Cgmdl1*Δ	Δ*Cgmdl1::NAT1*	This study
*Cgmdl2*Δ	Δ*Cgmdl2::NAT1*	This study
*Cgatm1*Δ	Δ*Cgatm1::NAT1*	This study
*Cgyor1*Δ	Δ*Cgyor1::NAT1*	This study
*Cgycf1*Δ	Δ*Cgycf1::NAT1*	This study
*Cgybt1*Δ	Δ*Cgybt1::NAT1*	This study

Cgvmr1Δ	*ΔCgvmr1::NAT1*	This study
Cgbpt1Δ	*ΔCgbpt1::NAT1*	This study
Cgpxa1Δ	*ΔCgpxa1::NAT1*	This study
Cgpxa2Δ	*ΔCgpxa2::NAT1*	This study
Cgcdr1Δ/Cgaus1Δ	*ΔCgcdr1::FRT, ΔCgaus1::NAT1*	This study
Cgcdr1Δ/Cgsnq2Δ	*ΔCgcdr1::FRT, ΔCgsnq2::NAT1*	This study
Cgcdr1Δ/Cgybt1Δ	*ΔCgcdr1::FRT, ΔCgybt1::NAT1*	This study
Cgcdr1Δ/Cgycf1Δ	*ΔCgcdr1::FRT, ΔCgycf1::NAT1*	This study
Cgcdr1Δ/Cgpdh1Δ	*ΔCgcdr1::FRT, ΔCgpdh1::NAT1*	This study
Cgcdr1Δ/Cgyor1Δ	*ΔCgcdr1::FRT, ΔCgyor1::NAT1*	This study
Cgyor1Δ/Cgpdh1Δ	*ΔCgyor1::FRT, ΔCgpdh1::NAT1*	This study
Cgyor1Δ/Cgsnq2Δ	*ΔCgyor1::FRT, ΔCgsnq2::NAT1*	This study
Cgyor1Δ/Cgaus1Δ	*ΔCgyor1::FRT, ΔCgaus1::NAT1*	This study
Cgyor1Δ/Cgycf1Δ	*ΔCgyor1::FRT, ΔCgycf1::NAT1*	This study
Cgyor1Δ/Cgybt1Δ	*ΔCgyor1::FRT, ΔCgybt1::NAT1*	This study
Cgckb1Δ	*ΔCgckb1::NAT1*	This study
Cgckb2Δ	*ΔCgckb2::NAT1*	This study
Cgcdr1Δ/Cgckb1Δ	*ΔCgcdr1::FRT, ΔCgckb1::NAT1*	This study
Cgcdr1Δ/Cgckb2Δ	*ΔCgcdr1::FRT, ΔCgckb2::NAT1*	This study
Cgyor1Δ/Cgckb1Δ	*ΔCgyor1::FRT, ΔCgckb1::NAT1*	This study
Cgyor1Δ/Cgckb2Δ	*ΔCgyor1::FRT, ΔCgckb2::NAT1*	This study
Cgcdr1Δ/Cgyor1Δ/Cgckb1Δ	*ΔCgcdr1::FRT, ΔCgyor1::FRT, ΔCgckb1::NAT1*	This study
Cgcdr1Δ/Cgyor1Δ/Cgckb2Δ	*ΔCgcdr1::FRT, ΔCgyor1::FRT, ΔCgckb1::NAT1*	This study
Cgyor1Δ/CgYOR1	*ΔCgyor1::FRT/CgYOR1*	This study
Cgcdr1Δ/CgCDR1	*ΔCgcdr1::FRT/CgCDR1*	This study
Cgsnq2Δ/CgSNQ2	*ΔCgsnq2::NAT1/CgSNQ2*	This study
Cgaus1Δ/CgAUS1	*ΔCgaus1::NAT1/CgAUS1*	This study
Cgpdh1Δ/CgPDH1	*ΔCgpdh1::NAT1/CgPDH1*	This study
Cgroa1Δ/CgROA1	*ΔCgroa1::NAT1/CgROA1*	This study
Cgpdr12Δ/CgPDR12	*ΔCgpdr12::NAT1/CgPDR12*	This study
Cgadp1Δ/CgADP1	*ΔCgadp1::NAT1/CgADP1*	This study
Cgste6Δ/CgSTE6	*ΔCgste6::NAT1/CgSTE6*	This study
Cgmdl1Δ/CgMDL1	*ΔCgmdl1::NAT1/CgMDL1*	This study
Cgmdl2Δ/CgMDL2	*ΔCgmdl2::NAT1/CgMDL2*	This study
Cgatm1Δ/CgATM1	*ΔCgatm1::NAT1/CgATM1*	This study
Cgycf1Δ/CgYCF1	*ΔCgycf1::NAT1/CgYCF1*	This study
Cgybt1Δ/YBT1	*ΔCgybt1::NAT1/YBT1*	This study
Cgvmr1Δ/VMR1	*ΔCgvmr1::NAT1/VMR1*	This study
Cgbpt1Δ/BPT1	*ΔCgbpt1::NAT1/BPT1*	This study

Cgpxa1Δ/PXA1	*ΔCgpxa1::NAT1/PXA1*	This study
Cgpxa2Δ/PXA2	*ΔCgpxa2::NAT1/PXA2*	This study
Scyor1Δ/CgYOR1	*BY4741/Scyor1Δ::KanMX/CgYOR1*	This study
AD1-8U-/CgYOR1	*AD1-8U-/CgYOR1*	This study
Cgyor1Δ BL	lucOPT 7/2/4, *ΔCgyor1::NAT1*	This study
Cgyor1Δ/CgYOR1 BL	lucOPT 7/2/4, *ΔCgyor1::NAT1/CgYOR1*	This study
WT^{GOF}	*Cgpdr1::CgPDR1^{G840C} FRT*	This study
MSY1	*ΔCgsnq2::FRT*	This study
MSY2	*ΔCgsnq2::FRT, ΔCgaus1::FRT*	This study
MSY3	*ΔCgsnq2::FRT, ΔCgaus1::FRT, ΔCgcdr1::FRT*	This study
MSY4	*ΔCgsnq2::FRT, ΔCgaus1::FRT, ΔCgcdr1::FRT, ΔCgpdh1::FRT*	This study
MSY5	*ΔCgsnq2::FRT, ΔCgaus1::FRT, ΔCgcdr1::FRT, ΔCgpdh1::FRT, ΔCgycf1::FRT*	This study
MSY6	*ΔCgsnq2::FRT, ΔCgaus1::FRT, ΔCgcdr1::FRT, ΔCgpdh1::FRT, ΔCgycf1::FRT, ΔCgybt1::FRT*	This study
MSY7	*ΔCgsnq2::FRT, ΔCgaus1::FRT, ΔCgcdr1::FRT, ΔCgpdh1::FRT, ΔCgycf1::FRT, ΔCgybt1::FRT, ΔCgyor1::FRT*	This study
MSY8	*ΔCgsnq2::FRT, ΔCgaus1::FRT, ΔCgcdr1::FRT, ΔCgpdh1::FRT, ΔCgycf1::FRT, ΔCgybt1::FRT, ΔCgyor1::FRT, Cgpdr1::CgPDR1^{G840C} FRT*	This study (Strain accession no. MTCC25307)
MSY9	*ΔCgsnq2::FRT, ΔCgaus1::FRT, ΔCgcdr1::FRT::CgCDR1-GFP::NAT1, ΔCgpdh1::FRT, ΔCgycf1::FRT, ΔCgybt1:: FRT, ΔCgyor1::FRT, Cgpdr1::CgPDR1^{G840C} FRT*	This study
MSY10	*ΔCgsnq2::FRT, ΔCgaus1::FRT, ΔCgcdr1::FRT::CgPDH1-GFP::NAT1, ΔCgpdh1::FRT, ΔCgycf1::FRT, ΔCgybt1:: FRT, ΔCgyor1::FRT, Cgpdr1::CgPDR1^{G840C} FRT*	This study
MSY11	*ΔCgsnq2::FRT, ΔCgaus1::FRT, ΔCgcdr1::FRT::CaCDR1-GFP::NAT1, ΔCgpdh1::FRT, ΔCgycf1::FRT, ΔCgybt1::FRT, ΔCgyor1::FRT, Cgpdr1::CgPDR1^{G840C} FRT*	This study
MSY12	*ΔCgsnq2::FRT, ΔCgaus1::FRT, ΔCgcdr1::FRT::ScPDR5-GFP::NAT1, ΔCgpdh1::FRT, ΔCgycf1::FRT, ΔCgybt1:: FRT, ΔCgyor1::FRT, Cgpdr1::CgPDR1^{G840C} FRT*	This study
MSY13	*ΔCgsnq2::FRT, ΔCgaus1::FRT, ΔCgcdr1::FRT::CgFLR1-GFP::NAT1, ΔCgpdh1::FRT, ΔCgycf1::FRT, ΔCgybt1:: FRT, ΔCgyor1::FRT, Cgpdr1::CgPDR1^{G840C} FRT*	This study
MSY14	*ΔCgsnq2::FRT, ΔCgaus1::FRT, ΔCgcdr1::FRT::CgYOR1-GFP::NAT1, ΔCgpdh1::FRT, ΔCgycf1::FRT, ΔCgybt1:: FRT, ΔCgyor1::FRT, Cgpdr1::CgPDR1^{G840C} FRT*	This study

MSY15	*∆Cgsnq2::FRT, ∆Cgaus1::FRT, ∆Cgcdr1::FRT::CaYORR1-GFP::NAT1, ∆Cgpdh1::FRT, ∆Cgycf1::FRT, ∆Cgybt1:: FRT, ∆Cgyor1::FRT, Cgpdr1::CgPDR1^{G840C} FRT*	This study
MSY16	*∆Cgsnq2::FRT, ∆Cgaus1::FRT, ∆Cgcdr1::FRT::ScYOR1-GFP::NAT1, ∆Cgpdh1::FRT, ∆Cgycf1::FRT, ∆Cgybt1:: FRT, ∆Cgyor1::FRT, Cgpdr1::CgPDR1^{G840C} FRT*	This study

7.3: Plasmids used in the study

Table 7.3: List of plasmids used in the study

Plasmids	**Description**	**Parent Plasmid**	**Source**
pBluescript KS+	Cloning plasmid	-	Lab stock
pRK70	FLP1 containing plasmid under EPA1 promoter	-	Lab of Fungal Pathogenesis, CDFD
pRK625	NAT1 plasmid	-	Lab of Fungal Pathogenesis, CDFD
pGRB2.3	*C. glabrata* expression plasmid	-	Addgene, #45343
pSH69	HphB containing plasmid	-	Euroscarf #P30675
pGPD2	Yeast expression plasmid	-	Addgene, #43972
pGRB2.3_HphB	*C. glabrata* expression plasmid with Hygromycin selection marker	pGRB2.3	This study
pGRB2.3_HphB_Rev1	CgCDR1 expressing plasmid	pGRB2.3_HphB	This study
pGRB2.3_HphB_Rev2	CgSNQ2 expressing plasmid	pGRB2.3_HphB	This study
pGRB2.3_HphB_Rev3	CgPDH1 expressing plasmid	pGRB2.3_HphB	This study
pGRB2.3_HphB_Rev4	CgAUS1 expressing plasmid	pGRB2.3_HphB	This study
pGRB2.3_HphB_Rev5	CgROA1 expressing plasmid	pGRB2.3_HphB	This study
pGRB2.3_HphB_Rev6	CgPDR12 expressing plasmid	pGRB2.3_HphB	This study
pGRB2.3_HphB_Rev7	CgADP1 expressing plasmid	pGRB2.3_HphB	This study
pGRB2.3_HphB_Rev8	CgYOR1 expressing plasmid	pGRB2.3_HphB	This study
pGRB2.3_HphB_Rev9	CgYCF1 expressing plasmid	pGRB2.3_HphB	This study
pGRB2.3_HphB_Rev10	CgYBT1 expressing plasmid	pGRB2.3_HphB	This study
pGRB2.3_HphB_Rev11	CgVMR1 expressing plasmid	pGRB2.3_HphB	This study
pGRB2.3_HphB_Rev12	CgBPT1 expressing plasmid	pGRB2.3_HphB	This study

pGRB2.3_HphB_Rev13	CgATM1 expressing plasmid	pGRB2.3_HphB	This study
pGRB2.3_HphB_Rev14	CgMDL1 expressing plasmid	pGRB2.3_HphB	This study
pGRB2.3_HphB_Rev15	CgMDL2 expressing plasmid	pGRB2.3_HphB	This study
pGRB2.3_HphB_Rev16	CgSTE6 expressing plasmid	pGRB2.3_HphB	This study
pGRB2.3_HphB_Rev17	CgPXA1 expressing plasmid	pGRB2.3_HphB	This study
pGRB2.3_HphB_Rev18	CgPXA2 expressing plasmid	pGRB2.3_HphB	This study
pMS1	FRT-NAT1-FRT was cloned at EcoRV site	pBluescript KS+	This study
pMS2	CgPDR1_ter cloned at KpnI/ ClaI site	pMS1	This study
pMS3	Mutated CgPDR1G840C coding sequence with 741 bp promoter and 587 bp terminator regions from DSY565 cloned at SacI/ SacII site	pMS2	This study
pMS4	CgCDR1_ter cloned at KpnI/ ClaI site	pMS1	This study
pMS5	CgCDR1_pro cloned at SacI/ SacII site	pMS4	This study
pMS6	YeGFP-HISt cloned at SpeI/ XmaI site	pMS5	This study
pMS7	CgCDR1 cloned at NotI/ PacI site	pMS6	This study
pMS8	CgPDH1 cloned at NotI/ PacI site	pMS6	This study
pMS9	CaCDR1 cloned at NotI/ PacI site	pMS6	This study
pMS10	ScPDR5 cloned at NotI/ PacI site	pMS6	This study
pMS11	CgFLR1 cloned at NotI/ PacI site	pMS6	This study
pMS12	CgYOR1 cloned at NotI/ PacI site	pMS6	This study
pMS13	CaYOR1 cloned at NotI/ PacI site	pMS6	This study
pMS14	ScYOR1 cloned at NotI/ PacI site	pMS6	This study
pGPD2_CgYOR1	CgYOR1 expressing plasmid	pGPD2	This study

REFERENCES

8. References

Abele R, Tampé R (2018) Moving the Cellular Peptidome by Transporters. Front Cell Dev Biol 6:. https://doi.org/10.3389/fcell.2018.00043

Achkar JM, Fries BC (2010) *Candida* infections of the genitourinary tract. Clin Microbiol Rev 23:253–273. https://doi.org/10.1128/CMR.00076-09

Adhikary R, Joshi S (2011) Species distribution and anti-fungal susceptibility of Candidaemia at a multi super-specialty center in Southern India. Indian J Med Microbiol 29:309. https://doi.org/10.4103/0255-0857.83920

Adler-Moore JP, Proffitt RT (2008) Amphotericin B lipid preparations: what are the differences? Clin Microbiol Infect 14:25–36. https://doi.org/10.1111/j.1469-0691.2008.01979.x

Al-Fakih AA (2014) Overview on the Fungal Metabolites Involved in Mycopathy. Open J Med Microbiol 2014:. https://doi.org/10.4236/ojmm.2014.41006

Almeida F, Rodrigues ML, Coelho C (2019) The Still Underestimated Problem of Fungal Diseases Worldwide. Front Microbiol 10:. https://doi.org/10.3389/fmicb.2019.00214

Almshawit H (2015) Studies on the effect of thymoquinone on oxidative stress and cell wall integrity of Candida glabrata

Anderson HW (1917) The Yeast-like Fungi of the Human Intestinal Tract. University of Illinois

Anjard C, Consortium the DS, Loomis WF (2002) Evolutionary Analyses of ABC Transporters of *Dictyostelium discoideum*. Eukaryot Cell 1:643–652. https://doi.org/10.1128/EC.1.4.643-652.2002

Arendrup MC, Dzajic E, Jensen RH, et al (2013) Epidemiological changes with potential implication for antifungal prescription recommendations for fungaemia: data from

a nationwide fungaemia surveillance programme. Clin Microbiol Infect 19:e343–e353. https://doi.org/10.1111/1469-0691.12212

Badiee P, Hashemizadeh Z (2014) Opportunistic invasive fungal infections: diagnosis & clinical management. Indian J Med Res 139:195–204

Bairwa G, Kaur R (2011) A novel role for a glycosylphosphatidylinositol-anchored aspartyl protease, CgYps1, in the regulation of pH homeostasis in *Candida glabrata*. Mol Microbiol 79:900–913. https://doi.org/10.1111/j.1365-2958.2010.07496.x

Bairwa G, Rasheed M, Taigwal R, et al (2014) GPI (glycosylphosphatidylinositol)-linked aspartyl proteases regulate vacuole homoeostasis in *Candida glabrata.* Biochem J 458:323–334. https://doi.org/10.1042/BJ20130757

Bajpai VK, Khan I, Shukla S, et al (2019) Invasive Fungal Infections and Their Epidemiology: Measures in the Clinical Scenario. Biotechnol Bioprocess Eng 24:436–444. https://doi.org/10.1007/s12257-018-0477-0

Bassetti M, Merelli M, Righi E, et al (2013) Epidemiology, Species Distribution, Antifungal Susceptibility, and Outcome of Candidemia across Five Sites in Italy and Spain. J Clin Microbiol 51:4167–4172. https://doi.org/10.1128/JCM.01998-13

Belanger ES, Yang E, Forrest GN (2015) Combination antifungal therapy: when, where, and why. Curr Clin Microbiol Rep 2:67–75

Ben-Ami R, Zimmerman O, Finn T, et al (2016) Heteroresistance to Fluconazole Is a Continuously Distributed Phenotype among *Candida glabrata* Clinical Strains Associated with In Vivo Persistence. mBio 7:. https://doi.org/10.1128/mBio.00655-16

Berbee ML, James TY, Strullu-Derrien C (2017) Early Diverging Fungi: Diversity and Impact at the Dawn of Terrestrial Life. Annu Rev Microbiol 71:41–60. https://doi.org/10.1146/annurev-micro-030117-020324

Berkower C, Michaelis S (1991) Mutational analysis of the yeast a-factor transporter STE6, a member of the ATP binding cassette (ABC) protein superfamily. EMBO J 10:3777–3785

Bhattacharya S, Fries BC (2018) Enhanced Efflux Pump Activity in Old *Candida glabrata* Cells. Antimicrob Agents Chemother 62:. https://doi.org/10.1128/aac.02227-17

Biemans-Oldehinkel E, Doeven MK, Poolman B (2006) ABC transporter architecture and regulatory roles of accessory domains. FEBS Lett 580:1023–1035. https://doi.org/10.1016/j.febslet.2005.11.079

Birchler JA, Veitia RA (2010) The Gene Balance Hypothesis: implications for gene regulation, quantitative traits and evolution. New Phytol 186:54–62. https://doi.org/10.1111/j.1469-8137.2009.03087.x

Bitew A, Abebaw Y (2018) Vulvovaginal candidiasis: species distribution of *Candida* and their antifungal susceptibility pattern. BMC Womens Health 18:94. https://doi.org/10.1186/s12905-018-0607-z

Blackwell M (2011) The Fungi: 1, 2, 3 ... 5.1 million species? Am J Bot 98:426–438

Boisnard S, Zhou Li Y, Arnaise S, et al (2015) Efficient Mating-Type Switching in *Candida glabrata* Induces Cell Death. PloS One 10:e0140990. https://doi.org/10.1371/journal.pone.0140990

Bongomin F, Gago S, Oladele R, Denning D (2017) Global and Multi-National Prevalence of Fungal Diseases—Estimate Precision. J Fungi 3:57. https://doi.org/10.3390/jof3040057

Borah S, Shivarathri R, Kaur R (2011) The Rho1 GTPase-activating protein CgBem2 is required for survival of azole stress in *Candida glabrata*. J Biol Chem 286:34311–34324. https://doi.org/10.1074/jbc.M111.264671

Borba-Santos LP, Reis de Sá LF, Ramos JA, et al (2017) Tacrolimus Increases the Effectiveness of Itraconazole and Fluconazole against Sporothrix spp. Front Microbiol 8:. https://doi.org/10.3389/fmicb.2017.01759

Borkovich K, Ebbole DJ (2010) Cellular and molecular biology of filamentous fungi. American Society for Microbiology Press

Borst P, Evers R, Kool M, Wijnholds J (2000) A Family of Drug Transporters: the Multidrug Resistance-Associated Proteins. JNCI J Natl Cancer Inst 92:1295–1302. https://doi.org/10.1093/jnci/92.16.1295

Bourgeois C, Majer O, Frohner IE, et al (2011) Conventional Dendritic Cells Mount a Type I IFN Response against Candida spp. Requiring Novel Phagosomal TLR7-Mediated IFN-β Signaling. J Immunol 186:3104–3112. https://doi.org/10.4049/jimmunol.1002599

Bourgeois N, Laurens C, Bertout S, et al (2014) Assessment of caspofungin susceptibility of Candida glabrata by the Etest®, CLSI, and EUCAST methods, and detection of FKS1 and FKS2 mutations. Eur J Clin Microbiol Infect Dis 33:1247–1252. https://doi.org/10.1007/s10096-014-2069-z

Brisse S, Pannier C, Angoulvant A, et al (2009) Uneven distribution of mating types among genotypes of *Candida glabrata i*solates from clinical samples. Eukaryot Cell 8:287–295

Brockert PJ, Lachke SA, Srikantha T, et al (2003) Phenotypic Switching and Mating Type Switching of *Candida glabrata* at Sites of Colonization. Infect Immun 71:7109–7118. https://doi.org/10.1128/IAI.71.12.7109-7118.2003

Brown GD, Denning DW, Gow NAR, et al (2012) Hidden Killers: Human Fungal Infections. Sci Transl Med 4:165rv13-165rv13. https://doi.org/10.1126/scitranslmed.3004404

Brüggemann RJM, Alffenaar J-WC, Blijlevens NMA, et al (2009) Clinical relevance of the pharmacokinetic interactions of azole antifungal drugs with other

coadministered agents. Clin Infect Dis Off Publ Infect Dis Soc Am 48:1441–1458. https://doi.org/10.1086/598327

Brun S, Bergès T, Poupard P, et al (2004) Mechanisms of Azole Resistance in Petite Mutants of *Candida glabrata* Mechanisms of Azole Resistance in Petite Mutants of Candida glabrata. Society 1788–1796. https://doi.org/10.1128/AAC.48.5.1788

Brunke S, Hube B (2013) Two unlike cousins: *Candida albicans* and *C. glabrata* *i*nfection strategies. Cell Microbiol 15:701–708. https://doi.org/10.1111/cmi.12091

Bruno VM, Mitchell AP (2005) Regulation of azole drug susceptibility by *Candida albicans* protein kinase CK2: Azole susceptibility and protein kinase CK2 of *C. albicans*. Mol Microbiol 56:559–573. https://doi.org/10.1111/j.1365-2958.2005.04562.x

Byadarahally Raju S, Rajappa S (2011) Isolation and identification of *Candida* from the oral cavity. ISRN Dent 2011:

Canuto MM, Rodero FG (2002) Antifungal drug resistance to azoles and polyenes. Lancet Infect Dis 2:550–563. https://doi.org/10.1016/S1473-3099(02)00371-7

Carreté L, Ksiezopolska E, Pegueroles C, et al (2018) Patterns of Genomic Variation in the Opportunistic Pathogen *Candida glabrata* Suggest the Existence of Mating and a Secondary Association with Humans. Curr Biol 28:15-27.e7. https://doi.org/10.1016/j.cub.2017.11.027

Casadevall A (2007) Determinants of virulence in the pathogenic fungi. Fungal Biol Rev 21:130–132. https://doi.org/10.1016/j.fbr.2007.02.007

Casal M, Paiva S, Queirós O, Soares-Silva I (2008) Transport of carboxylic acids in yeasts. FEMS Microbiol Rev 32:974–994. https://doi.org/10.1111/j.1574-6976.2008.00128.x

Castanheira M, Messer SA, Rhomberg PR, Pfaller MA (2016) Antifungal susceptibility patterns of a global collection of fungal isolates: results of the SENTRY

Antifungal Surveillance Program (2013). Diagn Microbiol Infect Dis 85:200–204. https://doi.org/10.1016/j.diagmicrobio.2016.02.009

Caudle KE, Barker KS, Wiederhold NP, et al (2011) Genomewide Expression Profile Analysis of the *Candida glabrata* Pdr1 Regulon. Eukaryot Cell 10:373–383. https://doi.org/10.1128/EC.00073-10

Cavalheiro M, Teixeira MC (2018) Candida Biofilms: Threats, Challenges, and Promising Strategies. Front Med 5:. https://doi.org/10.3389/fmed.2018.00028

Chaillot J, Tebbji F, Remmal A, et al (2015) The Monoterpene Carvacrol Generates Endoplasmic Reticulum Stress in the Pathogenic Fungus *Candida albicans*. Antimicrob Agents Chemother 59:4584–4592. https://doi.org/10.1128/AAC.00551-15

Chakrabarti A, Sood P, Rudramurthy SM, et al (2015) Incidence, characteristics and outcome of ICU-acquired candidemia in India. Intensive Care Med 41:285–295. https://doi.org/10.1007/s00134-014-3603-2

Chapman B, Slavin M, Marriott D, et al (2017) Changing epidemiology of candidaemia in Australia. J Antimicrob Chemother 72:1103–1108. https://doi.org/10.1093/jac/dkw422

Chaturvedi V, Springer DJ, Behr MJ, et al (2010) Morphological and Molecular Characterizations of Psychrophilic Fungus Geomyces destructans from New York Bats with White Nose Syndrome (WNS). PLoS ONE 5:e10783. https://doi.org/10.1371/journal.pone.0010783

Chen K-H, Miyazaki T, Tsai H-F, Bennett JE (2007) The bZip transcription factor Cgap1p is involved in multidrug resistance and required for activation of multidrug transporter gene CgFLR1 in *Candida glabrata.* Gene 386:63–72. https://doi.org/10.1016/j.gene.2006.08.010

Chen S, Chen Y, Zhou Y, et al (2019) *Candida glabrata*-Induced Refractory Infectious Arthritis: A Case Report and Literature Review. Mycopathologia 184:283–293. https://doi.org/10.1007/s11046-019-00329-8

Chloupková M, Reaves SK, LeBard LM, Koeller DM (2004) The mitochondrial ABC transporter Atm1p functions as a homodimer. FEBS Lett 569:65–69. https://doi.org/10.1016/j.febslet.2004.05.051

Chouhan S, Kallianpur S, Prabhu KT, et al (2019) Candidal prevalence in diabetics and its species identification. Int J Appl Basic Med Res 9:49. https://doi.org/10.4103/ijabmr.IJABMR_259_18

Chuang C-Y, Chen L-Y, Fu R-H, et al (2014) Involvement of the Carboxyl-Terminal Region of the Yeast Peroxisomal Half ABC Transporter Pxa2p in Its Interaction with Pxa1p and in Transporter Function. PLOS ONE 9:e104892. https://doi.org/10.1371/journal.pone.0104892

Colombo AL, Guimarães T, Silva LRBF, et al (2007) Prospective observational study of candidemia in São Paulo, Brazil: incidence rate, epidemiology, and predictors of mortality. Infect Control Hosp Epidemiol 28:570–576. https://doi.org/10.1086/513615

Cortegiani A, Misseri G, Fasciana T, et al (2018) Epidemiology, clinical characteristics, resistance, and treatment of infections by Candida auris. J Intensive Care 6:. https://doi.org/10.1186/s40560-018-0342-4

Cortés JA, Corrales IF (2018) Invasive Candidiasis: Epidemiology and Risk Factors. Fungal Infect. https://doi.org/10.5772/intechopen.81813

Cowen LE (2005) Hsp90 Potentiates the Rapid Evolution of New Traits: Drug Resistance in Diverse Fungi. Science 309:2185–2189. https://doi.org/10.1126/science.1118370

Cowen LE, Carpenter AE, Matangkasombut O, et al (2006) Genetic Architecture of Hsp90-Dependent Drug Resistance. Eukaryot Cell 5:2184–2188. https://doi.org/10.1128/EC.00274-06

Cowen LE, Sanglard D, Howard SJ, et al (2015) Mechanisms of Antifungal Drug Resistance. Cold Spring Harb Perspect Med 5:. https://doi.org/10.1101/cshperspect.a019752

Cowen LE, Singh SD, Köhler JR, et al (2009) Harnessing Hsp90 function as a powerful, broadly effective therapeutic strategy for fungal infectious disease. Proc Natl Acad Sci 106:2818–2823. https://doi.org/10.1073/pnas.0813394106

Csank C, Haynes K (2000) Candida glabrata displays pseudohyphal growth. FEMS Microbiol Lett 189:115–120. https://doi.org/10.1111/j.1574-6968.2000.tb09216.x

Cuéllar-Cruz M, Briones-Martin-del-Campo M, Cañas-Villamar I, et al (2008) High Resistance to Oxidative Stress in the Fungal Pathogen *Candida glabrata* Is Mediated by a Single Catalase, Cta1p, and Is Controlled by the Transcription Factors Yap1p, Skn7p, Msn2p, and Msn4p. Eukaryot Cell 7:814–825. https://doi.org/10.1128/EC.00011-08

Cui Z, Hirata D, Tsuchiya E, et al (1996) The multidrug resistance-associated protein (MRP) subfamily (Yrs1/Yor1) of *Saccharomyces cerevisiae* is important for the tolerance to a broad range of organic anions. J Biol Chem 271:14712–14716

Cutler JE, Deepe GS, Klein BS (2007) Advances in combating fungal diseases: vaccines on the threshold. Nat Rev Microbiol 5:13–28. https://doi.org/10.1038/nrmicro1537

d'Enfert C, Janbon G (2016) Biofilm formation in *Candida glabrata*: What have we learnt from functional genomics approaches? FEMS Yeast Res 16:. https://doi.org/10.1093/femsyr/fov111

Davidson AL, Chen J (2004) ATP-binding cassette transporters in bacteria. Annu Rev Biochem 73:241–268. https://doi.org/10.1146/annurev.biochem.73.011303.073626

de Oliveira Santos GC, Vasconcelos CC, Lopes AJO, et al (2018) *Candida* Infections and Therapeutic Strategies: Mechanisms of Action for Traditional and Alternative Agents. Front Microbiol 9:. https://doi.org/10.3389/fmicb.2018.01351

de Pauw BE (2011) What Are Fungal Infections? Mediterr J Hematol Infect Dis 3:. https://doi.org/10.4084/MJHID.2011.001

Dean M, Allikmets R, Gerrard B, et al (1994) Mapping and sequencing of two yeast genes belonging to the ATP- binding cassette superfamily. Yeast 10:377–383

Dean M, Hamon Y, Chimini G (2001) The human ATP-binding cassette (ABC) transporter superfamily. J Lipid Res 42:1007–1017

Decottignies A, Goffeau A (1997) Complete inventory of the yeast ABC proteins. Nat Genet 15:137–145. https://doi.org/10.1038/ng0297-137

Decottignies A, Grant AM, Nichols JW, et al (1998) ATPase and Multidrug Transport Activities of the Overexpressed Yeast ABC Protein Yor1p. J Biol Chem 273:12612–12622. https://doi.org/10.1074/jbc.273.20.12612

Decottignies A, Lambert L, Catty P, et al (1995) Identification and Characterization of SNQ2, a New Multidrug ATP Binding Cassette Transporter of the Yeast Plasma Membrane. J Biol Chem 270:18150–18157. https://doi.org/10.1074/jbc.270.30.18150

Delaloye J, Calandra T (2014) Invasive candidiasis as a cause of sepsis in the critically ill patient. Virulence 5:161–169. https://doi.org/10.4161/viru.26187

Delattin N, Cammue BP, Thevissen K (2013) Reactive oxygen species-inducing antifungal agents and their activity against fungal biofilms. Future Med Chem 6:77–90. https://doi.org/10.4155/fmc.13.189

Dellière S, Healey K, Gits-Muselli M, et al (2016) Fluconazole and Echinocandin Resistance of *Candida glabrata* Correlates Better with Antifungal Drug Exposure Rather than with MSH2 Mutator Genotype in a French Cohort of Patients Harboring Low Rates of Resistance. Front Microbiol 7:. https://doi.org/10.3389/fmicb.2016.02038

Denning DW (2003) Echinocandin antifungal drugs. Lancet Lond Engl 362:1142–1151. https://doi.org/10.1016/S0140-6736(03)14472-8

Dermauw W, Van Leeuwen T (2014) The ABC gene family in arthropods: comparative genomics and role in insecticide transport and resistance. Insect Biochem Mol Biol 45:89–110. https://doi.org/10.1016/j.ibmb.2013.11.001

Desai C, Mavrianos J, Chauhan N (2011) *Candida glabrata* Pwp7p and Aed1p are required for Adherence to Human Endothelial Cells. FEMS Yeast Res 11:595–601. https://doi.org/10.1111/j.1567-1364.2011.00743.x

Detmers FJ, Lanfermeijer FC, Poolman B (2001) Peptides and ATP binding cassette peptide transporters. Res Microbiol 152:245–258. https://doi.org/10.1016/s0923-2508(01)01196-2

Di Mambro T, Guerriero I, Aurisicchio L, et al (2019) The Yin and Yang of Current Antifungal Therapeutic Strategies: How Can We Harness Our Natural Defenses? Front Pharmacol 10:. https://doi.org/10.3389/fphar.2019.00080

Diezmann S, Michaut M, Shapiro RS, et al (2012) Mapping the Hsp90 Genetic Interaction Network in *Candida albicans* Reveals Environmental Contingency and Rewired Circuitry. PLoS Genet 8:. https://doi.org/10.1371/journal.pgen.1002562

Do E, Park S, Li M-H, et al (2018) The mitochondrial ABC transporter Atm1 plays a role in iron metabolism and virulence in the human fungal pathogen *Cryptococcus neoformans*. Med Mycol 56:458–468. https://doi.org/10.1093/mmy/myx073

Doi AM, Pignatari ACC, Edmond MB, et al (2016) Epidemiology and Microbiologic Characterization of Nosocomial Candidemia from a Brazilian National

Surveillance Program. PLOS ONE 11:e0146909. https://doi.org/10.1371/journal.pone.0146909

Dong J, Lai R, Nielsen K, et al (2004) The essential ATP-binding cassette protein RLI1 functions in translation by promoting preinitiation complex assembly. J Biol Chem 279:42157–42168. https://doi.org/10.1074/jbc.M404502200

Drinnenberg IA, Weinberg DE, Xie KT, et al (2009) RNAi in budding yeast. Science 326:544–550. https://doi.org/10.1126/science.1176945

Drummond RA, Gaffen SL, Hise AG, Brown GD (2015) Innate Defense against Fungal Pathogens. Cold Spring Harb Perspect Med 5:. https://doi.org/10.1101/cshperspect.a019620

Dujon B, Sherman D, Fischer G, et al (2004a) Genome evolution in yeasts. Nature 430:35–44

El-Awady R, Saleh E, Hashim A, et al (2017) The Role of Eukaryotic and Prokaryotic ABC Transporter Family in Failure of Chemotherapy. Front Pharmacol 7:. https://doi.org/10.3389/fphar.2016.00535

Elefanti A, Mouton JW, Verweij PE, et al (2013) Amphotericin B- and voriconazole-echinocandin combinations against Aspergillus spp.: Effect of serum on inhibitory and fungicidal interactions. Antimicrob Agents Chemother 57:4656–4663. https://doi.org/10.1128/AAC.00597-13

Falcón-Pérez JM, Martínez-Burgos M, Molano J, et al (2001) Domain Interactions in the Yeast ATP Binding Cassette Transporter Ycf1p: Intragenic Suppressor Analysis of Mutations in the Nucleotide Binding Domains. J Bacteriol 183:4761–4770. https://doi.org/10.1128/JB.183.16.4761-4770.2001

Ferrari S, Ischer F, Calabrese D, et al (2009a) Gain of function mutations in CgPDR1 of *Candida glabrata* not only mediate antifungal resistance but also enhance virulence. PLoS Pathog 5:e1000268. https://doi.org/10.1371/journal.ppat.1000268

Ferrari S, Sanguinetti M, De Bernardis F, et al (2011a) Loss of Mitochondrial Functions Associated with Azole Resistance in *Candida glabrata* Results in Enhanced Virulence in Mice. Antimicrob Agents Chemother 55:1852–1860. https://doi.org/10.1128/AAC.01271-10

Fidel PL, Vazquez JA, Sobel JD (1999) *Candida glabrata*: Review of Epidemiology, Pathogenesis, and Clinical Disease with Comparison toC. albicans. Clin Microbiol Rev 12:80–96. https://doi.org/10.1128/CMR.12.1.80

Fincham JRS (2001) Fungal Genetics. In: eLS. American Cancer Society

Fisher MC, Hawkins NJ, Sanglard D, Gurr SJ (2018) Worldwide emergence of resistance to antifungal drugs challenges human health and food security. Science 360:739–742. https://doi.org/10.1126/science.aap7999

Flanagan JU, Huber T (2007) Structural Evolution of the ABC Transporter Subfamily B. Evol Bioinforma Online 3:309–316

Fonseca E, Silva S, Rodrigues CF, et al (2014) Effects of fluconazole on *Candida glabrata* biofilms and its relationship with ABC transporter gene expression. Biofouling 30:447–457. https://doi.org/10.1080/08927014.2014.886108

Fu J, Ding Y, Wei B, et al (2017) Epidemiology of *Candida* albicans and *non-C. albicans* of neonatal candidemia at a tertiary care hospital in western China. BMC Infect Dis 17:329. https://doi.org/10.1186/s12879-017-2423-8

Gabaldón T, Carreté L (2016) The birth of a deadly yeast: tracing the evolutionary emergence of virulence traits in *Candida glabrata*. FEMS Yeast Res 16:. https://doi.org/10.1093/femsyr/fov110

Gabaldón T, Fairhead C (2019) Genomes shed light on the secret life of *Candida glabrata*: not so asexual, not so commensal. Curr Genet 65:93–98. https://doi.org/10.1007/s00294-018-0867-z

Gagliano M, Marchiani C, Bandini G, et al (2018) A rare case of *Candida glabrata* spondylodiscitis: case report and literature review. Int J Infect Dis 68:31–35. https://doi.org/10.1016/j.ijid.2018.01.003

Galocha M, Pais P, Cavalheiro M, et al (2019) Divergent Approaches to Virulence in *C. albicans* and *C. glabrata*: Two Sides of the Same Coin. Int J Mol Sci 20:. https://doi.org/10.3390/ijms20092345

Gao J, Wang H, Li Z, et al (2018) *Candida albicans* gains azole resistance by altering sphingolipid composition. Nat Commun 9:1–14. https://doi.org/10.1038/s41467-018-06944-1

Gaur M, Choudhury D, Prasad R (2005a) Complete inventory of ABC proteins in human pathogenic yeast, *Candida albicans*. J Mol Microbiol Biotechnol 9:3–15. https://doi.org/10.1159/000088141

Gaur M, Choudhury D, Prasad R (2005b) Complete inventory of ABC proteins in human pathogenic yeast, *Candida albicans*. J Mol Microbiol Biotechnol 9:3–15. https://doi.org/10.1159/000088141

Gbelska Y, Toth Hervay N, Dzugasova V, Konecna A (2017) Measurement of Energy-dependent Rhodamine 6G Efflux in Yeast Species. BIO-Protoc 7:. https://doi.org/10.21769/BioProtoc.2428

Gebre AA, Okada H, Kim C, et al (2015) Profiling of the effects of antifungal agents on yeast cells based on morphometric analysis. FEMS Yeast Res 15:. https://doi.org/10.1093/femsyr/fov040

Gietz D, St Jean A, Woods RA, Schiestl RH (1992) Improved method for high efficiency transformation of intact yeast cells. Nucleic Acids Res 20:1425. https://doi.org/10.1093/nar/20.6.1425

Glavinas H, Krajcsi P, Cserepes J, Sarkadi B (2004a) The role of ABC transporters in drug resistance, metabolism and toxicity. Curr Drug Deliv 1:27–42. https://doi.org/10.2174/1567201043480036

Goldman E, Green LH (2015) Practical handbook of microbiology. CRC press

Gostinčar C, Zajc J, Lenassi M, et al (2018) Fungi between extremotolerance and opportunistic pathogenicity on humans. Fungal Divers 93:195–213. https://doi.org/10.1007/s13225-018-0414-8

Gregori C, Schüller C, Frohner IE, et al (2008) Weak Organic Acids Trigger Conformational Changes of the Yeast Transcription Factor War1 in Vivo to Elicit Stress Adaptation. J Biol Chem 283:25752–25764. https://doi.org/10.1074/jbc.M803095200

Guarana M, Nucci M (2018) Acute disseminated candidiasis with skin lesions: a systematic review. Clin Microbiol Infect 24:246–250. https://doi.org/10.1016/j.cmi.2017.08.016

Gupta AK, Lyons DCA (2015) The Rise and Fall of Oral Ketoconazole. J Cutan Med Surg 19:352–357. https://doi.org/10.1177/1203475415574970

Gupta B, Gupta S, Chaudhary M, et al (2019) Oral candida prevalence and species specificity in leprosy. Dis Mon 100920

Hameed S, Dhamgaye S, Singh A, et al (2011) Calcineurin Signaling and Membrane Lipid Homeostasis Regulates Iron Mediated MultiDrug Resistance Mechanisms in Candida albicans. PLoS ONE 6:e18684. https://doi.org/10.1371/journal.pone.0018684

Hani U, Shivakumar HG, Vaghela R, et al (2015) Candidiasis: a fungal infection--current challenges and progress in prevention and treatment. Infect Disord Drug Targets 15:42–52. https://doi.org/10.2174/1871526515666150320162036

Hassan DM, Yousef RHA, Elhamed WAA, et al (2019) Candidemia in the Neonatal Intensive Care Unit: Insights on Epidemiology and Antifungal Drug Susceptibility Patterns. Arch Pediatr Infect Dis 7:. https://doi.org/10.5812/pedinfect.81090

Hawksworth DL, Lücking R (2017) Fungal Diversity Revisited: 2.2 to 3.8 Million Species. Microbiol Spectr 5:. https://doi.org/10.1128/microbiolspec.FUNK-0052-2016

Healey KR, Zhao Y, Perez WB, et al (2016) Prevalent mutator genotype identified in fungal pathogen *Candida glabrata* promotes multi-drug resistance. Nat Commun 7:11128. https://doi.org/10.1038/ncomms11128

Hernández-Chávez MJ, Pérez-García LA, Niño-Vega GA, Mora-Montes HM (2017) Fungal Strategies to Evade the Host Immune Recognition. J Fungi 3:. https://doi.org/10.3390/jof3040051

Hernández-Elvira M, Martínez-Gómez R, Domínguez-Martin E, et al (2019) Tunicamycin Sensitivity-Suppression by High Gene Dosage Reveals New Functions of the Yeast Hog1 MAP Kinase. Cells 8:. https://doi.org/10.3390/cells8070710

Heung LJ, Luberto C, Poeta MD (2006) Role of Sphingolipids in Microbial Pathogenesis. Infect Immun 74:28–39. https://doi.org/10.1128/IAI.74.1.28-39.2006

Higgins CF (2001) ABC transporters: physiology, structure and mechanism--an overview. Res Microbiol 152:205–210. https://doi.org/10.1016/s0923-2508(01)01193-7

Holmes AR, Cardno TS, Strouse JJ, et al (2016) Targeting efflux pumps to overcome antifungal drug resistance. Future Med Chem 8:1485–1501. https://doi.org/10.4155/fmc-2016-0050

Hull CM, Bader O, Parker JE, et al (2012a) Two clinical isolates of *Candida glabrata* exhibiting reduced sensitivity to amphotericin B both harbor mutations in ERG2. Antimicrob Agents Chemother 56:6417–6421. https://doi.org/10.1128/AAC.01145-12

Hull CM, Johnson AD (1999) Identification of a mating type-like locus in the asexual pathogenic yeast *Candida albicans*. Science 285:1271–1275. https://doi.org/10.1126/science.285.5431.1271

Hull CM, Parker JE, Bader O, et al (2012b) Facultative Sterol Uptake in an Ergosterol-Deficient Clinical Isolate of *Candida glabrata* Harboring a Missense Mutation in ERG11 and Exhibiting Cross-Resistance to Azoles and Amphotericin B. Antimicrob Agents Chemother 56:4223–4232. https://doi.org/10.1128/AAC.06253-11

Ibilibor C, Cammack JT (2018) C*andida glabrata*: A Unique Cause of Necrotizing Urethritis. In: Case Rep. Infect. Dis. https://www.hindawi.com/journals/criid/2018/5263438/. Accessed 29 Jan 2020

Inoue Y, Nomura W (2017) TOR Signaling in Budding Yeast. Yeast Role Med Appl. https://doi.org/10.5772/intechopen.70784

Istel F, Schwarzmüller T, Tscherner M, Kuchler K (2015) Genetic Transformation of *Candida glabrata* by Electroporation. Bio-Protoc 5:. https://doi.org/10.21769/BioProtoc.1528

Izumikawa K, Kakeya H, Tsai HF, et al (2003a) Function of C*andida glabrata* ABC transporter gene, PDH1. Yeast 20:249–261. https://doi.org/10.1002/yea.962

Jacob TR, Peres NTA, Martins MP, et al (2015) Heat Shock Protein 90 (Hsp90) as a Molecular Target for the Development of Novel Drugs Against the Dermatophyte *Trichophyton rubrum*. Front Microbiol 6:. https://doi.org/10.3389/fmicb.2015.01241

Jandric Z, Gregori C, Klopf E, et al (2013) Sorbic acid stress activates the *Candida glabrata* high osmolarity glycerol MAP kinase pathway. Front Microbiol 4:. https://doi.org/10.3389/fmicb.2013.00350

Jenks P, Brown J, Warnock D, Barnes N (1995) *Candida glabrata* epididymo-orchitis: An unusual infection rapidly cured with surgical and antifungal treatment. J Infect 31:71–72. https://doi.org/10.1016/S0163-4453(95)91612-1

Jeong CB, Kim DH, Kang HM, et al (2017) Genome-wide identification of ATP-binding cassette (ABC) transporters and their roles in response to polycyclic aromatic

hydrocarbons (PAHs) in the copepod *Paracyclopina nana*. Aquat Toxicol 183:144–155. https://doi.org/10.1016/j.aquatox.2016.12.022

Jia Y, Tang R-J, Wang L, et al (2012) Calcium-Activated-Calcineurin Reduces the In Vitro and In Vivo Sensitivity of Fluconazole to *Candida albicans* via Rta2p. PLoS ONE 7:. https://doi.org/10.1371/journal.pone.0048369

Jiang L, Xu D, Chen Z, et al (2016) The putative ABC transporter encoded by the orf19.4531 plays a role in the sensitivity of *Candida albicans* cells to azole antifungal drugs. FEMS Yeast Res 16:. https://doi.org/10.1093/femsyr/fow024

Johnson CJ, Kernien JF, Hoyer AR, Nett JE (2017) Mechanisms involved in the triggering of neutrophil extracellular traps (NETs) by *Candida glabrata* during planktonic and biofilm growth. Sci Rep 7:. https://doi.org/10.1038/s41598-017-13588-6

Johnson ME, Katiyar SK, Edlind TD (2011) New Fks Hot Spot for Acquired Echinocandin Resistance in *Saccharomyces cerevisiae* and Its Contribution to Intrinsic Resistance of Scedosporium Species. Antimicrob Agents Chemother 55:3774–3781. https://doi.org/10.1128/AAC.01811-10

Johnson ZL, Chen J (2017) Structural Basis of Substrate Recognition by the Multidrug Resistance Protein MRP1. Cell 168:1075-1085.e9. https://doi.org/10.1016/j.cell.2017.01.041

Jones PM, George AM (1999) Subunit interactions in ABC transporters: towards a functional architecture. FEMS Microbiol Lett 179:187–202. https://doi.org/10.1111/j.1574-6968.1999.tb08727.x

Jones PM, George AM (2002) Mechanism of ABC transporters: A molecular dynamics simulation of a well characterized nucleotide-binding subunit. Proc Natl Acad Sci 99:12639–12644. https://doi.org/10.1073/pnas.152439599

Jung EH (2017) Proteomics, drugs and nonlytic exocytosis: The pursuit of novel therapies against Cryptococcus neoformans

Jungwirth H, Kuchler K (2006) Yeast ABC transporters – A tale of sex, stress, drugs and aging. FEBS Lett 580:1131–1138. https://doi.org/10.1016/j.febslet.2005.12.050

Juvvadi PR, Lamoth F, Steinbach WJ (2014) Calcineurin as a multifunctional regulator: Unraveling novel functions in fungal stress responses, hyphal growth, drug resistance, and pathogenesis. Fungal Biol Rev 28:56–69. https://doi.org/10.1016/j.fbr.2014.02.004

Karababa M, Valentino E, Pardini G, et al (2006) *CRZ1* , a target of the calcineurin pathway in *Candida albicans*: Calcineurin targets in *Candida albicans*. Mol Microbiol 59:1429–1451. https://doi.org/10.1111/j.1365-2958.2005.05037.x

Kasper L, Seider K, Gerwien F, et al (2014) Identification of *Candida glabrata* Genes Involved in pH Modulation and Modification of the Phagosomal Environment in Macrophages. PLoS ONE 9:. https://doi.org/10.1371/journal.pone.0096015

Kasper L, Seider K, Hube B (2015a) Intracellular survival of *Candida glabrata* in macrophages: immune evasion and persistence. FEMS Yeast Res 15:fov042. https://doi.org/10.1093/femsyr/fov042

Katragkou A, McCarthy M, Meletiadis J, et al (2014) In vitro combination of isavuconazole with micafungin or amphotericin B deoxycholate against medically important molds. Antimicrob Agents Chemother 58:6934–6937. https://doi.org/10.1128/AAC.03261-14

Katzmann DJ, Hallstrom TC, Voet M, et al (1995a) Expression of an ATP-binding cassette transporter-encoding gene (YOR1) is required for oligomycin resistance in *Saccharomyces cerevisiae*. Mol Cell Biol 15:6875–6883. https://doi.org/10.1128/mcb.15.12.6875

Kaur R, Domergue R, Zupancic ML, Cormack BP (2005) A yeast by any other name: *Candida glabrata* and its interaction with the host. Curr Opin Microbiol 8:378–384. https://doi.org/10.1016/j.mib.2005.06.012

Kaur R, Goyal R, Dhakad MS, et al (2014) Epidemiology and Virulence Determinants including Biofilm Profile of *Candida* Infections in an ICU in a Tertiary Hospital in India. In: J. Mycol. https://www.hindawi.com/journals/jmy/2014/303491/. Accessed 12 Apr 2020

Kean R, Delaney C, Sherry L, et al (2018) Transcriptome Assembly and Profiling of *Candida auris* Reveals Novel Insights into Biofilm-Mediated Resistance. mSphere 3:. https://doi.org/10.1128/mSphere.00334-18

Keniya MV, Fleischer E, Klinger A, et al (2015) Inhibitors of the *Candida albicans* Major Facilitator Superfamily Transporter Mdr1p Responsible for Fluconazole Resistance. PLOS ONE 10:e0126350. https://doi.org/10.1371/journal.pone.0126350

Khakhina S, Johnson SS, Manoharlal R, et al (2015) Control of Plasma Membrane Permeability by ABC Transporters. Eukaryot Cell 14:442–453. https://doi.org/10.1128/EC.00021-15

Khandelwal NK, Chauhan N, Sarkar P, et al (2018) Azole resistance in a *Candida albicans* mutant lacking the ABC transporter *CDR6/ROA1* depends on TOR signaling. J Biol Chem 293:412–432. https://doi.org/10.1074/jbc.M117.807032

Khandelwal NK, Kaemmer P, Förster TM, et al (2016) Pleiotropic effects of the vacuolar ABC transporter MLT1 of *Candida albicans* on cell function and virulence. Biochem J 473:1537–1552. https://doi.org/10.1042/BCJ20160024

Khandelwal NK, Wasi M, Nair R, et al (2019) Vacuolar Sequestration of Azoles, a Novel Strategy of Azole Antifungal Resistance Conserved across Pathogenic and Nonpathogenic Yeast. Antimicrob Agents Chemother 63:. https://doi.org/10.1128/AAC.01347-18

Khoshnevis S, Gross T, Rotte C, et al (2010) The iron-sulphur protein RNase L inhibitor functions in translation termination. EMBO Rep 11:214–219. https://doi.org/10.1038/embor.2009.272

Khunweeraphong N, Stockner T, Kuchler K (2017) The structure of the human ABC transporter ABCG2 reveals a novel mechanism for drug extrusion. Sci Rep 7:13767. https://doi.org/10.1038/s41598-017-11794-w

Kim SH, Iyer KR, Pardeshi L, et al (2019a) Erratum for Kim et al., "Genetic Analysis of Candida auris Implicates Hsp90 in Morphogenesis and Azole Tolerance and Cdr1 in Azole Resistance." mBio 10:. https://doi.org/10.1128/mBio.00346-19

Kim SJ, Ryu JH, Kim YB, Yang SO (2019b) Management of Candida Urinary Tract Infection in the Elderly. Urogenit Tract Infect 14:33–41. https://doi.org/10.14777/uti.2019.14.2.33

Kispal G, Csere P, Guiard B, Lill R (1997) The ABC transport Atm1p is required for mitochondrial iron homeostasis. FEBS Lett 418:346–350. https://doi.org/10.1016/S0014-5793(97)01414-2

Klein C, Kuchler K, Valachovic M (2011) ABC proteins in yeast and fungal pathogens. Essays Biochem 50:101–19. https://doi.org/10.1042/bse0500101

Klein M, Burla B, Martinoia E (2006) The multidrug resistance-associated protein (MRP/ABCC) subfamily of ATP-binding cassette transporters in plants. FEBS Lett 580:1112–1122. https://doi.org/10.1016/j.febslet.2005.11.056

Klein M, Mamnun YM, Eggmann T, et al (2002) The ATP-binding cassette (ABC) transporter Bpt1p mediates vacuolar sequestration of glutathione conjugates in yeast. FEBS Lett 520:63–67. https://doi.org/10.1016/S0014-5793(02)02767-9

Klotz U, Schmidt D, Willinger B, et al (2016) Echinocandin resistance and population structure of invasive *Candida glabrata* isolates from two university hospitals in Germany and Austria. Mycoses 59:312–318. https://doi.org/10.1111/myc.12472

Köhler JR, Casadevall A, Perfect J (2015) The Spectrum of Fungi That Infects Humans. Cold Spring Harb Perspect Med 5:. https://doi.org/10.1101/cshperspect.a019273

Kołaczkowska A, Kołaczkowski M (2016) Drug resistance mechanisms and their regulation in non-*albicans Candida* species. J Antimicrob Chemother 71:1438–1450. https://doi.org/10.1093/jac/dkv445

Kolaczkowska A, Kolaczkowski M, Goffeau A, Moye-Rowley WS (2008) Compensatory activation of the multidrug transporters Pdr5p, Snq2p, and Yor1p by Pdr1p in *Saccharomyces cerevisiae*. FEBS Lett 582:977–983. https://doi.org/10.1016/j.febslet.2008.02.045

Kolaczkowski M, Cybularz-Kolaczkowska A, Soumillion J-P, et al (1996a) Anticancer drugs, ionophoric peptides, and steroids as substrates of the yeast multidrug transporter Pdr5p. J Biol Chem 271:31543–31548

Kolaczkowski M, Kolaczowska A, Luczynski J, et al (1998) In vivo characterization of the drug resistance profile of the major ABC transporters and other components of the yeast pleiotropic drug resistance network. Microb Drug Resist Larchmt N 4:143–158. https://doi.org/10.1089/mdr.1998.4.143

Kolaczkowski M, Van der Rest M, Cybularz-Kolaczkowska A, et al (1996b) Anticancer drugs, ionophoric peptides, and steroids as substrates of the yeast multidrug transporter Pdr5p. J Biol Chem 271:31543–31548. https://doi.org/10.1074/jbc.271.49.31543

Kothalawala M, Jayaweera JAAS, Arunan S, Jayathilake A (2019) The emergence of non-albicans candidemia and evaluation of HiChrome Candida differential agar and VITEK2 YST® platform for differentiation of *Candida* bloodstream isolates in teaching hospital Kandy, Sri Lanka. BMC Microbiol 19:136. https://doi.org/10.1186/s12866-019-1518-3

Kovalchuk A, Driessen AJ (2010a) Phylogenetic analysis of fungal ABC transporters. BMC Genomics 11:177. https://doi.org/10.1186/1471-2164-11-177

Kovalchuk A, Driessen AJM (2010b) Phylogenetic analysis of fungal ABC transporters. BMC Genomics 11:177. https://doi.org/10.1186/1471-2164-11-177

Kozubowski L, Heitman J (2012) Profiling a killer, the development of *Cryptococcus neoformans*. FEMS Microbiol Rev 36:78–94. https://doi.org/10.1111/j.1574-6976.2011.00286.x

Kraneveld EA, de Soet JJ, Deng DM, et al (2011) Identification and Differential Gene Expression of Adhesin-Like Wall Proteins in *Candida glabrata* Biofilms. Mycopathologia 172:415–427. https://doi.org/10.1007/s11046-011-9446-2

Ksiezopolska E, Gabaldón T (2018) Evolutionary Emergence of Drug Resistance in *Candida* Opportunistic Pathogens. Genes 9:. https://doi.org/10.3390/genes9090461

Kuchler K, Sterne RE, Thorner J (1989a) *Saccharomyces cerevisiae* STE6 gene product: a novel pathway for protein export in eukaryotic cells. EMBO J 8:3973–3984

Kullberg BJ, Arendrup MC (2015) Invasive Candidiasis. In: http://dx.doi.org/10.1056/NEJMra1315399. https://www.nejm.org/doi/pdf/10.1056/NEJMra1315399. Accessed 25 Jan 2020

Kumar A, Nair R, Kumar M, et al (2020) Assessment of antifungal resistance and associated molecular mechanism in *Candida albicans* isolates from different cohorts of patients in North Indian state of Haryana. Folia Microbiol (Praha). https://doi.org/10.1007/s12223-020-00785-6

Kumar K, Askari F, Sahu MS, Kaur R (2019) *Candida glabrata:* A Lot More Than Meets the Eye. Microorganisms 7:. https://doi.org/10.3390/microorganisms7020039

Kumari S, Kumar M, Khandelwal NK, et al (2018) ABC transportome inventory of human pathogenic yeast *Candida glabrata:* Phylogenetic and expression analysis. PLOS ONE 13:e0202993. https://doi.org/10.1371/journal.pone.0202993

Kurtzman C, Fell JW, Boekhout T (2011) The yeasts: a taxonomic study. Elsevier

Kurtzman CP, Robnett CJ (2003) Phylogenetic relationships among yeasts of the '*Saccharomyces* complex' determined from multigene sequence analyses. FEMS Yeast Res 3:417–432. https://doi.org/10.1016/S1567-1356(03)00012-6

Lachke SA, Joly S, Daniels K, Soll DR (2002) Phenotypic switching and filamentation in *Candida glabrata*. Microbiology 148:2661–2674

Lachke SA, Srikantha T, Tsai LK, et al (2000) Phenotypic switching in *Candida glabrata* involves phase-specific regulation of the Metallothionein gene MT-IIand the newly discovered hemolysin gene HLP. Infect Immun 68:884–895

Lamoth F, Alexander BD, Juvvadi PR, Steinbach WJ (2015) Antifungal activity of compounds targeting the Hsp90-calcineurin pathway against various mould species: Table 1. J Antimicrob Chemother 70:1408–1411. https://doi.org/10.1093/jac/dku549

Lamoth F, Lockhart SR, Berkow EL, Calandra T (2018) Changes in the epidemiological landscape of invasive candidiasis. J Antimicrob Chemother 73:i4–i13. https://doi.org/10.1093/jac/dkx444

Lamping E, Monk BC, Niimi K, et al (2007a) Characterization of three classes of membrane proteins involved in fungal azole resistance by functional hyperexpression in *Saccharomyces cerevisiae*. Eukaryot Cell 6:1150–1165. https://doi.org/10.1128/EC.00091-07

Lazard M, Ha-Duong N-T, Mounié S, et al (2011) Selenodiglutathione uptake by the *Saccharomyces cerevisiae* vacuolar ATP-binding cassette transporter Ycf1p. FEBS J 278:4112–4121. https://doi.org/10.1111/j.1742-4658.2011.08318.x

Lefèvre F, Boutry M (2018) Towards identification of the substrates of ATP-binding cassette transporters. Plant Physiol pp.00325.2018. https://doi.org/10.1104/pp.18.00325

Li QQ, Tsai H-F, Mandal A, et al (2018) Sterol uptake and sterol biosynthesis act coordinately to mediate antifungal resistance in *Candida glabrata* under azole

and hypoxic stress. Mol Med Rep 17:6585–6597. https://doi.org/10.3892/mmr.2018.8716

Lin MY, Carmeli Y, Zumsteg J, et al (2005) Prior Antimicrobial Therapy and Risk for Hospital-Acquired Candida glabrata and *Candida krusei* Fungemia: a Case-Case-Control Study. Antimicrob Agents Chemother 49:4555–4560. https://doi.org/10.1128/AAC.49.11.4555-4560.2005

Ling H, Chen B, Kang A, et al (2013) Transcriptome response to alkane biofuels in *Saccharomyces cerevisiae*: identification of efflux pumps involved in alkane tolerance. Biotechnol Biofuels 6:95. https://doi.org/10.1186/1754-6834-6-95

Linton KJ, Higgins CF (2007) Structure and function of ABC transporters: the ATP switch provides flexible control. Pflugers Arch 453:555–567. https://doi.org/10.1007/s00424-006-0126-x

Litchfield DW (2003) Protein kinase CK2: structure, regulation and role in cellular decisions of life and death. Biochem J 369:1–15. https://doi.org/10.1042/BJ20021469

Liu HY, Chiang YC, Pan J, et al (2001) Characterization of CAF4 and CAF16 Reveals a Functional Connection between the CCR4-NOT Complex and a Subset of SRB Proteins of the RNA Polymerase II Holoenzyme. J Biol Chem 276:7541–7548. https://doi.org/10.1074/jbc.M009112200

Liu N-N, Flanagan PR, Zeng J, et al (2017) Phosphate is the third nutrient monitored by TOR in *Candida albicans* and provides a target for fungal-specific indirect TOR inhibition. Proc Natl Acad Sci 114:6346–6351. https://doi.org/10.1073/pnas.1617799114

Liu S, Hou Y, Liu W, et al (2015) Components of the Calcium-Calcineurin Signaling Pathway in Fungal Cells and Their Potential as Antifungal Targets. Eukaryot Cell 14:324–334. https://doi.org/10.1128/EC.00271-14

Liu S, Yue L, Gu W, et al (2016) Synergistic Effect of Fluconazole and Calcium Channel Blockers against Resistant *Candida albicans*. PloS One 11:e0150859. https://doi.org/10.1371/journal.pone.0150859

Loewith R, Hall MN (2011) Target of Rapamycin (TOR) in Nutrient Signaling and Growth Control. Genetics 189:1177–1201. https://doi.org/10.1534/genetics.111.133363

Lu R-Y, Ni T-J-H, Wu J, et al (2019) New Triazole NT-a9 has Potent Antifungal Efficacy against *Cryptococcus neoformans* In Vitro and In Vivo. Antimicrob Agents Chemother. https://doi.org/10.1128/AAC.01628-19

Makanjuola O, Bongomin F, Fayemiwo S (2018) An Update on the Roles of Non-*albicans Candida* Species in Vulvovaginitis. J Fungi 4:121. https://doi.org/10.3390/jof4040121

Mamnun YM, Schüller C, Kuchler K (2004) Expression regulation of the yeast PDR5 ATP-binding cassette (ABC) transporter suggests a role in cellular detoxification during the exponential growth phase. FEBS Lett 559:111–117. https://doi.org/10.1016/S0014-5793(04)00046-8

Marr KA, Schlamm HT, Herbrecht R, et al (2015) Combination antifungal therapy for invasive aspergillosis: a randomized trial. Ann Intern Med 162:81–89. https://doi.org/10.7326/M13-2508

Megri Y, Arastehfar A, Boekhout T, et al (2020) *Candida tropicalis* is the most prevalent yeast species causing candidemia in Algeria: the urgent need for antifungal stewardship and infection control measures. Antimicrob Resist Infect Control 9:. https://doi.org/10.1186/s13756-020-00710-z

Mendes-Giannini MJS, Soares CP, da Silva JLM, Andreotti PF (2005) Interaction of pathogenic fungi with host cells: Molecular and cellular approaches. FEMS Immunol Med Microbiol 45:383–394. https://doi.org/10.1016/j.femsim.2005.05.014

Mesa-Arango AC, Trevijano-Contador N, Román E, et al (2014) The production of reactive oxygen species is a universal action mechanism of Amphotericin B against pathogenic yeasts and contributes to the fungicidal effect of this drug. Antimicrob Agents Chemother 58:6627–6638. https://doi.org/10.1128/AAC.03570-14

Michaelis S, Barrowman J (2012) Biogenesis of the *Saccharomyces cerevisiae* Pheromone a-Factor, from Yeast Mating to Human Disease. Microbiol Mol Biol Rev 76:626–651. https://doi.org/10.1128/MMBR.00010-12

Miller JD (1992) Fungi as contaminants in indoor air. Atmospheric Environ Part Gen Top 26:2163–2172. https://doi.org/10.1016/0960-1686(92)90404-9

Minnebruggen GV, François I, Cammue BPA, et al (2010) A general overview on past, present and future antimycotics. Open Mycol J 4:

Miyazaki H, Miyazaki Y, Geber A, et al (1998b) Fluconazole Resistance Associated with Drug Efflux and Increased Transcription of a Drug Transporter Gene, *PDH1* , in *Candida glabrata*. Antimicrob Agents Chemother 42:1695–1701. https://doi.org/10.1128/AAC.42.7.1695

Miyazaki T, Kohno S (2014) ER stress response mechanisms in the pathogenic yeast *Candida glabrata* and their roles in virulence. Virulence 5:365–370. https://doi.org/10.4161/viru.27373

Moore-Landecker E (1996) Fundamentals of the fungi. prentice Hall

Mor V, Rella A, Farnoud AM, et al (2015) Identification of a New Class of Antifungals Targeting the Synthesis of Fungal Sphingolipids. mBio 6:. https://doi.org/10.1128/mBio.00647-15

Morita M, Imanaka T (2012) Peroxisomal ABC transporters: structure, function and role in disease. Biochim Biophys Acta 1822:1387–1396. https://doi.org/10.1016/j.bbadis.2012.02.009

Movahed E, Tan GMY, Munusamy K, et al (2016) Triclosan Demonstrates Synergic Effect with Amphotericin B and Fluconazole and Induces Apoptosis-Like Cell Death in *Cryptococcus neoformans.* Front Microbiol 7:360. https://doi.org/10.3389/fmicb.2016.00360

Mukhopadhyay K, Prasad T, Saini P, et al (2004) Membrane Sphingolipid-Ergosterol Interactions Are Important Determinants of Multidrug Resistance in *Candida albicans*. Antimicrob Agents Chemother 48:1778–1787. https://doi.org/10.1128/AAC.48.5.1778-1787.2004

Murai T, Nakase Y, Fukuda K, et al (2009) Distinctive Responses to Nitrogen Starvation in the Dominant Active Mutants of the Fission Yeast Rheb GTPase. Genetics 183:517–527. https://doi.org/10.1534/genetics.109.105379

Nagi M, Tanabe K, Nakayama H, et al (2013a) Serum cholesterol promotes the growth of *Candida glabrata* in the presence of fluconazole. J Infect Chemother 19:138–143. https://doi.org/10.1007/s10156-012-0531-3

Nagy Z, Montigny C, Leverrier P, et al (2006) Role of the yeast ABC transporter Yor1p in cadmium detoxification. Biochimie 88:1665–1671. https://doi.org/10.1016/j.biochi.2006.05.014

Nakayama H, Izuta M, Nagahashi S, et al (1998) A controllable gene-expression system for the pathogenic fungus *Candida glabrata*. Microbiol Read Engl 144 (Pt 9:2407–2415. https://doi.org/10.1099/00221287-144-9-2407

Nakayama H, Tanabe K, Bard M, et al (2007) The *Candida glabrata* putative sterol transporter gene CgAUS1 protects cells against azoles in the presence of serum. J Antimicrob Chemother 60:1264–1272. https://doi.org/10.1093/jac/dkm321

Nami S, Aghebati-Maleki A, Morovati H, Aghebati-Maleki L (2019) Current antifungal drugs and immunotherapeutic approaches as promising strategies to treatment of fungal diseases. Biomed Pharmacother 110:857–868. https://doi.org/10.1016/j.biopha.2018.12.009

Nucci M, Marr KA (2005) Emerging Fungal Diseases. Clin Infect Dis 41:521–526. https://doi.org/10.1086/432060

Nygård Y, Mojzita D, Toivari M, et al (2014) The diverse role of Pdr12 in resistance to weak organic acids. Yeast 31:219–232. https://doi.org/10.1002/yea.3011

Oberoi JK, Wattal C, Goel N, et al (2012) Non-*albicans Candida* species in blood stream infections in a tertiary care hospital at New Delhi, India. Indian J Med Res 136:997–1003

Olsen L, Choffnes ER, Relman DA, Pray L (2011) Fungal diseases: an emerging threat to human, animal and plant health. Workshop summary. Fungal Dis Emerg Threat Hum Anim Plant Health Workshop Summ

Ong BX, Yoo Y, Han MG, et al (2019) Structural analysis of fungal pathogenicity-related casein kinase α subunit, Cka1, in the human fungal pathogen *Cryptococcus neoformans*. Sci Rep 9:1–13. https://doi.org/10.1038/s41598-019-50678-z

Onyewu C, Wormley FL, Perfect JR, Heitman J (2004) The Calcineurin Target, Crz1, Functions in Azole Tolerance but Is Not Required for Virulence of *Candida albicans*. Infect Immun 72:7330–7333. https://doi.org/10.1128/IAI.72.12.7330-7333.2004

Opekarová M, Tanner W (2003) Specific lipid requirements of membrane proteins—a putative bottleneck in heterologous expression. Biochim Biophys Acta BBA - Biomembr 1610:11–22. https://doi.org/10.1016/S0005-2736(02)00708-3

Orozco PA, Cortés JA, Parra CM (2009) [Colonization by yeasts in newborns and healthcare personnel in a neonatal intensive care unit at a university hospital in Bogotá, Colombia]. Rev Iberoam Micol 26:108–111. https://doi.org/10.1016/S1130-1406(09)70020-8

Orsi CF, Colombari B, Ardizzoni A, et al (2009) The ABC transporter-encoding gene AFR1 affects the resistance of *Cryptococcus neoformans* to microglia-mediated

antifungal activity by delaying phagosomal maturation. FEMS Yeast Res 9:301–310. https://doi.org/10.1111/j.1567-1364.2008.00470.x

Otsubo Y, Nakashima A, Yamamoto M, Yamashita A (2017) TORC1-Dependent Phosphorylation Targets in Fission Yeast. Biomolecules 7:50. https://doi.org/10.3390/biom7030050

Oxman DA, Chow JK, Frendl G, et al (2010) Candidaemia associated with decreased in vitro fluconazole susceptibility: is *Candida* speciation predictive of the susceptibility pattern? J Antimicrob Chemother 65:1460–1465. https://doi.org/10.1093/jac/dkq136

Pais P, Pires C, Costa C, et al (2016) Membrane Proteomics Analysis of the *Candida glabrata* Response to 5-Flucytosine: Unveiling the Role and Regulation of the Drug Efflux Transporters CgFlr1 and CgFlr2. Front Microbiol 7:. https://doi.org/10.3389/fmicb.2016.02045

Panapruksachat S, Iwatani S, Oura T, et al (2016) Identification and functional characterization of *Penicillium marneffei* pleiotropic drug resistance transporters ABC1 and ABC2. Med Mycol 54:478–491. https://doi.org/10.1093/mmy/myv117

Pappas PG, Lionakis MS, Arendrup MC, et al (2018) Invasive candidiasis. Nat Rev Dis Primer 4:18026. https://doi.org/10.1038/nrdp.2018.26

Paramythiotou E, Frantzeskaki F, Flevari A, et al (2014) Invasive fungal infections in the ICU: how to approach, how to treat. Mol Basel Switz 19:1085–1119. https://doi.org/10.3390/molecules19011085

Parente-Rocha JA, Bailão AM, Amaral AC, et al (2017) Antifungal Resistance, Metabolic Routes as Drug Targets, and New Antifungal Agents: An Overview about Endemic Dimorphic Fungi. In: Mediators Inflamm. https://www.hindawi.com/journals/mi/2017/9870679/. Accessed 28 Jan 2020

Park HL, Yoo Y, Hahn T-R, et al (2014) Antimicrobial Activity of UV-Induced Phenylamides from Rice Leaves. Molecules 19:18139–18151. https://doi.org/10.3390/molecules191118139

Pasrija R, Panwar SL, Prasad R (2008) Multidrug Transporters CaCdr1p and CaMdr1p of *Candida albicans* Display Different Lipid Specificities: both Ergosterol and Sphingolipids Are Essential for Targeting of CaCdr1p to Membrane Rafts. Antimicrob Agents Chemother 52:694–704. https://doi.org/10.1128/AAC.00861-07

Patil S, Rao RS, Majumdar B, Anil S (2015) Clinical Appearance of Oral *Candida* Infection and Therapeutic Strategies. Front Microbiol 6:1391. https://doi.org/10.3389/fmicb.2015.01391

Paul S, Diekema D, Moye-Rowley WS (2013) Contributions of *Aspergillus fumigatus* ATP-binding cassette transporter proteins to drug resistance and virulence. Eukaryot Cell 12:1619–1628. https://doi.org/10.1128/EC.00171-13

Paumi CM, Chuk M, Snider J, et al (2009) ABC Transporters in *Saccharomyces cerevisiae* and Their Interactors: New Technology Advances the Biology of the ABCC (MRP) Subfamily. Microbiol Mol Biol Rev MMBR 73:577–593. https://doi.org/10.1128/MMBR.00020-09

Pauwels A-M, Trost M, Beyaert R, Hoffmann E (2017) Patterns, Receptors, and Signals: Regulation of Phagosome Maturation. Trends Immunol 38:407–422. https://doi.org/10.1016/j.it.2017.03.006

Perlin DS (2011) Current perspectives on echinocandin class drugs. Future Microbiol 6:441–457. https://doi.org/10.2217/fmb.11.19

Perlroth J, Choi B, Spellberg B (2007) Nosocomial fungal infections: epidemiology, diagnosis, and treatment. Med Mycol 45:321–346. https://doi.org/10.1080/13693780701218689

Persyn A, Rogiers O, Brock M, et al (2019) Monitoring of Fluconazole and Caspofungin Activity against In Vivo *Candida glabrata* Biofilms by Bioluminescence Imaging. Antimicrob Agents Chemother 63:. https://doi.org/10.1128/AAC.01555-18

Pfaller MA, Andes DR, Diekema DJ, et al (2014) Epidemiology and Outcomes of Invasive Candidiasis Due to Non-*albicans* Species of *Candida* in 2,496 Patients: Data from the Prospective Antifungal Therapy (PATH) Registry 2004–2008. PLOS ONE 9:e101510. https://doi.org/10.1371/journal.pone.0101510

Pfaller MA, Diekema DJ (2012) Progress in Antifungal Susceptibility Testing of *Candida* spp. by Use of Clinical and Laboratory Standards Institute Broth Microdilution Methods, 2010 to 2012. J Clin Microbiol 50:2846–2856. https://doi.org/10.1128/JCM.00937-12

Pfaller MA, Diekema DJ (2007a) Epidemiology of invasive candidiasis: a persistent public health problem. Clin Microbiol Rev 20:133–163. https://doi.org/10.1128/CMR.00029-06

Pfaller MA, Diekema DJ (2007b) Epidemiology of invasive candidiasis: a persistent public health problem. Clin Microbiol Rev 20:133–163. https://doi.org/10.1128/CMR.00029-06

Pfaller MA, Diekema DJ, Gibbs DL, et al (2010) Results from the ARTEMIS DISK Global Antifungal Surveillance Study, 1997 to 2007: a 10.5-Year Analysis of Susceptibilities of C*andida* Species to Fluconazole and Voriconazole as Determined by CLSI Standardized Disk Diffusion. J Clin Microbiol 48:1366–1377. https://doi.org/10.1128/JCM.02117-09

Pfaller MA, Diekema DJ, Turnidge JD, et al (2019) Twenty Years of the SENTRY Antifungal Surveillance Program: Results for *Candida* Species From 1997–2016. Open Forum Infect Dis 6:S79–S94. https://doi.org/10.1093/ofid/ofy358

Pham CD, Iqbal N, Bolden CB, et al (2014) Role of FKS Mutations in *Candida glabrata*: MIC Values, Echinocandin Resistance, and Multidrug Resistance. Antimicrob Agents Chemother 58:4690–4696. https://doi.org/10.1128/AAC.03255-14

Piper P, Mahe Y, Thompson S, et al (1998) The pdr12 ABC transporter is required for the development of weak organic acid resistance in yeast. EMBO J 17:4257–4265. https://doi.org/10.1093/emboj/17.15.4257

Prasad Dr R, Rawal MK (2014) Efflux pump proteins in antifungal resistance. Front Pharmacol 5 AUG:1–13. https://doi.org/10.3389/fphar.2014.00202

Prasad R, Banerjee A, Khandelwal NK, Dhamgaye S (2015) The ABCs of *Candida albicans* multidrug transporter Cdr1. Eukaryot Cell 14:EC.00137-15. https://doi.org/10.1128/EC.00137-15

Prasad R, Gaur NA, Gaur M, Komath SS (2006) Efflux pumps in drug resistance of *Candida.* Infect Disord Drug Targets 6:69–83. https://doi.org/10.2174/187152606784112164

Prasad R, Goffeau A (2012) Yeast ATP-Binding Cassette Transporters Conferring Multidrug Resistance. Annu Rev Microbiol 66:39–63. https://doi.org/10.1146/annurev-micro-092611-150111

Prasad R, Khandelwal NK, Banerjee A (2016a) Yeast ABC transporters in lipid trafficking. Fungal Genet Biol FG B 93:25–34. https://doi.org/10.1016/j.fgb.2016.05.008

Prasad R, Khandelwal NK, Banerjee A (2016b) Yeast ABC transporters in lipid trafficking. Fungal Genet Biol FG B 93:25–34. https://doi.org/10.1016/j.fgb.2016.05.008

Prasad T, Saini P, Gaur NA, et al (2005) Functional Analysis of CaIPT1, a Sphingolipid Biosynthetic Gene Involved in Multidrug Resistance and Morphogenesis of *Candida albicans*. Antimicrob Agents Chemother 49:3442–3452. https://doi.org/10.1128/AAC.49.8.3442-3452.2005

Pujol A, Ferrer I, Camps C, et al (2004) Functional overlap between ABCD1 (ALD) and ABCD2 (ALDR) transporters: a therapeutic target for X-adrenoleukodystrophy. Hum Mol Genet 13:2997–3006. https://doi.org/10.1093/hmg/ddh323

Rai V, Gaur M, Shukla S, et al (2006) Conserved Asp327 of Walker B motif in the N-terminal Nucleotide Binding Domain (NBD-1) of Cdr1p of *Candida albicans* has acquired a new role in ATP hydrolysis. Biochemistry 45:14726–14739. https://doi.org/10.1021/bi061535t

Ramage G, Rajendran R, Sherry L, Williams C (2012) Fungal Biofilm Resistance. Int J Microbiol 2012:. https://doi.org/10.1155/2012/528521

Ramírez-Zavala B, Manz H, Englert F, et al (2018) A Hyperactive Form of the Zinc Cluster Transcription Factor Stb5 Causes *YOR1* Overexpression and Beauvericin Resistance in *Candida albicans*. Antimicrob Agents Chemother 62:e01655-18, /aac/62/12/e01655-18.atom. https://doi.org/10.1128/AAC.01655-18

Rasheed M, Battu A, Kaur R (2018) Aspartyl proteases in C*andida glabrata* are required for suppression of the host innate immune response. J Biol Chem 293:6410–6433. https://doi.org/10.1074/jbc.M117.813741

Raska M, Beláková J, Wudattu NK, et al (2005) Comparison of protective effect of protein and DNA vaccines hsp90 in murine model of systemic candidiasis. Folia Microbiol (Praha) 50:77–82. https://doi.org/10.1007/bf02931297

Raspor P, Zupan J (2006) Yeasts in Extreme Environments. In: Péter G, Rosa C (eds) Biodiversity and Ecophysiology of Yeasts. Springer, Berlin, Heidelberg, pp 371–417

Rastogi RP, Singh SP, Häder D-P, Sinha RP (2010) Detection of reactive oxygen species (ROS) by the oxidant-sensing probe 2',7'-dichlorodihydrofluorescein diacetate in the cyanobacterium *Anabaena variabilis* PCC 7937. Biochem Biophys Res Commun 397:603–607. https://doi.org/10.1016/j.bbrc.2010.06.006

Rathinasamy K, Jindal B, Asthana J, et al (2010) Griseofulvin stabilizes microtubule dynamics, activates p53 and inhibits the proliferation of MCF-7 cells synergistically with vinblastine. BMC Cancer 10:213. https://doi.org/10.1186/1471-2407-10-213

Raymond M, Dignard D, Alarco AM, et al (1998) A Ste6p/P-glycoprotein homologue from the asexual yeast *Candida albicans* transports the a-factor mating pheromone in Saccharomyces cerevisiae. Mol Microbiol 27:587–598. https://doi.org/10.1046/j.1365-2958.1998.00704.x

Rea PA (1999) MRP subfamily ABC transporters from plants and yeast. J Exp Bot 895–913

Redhu AK, Banerjee A, Shah AH, et al (2018) Molecular Basis of Substrate Polyspecificity of the *Candida albicans* Mdr1p Multidrug/H+ Antiporter. J Mol Biol 430:682–694. https://doi.org/10.1016/j.jmb.2018.01.005

Rees DC, Johnson E, Lewinson O (2009) ABC transporters: the power to change. Nat Rev Mol Cell Biol 10:218–227. https://doi.org/10.1038/nrm2646

Rella A, Mor V, Farnoud AM, et al (2015) Role of Sterylglucosidase 1 (Sgl1) on the pathogenicity of *Cryptococcus neoformans:* potential applications for vaccine development. Front Microbiol 6:. https://doi.org/10.3389/fmicb.2015.00836

Richardson M, Lass-Flörl C (2008) Changing epidemiology of systemic fungal infections. Clin Microbiol Infect 14:5–24. https://doi.org/10.1111/j.1469-0691.2008.01978.x

Riquelme M, Aguirre J, Bartnicki-García S, et al (2018) Fungal Morphogenesis, from the Polarized Growth of Hyphae to Complex Reproduction and Infection Structures. Microbiol Mol Biol Rev 82:. https://doi.org/10.1128/MMBR.00068-17

Rivero-Menendez O, Navarro-Rodriguez P, Bernal-Martinez L, et al (2019) Clinical and Laboratory Development of Echinocandin Resistance in *Candida glabrata*: Molecular Characterization. Front Microbiol 10:. https://doi.org/10.3389/fmicb.2019.01585

Rizzo J, Stanchev LD, da Silva VKA, et al (2019) Role of lipid transporters in fungal physiology and pathogenicity. Comput Struct Biotechnol J 17:1278–1289. https://doi.org/10.1016/j.csbj.2019.09.001

Robbins N, Collins C, Morhayim J, Cowen LE (2010) Metabolic control of antifungal drug resistance. Fungal Genet Biol 47:81–93. https://doi.org/10.1016/j.fgb.2009.07.004

Rodrigues CF, Rodrigues ME, Silva S, Henriques M (2017) *Candida glabrata* Biofilms: How Far Have We Come? J Fungi 3:. https://doi.org/10.3390/jof3010011

Rodrigues CF, Silva S, Henriques M (2014) *Candida glabrata:* a review of its features and resistance. Eur J Clin Microbiol Infect Dis 33:673–688. https://doi.org/10.1007/s10096-013-2009-3

Roelants FM, Breslow DK, Muir A, et al (2011) Protein kinase Ypk1 phosphorylates regulatory proteins Orm1 and Orm2 to control sphingolipid homeostasis in *Saccharomyces cerevisiae*. Proc Natl Acad Sci 108:19222–19227. https://doi.org/10.1073/pnas.1116948108

Roetzer A, Gratz N, Kovarik P, Schüller C (2010) Autophagy supports *Candida glabrata* survival during phagocytosis. Cell Microbiol 12:199–216. https://doi.org/10.1111/j.1462-5822.2009.01391.x

Rogers B, Decottignies a, Kolaczkowski M, et al (2001) The pleitropic drug ABC transporters from S*accharomyces cerevisiae*. J Mol Microbiol Biotechnol 3:207–214

Rollin-Pinheiro R, Singh A, Barreto-Bergter E, Del Poeta M (2016) Sphingolipids as targets for treatment of fungal infections. Future Med Chem 8:1469–1484. https://doi.org/10.4155/fmc-2016-0053

Romani L (2004) Immunity to fungal infections. Nat Rev Immunol 4:1–23. https://doi.org/10.1038/nri1255

Rosinha GMS, Freitas DA, Miyoshi A, et al (2002) Identification and Characterization of a Brucella abortus ATP-Binding Cassette Transporter Homolog to *Rhizobium meliloti* ExsA and Its Role in Virulence and Protection in Mice. Infect Immun 70:5036–5044. https://doi.org/10.1128/IAI.70.9.5036-5044.2002

Ruckenstuhl C, Lang S, Poschenel A, et al (2007) Characterization of Squalene Epoxidase of *Saccharomyces cerevisiae* by Applying Terbinafine-Sensitive Variants. Antimicrob Agents Chemother 51:275–284. https://doi.org/10.1128/AAC.00988-06

Rutledge RM, Esser L, Ma J, Xia D (2011) Toward Understanding the Mechanism of Action of the Yeast Multidrug Resistance Transporter Pdr5p: A Molecular Modeling Study. J Struct Biol 173:333–344. https://doi.org/10.1016/j.jsb.2010.10.012

Rybak JM, Doorley LA, Nishimoto AT, et al (2019) Abrogation of Triazole Resistance upon Deletion of CDR1 in a Clinical Isolate of *Candida auris*. Antimicrob Agents Chemother 63:. https://doi.org/10.1128/AAC.00057-19

Samaranayake YH, Cheung BPK, Wang Y, et al (2013) Fluconazole resistance in *Candida glabrata* is associated with increased bud formation and metallothionein production. J Med Microbiol 62:303–318. https://doi.org/10.1099/jmm.0.044123-0

Sanglard D (2019) Finding the needle in a haystack: Mapping antifungal drug resistance in fungal pathogen by genomic approaches. PLoS Pathog 15:e1007478. https://doi.org/10.1371/journal.ppat.1007478

Sanglard D, Ischer F, Bille J (2001a) Role of ATP-Binding-Cassette Transporter Genes in High-Frequency Acquisition of Resistance to Azole Antifungals in *Candida glabrata*. Antimicrob Agents Chemother 45:1174–1183. https://doi.org/10.1128/AAC.45.4.1174-1183.2001

Sanglard D, Ischer F, Bille J (2001b) Role of ATP-binding-cassette transporter genes in high-frequency acquisition of resistance to azole antifungals in *Candida glabrata*. Antimicrob Agents Chemother 45:1174–1183. https://doi.org/10.1128/AAC.45.4.1174-1183.2001

Sanglard D, Ischer F, Calabrese D, et al (1999a) The ATP Binding Cassette Transporter Gene *CgCDR1* from *Candida glabrata* Is Involved in the Resistance of Clinical

Isolates to Azole Antifungal Agents. Antimicrob Agents Chemother 43:2753–2765. https://doi.org/10.1128/AAC.43.11.2753

Sanglard D, Ischer F, Marchetti O, et al (2003) Calcineurin A of Candida albicans: involvement in antifungal tolerance, cell morphogenesis and virulence. Mol Microbiol 48:959–976. https://doi.org/10.1046/j.1365-2958.2003.03495.x

Sanguinetti M, Posteraro B, Fiori B, et al (2005a) Mechanisms of Azole Resistance in Clinical Isolates of *Candida glabrata* Collected during a Hospital Survey of Antifungal Resistance. Antimicrob Agents Chemother 49:668–679. https://doi.org/10.1128/AAC.49.2.668-679.2005

Sanguinetti M, Posteraro B, Sorda ML, et al (2006) Role of AFR1, an ABC Transporter-Encoding Gene, in the In Vivo Response to Fluconazole and Virulence of *Cryptococcus neoformans*. Infect Immun 74:1352–1359. https://doi.org/10.1128/IAI.74.2.1352-1359.2006

Sasani E, Khodavaisy S, Agha Kuchak Afshari S, et al (2016) Pseudohyphae formation in *Candida glabrata* due to CO2 exposure. Curr Med Mycol 2:49–52. https://doi.org/10.18869/acadpub.cmm.2.4.49

Saurin W, Hofnung M, Dassa E (1999) Getting in or out: early segregation between importers and exporters in the evolution of ATP-binding cassette (ABC) transporters. J Mol Evol 48:22–41. https://doi.org/10.1007/pl00006442

Scheid LA, Mario DAN, Kubiça TF, et al (2012) In vitro activities of antifungal agents alone and in combination against fluconazole-susceptible and -resistant strains of *Candida dubliniensis*. Braz J Infect Dis Off Publ Braz Soc Infect Dis 16:78–81. https://doi.org/10.1016/s1413-8670(12)70279-9

Schmidt P, Walker J, Selway L, et al (2008) Proteomic analysis of the pH response in the fungal pathogen *Candida glabrata*. Proteomics 8:534–544. https://doi.org/10.1002/pmic.200700845

Schmitt L, Tampé R (2002) Structure and mechanism of ABC transporters. Curr Opin Struct Biol 12:754–760. https://doi.org/10.1016/s0959-440x(02)00399-8

Schwarzmuller T, Ma B, Hiller E, et al (2014) Systematic phenotyping of a large-scale Candida glabrata deletion collection reveals novel antifungal tolerance genes. PLoS Pathog 10:e1004211. https://doi.org/10.1371/journal.ppat.1004211

Scorzoni L, de Paula e Silva ACA, Marcos CM, et al (2017) Antifungal Therapy: New Advances in the Understanding and Treatment of Mycosis. Front Microbiol 8:. https://doi.org/10.3389/fmicb.2017.00036

Seider K, Brunke S, Schild L, et al (2011) The Facultative Intracellular Pathogen *Candida glabrata* Subverts Macrophage Cytokine Production and Phagolysosome Maturation. J Immunol 187:3072–3086. https://doi.org/10.4049/jimmunol.1003730

Shah AH, Shukla S, Prasad R (2017) Tools and Techniques to Study Multidrug Transporters of Yeasts. In: Varma A, Sharma AK (eds) Modern Tools and Techniques to Understand Microbes. Springer International Publishing, Cham, pp 183–207

Shahid SK (2016) Newer patents in antimycotic therapy. Pharm Pat Anal 5:115–134. https://doi.org/10.4155/ppa-2015-0001

Shani N, Valle D (1996) A S*accharomyces cerevisiae* homolog of the human adrenoleukodystrophy transporter is a heterodimer of two half ATP-binding cassette transporters. Proc Natl Acad Sci U S A 93:11901–11906

Shani N, Watkins PA, Valle D (1995) PXA1, a possible *Saccharomyces cerevisiae* ortholog of the human adrenoleukodystrophy gene. Proc Natl Acad Sci U S A 92:6012–6016. https://doi.org/10.1073/pnas.92.13.6012

Shapiro RS, Robbins N, Cowen LE (2011) Regulatory Circuitry Governing Fungal Development, Drug Resistance, and Disease. Microbiol Mol Biol Rev 75:213–267. https://doi.org/10.1128/MMBR.00045-10

Sharma S, Alfatah Md, Bari VK, et al (2014) Sphingolipid Biosynthetic Pathway Genes FEN1 and SUR4 Modulate Amphotericin B Resistance. Antimicrob Agents Chemother 58:2409–2414. https://doi.org/10.1128/AAC.02130-13

Sheehan DJ, Hitchcock CA, Sibley CM (1999) Current and Emerging Azole Antifungal Agents. Clin Microbiol Rev 12:40–79

Shekhar-Guturja T, Gunaherath GMKB, Wijeratne EMK, et al (2016a) Dual action antifungal small molecule modulates multidrug efflux and TOR signaling. Nat Chem Biol 12:867–875. https://doi.org/10.1038/nchembio.2165

Shertz CA, Bastidas RJ, Li W, et al (2010) Conservation, duplication, and loss of the Tor signaling pathway in the fungal kingdom. BMC Genomics 11:510. https://doi.org/10.1186/1471-2164-11-510

Shimobayashi M, Oppliger W, Moes S, et al (2013) TORC1-regulated protein kinase Npr1 phosphorylates Orm to stimulate complex sphingolipid synthesis. Mol Biol Cell 24:870–881. https://doi.org/10.1091/mbc.e12-10-0753

Shukla S, Saini P, Smriti, et al (2003) Functional Characterization of *Candida albicans* ABC Transporter Cdr1p. Eukaryot Cell 2:1361–1375. https://doi.org/10.1128/EC.2.6.1361-1375.2003

Silva S, Negri M, Henriques M, et al (2012) *Candida glabrata, Candida parapsilosis* and *Candida tropicalis*: biology, epidemiology, pathogenicity and antifungal resistance. FEMS Microbiol Rev 36:288–305. https://doi.org/10.1111/j.1574-6976.2011.00278.x

Silverman-Gavrila LB, Lew RR (2000) Calcium and tip growth in *Neurospora crassa*. Protoplasma 213:203–217. https://doi.org/10.1007/BF01282158

Singh T, Kashyap AK, Ahluwalia G, et al (2014) Epidemiology of fungal infections in critical care setting of a tertiary care teaching hospital in North India: a prospective surveillance study. mortality 1:19–25

Singh-Babak SD, Babak T, Diezmann S, et al (2012) Global Analysis of the Evolution and Mechanism of Echinocandin Resistance in *Candida glabrata*. PLoS Pathog 8:e1002718. https://doi.org/10.1371/journal.ppat.1002718

Slomka M, Sobalska-Kwapis M, Korycka-Machala M, et al (2015) Genetic variation of the ABC transporter gene ABCC1 (Multidrug resistance protein 1-MRP1) in the Polish population. BMC Genet 16:114. https://doi.org/10.1186/s12863-015-0271-3

Smriti, Krishnamurthy S, Dixit BL, et al (2002) ABC transporters Cdr1p, Cdr2p and Cdr3p of a human pathogen *Candida albicans* are general phospholipid translocators. Yeast Chichester Engl 19:303–318. https://doi.org/10.1002/yea.818

Song T-T, Zhao J, Ying S-H, Feng M-G (2013) Differential Contributions of Five ABC Transporters to Mutidrug Resistance, Antioxidion and Virulence of *Beauveria bassiana*, an Entomopathogenic Fungus. PLOS ONE 8:e62179. https://doi.org/10.1371/journal.pone.0062179

Sousa CA, Hanselaer S, Soares EV (2015) ABCC Subfamily Vacuolar Transporters are Involved in Pb (Lead) Detoxification in *Saccharomyces cerevisiae*. Appl Biochem Biotechnol 175:65–74. https://doi.org/10.1007/s12010-014-1252-0

Spellberg BJ, Filler SG, Edwards JE (2006) Current treatment strategies for disseminated candidiasis. Clin Infect Dis Off Publ Infect Dis Soc Am 42:244–251. https://doi.org/10.1086/499057

Srikantha T, Zhao R, Daniels K, et al (2005) Phenotypic Switching in *Candida glabrata* Accompanied by Changes in Expression of Genes with Deduced Functions in Copper Detoxification and Stress. Eukaryot Cell 4:1434–1445. https://doi.org/10.1128/EC.4.8.1434-1445.2005

Srinivasan V, Pierik AJ, Lill R (2014) Crystal structures of nucleotide-free and glutathione-bound mitochondrial ABC transporter Atm1. Science 343:1137–1140. https://doi.org/10.1126/science.1246729

Srivastava VK, Suneetha KJ, Kaur R (2015) The mitogen-activated protein kinase CgHog1 is required for iron homeostasis, adherence and virulence in *Candida glabrata*. FEBS J 282:2142–2166. https://doi.org/10.1111/febs.13264

Steinbach WJ (2016) Pediatric Invasive Candidiasis: Epidemiology and Diagnosis in Children. J Fungi 2:. https://doi.org/10.3390/jof2010005

Steinbach WJ, Reedy JL, Cramer RA, et al (2007) Harnessing calcineurin as a novel anti-infective agent against invasive fungal infections. Nat Rev Microbiol 5:418–430. https://doi.org/10.1038/nrmicro1680

Tam P, Gee K, Piechocinski M, Macreadie I (2015) *Candida glabrata*, Friend and Foe. J Fungi 1:277–292. https://doi.org/10.3390/jof1020277

Tarling EJ, de Aguiar Vallim TQ, Edwards PA (2013) Role of ABC transporters in lipid transport and human disease. Trends Endocrinol Metab TEM 24:342–350. https://doi.org/10.1016/j.tem.2013.01.006

Taylor J, Jacobson D, Fisher M (1999) THE EVOLUTION OF ASEXUAL FUNGI: Reproduction, Speciation and Classification. Annu Rev Phytopathol 37:197–246. https://doi.org/10.1146/annurev.phyto.37.1.197

Taylor LH, Latham SM, Woolhouse ME (2001) Risk factors for human disease emergence. Philos Trans R Soc Lond B Biol Sci 356:983–989. https://doi.org/10.1098/rstb.2001.0888

Teo JQ-M, Lee SJ-Y, Tan A-L, et al (2019) Molecular mechanisms of azole resistance in *Candida* bloodstream isolates. BMC Infect Dis 19:63. https://doi.org/10.1186/s12879-019-3672-5

ter Beek J, Guskov A, Slotboom DJ (2014a) Structural diversity of ABC transporters. J Gen Physiol 143:419–435. https://doi.org/10.1085/jgp.201411164

Tesnière C, Pradal M, Bessière C, et al (2017) Relief from nitrogen starvation triggers transient destabilization of glycolytic mRNAs in *Saccharomyces cerevisiae* cells. Mol Biol Cell 29:490–498. https://doi.org/10.1091/mbc.E17-01-0061

Thakur JK, Arthanari H, Yang F, et al (2008) A nuclear receptor-like pathway regulating multidrug resistance in fungi. Nature 452:604–609. https://doi.org/10.1038/nature06836

Theodoulou FL, Holdsworth M, Baker A (2006) Peroxisomal ABC transporters. FEBS Lett 580:1139–1155. https://doi.org/10.1016/j.febslet.2005.12.095

Theodoulou FL, Kerr ID (2015) ABC transporter research: going strong 40 years on. Biochem Soc Trans 43:1033–1040. https://doi.org/10.1042/BST20150139

Tian L, Song T, He R, et al (2017) Genome-wide analysis of ATP-binding cassette (ABC) transporters in the sweetpotato whitefly, *Bemisia tabaci*. BMC Genomics 18:330. https://doi.org/10.1186/s12864-017-3706-6

Timmermans B, De Las Peñas A, Castaño I, Van Dijck P (2018) Adhesins in *Candida glabrata*. J Fungi 4:. https://doi.org/10.3390/jof4020060

Torelli R, Posteraro B, Ferrari S, et al (2008a) The ATP-binding cassette transporter–encoding gene *CgSNQ2* is contributing to the *CgPDR1*-dependent azole resistance of *Candida glabrata*. Mol Microbiol 68:186–201. https://doi.org/10.1111/j.1365-2958.2008.06143.x

Tortorano AM, Prigitano A, Lazzarini C, et al (2013) A 1-year prospective survey of candidemia in Italy and changing epidemiology over one decade. Infection 41:655–662. https://doi.org/10.1007/s15010-013-0455-6

Tsai H-F, Sammons LR, Zhang X, et al (2010a) Microarray and Molecular Analyses of the Azole Resistance Mechanism in *Candida glabrata* Oropharyngeal Isolates. Antimicrob Agents Chemother 54:3308–3317. https://doi.org/10.1128/AAC.00535-10

Tsai H-F, Sammons LR, Zhang X, et al (2010b) Microarray and molecular analyses of the azole resistance mechanism in *Candida glabrata* oropharyngeal isolates. Antimicrob Agents Chemother 54:3308–3317. https://doi.org/10.1128/AAC.00535-10

Uribe-Querol E, Rosales C (2017) Control of Phagocytosis by Microbial Pathogens. Front Immunol 8:. https://doi.org/10.3389/fimmu.2017.01368

Vale-Silva L, Ischer F, Leibundgut-Landmann S, Sanglard D (2013a) Gain-of-function mutations in PDR1, a regulator of antifungal drug resistance in *Candida glabrata*, control adherence to host cells. Infect Immun 81:1709–1720. https://doi.org/10.1128/IAI.00074-13

Vale-Silva LA, Moeckli B, Torelli R, et al (2016) Upregulation of the Adhesin Gene EPA1 Mediated by PDR1 in *Candida glabrata* Leads to Enhanced Host Colonization. mSphere 1:. https://doi.org/10.1128/mSphere.00065-15

Vale-Silva LA, Sanglard D (2015) Tipping the balance both ways: drug resistance and virulence in *Candida glabrata*. FEMS Yeast Res 15:. https://doi.org/10.1093/femsyr/fov025

Valotteau C, Prystopiuk V, Cormack BP, Dufrêne YF (2019) Atomic Force Microscopy Demonstrates that *Candida glabrata* Uses Three Epa Proteins To Mediate Adhesion to Abiotic Surfaces. mSphere 4:. https://doi.org/10.1128/mSphere.00277-19

Van Daele R, Spriet I, Wauters J, et al (2019) Antifungal drugs: What brings the future? Med Mycol 57:S328–S343. https://doi.org/10.1093/mmy/myz012

van Roermund CWT, Visser WF, Ijlst L, et al (2011) Differential substrate specificities of human ABCD1 and ABCD2 in peroxisomal fatty acid beta-oxidation. Biochim Biophys Acta 1811:148–152. https://doi.org/10.1016/j.bbalip.2010.11.010

van Schalkwyk E, Iyaloo S, Naicker SD, et al (2018) Large Outbreaks of Fungal and Bacterial Bloodstream Infections in a Neonatal Unit, South Africa, 2012-2016. Emerg Infect Dis 24:1204–1212. https://doi.org/10.3201/eid2407.171087

Vandeputte P, Ferrari S, Coste AT (2012) Antifungal Resistance and New Strategies to Control Fungal Infections. In: Int. J. Microbiol. https://www.hindawi.com/journals/ijmicro/2012/713687/. Accessed 27 Jan 2020

Vandeputte P, Tronchin G, Larcher G, et al (2008) A nonsense mutation in the ERG6 gene leads to reduced susceptibility to polyenes in a clinical isolate of Candida glabrata. Antimicrob Agents Chemother 52:3701–3709

Vazquez de Aldana CR, Marton MJ, Hinnebusch AG (1995) GCN20, a novel ATP binding cassette protein, and GCN1 reside in a complex that mediates activation of the eIF-2 alpha kinase GCN2 in amino acid-starved cells. EMBO J 14:3184–99

Veri A, Cowen LE (2014) Progress and prospects for targeting Hsp90 to treat fungal infections. Parasitology 141:1127–1137. https://doi.org/10.1017/S0031182013002072

Verma S, Shakya VPS, Idnurm A (2018) Exploring and exploiting the connection between mitochondria and the virulence of human pathogenic fungi. Virulence 9:426–446. https://doi.org/10.1080/21505594.2017.1414133

Vermitsky J-P, Earhart KD, Smith WL, et al (2006a) Pdr1 regulates multidrug resistance in *Candida glabrata*: gene disruption and genome-wide expression studies. Mol Microbiol 61:704–722. https://doi.org/10.1111/j.1365-2958.2006.05235.x

Vermitsky J-P, Edlind TD (2004) Azole Resistance in *Candida glabrata*: Coordinate Upregulation of Multidrug Transporters and Evidence for a Pdr1-Like Transcription Factor. Antimicrob Agents Chemother 48:3773–3781. https://doi.org/10.1128/AAC.48.10.3773-3781.2004

Vernon RM, Chong PA, Lin H, et al (2017) Stabilization of a nucleotide-binding domain of the cystic fibrosis transmembrane conductance regulator yields insight into disease-causing mutations. J Biol Chem 292:14147–14164. https://doi.org/10.1074/jbc.M116.772335

Vitenshtein A, Charpak-Amikam Y, Yamin R, et al (2016) NK cell recognition of *Candida glabrata* through binding of NKp46 and NCR1 to fungal ligands Epa1, Epa6, and Epa7. Cell Host Microbe 20:527–534. https://doi.org/10.1016/j.chom.2016.09.008

Walker GM, White NA (2017) Introduction to Fungal Physiology. In: Fungi. John Wiley & Sons, Ltd, pp 1–35

Walker JE, Saraste M, Runswick MJ, Gay NJ (1982) Distantly related sequences in the alpha- and beta-subunits of ATP synthase, myosin, kinases and other ATP-requiring enzymes and a common nucleotide binding fold. EMBO J 1:945–951

Walsh TJ, Anaissie EJ, Denning DW, et al (2008) Treatment of aspergillosis: clinical practice guidelines of the Infectious Diseases Society of America. Clin Infect Dis Off Publ Infect Dis Soc Am 46:327–360. https://doi.org/10.1086/525258

Wang H, Liu N, Yin M, et al (2014) The epidemiology, antifungal use and risk factors of death in elderly patients with candidemia: a multicentre retrospective study. BMC Infect Dis 14:609. https://doi.org/10.1186/s12879-014-0609-x

Wang H, Zhang L, Kudinha T, et al (2016) Investigation of an unrecognized large-scale outbreak of *Candida parapsilosis* sensu stricto fungaemia in a tertiary-care hospital in China. Sci Rep 6:1–11. https://doi.org/10.1038/srep27099

Wawrzycka D, Sobczak I, Bartosz G, et al (2010) Vmr 1p is a novel vacuolar multidrug resistance ABC transporter in Saccharomyces cerevisiae. FEMS Yeast Res 10:828–838. https://doi.org/10.1111/j.1567-1364.2010.00673.x

Webster J, Weber R (2007) Introduction to Fungi. Cambridge University Press

West L, Lowman DW, Mora-Montes HM, et al (2013) Differential Virulence of *Candida glabrata* Glycosylation Mutants. J Biol Chem 288:22006–22018. https://doi.org/10.1074/jbc.M113.478743

Whaley SG, Berkow EL, Rybak JM, et al (2017) Azole Antifungal Resistance in *Candida albicans* and Emerging Non- a*lbicans Candida* Species. 7:1–12. https://doi.org/10.3389/fmicb.2016.02173

Whaley SG, Berkow EL, Rybak JM, et al (2016) Azole Antifungal Resistance in *Candida albicans* and Emerging Non-albicans Candida Species. Front Microbiol 7:2173. https://doi.org/10.3389/fmicb.2016.02173

Whaley SG, Rogers PD (2016) Azole Resistance in *Candida glabrata.* Curr Infect Dis Rep 18:19–21. https://doi.org/10.1007/s11908-016-0554-5

Whaley SG, Zhang Q, Caudle KE, Rogers PD (2018) Relative Contribution of the ABC Transporters Cdr1, Pdh1, and Snq2 to Azole Resistance in *Candida glabrata*. Antimicrob Agents Chemother 62:. https://doi.org/10.1128/AAC.01070-18

Wilkens S (2015a) Structure and mechanism of ABC transporters. F1000Prime Rep 7:. https://doi.org/10.12703/P7-14

Willis KJ (2018) State of the World's Fungi. In: State Worlds Fungi. https://stateoftheworldsfungi.org/. Accessed 25 Jan 2020

Wolfger H, Mamnun YM, Kuchler K (2004) The Yeast Pdr15p ATP-binding Cassette (ABC) Protein Is a General Stress Response Factor Implicated in Cellular Detoxification. J Biol Chem 279:11593–11599. https://doi.org/10.1074/jbc.M311282200

Wu C-P, Calcagno AM, Ambudkar S V (2008) Reversal of ABC drug transporter-mediated multidrug resistance in cancer cells: Evaluation of current strategies. Curr Mol Pharmacol 1:93–105

Xiong J, Feng J, Yuan D, et al (2015) Tracing the structural evolution of eukaryotic ATP binding cassette transporter superfamily. Sci Rep 5:16724

Yapar N (2014a) Epidemiology and risk factors for invasive candidiasis. Ther Clin Risk Manag 10:95–105. https://doi.org/10.2147/TCRM.S40160

Yapar N (2014b) Epidemiology and risk factors for invasive candidiasis. Ther Clin Risk Manag 10:95–105. https://doi.org/10.2147/TCRM.S40160

Yazici O, Cortuk M, Casim H, et al (2016) *Candida glabrata* Pneumonia in a Patient with Chronic Obstructive Pulmonary Disease. In: Case Rep. Infect. Dis. https://www.hindawi.com/journals/criid/2016/4737321/. Accessed 28 Jan 2020

Yu A-Q, Pratomo Juwono NK, Foo JL, et al (2016) Metabolic engineering of *Saccharomyces cerevisiae* for the overproduction of short branched-chain fatty acids. Metab Eng 34:36–43. https://doi.org/10.1016/j.ymben.2015.12.005

Yu L, Ling G, Deng X, et al (2011) In vitro interaction between fluconazole and triclosan against clinical isolates of fluconazole-resistant *Candida albicans* determined by different methods. Antimicrob Agents Chemother 55:3609–3612. https://doi.org/10.1128/AAC.01313-10

Yu S-J, Chang Y-L, Chen Y-L (2015) Calcineurin signaling: lessons from *Candida* species. FEMS Yeast Res 15:. https://doi.org/10.1093/femsyr/fov016

Zeng Z, Tian G, Ding Y, et al (2019) Surveillance study of the prevalence, species distribution, antifungal susceptibility, risk factors and mortality of invasive candidiasis in a tertiary teaching hospital in Southwest China. BMC Infect Dis 19:939. https://doi.org/10.1186/s12879-019-4588-9

Zhou Y, Xu J, Zhu Y, et al (2016) Mechanism of action of the benzimidazole fungicide on *Fusarium graminearum*: interfering with polymerization of monomeric tubulin but not polymerized microtubule. Phytopathology 106:807–813

Zuccolo M, Kunova A, Musso L, et al (2019) Dual-active antifungal agents containing strobilurin and SDHI-based pharmacophores. Sci Rep 9:. https://doi.org/10.1038/s41598-019-47752

PUBLICATIONS AND PATENTS

9. Publications and patents

9.1 Publications

1. Kumari S, Kumar M, Khandelwal NK, Kumari P, Varma M, Vishwakarma P, Shahi G, Sharma S, Lynn AM, Prasad R, Gaur NA. ABC transportome inventory of human pathogenic yeast *Candida glabrata*: Phylogenetic and expression analysis. PLoS One. 2018 Aug 28;13(8):e0202993.

2. Pandey AK, Kumar M, **Kumari S**, Kumari P, Yusuf F, Jakeer S, Naz S, Chandna P, Bhatnagar I, Gaur NA. Evaluation of divergent yeast genera for fermentation-associated stresses and identification of a robust sugarcane distillery waste isolate *Saccharomyces cerevisiae* NGY10 for lignocellulosic ethanol production in SHF and SSF. Biotechnology for biofuels. 2019 Dec 1;12(1):40.

3. Kumari S, Kumar M, Khandelwal NK, Pandey AK, Bhakt P, Kaur R, Prasad R, Gaur NA. A homologous overexpression system to study roles of drug transporters in *Candida glabrata*. FEMS Yeast Research. 2020 Jun 3.

4. Shahi G, Kumar M, **Kumari S**, Rudramurthy SM, Chakrabarti A, Gaur NA, Singh A, Prasad R. A detailed lipidomic study of human pathogenic fungi Candida auris. FEMS Yeast Research. 2020 Aug 5.

5. Kumar M, Pandey AK, **Kumari S**, Wani SA, Jakeer S, Tiwari R, Prasad R, Gaur NA. Secretome produced by a newly isolated Aspergillus flavus strain in engineered medium shows synergy for biomass saccharification with a commercial cellulase. Biomass Conversion and Biorefinery. 2020 Aug 11:1-3.

6. Galkina KV, Finkelberg JM, Markova OV, Azbarova AV, Banerjee A, **Kumari S**, Sokolov SS, Severin FF, Prasad R, Knorre DA. Protonophore FCCP provides fitness advantage to PDR-deficient yeast cells. Journal of Bioenergetics and Biomembranes. 2020 Aug 17:1-3.

7. Kumari S, Kumar M, Gaur NA, Prasad R. A closer look at unconventional roles of ABC transporters in yeast. Fungal Genetics and Biology. (Under Revision).

8. Kumar M, Singh A, **Kumari S**, Kumar P, Wasi M, Mondal AK, Rudramurthy SM, Chakarbrati A, Gaur NA, Gow NAR, Prasad R. Sphingolipidomics of drug resistant *Candida auris* clinical isolates reveal distinct sphingolipid species signatures. BBA - Molecular and Cell Biology of Lipids. (Under Revision).

9. Onchieku NM, **Kumari S**, Pandey R, Sharma V, Kumar M, Deshmukh A, Gupta P, Kaur I, Gupta D, Kiboi D, Gaur NA, Malhotra P. Artemisinin acts by binding and inhibiting the protease activity of Ddi1 in *Plasmodium falciparum*. ACS Infectious Diseases. (Submitted).

10. Kumari S et al., CgYOR1 does not transport oligomycin, imparts TOR Kinases dependent azole resistance independent of major transporter CgCDR1 in *Candida glabrata.* (Manuscript under preparation).

11. **Kumari S** et al., Systematic phenotyping of disruptome of ABC transporters of *Candida glabrata*. (Manuscript under preparation).

9.2 Patents Filed

1. Kumari S, Kumar M, Prasad R, Gaur NA. ABC transporters deficient pathogenic yeast strain, its overexpression system, for characterization of membrane transporters and a process for the same. Indian Patent. IPA No. 201911008033, LIPC ref. IPO294. 2020.

2. Guleria I, Kumari A, Saini AK, **Kumari S**, Gaur NA. An Antifungal composition comprising bark and leaves extract of Populuss ciliate plant and method for preparing the same.Indian Patent. Patent filing No. 202011014386. 2020

PLOS ONE

RESEARCH ARTICLE

ABC transportome inventory of human pathogenic yeast *Candida glabrata*: Phylogenetic and expression analysis

Sonam Kumari[1], Mohit Kumar[1,2], Nitesh Kumar Khandelwal[1], Priya Kumari[1], Mahendra Varma[1], Poonam Vishwakarma[3], Garima Shahi[2], Suman Sharma[2], Andrew M. Lynn[3], Rajendra Prasad[2]*, Naseem A. Gaur[1]*

1 Yeast Biofuel Group, International Centre for Genetic Engineering and Biotechnology, New Delhi, India, **2** Amity Institute of Integrative Science and Health, Amity University Gurgaon, Haryana, India, **3** School of Computational and Integrative Sciences, Jawaharlal Nehru University, New Delhi, India

* naseem@icgeb.res.in (NAG); rprasad@amity.ggn.amity.edu (RP)

Citation: Kumari S, Kumar M, Khandelwal NK, Kumari P, Varma M, Vishwakarma P, et al. (2018) ABC transportome inventory of human pathogenic yeast *Candida glabrata*: Phylogenetic and expression analysis. PLoS ONE 13(8): e0202993. https://doi.org/10.1371/journal.pone.0202993

Editor: Anuradha Chowdhary, Vallabhbhai Patel Chest Institute, INDIA

Received: March 16, 2018

Accepted: August 12, 2018

Published: August 28, 2018

Data Availability Statement: All relevant data are within the paper and its Supporting Information files.

Funding: The work has been supported in parts by grants to R.P. from the Department of Biotechnology DBT [No. BT/01/CEIB/10/III/02], DBT [No. BT/PR7392/MED/29/652/2012] and DBT [No. BT/PR14117/BRB/10/1420/2015] and in parts by grants to N.A.G. by DST Ramanujan Fellowship grant [SR/S2/RJN-07/2012], DBT grants [No. BT/PR10684/PBD/26/403/2013] and DBT [No. BT/PB/

Abstract

ATP-binding cassette (ABC) is one of the two major superfamilies of transporters present across the evolutionary scale. ABC superfamily members came to prominence due to their ability to extrude broad spectrum of substrates and to confer multi drug resistance (MDR). Overexpression of some ABC transporters in clinical isolates of *Candida* species was attributed to the development of MDR phenotypes. Among *Candida* species, *Candida glabrata* is an emerging drug resistant species in human fungal infections. A comprehensive analysis of such proteins in *C*. *glabrata* is required to untangle their role not only in MDR but also in other biological processes. Bioinformatic analysis of proteins encoded by genome of human pathogenic yeast *C*. *glabrata* identified 25 putative ABC protein coding genes. On the basis of phylogenetic analysis, domain organization and nomenclature adopted by the Human Genome Organization (HUGO) scheme, these proteins were categorized into six subfamilies such as Pleiotropic Drug Resistance (PDR)/ABCG, Multi Drug Resistance (MDR)/ABCB, Multi Drug Resistance associated Protein (MRP)/ABCC, Adrenoleukodystrophy protein (ALDp)/ABCD, RNase L Inhibitor (RLI)/ABCE and Elongation Factor 3 (EF3)/ABCF. Among these, only 18 ABC proteins contained transmembrane domains (TMDs) and were grouped as membrane proteins, predominantly belonging to PDR, MDR, MRP, and ALDp subfamilies. A comparative phylogenetic analysis of these ABC proteins with other yeast species revealed their orthologous relationship and pointed towards their conserved functions. Quantitative real time PCR (qRT-PCR) analysis of putative membrane localized ABC protein encoding genes of *C*. *glabrata* confirmed their basal expression and showed variable transcriptional response towards antimycotic drugs. This study presents first comprehensive overview of ABC superfamily proteins of a human fungal pathogen *C*. *glabrata*, which is expected to provide an important platform for in depth analysis of their physiological relevance in cellular processes and drug resistance.

Centre/03/2011]. The funders had no role in study design, data collection and analysis, decision to publish, or preparation of the manuscript.

Competing interests: The authors have declared that no competing interests exist.

Introduction

ABC superfamily also known as 'Traffic ATPases' is very diverse and well-studied family of proteins known to exist from prokaryotes to higher eukaryotes [1]. These proteins are well known for their role as high affinity nutrient importers in bacterial cells and rose to prominence as exporters in higher eukaryotes. ABC proteins are promiscuous translocator of wide range of substrates such as sugars, amino acids, ions, peptides, cholesterol, metabolites, and toxins across the biological membranes, which are powered by ATP hydrolysis [2]. These proteins are known to perform diverse functions and their ability to confer MDR brought them to eminence. Typically, a full ABC transporter consists of four distinct domains: two TMDs consisting of six transmembrane helices (TMHs) and two nucleotide binding domains (NBD), located on the cytosolic side of the membrane [3]. The NBDs, which couple energy of ATP hydrolysis to power drug export are highly conserved structure [4]. Each NBD contains three characteristic motifs: Walker A and Walker B motifs, which form the nucleotide-binding site, and an ABC signature sequence, or C motif, for which several functions have been proposed, including communication between the TMDs and NBDs during the transport cycle [5,6]. The conserved sequence motifs Walker A and Walker B are separated by approximately 120 amino acids residues and the signature sequence is placed between these two motifs [7]. TMDs on the other hand with its homo- or heteromeric repeats of unrelated TMHs provide three dimensional structures for substrate binding and help in transport process [8]. In contrast to NBDs which consist of conserved sub-domains, TMHs of two TMDs are of variable structure which imparts poly specificity to these transporters [9]. While two NBDs and two TMDs are required to become a full functional ABC transporter, half ABC transporters also known to exist with one each of NBD and TMD and presumably function as homo-dimers [10]. The eukaryotic ABC superfamily is classified into nine subfamilies (A to I), according to the HUGO nomenclature [11]. The newly added ABC subfamily ABCI (the prokaryotic type ABC protein subfamily) contains ABC proteins without NBD, and is confined to plant taxa [12]. ABCH subfamily is identified in the genomes of arthropods but is absent in most of the plants, animals and fungal genomes [13]. Subfamily ABCA is known to exist in animal, plant and various protists but is absent in yeast genome [14].

Saccharomyces cerevisiae and *Candida albicans* possess a battery of ABC proteins, which are reasonably well characterized for their role in MDR [7,15]. However, such information is lacking for an emerging pathogenic haploid yeast *C. glabrata.* Recent epidemiological data revealed that *C. glabrata* is the second most frequently isolated nosocomial species among fungal infections [16], and exist as a commensal of normal microbiota of oral cavity, gastrointestinal and genital tract in humans [17]. Notably, *C. glabrata* is phylogenetically distant from pathogenic *C. albicans* and closer to nonpathogenic yeast *S. cerevisiae* [18]. The clinical isolates of *C. glabrata* show high level of resistance towards commonly used antifungal such as azoles [19]. MDR, the acquisition of resistance towards various classes of antifungal drugs is a serious clinical challenge for candidiasis treatment. Recently, high attention was derived by ABC proteins of *C. glabrata* due to the fact that some of the efflux pumps encoding genes such as *CAGL0M01760g* (*CgCDR1*), *CAGL0F02717g* (*CgPDH1*) and *CAGL0I04862g* (*CgSNQ2*) are highly expressed in clinical isolates of *C. glabrata* and contribute to the development of azole resistance [20–24]. Earlier, *CAGL0M01760g* (*CgCDR1*) and *CAGL0F02717g* (*CgPDH1*) upregulation independent of *CgPDR1* mutation in fluconazole heteroresistant *C. glabrata* clinical isolates has been also reported [25]. Therefore, an in depth analysis of large members of ABC superfamily of *C. glabrata* is required to dissect their physiological relevance in MDR and other cellular processes.

This study represents the identification and phylogenetic analysis of proteins belonging to ABC superfamily of *C. glabrata*. Our analysis identified 25 putative ABC proteins, among

them 18 members possesses at least one each of NBD and TMD and categorized as ABC transporters. The remaining 7 possess only NBDs, hence are grouped as soluble ABC proteins. Basal expression analysis of all ABC transporters revealed that all coding sequences were transcribed under normal laboratory conditions. Transient treatment with antimycotic drugs leads to the differential expression of some ABC transporters, implying their potential role in development of MDR. The phylogenetic analysis and expression profiles presented here will pave the way for future investigations involving molecular and biological significance of ABC transporters in pathogenic yeast *C. glabrata*.

Materials and methods

Identification and sequence retrieval

C. glabrata genome sequences were downloaded from the NCBI genome database (ftp.ncbi.nlm.nih.gov/genomes) with assembly no. ASM254v2. ABC proteins were identified by using the model ABC-tran (accession PF00005) of the Pfam database (https://pfam.xfam.org/) and the HMM search program from the HMMER package (http://hmmer.org/) using the default settings. Positive hits above the default threshold were further filtered by a cutoff, defined from the plot of scores and e-values (S1 Fig). Hits with domain score greater than 56.4 and e-value less than 1.2e-20 were considered true positives containing the NBD domain and extracted as potential ABC sequences for further analysis (Table 1).

Multiple sequence alignment and phylogenetic analysis

Amino acid sequences of *C. glabrata* NBDs (accession PF00005) were extracted as per their locations in the ABC proteins and *S. cerevisiae* NBD sequences of ABC proteins were retrieved by UniProt (www.uniprot.org/). The complete amino acid sequences of ABC proteins of *S. cerevisiae*, *C. albicans*, *Cryptococcus neoformans*, *Kleyvuromyces lactis* and *Schizosaccharomyces pombe* were taken from previously published report [14]. ITS sequences were taken from online database SILVA (https://www.arb-silva.de/). Sequences were aligned by ClustalW with default parameters and phylogenetic trees were generated by MEGA6.06 using maximum likelihood (ML) method and poisson amino acid substitution model with 1000 bootstrap replications. Sequence identities of ABC proteins among different species were analyzed by using BLASTp (https://blast.ncbi.nlm.nih.gov/Blast.cgi?PAGE=Proteins) with default parameters.

Topology, Chromosomal location, and localization prediction of ABC proteins

The topology of *C. glabrata* ABC proteins was predicted by online softwares Scan Prosite (http://prosite.expasy.org/scanprosite/) and Topocons (http://topcons.cbr.su.se/). Scan Prosite was used to recognize the NBD location and Topocons was utilized for TMH identification. Size and chromosomal location of the ABC proteins were retrieved from the Candida Genome Database (http://www.candidagenome.org/) and a circular ideogram was generated by using Circos software (http://circos.ca/software/). To predict subcellular localization of ABC proteins, LocTree3 (https://rostlab.org/services/loctree2/) and WoLF PSORT (https://www.genscript.com/wolf-psort.html) were employed with input of putative ABC proteins amino acid sequences.

Strain and Chemicals

Two *C. glabrata* strains reference strain CBS138/ATCC2001 and BG2, gifted by New Jersey Medical School–Rutgers, Newark, New Jersey and Lab of fungal pathogenesis, CDFD, Hyderabad, India respectively, were used in present study. Yeast cultures were maintained in YPD

Table 1. Predicted ABC proteins in *C. glabrata*.

RefSeq ID	ORF Name	Gene names*	Length#	UniProt Entry
XP_448240.1	*CAGL0K00363g*		1227	Q6FNF4
XP_444820.1	*CAGL0A01133g*		801	Q6FXW2
XP_449941.1	*CAGL0M13739g*	*ATM1*	727	Q6FIK3
XP_445704.1	*CAGL0E00385g*		608	Q6FVP0
XP_445860.1	*CAGL0E03982g*		1659	Q6FV84
XP_445319.1	*CAGL0C03289g*	*YBT1*	1648	Q6FWS5
XP_445834.1	*CAGL0E03355g*		1535	Q6FVB0
XP_449053.1	*CAGL0L06402g*	*YCF1*	1535	Q6FL41
XP_446375.1	*CAGL0G00242g*	*YOR1*	1477	Q6FTR9
XP_445428.1	*CAGL0D00352g*		861	Q6FWG6
XP_449450.1	*CAGL0M02387g*		856	Q6FJZ4
XP_446712.1	*CAGL0G08041g*		607	Q6FST2
XP_445278.2	*CAGL0C02343g*	*ARB1*	720	Q6FWW6
XP_445575.1	*CAGL0D03674g*		1186	Q6FW19
XP_448674.1	*CAGL0K10472g*		752	Q6FM70
XP_445123.1	*CAGL0B03487g*	*TEF3*	1045	O93796
XP_447598.1	*CAGL0I08019g*		1285	Q6FQ96
XP_449421.1	*CAGL0M01760g*	*CDR1*	1499	Q6FK23
XP_447461.1	*CAGL0I04862g*	*SNQ2*	1507	Q6FQN3
XP_446088.1	*CAGL0F02717g*	*PDH1/CGR1*	1542	O74208
XP_449665.1	*CAGL0M07293g*		1515	Q6FJC9
XP_446033.1	*CAGL0F01419g*	*AUS1*	1398	Q6FUR1
XP_449114.1	*CAGL0L07744g*		1055	Q6FKY0
XP_446582.1	*CAGL0G05093g*		544	Q6FT62
XP_448758.1	*CAGL0K12474g*		294	Q6FLY6

* Name of genes given in the NCBI database

Length of proteins in amino acids

https://doi.org/10.1371/journal.pone.0202993.t001

broth (2% peptone, 1% yeast extract and 2% glucose) and YPD Agar (YPD broth with 2% agar). Antifungal drugs (fluconazole, amphotericin B, caspofungin and ketoconazole) were of analytical grade and purchased from Sigma Aldrich, India.

Total RNA isolation and cDNA synthesis

Total RNA was extracted by using RNeasy Mini Kit (QIAGEN, Germany) using prescribed protocol. Briefly, overnight grown cultures of *C. glabrata* were diluted to 0.1 OD_{600} and grown for 4 hrs. at 30˚C in YPD, followed by 60 minutes treatment with desired drugs (fluconazole, 16μg/ml; amphotericin B, 1μg/ml; caspofungin, 75ng/ml and ketoconazole, 0.5μg/ml) concentration as per MIC_{50} values. Cells were washed with PBS and total RNA was extracted as per the manufacturer's protocol. RNA samples were quantified using nanodrop 2000 spectrophotometer (Thermo Scientific, USA) and 5μg of total RNA was used for cDNA synthesis by using RevertAid H minus first strand cDNA synthesis kit (Thermo Scientific, Lithuania).

Quantitative real-time PCR

Quantitative gene expression profile was evaluated by using DyNAmo Flash SYBR Green qPCR kit (Thermo Scientific, Lithuania) and gene-specific primers (Table 2) including

Table 2. Primers used in this study.

ABC Gene ORF	Forward primers (5' - 3')	Reverse primers (5' - 3')
CAGL0G09383g	CCACGGTAGATACGCTGGTG	CAGAACCCCATGGCAAGTTAGC
CAGL0F02717g	CTTTATATGAGGCAAGACC	GAAGTTCACCAGGAAATAG
CAGL0F01419g	GTCACCATACACTTACTTC	CAACCATCCACCATATTC
CAGL0M01760g	TGATGGCTGTAAGACTATG	TCCATACTTCGTGGTAATC
CAGL0I04862g	GATCCAGGTGACTCTTATAC	GGATTCCCTTACCTCAAATA
CAGL0I08019g	CTTTAATGGATCACCAGAG	CTGGTCTTAGAGTGTATTTC
CAGL0M07293g	CACGATAAGAAGGTTGTATG	CACTATATGGGCAGTAGTT
CAGL0L07744g	CGAAATTCCTGGGTATAAG	GGTGATTGAGACACATAC
CAGL0G00242g	TCTTACGTGCTCTTACTC	CCATTAGTAGGCCAATTATC
CAGL0L06402g	CCTCTTCTACTGGTGATATTG	CCCACATAGAATGACCTAAA
CAGL0C03289g	GTCGACTATGACAAGATTC	ATCCAACTCTCCACTATC
CAGL0E03982g	CTCTCACGTATGCTATTTC	AGTAGTGATAGTACCTTCG
CAGL0E03355g	CACAGGAAGGAAACTATG	GAGAGAGCATCTTCTAGT
CAGL0D00352g	GGTGTTCAGCAAAGATTAG	CAGACAGATATAACCGAGAT
CAGL0M02387g	CCTCCCAGCTATTCTATTC	CTAGTCTTGCGACAAATAAG
CAGL0A01133g	CTAAGAGTCCTAAGTGAAAG	GAACGAGATACCACATAAG
CAGL0M13739g	CTGTACCTCTGAACTTCT	CCATCACTCTTGCTTATAC
CAGL0E00385g	GGGTTACCTATCACATTC	GACCCAGTCCTATAATAAC
CAGL0K00363g	CCAACACTATTCAACGATAC	TTCCACCAGAACCTATTC

https://doi.org/10.1371/journal.pone.0202993.t002

CAGL0G09383g (*CgTDH3*) for normalization in CFX96TM real time PCR system (Bio-Rad, USA). *CgTDH3* gene was used as reference gene because its expression was constant in presence of all tested conditions (data not shown). The basal expression level of ABC transporters was measured by comparing the Ct value of the gene with *CgTDH3*. Comparative expression profiles of ABC transporters in drug-treated versus untreated conditions were analyzed by $2^{-\Delta\Delta Ct}$ method [26]. qRT-PCR was performed in biological duplicate with technical triplicate.

Statistical analysis

The statistical analysis was performed by GraphPad Prism 6. Data obtained were expressed as means ± SDs. The significance of differences between control and experimental groups were analyzed by using two-way ANOVA and statistical significant differences relative to untreated condition (YPD) were determined by Sidak's multiple comparisons test with p value <0.0001.

Results and discussion

Identification of ABC proteins in *C. glabrata*

To investigate putative ABC proteins, the HMM profile of the ABC transporter domain (accession PF00005) was utilized as the queries to search against 5213 protein coding ORFs in *C. glabrata* genome. Initially, a total of 54 proteins consisting NBD domain in the range of 150 ±20 amino acids were found. Since, NBD is a member of the Rossman fold superfamily of nucleotide binding proteins, and to ensure that only NBD containing proteins are detected, a threshold was determined from the plot of domain scores and e-values (S1 Fig), and a large inflection at a score of 56.4 and e-value of 1.2 e-20 was observed. Further, examination of sequences below this score and with a higher e-value showed that canonical motifs associated with NBD were absent in 29, out of these 54 proteins. Hence, only 25 proteins with higher score and lower e-value than the set threshold were considered for further study (Table 1).

Phylogenetic analysis, domain organization and subfamily prediction

The complete genome sequence and phylogenetic analysis of *S. cerevisiae* and *C. albicans* identified 30 and 26 distinct ABC protein encoding genes, respectively [27]. Considering close phylogenetic similarity of *C. glabrata* with *S. cerevisiae* and to predict subfamilies, an unrooted phylogenetic tree was constructed by aligning NBDs of *C. glabrata* and *S. cerevisiae* ABC proteins as described in methods. Based on resemblance in domain organization with *S. cerevisiae*, putative ABC proteins of *C. glabrata* were segregated into six major clusters and were assigned to MDR/ABCB, MRP/ABCC, ALDp/ABCD, RLI/ABCE, EF3/ABCF and PDR/ABCG subfamilies (Fig 1). The domain organization of *C. glabrata* ABC proteins was consistent with that of *S. cerevisiae* in ML tree, wherein N- and C- terminal NBDs are segregated separately; indicating that full transporters could be the outcome of duplication of half transporters.

To attain a better understanding of evolutionary relationship in ABC proteins among yeast species another phylogenetic tree was constructed by using complete ABC proteins of six representative yeast species (*S. cerevisiae*, *C. albicans*, *C. neoformans*, *K. lactis* and *S. pombe*) including *C. glabrata* (Fig 2A). Among them, *S. pombe* possess the least member of ABC proteins (19 ABC proteins) while *C. neoformans* has maximum (33 ABC proteins) ABC protein members (Fig 2B). Notably, *S. pombe* was distinct with regard to a number of subfamilies since it does not have any member protein belonging to ALDp/ABCD subfamily. Our analysis further revealed that phylogenetically *C. glabrata* ABC subfamily proteins are closer to *S. cerevisiae* and *K. lactis* ABC proteins. Interestingly, in addition to the NBD, members of each family also have conserved amino acid sequences, which could help in providing a comparative evolutionary orthologous relationship among various yeast species. Considering almost similar size of *C. glabrata* (12.3Mb) and *S. cerevisiae* (12.1Mb) genome, it is notable that the former possess lesser number of ABC proteins, which could suggest loss of some of the genes during whole genome duplication (WGD) event [28]. In *S. cerevisiae* and *C. glabrata* ABCG/PDR family forms the largest subfamily, although it has significantly lower number in *C. glabrata*. Among subfamilies, preferentially MDR/ABCB, ALDp/ABCD and RLI/ABCE family members were retained during duplication event, indicating their significance in cell physiology.

ABC proteins have two characteristic topological structures: TMD and NBD. The presence of hydrophobic TMD in the protein makes it an eligible candidate of membrane-localized proteins, while presence of only NBD makes it a putative soluble protein. To investigate whether *C. glabrata* ABC proteins follow the same domain organization as reported in other organisms, the position of NBDs and TMDs were determined in each of the ABC protein sequences by using Topocons and Scan Prosite. Based on the order of NBDs and TMDs, the ABC proteins belonging to the subfamilies ABCB/MDR, ABCC/MRP, ABCD/ALDp were predicted to possess forward topology, wherein TMD precedes the NBD (TMD-NBD), while the members of ABCG/PDR subfamily have reverse orientation, where TMD follows NBD (NBD-TMD) [29] (Fig 3). A typical TMD is comprised of 6 to 10 TMHs [30], however the prediction with different topology predicting softwares indicated the presence of a variable number of TMH in ABC proteins containing TMDs (S1 File). All the proteins with only NBDs in primary structure belong to ABCE/RLI and ABCF/EF3 subfamilies and were predicted as soluble proteins.

Multi drug resistance (MDR)/ABCB subfamily

The MDR subfamily members comprise of both full and half transporters with forward topology, $(TMD\text{-}NBD)_2$ or (TMD-NBD). ABCB1 was the first characterized member of MDR subfamily for its ability to confer MDR in mammalian cells [1]. This subfamily is further divided into three subtypes: full transporters (involved in MDR), half transporters (involved in the transportation of peptides) and mitochondrial half membrane transporters [31]. Four ABC

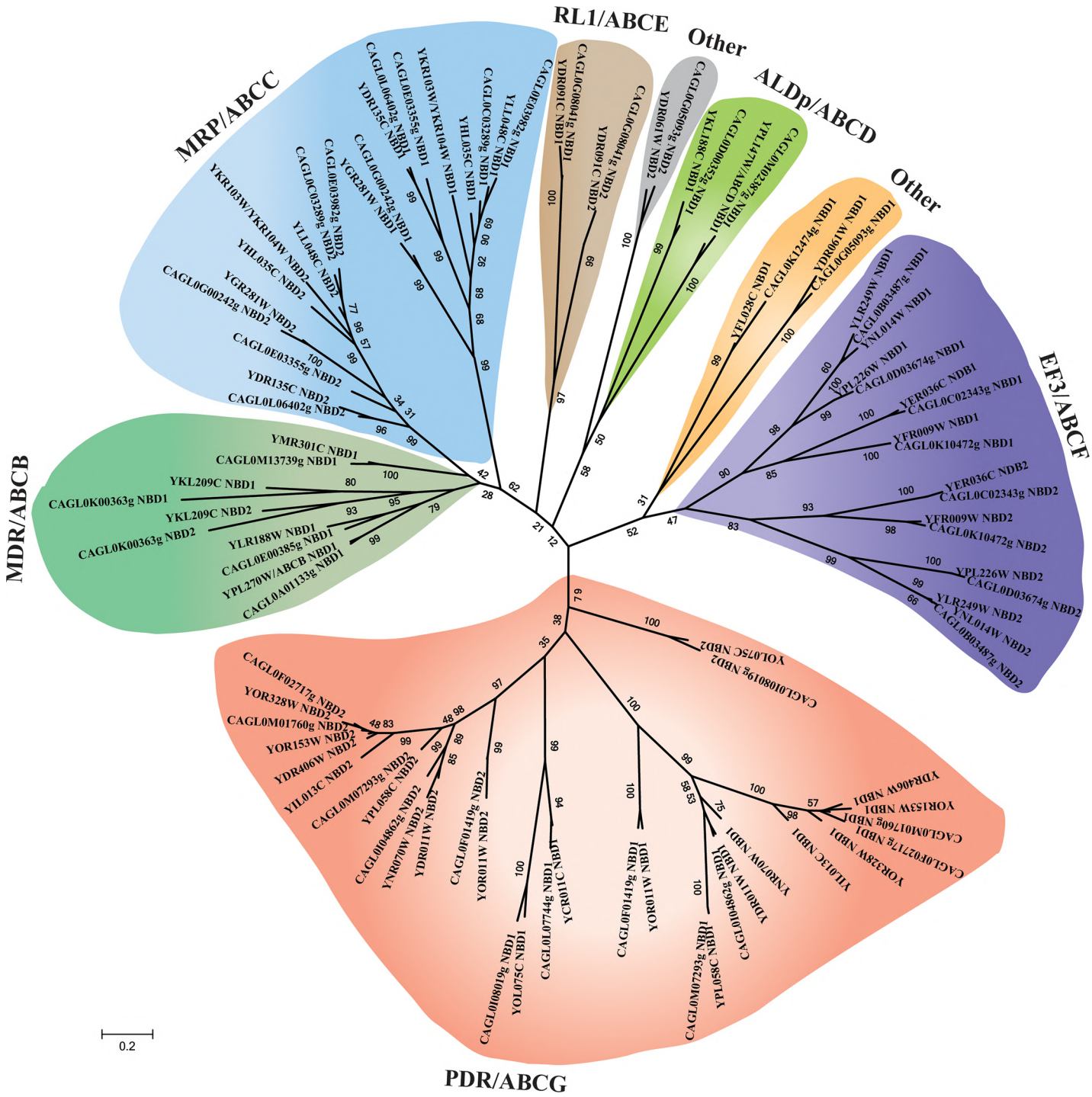

Fig 1. A schematic tree depicting the phylogenetic relationship among ABC subfamilies. NBDs of *C. glabrata* and *S. cerevisiae* ABC proteins were used in ML analysis. Clustering of *C. glabrata* NBDs is consistent with NBDs of *S. cerevisiae* ABC proteins. C-terminal NBDs of ABCC/MRP subfamily members clustered with ABCB/MDR subfamily NBDs. Phylogenetic tree is represented in radial form.

https://doi.org/10.1371/journal.pone.0202993.g001

proteins of *C. glabrata CAGL0K00363g*, *CAGL0E00385g*, *CAGL0M13739g* (*CgATM1*), and *CAGL0A01133g* belong to MDR subfamily but are remain to be characterized (Fig 1). Among these *CAGL0K00363g*, the only member of MDR/ABCB full transporter in *C. glabrata*, was

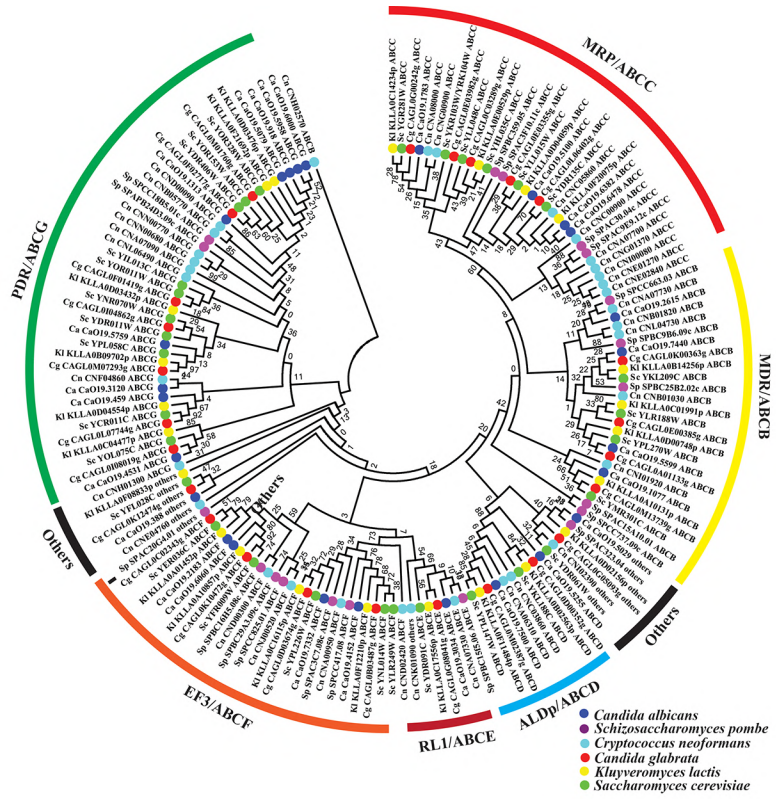

	MDR		MRP	ALDP	RL1	YEF3	PDR		Others	Total	
	Full	Half					Full	Half			
	1	3	4	2	1	4	4	2	2	23	*Kluyveromyces lactis*
	1	3	6	2	1	5	8	2	2	30	*Saccharomyces cerevisiae*
	1	3	5	2	1	4	6	1	2	25	*Candida glabrata*
	1	3	4	2	1	4	6	2	2	26	*Candida albicans*
	2	3	4	0	1	5	2	0	2	19	*Schizosaccharomyces pombe*
	2	4	9	2	1	4	6	2	3	33	*Cryptococcus neoformans*

Fig 2. Comparison of ABC proteins in different yeast species. (**A**) Phylogenetic tree of the ABC proteins of six yeast species: The analysis was performed with putative *C. glabrata* ABC protein sequences with *S. cerevisiae*, *C. albicans*, *C. neoformans*, *K. lactis* and *S. pombe*. The numbers on the branches indicate the percentage of bootstrap support from 1000 replicates. The ABC subfamilies are identified based on known subfamilies in fungal species. (**B**) Distribution of ABC proteins among fungal species: *C. glabrata* harbors less number of ABC proteins as compared to *S. cerevisiae*, *C. neoformans* and *C. albicans* but more in number as compared to *K. lactis* and *S. pombe*. Organism phylogeny presented based on their ITS sequences.

https://doi.org/10.1371/journal.pone.0202993.g002

clustered with similar full transporters in other yeasts. It showed 42% sequence identity with *S. cerevisiae* haploid-specific ABC transporter *STE6*, the a-factor pheromone transporter [32]. The three half transporters *CAGL0M13739g* (*CgATM1*), *CAGL0A01133g*, and *CAGL0E00385g* showed an orthologous relationship with *S. cerevisiae* mitochondrial half transporters. *CAGL0M13739g* (*CgATM1*) is ortholog of an inner mitochondrial membrane-localized transporters of *S. cerevisiae* (*ATM1*), which translocate iron-sulfur (Fe/S) clusters into the cytosol [33] and has a well-defined mitochondrial targeting signal sequence. Biogenesis of iron-sulfur (Fe/S) clusters as a function of *ATM1* is highly conserved among various fungal species [14]. In *C. glabrata*, *CAGL0M13739g* (*CgATM1*) is involved in osmosensitivity and echinocandin

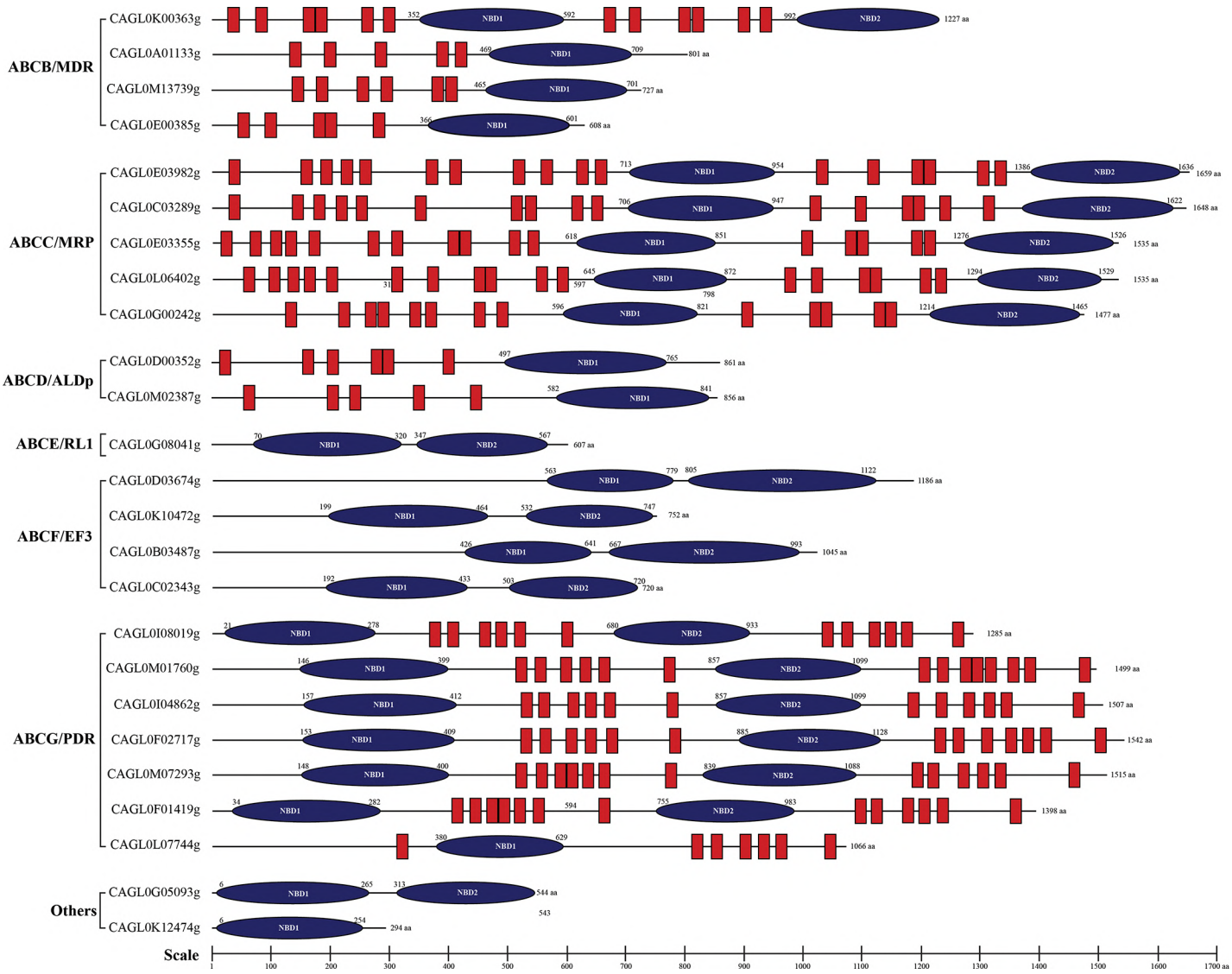

Fig 3. Pictorial depiction of ABC protein topology in *C. glabrata*. Topology prediction was performed by online softwares Scan Prosite and Topocons: All the subfamily members of ABC proteins harbor either one or two NBD. The MDR/ABCB subfamily displayed forward topology and consist of both full and half transporters, while members of the PDR/ABCG subfamily displayed reverse topology. One of the MRP/ABCC family members *CAGL0G00242g* (*CgYOR1*) does not contain extra set of transmembrane domains. ALDP/ABCD member proteins are half transporter with same topology as MDR half transporters. Members of the RLI/ABCE, EF3/ABCF and other soluble ABC proteins do not contain transmembrane domains. The scale indicates the number of amino acids.

https://doi.org/10.1371/journal.pone.0202993.g003

sensitivity [34]. *CAGL0E00385g* and *CAGL0A01133g* are orthologs of peptide transporter *MDL1* and *MDL2*, respectively, of *S. cerevisiae* localized in the mitochondrial inner membrane [35].

Multi drug resistance associated proteins (MRP)/ABCC subfamily. None of the ABC proteins of this subfamily are characterized in *C. glabrata*. MRP subfamily members belonging to mammalian cells and other major groups of eukaryotes are known to efflux diverse array of toxic substrates including drugs and xenobiotics compounds outside the cell or sequester into the vacuole [36]. The unique feature of this family is to recognize glutathione (GSH)-, glucuronate- and sulfate- conjugated organic anions and are involved in detoxification processes [37]. It has also been observed that MRPs synergistically act with a large number of enzymes viz,

GSH-S-transferase, UDP- glycosyltransferase to contribute resistance towards various substrates [38]. Notably, unlike MDR or PDR subfamilies, all the MRP members exist as full transporters. Five putative ABC proteins of *C. glabrata* were clustered into this group, among them *CAGL0E03982g*, *CAGL0C03289g* (*CgYBT1*), *CAGL0E03355g*, and *CAGL0L06402g* (*CgYCF1*) have an extra transmembrane region TMD_0(TMD- NBD)$_2$ and were considered as long MRPs, and *CAGL0G00242g* (*CgYOR1*) has topology of (TMD- NBD)$_{2,}$ considered to be short MRP (Fig 3). *C. glabrata* MRP members showed phylogenetic similarity with *K. lactis* and *S. cerevisiae* ABC proteins. However, *CAGL0G00242g* (*CgYOR1*) have 71% sequence identity with *S. cerevisiae YOR1*, a well-studied plasma membrane localized transporter involved in transport of various organic anions including oligomycin and phospholipids [39]. *CAGL0G00242g* (*CgYOR1*) also exhibited 31% sequence identity with the only known channel human *CFTR/ABCC7* in the ABC transporter superfamily protein, where mutations in its encoding gene sequence were linked to cystic fibrosis [40]. *CAGL0C03289g* (Cg*YBT1*) has a sequence identity of 53% with *S. cerevisiae YBT1*. *CAGL0G00242g* (Cg*YOR1*) and *CAGL0C03289g* (Cg*YBT1*), both were found to be upregulated in azole resistant lab mutant as well as in azole resistant clinical isolates [41,42]. 42% sequence identity of *CAGL0L06402g* (Cg*YCF1*) was observed with human *MRP1* which is involved in endobiotics and xenobiotics extrusion [43]. Previous report also suggested the upregulation of *CAGL0L06402g* (Cg*YCF1*), *CAGL0C03289g* (Cg*YBT1*) *and CAGL0G00242g* (Cg*YOR1*) in the petite strain isolates [44].

Adrenoleukodystrophy protein (ALDp)/ABCD). ALDp/ABCD subfamily proteins found in all eukaryotic organisms with an exception to some plants predominantly exist as half transporters [45]. Half ALDp members homogenously or heterogeneously dimerize to become functional [46]. In *C. glabrata CAGL0M02387g* and *CAGL0D00352g* belong to this subfamily which showed orthology with *S. cerevisiae PXA1* and *PXA2*, respectively. ALDps are peroxisomal membrane localized proteins in *S. cerevisiae*, involved in long and branched chain fatty acids import or their conjugate fatty acyl-CoA derivatives transport to peroxisome [47]. Interestingly, mutations in either *PXA1* or *PXA2* make cells incompetent to grow on oleic acid, suggesting that probably they function as a heterodimer [48]. Moreover, both ALDps of *C. glabrata* such as *CAGL0M02387g* and *CAGL0D00352g*, showed 32% and 33% sequence identity with human ABCD2 and 31% and 32% identity with *ABCD1*. The human *ABCD1* and *ABCD2* are involved in translocation of polyunsaturated VLCFA-CoA and mutation in these genes result in a human disease, X-linked Adrenoleukodystrophy (X-ALD) [49]. The clear evolutionary orthologous relationship between this family members in various species strongly point to their conserved functions.

RNase L Inhibitor (RLI)/ABCE subfamily. The RLI/ABCE subfamily proteins have a characteristic pair of linked NBDs with no TMDs. These soluble proteins are predicted to have a role in biological processes rather than in membrane transport [50]. In human *ABCE1*, an RLI protein is associated with polyribosomes and functions to inhibit RNase L to initiate translation [51]. *CAGL0G08041g*, the only member of this family in *C. glabrata*, displayed NBD-NBD topology and has a characteristic ferredoxin iron-sulfur type binding domain (4Fe-4S) with the consensus sequence of C-X-{P}-C-X(2)-C-{CP}-X(2)-C-[PEG], (pfam00037, where four C's are the 4Fe-4S center) which is a typical motif found in nucleic acid binding proteins. *CAGL0G08041g* showed high sequence identity with *S. cerevisiae RLI1* (89%) and *K. lactis KLLA0C17556p* (88%). *RLI1* of *S. cerevisiae*, an iron-sulfur (4Fe-4S) protein, is involved in maturation of ribosomal subunit, translation initiation through interaction with eIF3 complex and also have a role in translational termination [52], however, this protein remains uncharacterized in *C. glabrata*.

Elongation factor 3 (EF3)/ABCF subfamilies. The members of this subfamily are topologically similar to RLI subfamily proteins with paired NBDs without TMDs. In human and yeast species, *EF3* is involved in several aspects of translation such as ribosome biogenesis, translational control of gene expression, exporting mRNA into cytoplasm, or act as a

translational elongation factor [14]. A total of four members namely, *CAGL0K10472g*, *CAGL0C02343g*, *CAGL0D03674g*, and *CAGL0B03487g* (*CgTEF3*) of ABC proteins in *C. glabrata* belonged to this subfamily. *CAGL0B03487g* (*CgTEF3*) and *CAGL0C02343g* showed 88% and 90% sequence identity with *S. cerevisiae TEF3* and *ARB1*, respectively. In *C. glabrata*, *CAGL0B03487g* (*CgTEF3*) is an essential gene for growth and at protein level, it has been reported to be down regulated at alkaline pH [53,54]. The best characterized member of this subfamily in *S. cerevisiae* is *GCN20*, which mediates the activation of eIF-2α kinase [55] and showed 89% sequence identity with *CAGL0K10472g*. All members of this family are remain uncharacterized in *C. glabrata*.

Pleiotropic Drug Resistance (PDR)/ABCG subfamily. PDR/ABCG subfamily is ubiquitous throughout the plants, fungi and animal kingdom but absent in bacteria. In animals, PDR subfamily members exist as half transporters and are homologous to the white-brown-complex (WBC) family transporter of *Drosophila*. In previous report, it is suggested that there could be two possibilities of generation of PDR/ABCG subfamily, 1) by fusion of independent NBD and TMD, because it is the only subfamily in which NBD precedes the TMD (reverse topology) or 2) by direct origin from the central portion of a member of the ABCA, ABCB, or ABCC subfamilies [56]. Notably, PDR/ABCG subfamily members play important roles in extruding a variety of xenobiotics including agricultural fungicides, azoles, mycotoxins, herbicides, and antifungal drugs [57]. Similar to *S. cerevisiae* and *C. albicans*, PDR/ABCG subfamily with 7 members; *CAGL0F02717g* (*CgPDH1*), *CAGL0F01419g* (*CgAUS1*), *CAGL0M01760g* (*CgCDR1*), *CAGL0I04862g* (*CgSNQ2*), *CAGL0I08019g*, *CAGL0M07293g*, and *CAGL0L07744g* represents the largest group in *C. glabrata* wherein, all the members except *CAGL0L07744g* are full transporters. Importantly, *CAGL0M01760g* (*CgCDR1*), *CAGL0I04862g* (*CgSNQ2*) and *CAGL0F02717g* (*CgPDH1*) have been shown to play major role in the development of MDR phenotypes in clinical isolates and petite mutants of *C. glabrata* [58–61]. These three transporters are regulated by transcription factor PDR1 and their upregulation is linked to the azole resistance [24]. *CAGL0F01419g* (*CgAUS1*) is a sterol transporter and protects cells against azole antifungals in the presence of serum [62,63]. These *C. glabrata* genes showed sequence similarity with human ABCG members involved in exporting anti-cancerous drugs and cholesterol transport. Other members of PDR subfamily are poorly characterized in *C. glabrata*. However, their functions can be predicted based on sequence identity with PDR/ABCG members of other yeast species. For instance, *CAGL0M07293g* is an ortholog of *S. cerevisiae PDR12* with 85% sequence identity, which is involved in organic acid transport [64], while *CAGL0I08019g* with 36% sequence identity to *CDR6/ROA1* of *C. albicans* governs resistance to azoles [65]. The half transporter *CAGL0L07744g* shows 67% sequence identity with *S. cerevisiae ADP1*, the first identified half transporter belongs to the WBC family of *Drosophila* [66].

Others. Soluble ABC proteins that do not cluster into any specified subfamily has been kept under the category of others. In *C. glabrata* two proteins, *CAGL0G05093g* and *CAGL0K12474g* come into this category with two NBD and one NBD, respectively. *CAGL0G05093g* showed an orthologous relationship with uncharacterized protein in *S. cerevisiae* (*YDR061W*) and have 32% sequence identity with *C. albicans MODF*. *CAGL0K12474g* gene has orthologous relationship with *CAF16* of *S. cerevisiae* which is known to be a part of CCR4-NOT regulatory complex involved in transcriptional control of gene regulation [67].

Chromosomal position and localization prediction

C. glabrata with haploid genome consists of 13 chromosomes (Chr A to Chr M) [18]. Chr M harbors maximum number of ABC protein encoding genes (4 genes) followed by Chr E, Chr G and Chr K, each possess 3 genes. Each of Chr C, Chr D, Chr F, Chr I and Chr L

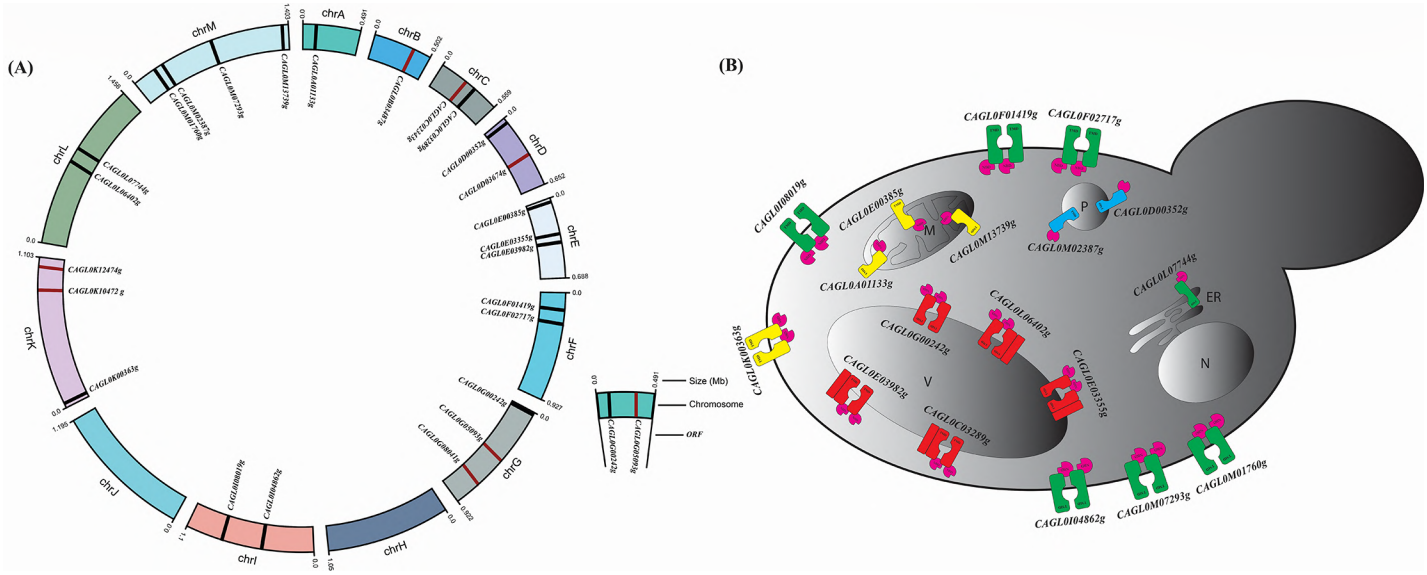

Fig 4. Chromosomal location and subcellular localization of ABC proteins in *C. glabrata*. **(A)** *C. glabrata* chromosomes (chrA—chrM) are displayed in circular ideogram. Black color indicates location of ABC transporter and dark maroon indicates soluble ABC proteins location. Chromosome M harbors maximum number of ABC genes and Chromosome H and J do not contain ABC genes. (**B**) Subcellular localization of the ABC transporters were predicted by LocTree3 and WoLF PSORT: Only membrane proteins are depicted.

https://doi.org/10.1371/journal.pone.0202993.g004

accommodate 2 genes. Each Chr A and Chr B reside only 1 gene, however, Chr H and Chr J do not contain any ABC protein coding gene (Fig 4A).

Subcellular localization (SCL) of a protein is important to elucidate the potential function in various cellular processes. It is anticipated that proteins localized in the same cellular compartment of different organisms could perform similar type of function. SCLs of ABC proteins of *C. glabrata* were analysed by using online software LocTree3. The results obtained suggested that most of the *C. glabrata* MDR/ABCB members are localized in mitochondrial membrane and MRP/ABCC members are localized in vacuolar membrane (VM). As expected, ALDp/ABCD members were predicted to be localized on peroxisomal membrane. ABC proteins of PDR/ABCG subfamily were predicted in plasma membrane (PM) except *CAGL0L07744g*, which was found to be localized on endoplasmic reticulum (ER) (Fig 4B). Previous reports supported our localization prediction as two of the known PDR/ABCG members, *CAGL0M01760g* (*CgCDR1*) and *CAGL0F02717g* (*CgPDH1*) were shown to be plasma membrane localized [68]. Notably, localization prediction varies by the use of different softwares. ABC proteins, *CAGL0I08019g* and *CAGL0K00363g* belonging to PDR/ABCG and MDR/ABCB subfamilies, respectively, were predicted to be localized at the nucleus by LocTree3 software, however, WoLF PSORT predicted these proteins localization at PM. WoLF PSORT predicted *CAGL0G00242g* (*CgYOR1*) and *CAGL0L07744g* localization to PM, while LocTree3 predicted in VM and ER membranes, respectively. The predicted localization of 18 ABC membrane proteins are depicted in Fig 4B, while soluble ABC proteins are predicted to be confined to the cytosol or nucleus are listed in S2 File.

Membrane localized ABC subfamily genes displayed variable response to drug exposure

Our long term goal is to unravel the role of membrane localized efflux pumps in development of MDR. Hence, for expression analysis, we selected 18 potential membrane localized

members of the ABC superfamily. It is expected that expression level of genes may vary among strains with different genetic background and source of isolation. Therefore, in this study we evaluated the expression level of ABC transporter genes between the two strains of *C. glabrata*: a reference strain CBS138/ATCC2001 and a widely used clinical isolate BG2.

Initially, we tested the basal expression level of these gene under laboratory growth conditions. qRT-PCR analysis of the mid-log phage grown cells in YPD media at 30˚C confirmed that all selected ABC transporter were transcribed under normal growth condition in both the strains. However, the degree of basal expression showed considerable variation in these strains. Since strain BG2 was an isolate from a patient with initial exposure to fluconazole treatment, expectedly, in comparison to CBS138/ATCC2001, its encoding transporter genes were upregulated at basal level (Fig 5). Therefore, after transient drug exposure, the ABC transporter genes of BG2 show lesser changes in their expression. But in CBS138/ATCC2001 strain, the transient drug induction yielded stronger response and comparatively showed higher changes in expression pattern of ABC genes in all tested condition (Fig 6A–6D).

Frequently, enhanced expression of several ABC superfamily genes was directly linked to the acquisition of drug resistance among different yeast species. Earlier, several reports demonstrated that in clinical MDR isolates of *C. glabrata*, ABC transporters such as *CAGL0M01760g* (*CgCDR1*), *CAGL0I04862g* (*CgSNQ2*) and *CAGL0F02717g* (*CgPDH1*) were highly expressed and their expression varied in laboratory strains during transient drug induction and environmental conditions [69,70]. For evaluating the role of ABC membrane proteins coding genes, we further tested expression of all selected ABC transporters followed by 60 min exposure to azoles

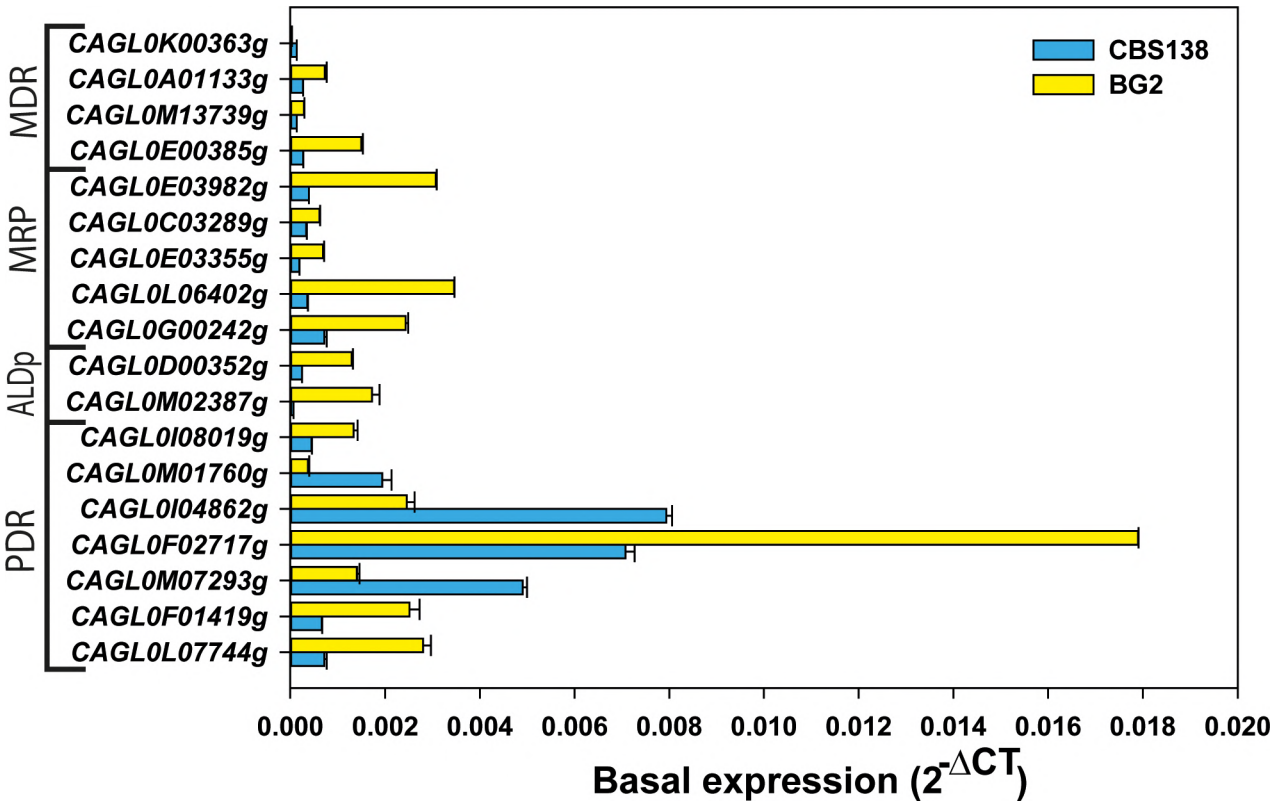

Fig 5. Comparative basal expression of ABC transporters in CBS138/ATCC2001 and BG2 strains. The basal expression of ABC transporters were tested by qRT-PCR in log phase grown cell under laboratory conditions (YPD, 30˚C) and data was measured in $2^{-\Delta CT}$ by normalizing with housekeeping gene *CgTDH3*. Among all ABC transporters *CAGL0K00363g* exhibited minimum expression level in both the strains.

https://doi.org/10.1371/journal.pone.0202993.g005

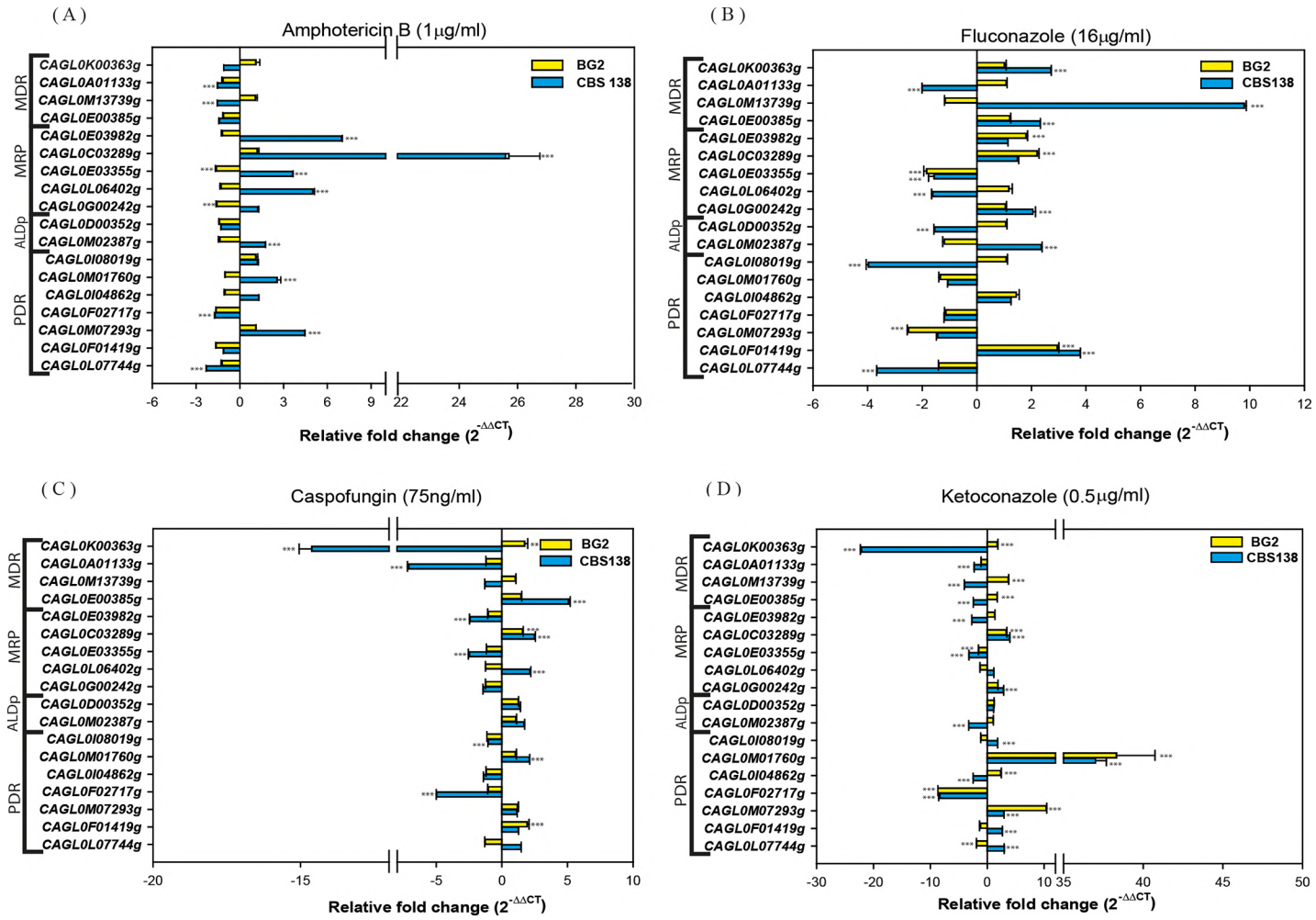

Fig 6. Comparative expression of ABC transporters encoding genes after transient drug exposure of CBS138/ATCC2001 and BG2 strains. The expression level was tested by qRT-PCR and data was measured by $2^{-\Delta\Delta CT}$ method in the presence of amphotericin B (A), fluconazole (B), caspofungin (C), and ketoconazole (D). Transporters behaved differently in these four conditions. Expression data were assessed by two-way ANOVA and statistical significant differences relative to untreated condition (YPD) were determined by Sidak's multiple comparisons test and are indicated as stars with p value <0.0001.

https://doi.org/10.1371/journal.pone.0202993.g006

(fluconazole, ketoconazole), echinocandin (caspofungin) and polyene (amphotericin B) drugs. The data obtained by qRT-PCR provided an interesting insight on to the expression pattern of ABC transporters under stress conditions. For instance, all the tested drugs exhibited differential expression pattern of membrane ABC superfamily genes, implying their role in the development of drug resistance phenotypes.

Among MDR members, basal expression of *CAGL0K00363g* was lowest, in both the strains. Notably, *CAGL0K00363g* ortholog in *S. cerevisiae* (*STE6*) is a dedicated pheromone transporter and its human homolog (*ABCB1*) mediated MDR in various chemotherapy resistant tumors by effluxing toxic compounds [71]. Although *CAGL0K00363g* was 1.7 fold upregulated in presence of both caspofungin and ketoconazole in BG2 strain, but in CBS138/ATCC2001 strain it was down regulated to 14.6 and 22.1 fold in presence these drugs. Most of the MDR genes in CBS138/ATCC2001 strain displayed down regulation following amphotericin B, caspofungin, and ketoconazole treatment but were up regulated in fluconazole exposed cells. Interestingly, in BG2 strain the expression level of other MDR members remained unchanged during

fluconazole, amphotericin B and caspofungin inductions except *CAGL0E00385g* and *CAGL0M13739g* (*CgATM1*), wherein expression level was significantly higher followed by ketoconazole exposure (Fig 6D).

Among MRP subfamily members, basal expression level of *CAGL0E03355g* was low in both the strains. *CAGL0G00242g* (*CgYOR1*) was upregulated by azoles in CBS138//ATCC2001, while, in BG2 strain the expression level was down regulated by 1.5 fold following amphotericin B treatment. However, in case of ketoconazole exposed cells, it was 1.8 fold upregulated. *CAGL0G00242g* (*CgYOR1*) ortholog in *S. cerevisiae* (*YOR1*) has a well demonstrated role in pleiotropic drug resistance [72]. *CAGL0C03289g* (*CgYBT1*) displayed higher expression following drug treatment in both strains. While, *CAGL0E03982g* transcript level was significantly upregulated only in fluconazole treated BG2 cells, whereas in CBS138/ATCC2001 strain, it was upregulated by amphotericin B treatment only. *CAGL0E03355g* transcript level was significantly down regulated in both tested strains followed by most of the inducing conditions. Notably, human MRP family member *ABCC1* is involved in multidrug resistance, especially during cancer and leukemia chemotherapy treatments [73] However, its ortholog *CAGL0L06402g* (*CgYCF1*) in *C. glabrata* does not respond to tested drug in BG2 strain but were significantly upregulated in case of amphotericin B and caspofungin exposed CBS138/ATCC2001 strain. Together, qRT-PCR analysis of MRP subfamily genes in *C. glabrata* similar to other yeast species do point to their involvement in drug detoxification.

Both ALDp members exhibited significantly higher expression at basal level in BG2 than in CBS138/ATCC2001. The expression level of ALDp members remained unresponsive to drug treatment in BG2. However, in CBS138/ATCC2001 strain *CAGL0M02387g* was significantly down regulated in ketoconazole and upregulated with other tested inducing conditions while *CAGL0D00352g* showed significant down regulation in fluconazole treatment.

Together, PDR subfamily member genes revealed constitutive expression, and they are the best responders to transient drug treatments. *CAGL0M01760g* (*CgCDR1*) and *CAGL0F02717g* (*CgPDH1*) have similar behavior with ketoconazole treatment in both the strains. The expression of *CAGL0M07293g*, an ortholog of *S. cerevisiae PDR12* (weak acid transporter) was higher following ketoconazole treatment in both the strains. The low level of expression of *CAGL0M07293g* in fluconazole resistant isolates of *C. glabrata* was earlier recorded by Vermitsky *et. al.* [41], which could be consistent with the low expression in BG2 strain. In BG2 strain *CAGL0M07293g* gene behaved differently in different azoles, where an imidazole and a triazole yielded opposite response. *CAGL0F02717g* (*CgPDH1*) was down regulated in most of the treatment condition in both the strain. Based on homology with *CaCDR1* and *CaCDR2*, it is reasonable to expect that *CAGL0F02717g* (*CgPDH1*) could be involved in phospholipid translocation and membrane lipid asymmetry maintenance [74]. As expected, fluconazole treatment induced *CAGL0F01419g* (*CgAUS1*) expression in both the strains. PDR members displayed varying degree of changes in expression, which strongly indicate their role in multi drug resistance.

Conclusion

The study presents a first comprehensive transportome analysis of ABC proteins in *C. glabrata*, which led to the identification of 25 ABC proteins, representing 0.479% of protein coding genes, distributed on 11 out of 13 chromosomes. The phylogenetic comparison with other fungal species clustered these ABC members into six major subfamilies: MDR/ABCB, MRP/ABCC, ALD/ABCD, RLI/ABCE, EF3/ABCF and PDR/ABCG. The constitutive expression of all the genes encoding putative membrane localized ABC members not only confirmed their genomic presence but also reflected their biological relevance. The exposure to drugs presented variable transcriptional response among ABC membrane proteins, nonetheless, it

provided sufficient clue for their potential contribution in emerging clinical drug resistance in *C. glabrata* isolates. Of note, majority of members of subfamilies remain unexplored. The sequence identity of *C. glabrata* ABC proteins with other organism could provide a basis for functional characterization of these unexplored important proteins; however, our analysis could only predict their localization and putative function. Based on the information available in *S. cerevisiae* and other yeasts, most of the ABC transporter genes are non-essential and hence construction of homozygous knockouts (KOs) should be realtively easy. The analysis of KOs of each member is a way forward in dissecting their role in MDR, pathogenicity and virulence. The studies so far do suggest that some of the ABC members, particularly those belonging to PDR family (*CgCDR1*, *CgPDH1* and *CgSNQ2*) have demonstrable role in developing drug resistance but considering the vast information about the role of ABC members in *C. albicans* and in other organisms, it is a long way before their physiological relevance of these ABC proteins could be unraveled.

Supporting information

S1 Fig. Identification of ABC proteins in *C. glabrata*. ABC proteins were identified by using the model ABC-tran (accession PF00005) of the Pfam database and the HMM search program. A total of 25 ABC proteins are extracted as potential ABC protein sequence. Hits with domain score greater than 56.4 and e-value less than 1.2e-20 were considered true positives containing the NBD domain.
(TIF)

S1 File. Number of transmembrane helix in *C. glabrata* ABC protein by using different softwares.
(XLSX)

S2 File. Localization prediction of all *C. glabrata* ABC proteins.
(XLSX)

S3 File. NBD sequences of *C. glabrata* and *S. cerevisiae* ABC proteins.
(XLSX)

S4 File. Complete sequences of ABC proteins and their ITS sequences of six yeast species.
(XLSX)

S5 File. Chromosomal location of putative ABC protein coding genes in *C. glabrata*.
(XLSX)

S6 File. Percent identity of putative ABC proteins of *C. glabrata* with other species.
(XLSX)

Acknowledgments

The authors are grateful to Dr. Rupinder Kaur, CDFD, Hyderabad, India and Neeraj Chauhan, Public Health Research Institute Center, New Jersey Medical School–Rutgers, Newark, New Jersey for their kind gift of *C. glabrata* BG2 and CBS138/ATCC2001 strain respectively. The authors are also thankful to Dr. Ajay Kumar Pandey for English and grammatical correction of the manuscript.

Author Contributions

Conceptualization: Nitesh Kumar Khandelwal.

Data curation: Sonam Kumari, Nitesh Kumar Khandelwal.

Funding acquisition: Rajendra Prasad, Naseem A. Gaur.

Investigation: Sonam Kumari, Mohit Kumar, Priya Kumari, Mahendra Varma.

Methodology: Sonam Kumari, Mohit Kumar, Nitesh Kumar Khandelwal, Mahendra Varma, Poonam Vishwakarma, Garima Shahi, Suman Sharma.

Project administration: Rajendra Prasad, Naseem A. Gaur.

Software: Sonam Kumari, Mohit Kumar, Mahendra Varma, Poonam Vishwakarma, Andrew M. Lynn.

Supervision: Andrew M. Lynn, Rajendra Prasad, Naseem A. Gaur.

Validation: Sonam Kumari, Mohit Kumar.

Visualization: Sonam Kumari.

Writing – original draft: Sonam Kumari, Rajendra Prasad, Naseem A. Gaur.

Writing – review & editing: Sonam Kumari, Mohit Kumar, Nitesh Kumar Khandelwal, Priya Kumari, Poonam Vishwakarma, Andrew M. Lynn, Rajendra Prasad, Naseem A. Gaur.

References

1. Glavinas H, Krajcsi P, Cserepes J, Sarkadi B. The role of ABC transporters in drug resistance, metabolism and toxicity. Curr Drug Deliv. United Arab Emirates; 2004; 1: 27–42. PMID: 16305368
2. Davidson AL, Dassa E, Orelle C, Chen J. Structure, Function, and Evolution of Bacterial ATP-Binding Cassette Systems. Microbiol Mol Biol Rev. American Society for Microbiology (ASM); 2008; 72: 317–364. https://doi.org/10.1128/MMBR.00031-07 PMID: 18535149
3. Wilkens S. Structure and mechanism of ABC transporters. F1000Prime Rep. 2015; 7: 1–9. https://doi.org/10.12703/P7-14 PMID: 25750732
4. Linton KJ, Higgins CF. Structure and function of ABC transporters: the ATP switch provides flexible control. Pflugers Arch. Germany; 2007; 453: 555–567. https://doi.org/10.1007/s00424-006-0126-x PMID: 16937116
5. Rai V, Gaur M, Shukla S, Shukla S, Ambudkar S V, Komath SS, et al. Conserved Asp327 of Walker B motif in the N-terminal Nucleotide Binding Domain (NBD-1) of Cdr1p of Candida albicans has acquired a new role in ATP hydrolysis. Biochemistry. 2006; 45: 14726–14739. https://doi.org/10.1021/bi061535t PMID: 17144665
6. Prasad R, Banerjee A, Khandelwal NK, Dhamgaye S. The ABCs of *Candida albicans* multidrug transporter Cdr1. Eukaryot Cell. 2015; 14: EC.00137-15. https://doi.org/10.1128/EC.00137-15 PMID: 26407965
7. Gaur M, Choudhury D, Prasad R. Complete inventory of ABC proteins in human pathogenic yeast, Candida albicans. J Mol Microbiol Biotechnol. Switzerland; 2005; 9: 3–15. https://doi.org/10.1159/000088141 PMID: 16254441
8. ter Beek J, Guskov A, Slotboom DJ. Structural diversity of ABC transporters. J Gen Physiol. United States; 2014; 143: 419–435. https://doi.org/10.1085/jgp.201411164 PMID: 24638992
9. Prasad R Dr, Rawal MK. Efflux pump proteins in antifungal resistance. Front Pharmacol. 2014; 5 AUG: 1–13. https://doi.org/10.3389/fphar.2014.00001
10. Wilkens S. Structure and mechanism of ABC transporters. F1000Prime Rep. England; 2015; 7: 14. https://doi.org/10.12703/P7-14 PMID: 25750732
11. Dean M, Hamon Y, Chimini G. The human ATP-binding cassette (ABC) transporter superfamily. J Lipid Res. United States; 2001; 42: 1007–1017. PMID: 11441126
12. Verrier PJ, Bird D, Burla B, Dassa E, Forestier C, Geisler M, et al. Plant ABC proteins—a unified nomenclature and updated inventory. Trends Plant Sci. England; 2008; 13: 151–159. https://doi.org/10.1016/j.tplants.2008.02.001 PMID: 18299247
13. Annilo T, Chen Z-Q, Shulenin S, Costantino J, Thomas L, Lou H, et al. Evolution of the vertebrate ABC gene family: analysis of gene birth and death. Genomics. United States; 2006; 88: 1–11. https://doi.org/10.1016/j.ygeno.2006.03.001 PMID: 16631343

14. Kovalchuk A, Driessen AJM. Phylogenetic analysis of fungal ABC transporters. BMC Genomics. 2010; 11: 177. https://doi.org/10.1186/1471-2164-11-177 PMID: 20233411

15. Decottignies A, Goffeau A. Complete inventory of the yeast ABC proteins. Nat Genet. United States; 1997; 15: 137–145. https://doi.org/10.1038/ng0297-137 PMID: 9020838

16. Pfaller MA, Diekema DJ. Epidemiology of invasive candidiasis: a persistent public health problem. Clin Microbiol Rev. United States; 2007; 20: 133–163. https://doi.org/10.1128/CMR.00029-06 PMID: 17223626

17. Kaur R, Domergue R, Zupancic ML, Cormack BP. A yeast by any other name: Candida glabrata and its interaction with the host. Curr Opin Microbiol. England; 2005; 8: 378–384. https://doi.org/10.1016/j.mib.2005.06.012 PMID: 15996895

18. Dujon B, Sherman D, Fischer G, Durrens P, Casaregola S, Lafontaine I, et al. Genome evolution in yeasts. Nature. England; 2004; 430: 35–44. https://doi.org/10.1038/nature02579 PMID: 15229592

19. Oxman DA, Chow JK, Frendl G, Hadley S, Hershkovitz S, Ireland P, et al. Candidaemia associated with decreased in vitro fluconazole susceptibility: is Candida speciation predictive of the susceptibility pattern? J Antimicrob Chemother. England; 2010; 65: 1460–1465. https://doi.org/10.1093/jac/dkq136 PMID: 20430790

20. Sanglard D, Ischer F, Calabrese D, Majcherczyk PA, Bille J. The ATP binding cassette transporter GeneCgCDR1 from Candida glabrata is involved in the resistance of clinical isolates to azole antifungal agents. Antimicrob Agents Chemother. Am Soc Microbiol; 1999; 43: 2753–2765. PMID: 10543759

21. Sanglard D, Ischer F, Bille J. Role of ATP-binding-cassette transporter genes in high-frequency acquisition of resistance to azole antifungals in Candida glabrata. Antimicrob Agents Chemother. 2001; 45: 1174–1183. https://doi.org/10.1128/AAC.45.4.1174-1183.2001 PMID: 11257032

22. Whaley SG, Berkow EL, Rybak JM, Nishimoto AT, Barker KS, Rogers PD, et al. Azole Antifungal Resistance in Candida albicans and Emerging Non- albicans Candida Species. 2017; 7: 1–12. https://doi.org/10.3389/fmicb.2016.02173 PMID: 28127295

23. Sanguinetti M, Posteraro B, Fiori B, Ranno S, Torelli R, Fadda G. Mechanisms of azole resistance in clinical isolates of Candida glabrata collected during a hospital survey of antifungal resistance. Antimicrob Agents Chemother. United States; 2005; 49: 668–679. https://doi.org/10.1128/AAC.49.2.668-679.2005 PMID: 15673750

24. Torelli R, Posteraro B, Ferrari S, La Sorda M, Fadda G, Sanglard D, et al. The ATP-binding cassette transporter-encoding gene CgSNQ2 is contributing to the CgPDR1-dependent azole resistance of Candida glabrata. Mol Microbiol. 2008; 68: 186–201. https://doi.org/10.1111/j.1365-2958.2008.06143.x PMID: 18312269

25. Ben-Ami R, Zimmerman O, Finn T, Amit S, Novikov A, Wertheimer N, et al. Heteroresistance to Fluconazole Is a Continuously Distributed Phenotype among Candida glabrata Clinical Strains Associated with In Vivo Persistence. MBio. United States; 2016; 7. https://doi.org/10.1128/mBio.00655-16 PMID: 27486188

26. Livak KJ, Schmittgen TD. Analysis of relative gene expression data using real-time quantitative PCR and the 2-$^{\Delta\Delta}$CT method. Methods. 2001; 25: 402–408. https://doi.org/10.1006/meth.2001.1262 PMID: 11846609

27. Prasad R, Khandelwal NK, Banerjee A. Yeast ABC transporters in lipid trafficking. Fungal Genet Biol. United States; 2016; 93: 25–34. https://doi.org/10.1016/j.fgb.2016.05.008 PMID: 27259587

28. Birchler JA, Veitia RA. The Gene Balance Hypothesis: implications for gene regulation, quantitative traits and evolution. New Phytol. 2010; 186: 54–62. https://doi.org/10.1111/j.1469-8137.2009.03087.x PMID: 19925558

29. Xiong J, Feng J, Yuan D, Zhou J, Miao W. Tracing the structural evolution of eukaryotic ATP binding cassette transporter superfamily. Sci Rep. The Author(s); 2015; 5: 16724. Available: https://doi.org/10.1038/srep16724 PMID: 26577702

30. Khunweeraphong N, Stockner T, Kuchler K. The structure of the human ABC transporter ABCG2 reveals a novel mechanism for drug extrusion. Sci Rep. 2017; 7: 13767. https://doi.org/10.1038/s41598-017-11794-w PMID: 29061978

31. Anjard C, Consortium the DS, Loomis WF. Evolutionary Analyses of ABC Transporters of Dictyostelium discoideum. Eukaryot Cell. American Society for Microbiology; 2002; 1: 643–652. https://doi.org/10.1128/EC.1.4.643-652.2002 PMID: 12456012

32. Kuchler K, Sterne RE, Thorner J. Saccharomyces cerevisiae STE6 gene product: a novel pathway for protein export in eukaryotic cells. EMBO J. England; 1989; 8: 3973–3984.

33. Kispal G, Csere P, Guiard B, Lill R. The ABC transport Atm1p is required for mitochondrial iron homeostasis. FEBS Lett. Federation of European Biochemical Societies; 1997; 418: 346–350. https://doi.org/10.1016/S0014-5793(97)01414-2 PMID: 9428742

34. Schwarzmuller T, Ma B, Hiller E, Istel F, Tscherner M, Brunke S, et al. Systematic phenotyping of a large-scale Candida glabrata deletion collection reveals novel antifungal tolerance genes. PLoS Pathog. United States; 2014; 10: e1004211. https://doi.org/10.1371/journal.ppat.1004211 PMID: 24945925

35. Dean M, Allikmets R, Gerrard B, Stewart C, Kistler A, Shafer B, et al. Mapping and sequencing of two yeast genes belonging to the ATP- binding cassette superfamily. Yeast. 1994; 10: 377–383. https://doi.org/10.1002/yea.320100310 PMID: 7912468

36. Klein M, Burla B, Martinoia E. The multidrug resistance-associated protein (MRP/ABCC) subfamily of ATP-binding cassette transporters in plants. FEBS Lett. England; 2006; 580: 1112–1122. https://doi.org/10.1016/j.febslet.2005.11.056 PMID: 16375897

37. Jeong CB, Kim DH, Kang HM, Lee YH, Kim HS, Kim IC, et al. Genome-wide identification of ATP-binding cassette (ABC) transporters and their roles in response to polycyclic aromatic hydrocarbons (PAHs) in the copepod Paracyclopina nana. Aquat Toxicol. Elsevier B.V.; 2017; 183: 144–155. https://doi.org/10.1016/j.aquatox.2016.12.022 PMID: 28073050

38. Dermauw W, Van Leeuwen T. The ABC gene family in arthropods: comparative genomics and role in insecticide transport and resistance. Insect Biochem Mol Biol. England; 2014; 45: 89–110. https://doi.org/10.1016/j.ibmb.2013.11.001 PMID: 24291285

39. Cui Z, Hirata D, Tsuchiya E, Osada H, Miyakawa T. The multidrug resistance-associated protein (MRP) subfamily (Yrs1/Yor1) of Saccharomyces cerevisiae is important for the tolerance to a broad range of organic anions. J Biol Chem. United States; 1996; 271: 14712–14716. PMID: 8663018

40. Vernon RM, Chong PA, Lin H, Yang Z, Zhou Q, Aleksandrov AA, et al. Stabilization of a nucleotide-binding domain of the cystic fibrosis transmembrane conductance regulator yields insight into disease-causing mutations. J Biol Chem. United States; 2017; 292: 14147–14164. https://doi.org/10.1074/jbc.M116.772335 PMID: 28655774

41. Vermitsky J-P, Earhart KD, Smith WL, Homayouni R, Edlind TD, Rogers PD. Pdr1 regulates multidrug resistance in Candida glabrata: gene disruption and genome-wide expression studies. Mol Microbiol. 2006; 61: 704–722. https://doi.org/10.1111/j.1365-2958.2006.05235.x PMID: 16803598

42. Tsai H-F, Sammons LR, Zhang X, Suffis SD, Su Q, Myers TG, et al. Microarray and molecular analyses of the azole resistance mechanism in Candida glabrata oropharyngeal isolates. Antimicrob Agents Chemother. United States; 2010; 54: 3308–3317. https://doi.org/10.1128/AAC.00535-10 PMID: 20547810

43. Johnson ZL, Chen J. Structural Basis of Substrate Recognition by the Multidrug Resistance Protein MRP1. Cell. United States; 2017; 168: 1075–1085.e9. https://doi.org/10.1016/j.cell.2017.01.041 PMID: 28238471

44. Ferrari S, Sanguinetti M, De Bernardis F, Torelli R, Posteraro B, Vandeputte P, et al. Loss of mitochondrial functions associated with azole resistance in Candida glabrata results in enhanced virulence in mice. Antimicrob Agents Chemother. United States; 2011; 55: 1852–1860. https://doi.org/10.1128/AAC.01271-10 PMID: 21321146

45. Theodoulou FL, Holdsworth M, Baker A. Peroxisomal ABC transporters. FEBS Lett. 2006; 580: 1139–1155. https://doi.org/10.1016/j.febslet.2005.12.095 PMID: 16413537

46. Morita M, Imanaka T. Peroxisomal ABC transporters: structure, function and role in disease. Biochim Biophys Acta. Netherlands; 2012; 1822: 1387–1396. https://doi.org/10.1016/j.bbadis.2012.02.009 PMID: 22366764

47. van Roermund CWT, Visser WF, Ijlst L, Waterham HR, Wanders RJA. Differential substrate specificities of human ABCD1 and ABCD2 in peroxisomal fatty acid beta-oxidation. Biochim Biophys Acta. Netherlands; 2011; 1811: 148–152. https://doi.org/10.1016/j.bbalip.2010.11.010 PMID: 21145416

48. Shani N, Valle D. A Saccharomyces cerevisiae homolog of the human adrenoleukodystrophy transporter is a heterodimer of two half ATP-binding cassette transporters. Proc Natl Acad Sci U S A. 1996; 93: 11901–11906. PMID: 8876235

49. Pujol A, Ferrer I, Camps C, Metzger E, Hindelang C, Callizot N, et al. Functional overlap between ABCD1 (ALD) and ABCD2 (ALDR) transporters: a therapeutic target for X-adrenoleukodystrophy. Hum Mol Genet. England; 2004; 13: 2997–3006. https://doi.org/10.1093/hmg/ddh323 PMID: 15489218

50. Tian L, Song T, He R, Zeng Y, Xie W, Wu Q, et al. Genome-wide analysis of ATP-binding cassette (ABC) transporters in the sweetpotato whitefly, Bemisia tabaci. BMC Genomics. England; 2017; 18: 330. https://doi.org/10.1186/s12864-017-3706-6 PMID: 28446145

51. Dong J, Lai R, Nielsen K, Fekete CA, Qiu H, Hinnebusch AG. The essential ATP-binding cassette protein RLI1 functions in translation by promoting preinitiation complex assembly. J Biol Chem. United States; 2004; 279: 42157–42168. https://doi.org/10.1074/jbc.M404502200 PMID: 15277527

52. Khoshnevis S, Gross T, Rotte C, Baierlein C, Ficner R, Krebber H. The iron-sulphur protein RNase L inhibitor functions in translation termination. EMBO Rep. England; 2010; 11: 214–219. https://doi.org/10.1038/embor.2009.272 PMID: 20062004

53. Schmidt P, Walker J, Selway L, Stead D, Yin Z, Enjalbert B, et al. Proteomic analysis of the pH response in the fungal pathogen Candida glabrata. Proteomics. Germany; 2008; 8: 534–544. https://doi.org/10.1002/pmic.200700845 PMID: 18186024

54. Nakayama H, Izuta M, Nagahashi S, Sihta EY, Sato Y, Yamazaki T, et al. A controllable gene-expression system for the pathogenic fungus Candida glabrata. Microbiology. England; 1998; 144 (Pt 9: 2407–2415. https://doi.org/10.1099/00221287-144-9-2407 PMID: 9782488

55. Vazquez de Aldana CR, Marton MJ, Hinnebusch AG. GCN20, a novel ATP binding cassette protein, and GCN1 reside in a complex that mediates activation of the eIF-2 alpha kinase GCN2 in amino acid-starved cells. EMBO J. 1995; 14: 3184–99. PMID: 7621831

56. Anjard C, Loomis WF. Evolutionary analyses of ABC transporters of Dictyostelium discoideum. Eukaryot Cell. United States; 2002; 1: 643–652. https://doi.org/10.1128/EC.1.4.643-652.2002 PMID: 12456012

57. Kolaczkowski M, Van der Rest M, Cybularz-Kolaczkowska A, Soumillion JP, Konings WN, Goffeau A. Anticancer drugs, ionophoric peptides, and steroids as substrates of the yeast multidrug transporter Pdr5p. J Biol Chem. 1996; 271: 31543–31548. https://doi.org/10.1074/jbc.271.49.31543 PMID: 8940170

58. Miyazaki H, Miyazaki Y, Geber A, Parkinson T, Hitchcock C, Falconer DJ, et al. Fluconazole resistance associated with drug efflux and increased transcription of a drug transporter gene, PDH1, in Candida glabrata. Antimicrob Agents Chemother. United States; 1998; 42: 1695–1701. PMID: 9661006

59. Izumikawa K, Kakeya H, Tsai HF, Grimberg B, Bennett JE. Function of Candida glabrata ABC transporter gene, PDH1. Yeast. 2003; 20: 249–261. https://doi.org/10.1002/yea.962 PMID: 12557277

60. Brun S, Bergès T, Poupard P, Renier G, Chabasse D, Bouchara J, et al. Mechanisms of Azole Resistance in Petite Mutants of Candida glabrata Mechanisms of Azole Resistance in Petite Mutants of Candida glabrata. Society. 2004; 1788–1796. https://doi.org/10.1128/AAC.48.5.1788

61. Whaley SG, Rogers PD. Azole Resistance in Candida glabrata. Curr Infect Dis Rep. Current Infectious Disease Reports; 2016; 18: 19–21. https://doi.org/10.1007/s11908-016-0525-x

62. Nagi M, Tanabe K, Nakayama H, Yamagoe S, Umeyama T, Oura T, et al. Serum cholesterol promotes the growth of Candida glabrata in the presence of fluconazole. J Infect Chemother. Elsevier; 2013; 19: 138–143. https://doi.org/10.1007/s10156-012-0531-3 PMID: 23233084

63. Nakayama H, Tanabe K, Bard M, Hodgson W, Wu S, Takemori D, et al. The Candida glabrata putative sterol transporter gene CgAUS1 protects cells against azoles in the presence of serum. J Antimicrob Chemother. 2007; 60: 1264–1272. https://doi.org/10.1093/jac/dkm321 PMID: 17913716

64. Piper P, Mahe Y, Thompson S, Pandjaitan R, Holyoak C, Egner R, et al. The pdr12 ABC transporter is required for the development of weak organic acid resistance in yeast. EMBO J. England; 1998; 17: 4257–4265. https://doi.org/10.1093/emboj/17.15.4257 PMID: 9687494

65. Khandelwal NK, Chauhan N, Sarkar P, Esquivel BD, Coccetti P, Singh A, et al. Azole resistance in a Candida albicans mutant lacking the ABC transporter CDR6/ROA1 depends on TOR signaling. J Biol Chem. 2017; jbc.M117.807032. https://doi.org/10.1074/jbc.M117.807032 PMID: 29158264

66. Rogers B, Decottignies a, Kolaczkowski M, Carvajal E, Balzi E, Goffeau a. The pleitropic drug ABC transporters from Saccharomyces cerevisiae. J Mol Microbiol Biotechnol. 2001; 3: 207–214. PMID: 11321575

67. Liu HY, Chiang YC, Pan J, Chen J, Salvadore C, Audino DC, et al. Characterization of CAF4 and CAF16 Reveals a Functional Connection between the CCR4-NOT Complex and a Subset of SRB Proteins of the RNA Polymerase II Holoenzyme. J Biol Chem. 2001; 276: 7541–7548. https://doi.org/10.1074/jbc.M009112200 PMID: 11113136

68. Lamping E, Monk BC, Niimi K, Holmes AR, Tsao S, Tanabe K, et al. Characterization of three classes of membrane proteins involved in fungal azole resistance by functional hyperexpression in Saccharomyces cerevisiae. Eukaryot Cell. United States; 2007; 6: 1150–1165. https://doi.org/10.1128/EC.00091-07 PMID: 17513564

69. Vale-Silva L, Ischer F, Leibundgut-Landmann S, Sanglard D. Gain-of-function mutations in PDR1, a regulator of antifungal drug resistance in Candida glabrata, control adherence to host cells. Infect Immun. United States; 2013; 81: 1709–1720. https://doi.org/10.1128/IAI.00074-13 PMID: 23460523

70. Samaranayake YH, Cheung BPK, Wang Y, Yau JYY, Yeung KWS, Samaranayake LP. Fluconazole resistance in Candida glabrata is associated with increased bud formation and metallothionein production. J Med Microbiol. England; 2013; 62: 303–318. https://doi.org/10.1099/jmm.0.044123-0 PMID: 23002065

71. Wu C-P, Calcagno AM, Ambudkar S V. Reversal of ABC drug transporter-mediated multidrug resistance in cancer cells: Evaluation of current strategies. Curr Mol Pharmacol. 2008; 1: 93–105. PMID: 19079736

72. Klein C, Kuchler K, Valachovic M. ABC proteins in yeast and fungal pathogens. Essays Biochem. 2011; 50: 101–19. https://doi.org/10.1042/bse0500101 PMID: 21967054

73. Slomka M, Sobalska-Kwapis M, Korycka-Machala M, Bartosz G, Dziadek J, Strapagiel D. Genetic variation of the ABC transporter gene ABCC1 (Multidrug resistance protein 1-MRP1) in the Polish population. BMC Genet. England; 2015; 16: 114. https://doi.org/10.1186/s12863-015-0271-3 PMID: 26395522

74. Smriti Krishnamurthy S, Dixit BL, Gupta CM, Milewski S, Prasad R. ABC transporters Cdr1p, Cdr2p and Cdr3p of a human pathogen Candida albicans are general phospholipid translocators. Yeast. England; 2002; 19: 303–318. https://doi.org/10.1002/yea.818 PMID: 11870854

EDITOR'S CHOICE

A homologous overexpression system to study roles of drug transporters in *Candida glabrata* FREE

Sonam Kumari, Mohit Kumar, Nitesh Kumar Khandelwal, Ajay Kumar Pandey, Priyanka Bhakt, Rupinder Kaur, Rajendra Prasad ✉, Naseem A Gaur ✉ Author Notes

FEMS Yeast Research, Volume 20, Issue 4, June 2020, foaa032,
https://doi.org/10.1093/femsyr/foaa032
Published: 03 June 2020 **Article history** ▾

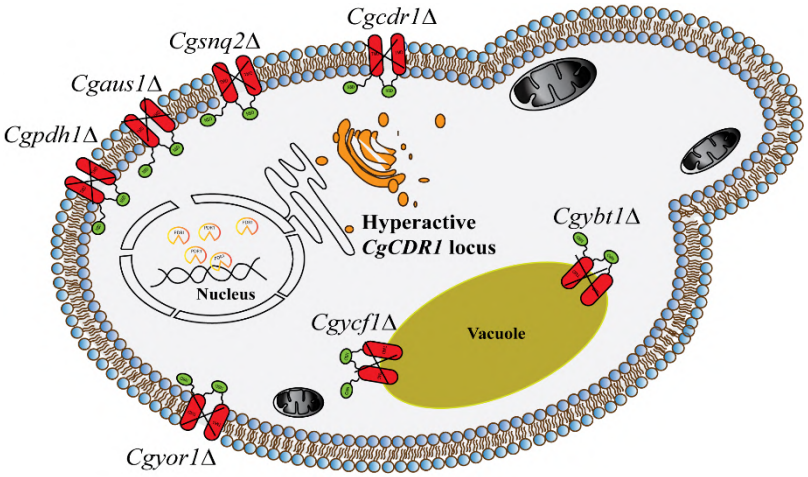

FEMS Yeast Research, 20, 2020, foaa032

doi: 10.1093/femsyr/foaa032
Advance Access Publication Date: 3 June 2020
Research Article

RESEARCH ARTICLE

A homologous overexpression system to study roles of drug transporters in *Candida glabrata*

Sonam Kumari[1,†], Mohit Kumar[1,2,†], Nitesh Kumar Khandelwal[1,‡], Ajay Kumar Pandey[1], Priyanka Bhakt[3], Rupinder Kaur[3], Rajendra Prasad[2,*,§] and Naseem A. Gaur[1,*]

[1]Yeast Biofuel Group, International Centre for Genetic Engineering and Biotechnology, New Delhi, 110067, India, [2]Amity Institute of Integrative Science and Health and Amity Institute of Biotechnology, Amity University, Gurgaon, 122413, Haryana, India and [3]Laboratory of Fungal Pathogenesis, Centre for DNA Fingerprinting and Diagnostics, Hyderabad, 500039, Telangana, India

*Corresponding author: Amity Institute of Integrative Sciences and Health, Amity University, Haryana, 122413, India. E-mail: rp47jnu@gmail.com; Yeast Biofuel Group, International Centre for Genetic Engineering and Biotechnology, New Delhi, 110067, India. E-mail: naseem@icgeb.res.in

‡Present address: Department of Chemistry and Biochemistry, University of Arizona, Tucson, AZ, 85721, USA.

One sentence summary: Development of a strain containing seven ABC transporter deletion with overexpressed CgCDR1 locus and its expression system for characterizing membrane protein in pathogenic yeast Candida glabrata.

†Contributed equally.

Editor: Miguel Teixeira

§Rajendra Prasad, http://orcid.org/0000-0002-8044-7042

ABSTRACT

Considering the relevance of drug transporters belonging to ABC and MFS superfamilies in pathogenic *Candida* species, there has always been a need to have an overexpression system where these membrane proteins for functional analysis could be expressed in a homologous background. We could address this unmet need by constructing a highly drug-susceptible *Candida glabrata* strain deleted in seven dominant ABC transporters genes such as *CgSNQ2, CgAUS1, CgCDR1*, *CgPDH1*, *CgYCF1*, *CgYBT1* and *CgYOR1* and introduced a GOF mutation in transcription factor (TF) *CgPDR1* leading to a hyper-activation of *CgCDR1* locus. The expression system was validated by overexpressing four GFP tagged ABC (*CgCDR1*, *CgPDH1*, *CaCDR1* and *ScPDR5*) and an MFS (*CgFLR1*) transporters genes facilitated by an engineered expression plasmid to integrate at the *CgCDR1* locus. The properly expressed and localized transporters were fully functional, as was revealed by their several-fold increased drug resistance, growth kinetics, localization studies and efflux activities. The present homologous system will facilitate in determining the role of an individual transporter for its substrate specificity, drug efflux, pathogenicity and virulence traits without the interference of other major transporters.

Keywords: ABC transporters; multi-deletion; azoles; GOF mutation; expression plasmid; *Candida glabrata*

INTRODUCTION

Candida glabrata, present as a commensal in the human microbiota, is the only second most common infectious agent to cause superficial skin infections to be severe and life-threatening bloodstream infections among genus *Candida* (Kasper, Seider and Hube 2015). The continuous use of antimycotic drugs, especially azoles, has led to an emergence of drug-resistant clinical strains (Ksiezopolska and Gabaldón 2018). *C. glabrata* exhibits intrinsically low susceptibility to azoles (Whaley *et al.* 2016). This clinically rising drug resistance in *C. glabrata* is a culmination of several mechanisms which also includes overexpression

Received: 24 April 2020; **Accepted:** 2 June 2020

of drug efflux pumps belonging to ATP Binding Cassette (ABC) superfamily and Major Facilitator Superfamily (MFS) of transporters which help cells to rapidly extrude antimycotic drugs to circumvent their lethality (Holmes *et al.* 2016). The existence of a large number of ABC transporters in *C. glabrata* genome makes it difficult to dissect the functional relevance of individual transporters (Kumari *et al.* 2018). Presently, a widely used *Saccharomyces cerevisiae* based heterologous expression system, that lacks several ABC transporters has been extensively used to study membrane proteins from different yeasts (Lamping *et al.* 2007). These studies helped in unraveling details of drug efflux, protein localization and directed mutagenesis to dissect the molecular basis of the promiscuity towards substrate recognition (Redhu *et al.* 2018). Notwithstanding, the immense importance of the *S. cerevisiae* system that has contributed immensely to the study of ABC transporters, questions are always raised concerning the differences among different species and non-pathogenic host strain's cellular environment, the lipid content of membrane and protein sorting behavior.

To circumvent these issues, we have developed a system in *C. glabrata* devoid of any masking effects by dominant drug transporters and an integrative plasmid for the expression of the gene of interest (GOI). For this, a strain of *C. glabrata* MSY8 was constructed by disrupting seven clinically relevant membrane-localized ABC drug transporter genes that included *CgSNQ2, CgAUS1, CgCDR1, CgPDH1, CgYCF1, CgYBT1* and *CgYOR1* and introduced a gain of function (GOF) mutation in the *CgPDR1* transcription factor (TF) resulting in a hyper-activation of *CgCDR1* locus. The integration of GOI by employing an engineered expression plasmid allowed overexpression of fully functional ABC and MFS transporters.

MATERIAL AND METHODS

Chemicals and strains

Antifungal drugs were of analytical grade and were purchased from Sigma-Aldrich, Bengaluru, India. Yeast strains were maintained in YPD media. Bacterial cultures were maintained in LB media with a final concentration of ampicillin at 100 μg/mL.

Deletion construction

A homologous recombination-based strategy was used to make deletion as described previously (Borah, Shivarathri and Kaur 2011). Sequential deletions were made by using a drug-based recyclable (*FRT-NAT1-FRT*) cassette. Briefly, 5' and 3'UTR flanking regions (500–700 bp) of the transporter gene were PCR amplified from wild type genomic DNA. The selection marker *NAT1* gene with FRT sites was also PCR amplified in two halves from plasmid pRK625. Both the UTRs were fused to one half of the *NAT1* gene, and these fused PCR products were co-transformed into the wild type strain. Positive transformants were selected on YPD agar medium containing 200 μg/mL nourseothricin, and deletions were confirmed by genomic DNA PCR. The primers used in ABC transporter gene deletion and confirmation are listed as File S1 (Supporting Information). The selection marker was then recycled by using plasmid pRK70, which contains the *Ura3* selection marker and flippase (*FLP1*) gene under the constitutive *EPA1* promoter. Then after rescuing both the selection marker and plasmid, the strain was used for the next round of deletion. The constructed strains are listed in Table 1.

Plasmid constructions

The integration-based plasmid was constructed to integrate mutated *CgPDR1* ORF in place of native *CgPDR1* locus. An integration-based expression plasmid that can integrate GOI at *CgCDR1* locus was constructed that contained *NAT1* selection marker, *CgCDR1* terminator and promoter regions, *YeGFP* and four unique restriction sites for cloning the GOI. The details of expression plasmid pMS6 construction and the list of the plasmids used are documented in File S2 (Supporting Information).

Growth analysis

Growth curve analysis was performed by a micro-cultivation method in a 96-well plate using the liquid handling system (Tecan, Grödig, Austria) in YPD broth at 30°C. Briefly, overnight grown cells were inoculated at a dilution of 0.1 OD_{600} in a 96-well plate and allowed to grow at 30°C. OD_{600} was measured every 30 min for an interval to up to 24 h. Doubling times of strains were calculated by measuring the time taken in doubling of logarithms values of the OD_{600} of the exponential phase.

Drug susceptibility and efflux assays

Susceptibility to antifungal drugs was estimated either by broth micro-dilution or serial dilution spot assays, as described earlier (Shah, Shukla and Prasad 2017). The MIC_{80} was defined at the lowest concentration inhibiting growth by at least 80% relative to the drug-free YPD control after incubation. Both Rhodamine-6-G (R6G) and Nile Red (NR) efflux assays were performed by spectrofluorometer based assays as per protocols used earlier (Keniya *et al.* 2015; Gbelska *et al.* 2017). For R6G efflux, 527 nm excitation and 555 nm emission, and for NR, 552 nm excitation and 636 nm emission were used. A straight line for the relation between fluorescence and concentration was plotted for both the substrates, and the concentration in the supernatant was determined by plotting the fluorescence to this graph.

cDNA synthesis and real-time PCR

Total RNA was extracted by using the RNeasy Mini Kit by following manufacturer instructions (QIAGEN, Hilden, Germany). 5 μg of total RNA was used to synthesize cDNA by using RevertAid H minus first-strand cDNA synthesis kit (Thermo Scientific, Vilnius, Lithuania) as per the protocol. The quantitative gene expression profile was evaluated by using iTaq universal SYBR green supermix (BioRad, Gurugram, India) and gene-specific primers, including *CgPGK1* as an internal control. Comparative expression profiles were analyzed by $2^{-\Delta\Delta Ct}$ method. qRT-PCR experiments were performed in triplicates. *P*-values were determined by students t-test with ≤ 0.05 were considered as significant.

RESULTS

Construction of multiple ABC transporters deleted strain of *C. glabrata*

ABC transporters extrude a wide variety of physiological compounds. Among ABC subfamilies, there is a greater similarity in the sequence and structure, which could make them share partial overlapping substrate profiles (Kolaczkowski *et al.* 1998). Due to the similarity in the substrate profile, some transporters

Table 1. List of strains used in the study.

Mutant Name	Genotype	Source
WT (BG14)	*ura3*Δ::*Tn903 Neo*^{R}	Lab strain
WT^{GOF}	*Cgpdr1*::*CgPDR1*^{G840C} *FRT*	This study
MSY1	Δ*Cgsnq2*::*FRT*	This study
MSY2	Δ*Cgsnq2*::*FRT*, Δ*Cgaus1*::*FRT*	This study
MSY3	Δ*Cgsnq2*::*FRT*, Δ*Cgaus1*::*FRT*, Δ*Cgcdr1*::*FRT*	This study
MSY4	Δ*Cgsnq2*::*FRT*, Δ*Cgaus1*::*FRT*, Δ*Cgcdr1*::*FRT*, Δ*Cgpdh1*::*FRT*	This study
MSY5	Δ*Cgsnq2*::*FRT*, Δ*Cgaus1*::*FRT*, Δ*Cgcdr1*::*FRT*, Δ*Cgpdh1*::*FRT*, Δ*Cgycf1*::*FRT*	This study
MSY6	Δ*Cgsnq2*::*FRT*, Δ*Cgaus1*::*FRT*, Δ*Cgcdr1*::*FRT*, Δ*Cgpdh1*::*FRT*, Δ*Cgycf1*::*FRT*, Δ*Cgybt1*::*FRT*	This study
MSY7	Δ*Cgsnq2*::*FRT*, Δ*Cgaus1*::*FRT*, Δ*Cgcdr1*::*FRT*, Δ*Cgpdh1*::*FRT*, Δ*Cgycf1*::*FRT*, Δ*Cgybt1*::*FRT*, Δ*Cgyor1*::*FRT*	This study
MSY8	Δ*Cgsnq2*::*FRT*, Δ*Cgaus1*::*FRT*, Δ*Cgcdr1*::*FRT*, Δ*Cgpdh1*::*FRT*, Δ*Cgycf1*::*FRT*, Δ*Cgybt1*::*FRT*, Δ*Cgyor1*::*FRT*, *Cgpdr1*::*CgPDR1*^{G840C} *FRT*	This study (Strain accession no. MTCC25307)
MSY9	Δ*Cgsnq2*::*FRT*, Δ*Cgaus1*::*FRT*, Δ*Cgcdr1*::*FRT*::*CgCDR1-GFP*::*NAT1*, Δ*Cgpdh1*::*FRT*, Δ*Cgycf1*::*FRT*, Δ*Cgybt1*:: *FRT*, Δ*Cgyor1*::*FRT*, *Cgpdr1*::*CgPDR1*^{G840C} *FRT*	This study
MSY10	Δ*Cgsnq2*::*FRT*, Δ*Cgaus1*::*FRT*, Δ*Cgcdr1*::*FRT*::*CgPDH1-GFP*::*NAT1*, Δ*Cgpdh1*::*FRT*, Δ*Cgycf1*::*FRT*, Δ*Cgybt1*:: *FRT*, Δ*Cgyor1*::*FRT*, *Cgpdr1*::*CgPDR1*^{G840C} *FRT*	This study
MSY11	Δ*Cgsnq2*::*FRT*, Δ*Cgaus1*::*FRT*, Δ*Cgcdr1*::*FRT*::*CaCDR1-GFP*::*NAT1*, Δ*Cgpdh1*::*FRT*, Δ*Cgycf1*::*FRT*, Δ*Cgybt1*::*FRT*, Δ*Cgyor1*::*FRT*, *Cgpdr1*::*CgPDR1*^{G840C} *FRT*	This study
MSY12	Δ*Cgsnq2*::*FRT*, Δ*Cgaus1*::*FRT*, Δ*Cgcdr1*::*FRT*::*ScPDR5-GFP*::*NAT1*, Δ*Cgpdh1*::*FRT*, Δ*Cgycf1*::*FRT*, Δ*Cgybt1*:: *FRT*, Δ*Cgyor1*::*FRT*, *Cgpdr1*::*CgPDR1*^{G840C} *FRT*	This study
MSY13	Δ*Cgsnq2*::*FRT*, Δ*Cgaus1*::*FRT*, Δ*Cgcdr1*::*FRT*::*CgFLR1-GFP*::*NAT1*, Δ*Cgpdh1*::*FRT*, Δ*Cgycf1*::*FRT*, Δ*Cgybt1*:: *FRT*, Δ*Cgyor1*::*FRT*, *Cgpdr1*::*CgPDR1*^{G840C} *FRT*	This study

may function as dominant transporters by masking the function of other transporters. The dominance of ABC transporters such as CaCdr1p and CgCdr1p and CgPdh1p in *C. albicans* and *C. glabrata*, respectively, or ScPdr5p in *S. cerevisiae*, are few examples which are well reported. Therefore, functional analysis of a transporter in the absence of dominant transporters is very important to evaluate its true potential for drug efflux and the development of multiple drug resistance. To generate such a host strain, we selected seven transporters genes (*CgSNQ2*, *CgAUS1*, *CgCDR1*, *CgPDH1*, *CgYCF1*, *CgYBT1* and *CgYOR1*) which were earlier shown to be upregulated in azole-resistant clinical isolates of *C. glabrata* or involved in azole drug resistance (Sanguinetti *et al.* 2005; Vermitsky *et al.* 2006; Torelli *et al.* 2008; Ferrari *et al.* 2011). For these deletions, a recyclable FRT based dominant selection marker *NAT1* was used by employing fusion PCR based homologous recombination (Borah, Shivarathri and Kaur 2011; Srivastava, Suneetha and Kaur 2015). Thus, we sequentially deleted these transporters' coding sequences, and resulting strains were designated as MSY1–MSY7. These deletions were not in a particular order. Each deletant was designated as MSY1 (*Cgsnq2*Δ), MSY2 (MSY1 + *Cgaus1*Δ), MSY3 (MSY2 + *Cgcdr1*Δ), MSY4 (MSY3 + *Cgpdh1*Δ), MSY5 (MSY4 + *Cgycf1*Δ), MSY6 (MSY5 + *Cgybt1*Δ), MSY7 (MSY6 + *Cgyor1*Δ).

Growth kinetics of MSY1–MSY7 strains

To determine the effect of each transporter deletion on growth, we performed growth kinetics by micro-cultivation method. The cells were grown in YPD broth at 30°C, and OD_{600} was recorded for 24 h. The growth curves of WT and deletion mutants MSY1–MSY7 are depicted in Fig. 1A. Notably, the doubling times of MSY1 to MSY6 were similar to WT strain (60 min); however, the deletion of *Cgyor1*Δ (MSY7) resulted in a slightly slower growth rate with a doubling time of 68.04 min (Fig. 1A). To further confirm if the slow growth phenotype of the MSY7 is due to *Cgyor1* deletion and not due to any other changes, we complemented the *CgYOR1* gene by episomal expression in plasmid pGRB2.2. While the episomal complementation reversed the drug sensitivity phenotype in MSY7 to a level up to MSY6 (data not shown), it could not restore the growth defect of MSY7. This growth defect is probably due to the cumulative effect of deletions.

Drug susceptibility profiling of MSY1–MSY7 mutants

The drug susceptibility profile of each deletion mutant was determined by spot assays, MIC_{80} determination by microdilution method and growth kinetics using fluconazole (FLC), ketoconazole (KTC), voriconazole (VRC), miconazole (MCZ) and itraconazole (ITZ), caspofungin (CSF), amphotericin B (AmB) and nystatin (NYS), allylamine terbinafine (TER), protein synthesis inhibitors cycloheximide (CHX) and anisomycin (ANY), DNA damaging agents 4-nitroquinoline (4-NQO) and metal chelator 1,10-phenanthroline (OP) at indicated concentrations (Fig. 1B and File S3, Supporting Information). The initial two deletions MSY1 (*Cgsnq2*Δ) and MSY2 (*Cgsnq2*Δ, *Cgaus1*Δ) did not show any alteration in MIC_{80} with respect to WT on all the tested drugs except for 4-NQO and OP which was supported by spot assays as well (Fig. 1B). However, when *Cgcdr1*Δ was deleted, in MSY3 strain, as expected, the mutant MIC_{80} were dropped dramatically for tested azoles, including FLC MIC_{80} drop from 64 μg/mL to 4 μg/mL. The MIC_{80} was two doubling dilution lower (1 μg/mL) for FLC when *Cgpdh1*Δ was deleted to make MSY4 strain. The subsequent deletion of *Cgycf1*Δ, in MSY5, and *Cgybt1*Δ in MSY6, did not yield any further change in MIC_{80} of FLC as well as of other tested drugs (except for KTC). The subsequent last deletion of *Cgyor1*Δ, MSY7, led to another 4-fold drop in MIC of FLC (0.25 μg/mL) in comparison to the MSY6 strain. A similar reduction of MIC_{80} of MSY7 was also observed with other azoles, protein synthesis inhibitors and allylamine. As expected, the deletion of *Cgsnq2*Δ, MSY1 displayed dramatic susceptibility towards 4-NQO and OP, which are the known substrates of ScSnq2p; however, no further change in susceptibility towards 4-NQO and OP was noticed in subsequent deletions MSY2–MSY7 (Fig. 1B, File S3, Supporting Information). This indicated that changes in

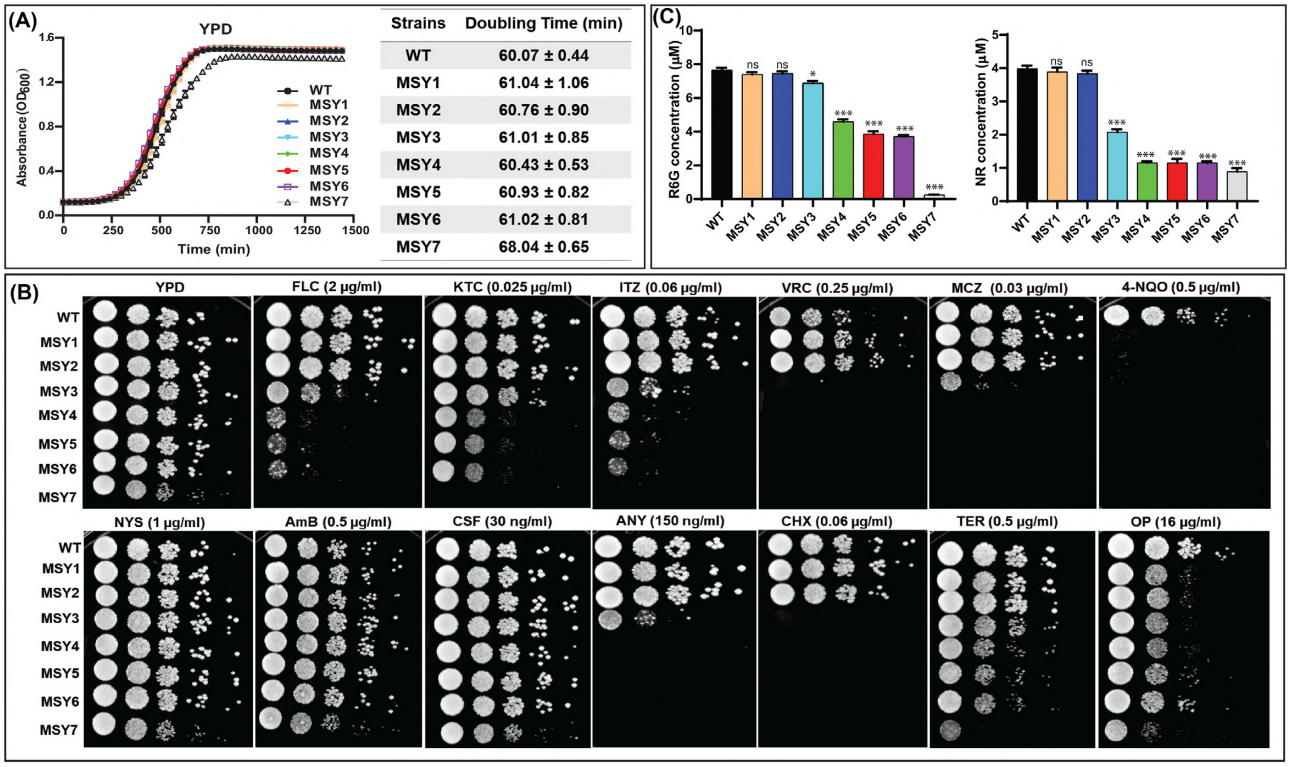

Figure 1. Phenotypic characterization of strains MSY1–MSY7. **(A)** Growth kinetics study of MSY1–MSY7 strains was performed by a micro-cultivation method in a 96-well plate using Liquid Handling System (Tecan, Austria) in YPD broth at 30°C. Doubling time for the strains was calculated by quantifying the time taken in doubling of logarithms values of the log phase. Experiments were conducted in triplicates (n = 3), and values are expressed in mean ± standard deviation. **(B)** Spot assays were performed by serial dilution spot assay to check the effect of deletion on the antifungals tested. **(C)** R6G and NR efflux in MSY1–MSY7 cells. The experiment was performed in biological triplicates with three technical replicates. Significance was determined by calculating the *P*-value for all the strains with respect to WT by employing the student's t-test. *P*-values ≤ 0.05 = *, ≤0.0005 = *** and ns = not significant.

drug susceptibility are transporter dependent. We further confirmed the drug susceptibility profile of each deletion mutant by growth curve analysis in the presence of tested drugs (File S4, Supporting Information). The MIC_{80} to tested echinocandin and polyenes remained unchanged in all the deletion strains even after the deletion of all the seven transporters (File S3, Supporting Information). Together, these results suggested that the deletion of seven ABC transporters, which generated the MSY7 strain, displayed supersensitive phenotype to a wide range of tested drugs.

Assessment of efflux capacity of MSY1–MSY7 mutants

Fluorescent compounds R6G and NR are the known substrates of some of the ABC transporters and have been commonly used to evaluate the efflux activity. Therefore, we tested the R6G and NR efflux by MSY1–MSY7 deletion mutants to confirm the transport defect in these mutants. Indicated cells were pre-incubated with R6G or NR for 4 h in the absence of energy source to accumulate the dyes inside the cells. The energy-starved cells were then supplemented with 2% glucose to initiate the efflux of fluorescent substrates. After 45 min, the fluorescence was recorded in the supernatant and quantified. As expected, there was no reduction in R6G efflux in MSY1–MSY2 mutant strains. Surprisingly, MSY3 strain (*Cgcdr1*Δ) showed only ∼10% reduction in R6G efflux and an almost 48% reduction in NR efflux as compared to WT cells. The subsequent *Cgpdh1*Δ in MSY4 resulted in 33 and 44% reduction of R6G and NR efflux, respectively, which coincided well with a recorded drop in MIC_{80} of FLC. Subsequent deletions (MSY5–MSY6) did not show any significant changes in R6G and NR efflux. However, the deletion of *Cgyor1*Δ (MSY7 strain) further decreased R6G efflux by ∼93% and NR efflux by ∼23% as compared to MSY4 (Fig. 1C).

GOF mutation in WT enhances azole resistance by < 100 fold

In *C. glabrata*, the upregulation of ABC transporters is linked to alterations in zinc-clustered TF *CgPDR1*. This TF recognizes PDRE present at promoters of several ABC transporters genes, including *CgCDR1*, *CgPDH1*, *CgSNQ2*, *CgYOR1*, *CgYCF1* and *CgYBT1*. Several GOF mutations in the *CgPDR1* coding region have been linked to an increase in the expression of transporters and resistance towards azoles (Ferrari *et al.* 2009). A *CgPDR1* GOF mutation ($CgPDR1^{G840C}$) in *C. glabrata* DSY565 strain showed MIC_{80} of FLC 128 μg/mL along with approximately 64-fold upregulation of *CgCDR1* transcript (Ferrari *et al.* 2009). We introduced this mutation ($CgPDR1^{G840C}$) in WT, and the resulting mutant was designated as WT^{GOF} (*Cgpdr1*::$CgPDR1^{G840C}$). For this, pMS3 plasmid was linearized with SacI/KpnI and transformed by electroporation, which replaced the native *CgPDR1* coding sequence (Fig. 2A). The drug susceptibility of WT^{GOF} was tested for azoles, and expectedly we observed increased resistance to FLC along with ∼114-fold upregulated transcript of the *CgCDR1* gene (Fig. 2B and C).

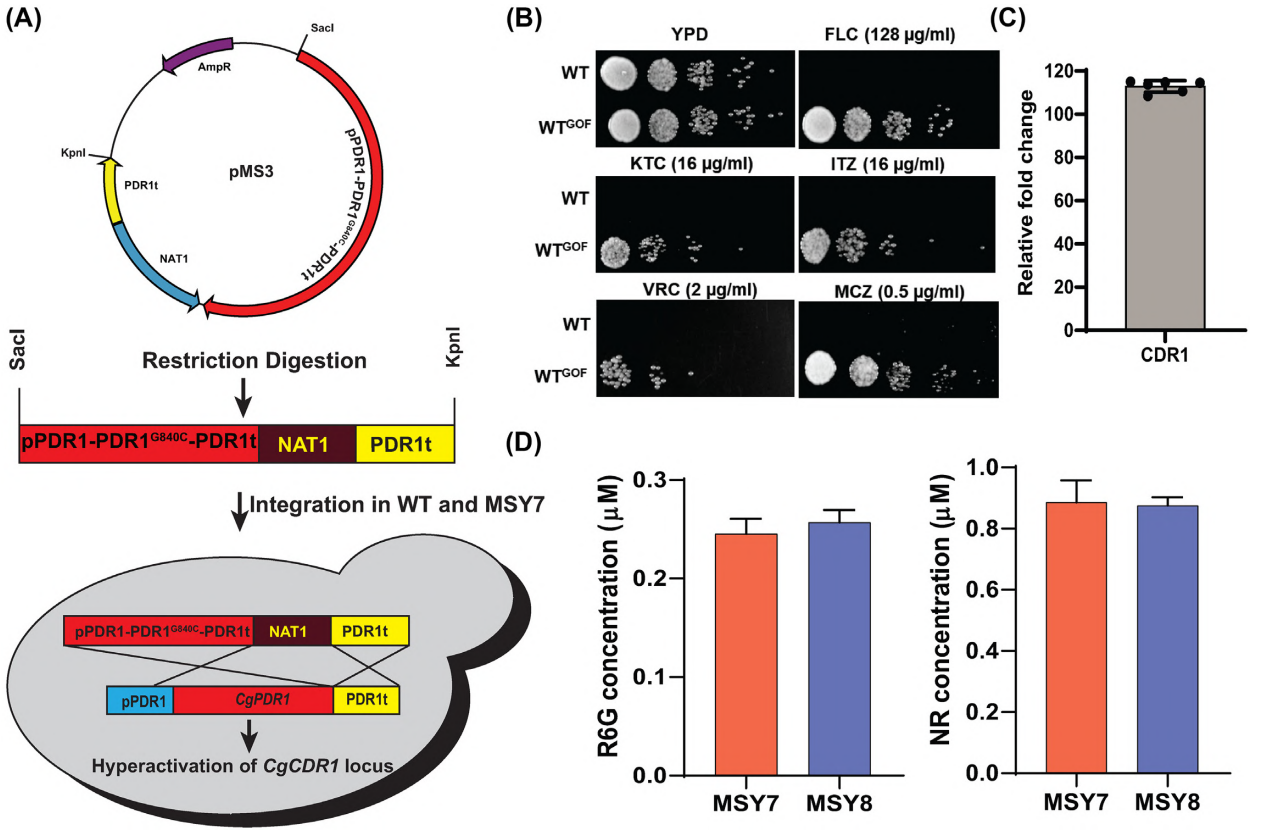

Figure 2. Introduction of GOF mutation (*CgPDR1*^{G840C}) in MSY7 and phenotypes tested with of MSY8 strain: **(A)** Integration plasmid for GOF TF *CgPDR1* was constructed by cloning mutated *CgPDR1* ORF (*CgPDR1*^{G840C}) from *C. glabrata* strain DSY565 (Ferrari *et al.* 2009). The resulting plasmid pMS3 was then digested with KpnI/SacI and transformed in WT and MSY7 strain to introduce the GOF in the genome to construct WT^{GOF} and MSY8, respectively. **(B)** Serial dilution spot assay to depicts drug susceptibility of WT^{GOF} cells. **(C)** Expression analysis of *CgCDR1* in WT^{GOF} cells as compared with WT cells. **(D)** Substrate transport assay (R6G and NR) with MSY7 and MSY8 strains.

GOF mutation in MSY8 does not impact growth, susceptibility to antifungals and substrate transport

To construct a supersensitive *C. glabrata* strain where GOI could be overexpressed without the interference of dominant transporters for functional analysis, we constructed MSY8 strain, with seven transporter deletions and hyperactive *CgCDR1* locus in its genome. For this, the above-constructed cassette from digested pMS3 plasmid was transformed in the above-constructed MSY7 strain to generate the MSY8 strain. The constructed MSY8 strain has a GOF *CgPDR1* (*CgPDR1*^{G840C}) and a hyperactive *CgCDR1* promoter. Since TF *CgPDR1* regulon includes several other genes apart from ABC transporters, we checked the possibility of altered growth and azole susceptibility in MSY8 strain. Interestingly MSY8 did not show a further change in susceptibility towards antifungals and efflux of substrates to MSY7 strain (Fig. 2C and D; File S3, Supporting Information).

Overexpression of ABC transporters validated the appropriateness of MSY8 as an expression system

To validate the expression system, we expressed well known ABC transporters of *C. glabrata* (*CgCDR1* and *CgPDH1*), *C. albicans* (*CaCDR1*) and *S. cerevisiae* (*ScPDR5*) in MSY8 strain. These transporters were cloned in pMS6 plasmid upstream of the *YeGFP* at either SacI/SacII or NotI/PacI sites, as described in File S2 (Supporting Information). The whole cassette containing GOI-GFP chimeric construct was then digested with SacI/KpnI and integrated into the MSY8 strain at *CgCDR1* locus. The constructed strains MSY9 (MSY8/*CgCDR1*), MSY10 (MSY8/*CgPDH1*), MSY11 (MSY8/*CaCDR1*) and MSY12 (MSY8/*ScPDR5*) were tested for the expression and localization. As evident from confocal images, all the GFP-chimeric transporters CgCdr1-GFP, CgPdh1-GFP, CaCdr1-GFP and ScPdr5-GFP showed precise plasma membrane localization (Fig. 3A). The transcripts levels of each transporter *CgCDR1, CgPDH1, CaCDR1 and ScPDR5* in MSY9, MSY10, MSY11 and MSY12 cells were confirmed by RT-PCR, which also displayed the overexpression of these transporters at the locus (Fig. 3C).

Functional analysis of CgCdr1-GFP, CgPdh1-GFP, CaCdr1-GFP and ScPdr5-GFP

The functionality of the recombinantly expressed ABC transporters in MSY9–MSY12 strains was analyzed by testing their susceptibility towards azoles, allylamines and protein synthesis inhibitors in comparison to parental strain MSY8. We rationalized that the overexpressing transporter proteins should be able to reverse the higher susceptibility of MSY8 cells. Expectedly, the expression of all four transporters drastically decreased the susceptibility of MSY8 cells, albeit to variable levels (Fig. 3B). R6G is a known substrate of ABC transporters, and these four transporters are known to efflux R6G (Lamping *et al.* 2007). Spectrofluorometric based efflux assay showed a 25 to 32-fold increased efflux of R6G as compared to MSY8 cells (Fig. 3D). Results

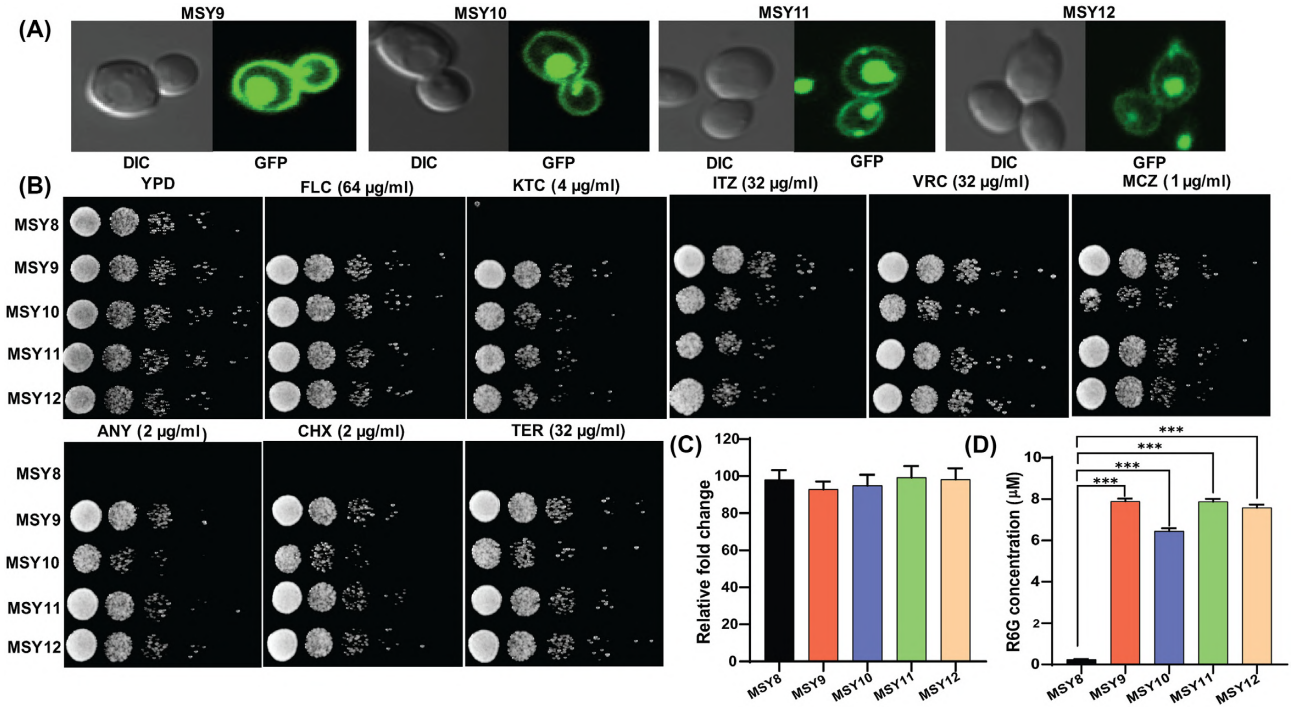

Figure 3. Overexpression of ABC transporters and their characterization: **(A)** Integration of ABC transporters *CgCDR1*, *CgPDH1*, *CaCDR1* and *ScPDR5* was performed as described in Methods and resulting strains designated as MSY9–MSY12. Confocal images of MSY9–MSY12 show the localization at the plasma membrane. Confocal images were taken by using the FITC filter. **(B)** Drug susceptibility tests were performed by spot assays at indicated concentrations. **(C)** Transcript levels of integrated transporters into MSY8 was determined by RT-PCR. **(D)** R6G substrate transport assay with the overexpressed transporters. *P*-value was determined by the student's t-test and *P*-value $\leq$ 0.0005 represented as (***).

indicated that ABC transporters from different fungal species could be expressed and functional in the MSY8 strain.

MSY8 expression system is suitable to study non-ABC transporters

We explored the suitability of our expression system for functional analysis of non-ABC membrane transporters. For this, we transformed and integrated a GFP-chimeric-*CgFLR1* transporter belonging to MFS superfamily in MSY8 strain to generate the MSY13 strain. Drug: H^+ antiporter CgFlr1p is a well-known drug transporter that confers 5-flucytosine (5-FC) antifungal resistance in *C. glabrata* (Pais *et al.* 2016). While the homolog CgFlr2p confers resistance to both azoles and 5-FC, the *Cgflr1*Δ deletant imparts susceptibility to 5-FC, but not to azoles (Chen *et al.* 2007). As expected, MSY13 strain became resistant to 5-FC and interestingly, also demonstrated increased resistance to azoles (Fig. 4A). The increased azole resistance could be attributed to the masking effect of *CgFLR2* on azole resistance phenotype of *CgFLR1*. MSY13 overexpressing CgFlr1-GFP showed proper localization at the plasma membrane, as was evident from confocal images (Fig. 4B), and 2-fold increased efflux of NR, a well-known MFS transporters substrate (Fig. 4C).

DISCUSSION

Several independent studies have called attention to the relevance of drug transporters belonging to ABC and MFS superfamilies in drug resistance and their posing of a serious hindrance to successful antifungal therapy. Such a situation demands an in-depth structure and function analysis of clinically relevant drug transporters. For this, there is always an unmet need for an overexpression system that can act as a platform to facilitate the functional characterization of these transporters to analyze the basis of their substrate poly-specificity, structural analysis and to develop inhibitors/modulators. Over the years, this requirement has been successfully met by the *S. cerevisiae* overexpression system established by Goffeau's and Cannon's groups (Decottignies *et al.* 1998; Lamping *et al.* 2007). Using this approach, efflux pumps not only from *S. cerevisiae* but from different fungal pathogens as well could be structurally and functionally analyzed (Shukla *et al.* 2003; Lamping *et al.* 2007; Panapruksachat *et al.* 2016). Notwithstanding, the extensive use of the *S. cerevisiae* system by several laboratories for nearly two decades, concerns have been raised pertaining to its artefactual environment posed by heterologous system, particularly applicable to the functionality of drug transporters of pathogenic *Candida* species. The differences in regulatory circuitry governing drug resistance and subtle differences in membrane lipid environment influencing the functionality of drug transporter proteins are some of the concerns faced by such studies. In this context, it is worth mentioning that membrane lipids do impact drug transporter protein insertion, integrity and overall functioning (Opekarová and Tanner 2003; Pasrija, Panwar and Prasad 2008).

Our present study is focused to resolve challenges imposed by the heterologous system for the overexpression of drug transporter proteins of *C. glabrata*. We took advantage of a GOF mutation of TF *CgPDR1* azole-resistant clinical isolate of *C. glabrata* and introduced it into an engineered hyper-susceptible MSY7 mutant strain, which was deleted for seven dominant ABC transporters. Thus the resulting strain MSY8 apart from major transporters deleted background also possessed hyper-activated *CgCDR1* locus. This followed by the construction of an integration-based plasmid for cloning GOI at the activated

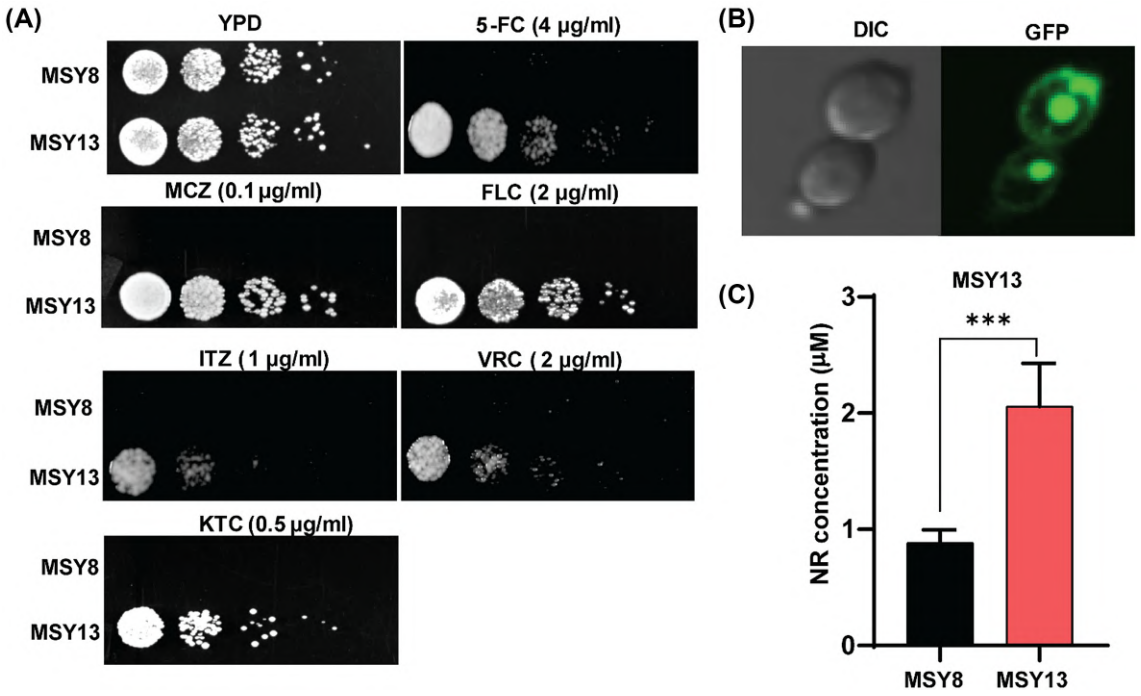

Figure 4. Expression of MFS transporter and its phenotypic characterization. **(A)** Drug spot assays of MSY13 by serial dilution at indicated concentrations. **(B)** Confocal images of localization of CgFlr-GFP taken from the FITC filter of the confocal microscope. **(C)** NR efflux in MSY13 cells. Each experiment was performed in biological triplicates with three technical replicates. P-value was determined by paired student *t*-test, and P-value ≤ 0.0005 was represented as (***).

CgCDR1 locus. The suitability of the expression system was well demonstrated by overexpressing fully functional clinically relevant ABC drug transporters of *C. glabrata* (*CgCDR1* and *CgPDH1*), *C. albicans* (*CaCDR1*), *S. cerevisiae* (*ScPDR5*) and *C. glabrata* MFS transporter *CgFLR1*. This MSY8 system thus presents a good platform for detailed substrate profiling and functional analysis of transporter proteins with minimum interference by major drug transporters of *C. glabrata*.

SUPPLEMENTARY DATA

Supplementary data are available at FEMSYR online.

ACKNOWLEDGMENTS

RP acknowledges support from the Indian Council of Medical Research, ICMR (AMR/149 (2)-2018-ECD-II) and DBT (BT/PR27264/Med/29/1277/2018 and BT/PR14117/BRB/10/1420/2015). NAG acknowledges ICGEB, New Delhi, and Department of Biotechnology (DBT), Government of India for financial support (Grant No.: BT/PB/Centre/03/ICGEB/2011-PhaseII). RK is a senior fellow of the Wellcome Trust/DBT India Alliance (IA/S/15/1/501831). MK and SK acknowledge the Department of Biotechnology (DBT), India, and the Council for Scientific and Industrial Research (CSIR), respectively, for providing fellowship support during the research work. Authors acknowledge Dominique Sanglard, Institute of Microbiology, Lausanne, for providing DSY565 strain.

Conflict of interest. None declared.

REFERENCES

Borah S, Shivarathri R, Kaur R. The Rho1 GTPase-activating protein CgBem2 is required for survival of azole stress in *Candida glabrata*. *J Biol Chem* 2011;**286**:34311–24.

Chen K-H, Miyazaki T, Tsai H-F *et al.* The bZip transcription factor Cgap1p is involved in multidrug resistance and required for activation of multidrug transporter gene *CgFLR1* in *Candida glabrata*. *Gene* 2007;**386**:63–72.

Decottignies A, Grant AM, Nichols JW *et al.* ATPase and multidrug transport activities of the overexpressed Yeast ABC protein Yor1p. *J Biol Chem* 1998;**273**:12612–22.

Ferrari S, Ischer F, Calabrese D *et al.* Gain of function mutations in *CgPDR1* of *Candida glabrata* not only mediate antifungal resistance but also enhance virulence. *PLoS Pathog* 2009;**5**:e1000268.

Ferrari S, Sanguinetti M, De Bernardis F *et al.* Loss of mitochondrial functions associated with azole resistance in *Candida glabrata* results in enhanced virulence in mice. *Antimicrob Agents Chemother* 2011;**55**:1852–60.

Gbelska Y, Toth Hervay N, Dzugasova V *et al.* Measurement of energy-dependent rhodamine 6 G efflux in yeast species. *BIO-Protoc* 2017;**7**, DOI: 10.21769/BioProtoc.2428.

Holmes AR, Cardno TS, Strouse JJ *et al.* Targeting efflux pumps to overcome antifungal drug resistance. *Future Med Chem* 2016;**8**:1485–501.

Kasper L, Seider K, Hube B. Intracellular survival of *Candida glabrata* in macrophages: immune evasion and persistence. *FEMS Yeast Res* 2015;**15**, DOI: 10.1093/femsyr/fov042fov042.

Keniya MV, Fleischer E, Klinger A *et al.* Inhibitors of the *Candida albicans* major facilitator superfamily transporter Mdr1p responsible for fluconazole resistance. *PLOS ONE* 2015;**10**:e0126350.

Kolaczkowski M, Kolaczowska A, Luczynski J *et al. In vivo* characterization of the drug resistance profile of the major ABC

transporters and other components of the yeast pleiotropic drug resistance network. *Microb Drug Resist Larchmt N* 1998;**4**:143–58.

Ksiezopolska E, Gabaldón T. Evolutionary emergence of drug resistance in *Candida* opportunistic pathogens. *Genes* 2018;**9**:461.

Kumari S, Kumar M, Khandelwal NK *et al.* ABC transportome inventory of human pathogenic yeast *Candida glabrata*: phylogenetic and expression analysis. *PLOS ONE* 2018;**13**:e0202993.

Lamping E, Monk BC, Niimi K *et al.* Characterization of three classes of membrane proteins involved in fungal azole resistance by functional hyperexpression in *Saccharomyces cerevisiae*. *Eukaryot Cell* 2007;**6**:1150–65.

Opekarová M, Tanner W. Specific lipid requirements of membrane proteins—a putative bottleneck in heterologous expression. *Biochim Biophys Acta BBA - Biomembr* 2003;**1610**:11–22.

Pais P, Pires C, Costa C *et al.* Membrane proteomics analysis of the *Candida glabrata* response to 5-Flucytosine: uveiling the role and regulation of the drug efflux transporters CgFlr1 and CgFlr2. *Front Microbiol* 2016;**7**, DOI: 10.3389/fmicb.2016.02045.

Panapruksachat S, Iwatani S, Oura T *et al.* Identification and functional characterization of *Penicillium marneffei* pleiotropic drug resistance transporters ABC1 and ABC2. *Med Mycol* 2016;**54**:478–91.

Pasrija R, Panwar SL, Prasad R. Multidrug transporters CaCdr1p and CaMdr1p of *Candida albicans* display different lipid Specificities: both ergosterol and sphingolipids are essential for targeting of CaCdr1p to membrane rafts. *Antimicrob Agents Chemother* 2008;**52**:694–704.

Redhu AK, Banerjee A, Shah AH *et al.* Molecular basis of substrate polyspecificity of the *Candida albicans* Mdr1p Multidrug/H+ antiporter. *J Mol Biol* 2018;**430**:682–94.

Sanguinetti M, Posteraro B, Fiori B *et al.* Mechanisms of Azole resistance in clinical isolates of *Candida glabrata* collected during a hospital survey of antifungal resistance. *Antimicrob Agents Chemother* 2005;**49**:668–79.

Shah AH, Shukla S, Prasad R. Tools and techniques to study multidrug transporters of yeasts. In: Varma A, Sharma AK (eds.). *Modern Tools and Techniques to Understand Microbes*. Cham: Springer International Publishing, 2017, 183–207.

Shukla S, Saini P, Smriti *et al.* Functional characterization of *Candida albicans* ABC transporter Cdr1p. *Eukaryot Cell* 2003;**2**:1361–75.

Srivastava VK, Suneetha KJ, Kaur R. The mitogen-activated protein kinase CgHog1 is required for iron homeostasis, adherence and virulence in *Candida glabrata*. *FEBS J* 2015;**282**:2142–66.

Torelli R, Posteraro B, Ferrari S *et al.* The ATP-binding cassette transporter–encoding gene *CgSNQ2* is contributing to the *CgPDR1*-dependent azole resistance of *Candida glabrata*. *Mol Microbiol* 2008;**68**:186–201.

Vermitsky J-P, Earhart KD, Smith WL *et al.* *Pdr1* regulates multidrug resistance in *Candida glabrata*: gene disruption and genome-wide expression studies. *Mol Microbiol* 2006;**61**:704–22.

Whaley SG, Berkow EL, Rybak JM *et al.* Azole antifungal resistance in *Candida albicans* and emerging Non-*albicans Candida* species. *Front Microbiol* 2016;**7**:2173.

FEMS Yeast Research, 20, 2020, foaa045

doi: 10.1093/femsyr/foaa045
Advance Access Publication Date: 5 August 2020
Research Article

RESEARCH ARTICLE

A detailed lipidomic study of human pathogenic fungi *Candida auris*

Garima Shahi[1,†], Mohit Kumar[1,2,†], Sonam Kumari[2], Shivaprakash M. Rudramurthy[3], Arunaloke Chakrabarti[3,‡], Naseem A. Gaur[2], Ashutosh Singh[4,*] and Rajendra Prasad[1,*,¤]

[1]Amity Institute of Integrative Science and Health and Amity Institute of Biotechnology, Amity University Gurugram,, Haryana, 122413, India, [2]Yeast Biofuel Group, International Centre for Genetic Engineering and Biotechnology, New Delhi, 110067, India, [3]Department of Medical Microbiology, Postgraduate Institute of Medical Education and Research,, Chandigarh, 160012, India and [4]Department of Biochemistry, University of Lucknow, Lucknow, Uttar Pradesh, 226007, India

*Corresponding author: Department of Biochemistry, University of Lucknow, Uttar Pradesh, 226007, India. E-mail: singh_ashutosh@lkouniv.ac.in; Amity Institute of Integrative Science and Health and Amity Institute of Biotechnology, Amity University Gurugram, Haryana, 122413, India. E-mail: rprasad@ggn.amity.edu

One sentence summary: The present study determines the lipid composition of *Candida auris* and highlights alterations in lipids that may be correlated to high drug resistance in fungi.

†Equal First Author

Editor: Carol Munro

‡Arunaloke Chakrabarti, http://orcid.org/0000-0003-1555-3807
¤Rajendra Prasad, http://orcid.org/0000-0002-8044-7042

ABSTRACT

The present study is an attempt to determine the lipid composition of *Candida auris* and to highlight if the changes in lipids can be correlated to high drug resistance encountered in *C. auris*. For this, the comparative lipidomics landscape between drug-susceptible (CBS10913T) and a resistant hospital isolate (NCCPF_470033) of *C. auris* was determined by employing high throughput mass spectrometry. All major groups of phosphoglycerides (PGL), sphingolipids, sterols, diacylglycerols (DAG) and triacylglycerols (TAG), were quantitated along with their molecular lipid species. Our analyses highlighted several key changes where the NCCPF_470033 showed an increase in PGL content, specifically phosphatidylcholine, phosphatidylglycerol, phosphatidylserine, phosphatidylinositol, and phosphatidylethanolamine; odd chain containing lipids and accumulation of 16:1-DAG and 16:0-DAG; depletion of 18:1-TAG and 18:0-TAG. The landscape of molecular species displayed a distinct imprint between isolates. For example, the levels of unsaturated PGLs, contributed by both odd and even-chain fatty acyls were higher in resistant NCCPF_470033 isolate, resulting in a higher unsaturation index. Notwithstanding, several commonalities of lipid compositional changes between resistant *C. auris* and other *Candida* spp., the study could also identify distinguishable changes in specific lipid species in *C. auris*. Together, the data highlights the modulation of membrane lipid homeostasis associated with drug-resistant phenotype of *C. auris*.

Keywords: Lipids; pathogenic fungi; functions; mass spectrometry

Received: 20 May 2020; **Accepted:** 27 July 2020

INTRODUCTION

The scope of diseases caused by human fungal pathogens ranged from superficial to chronic by a variety of *Candida* species. The prevalent human fungal infections are majorly caused by *Candida albicans* and non-albicans *Candida* (NAC) species. Apart from common fungal species, newer species of *Candida* are emerging as belligerent pathogens that display a high level of drug resistance (Brown *et al.* 2012; Fairlamb *et al.* 2017). In 2009 from Japan, a close relative of *Candida haemulonii* was identified and named as *Candida auris*, represents one such example (Satoh *et al.* 2009; Kathuria *et al.* 2015). Fungemia, due to *C. auris*, now prevalent worldwide, is associated with a high mortality rate and treatment failure, in addition to being highly resistant to commonly used antimycotics such as azoles, polyenes, and echinocandins (Chowdhary, Sharma and Meis 2017; Lockhart *et al.* 2017; Lone and Ahmad 2019).

The most common contributors involved in reducing the impact of antifungals used by other pathogenic fungi include overexpression of multidrug transporters (Kumari *et al.* 2018; Wasi *et al.* 2019) and drug target alterations also represent another common strategy that excludes the antifungals from reaching out to its target (Lupetti *et al.* 2002; Shor and Perlin 2015). Azoles target 14α-demethylase encoded by *ERG11*, while echinocandins target 1,3-β-glucan synthase encoded by *FKS* genes. Both the targets are widely reported to acquire mutations in drug-resistant isolates in *Candida* isolates (Lupetti *et al.* 2002; Hou *et al.* 2019). Notwithstanding, the well understood and widely documented features of drug resistance, microorganisms are continually developing new and varied ways of rendering generally used antifungal drugs. (Anderson 2005). Several recent reports have shown new resistance mechanisms that fungal cells resort to thwart drug effectiveness includes stress responses that are crucial in assuring the survival of the cell (Shor and Perlin 2015).

In *Candida*, the enzymes of lipid biosynthetic pathways represent a target of many known antifungal drugs (Prasad and Singh 2013). Previous independent studies on *Candida* by our group and others demonstrated that membrane lipids composition could influence the drug susceptibilities in *Candida* cells (Lattif *et al.* 2011; Singh, Yadav and Prasad 2012). Besides, the virulence of many pathogens is also impacted by lipids, the phospholipid synthesis genes, *PSD1* and *PDS2* play a crucial role in azole resistance, cell wall integrity and virulence of *C. albicans* (Gonçalves *et al.* 2017; Khandelwal *et al.* 2018). Moreover, any changes in the lipid homeostasis and membrane lipid asymmetric distributions between two monolayers of the plasma membrane also shown to affect drug resistance and virulence (Gonçalves *et al.* 2017; Khandelwal *et al.* 2018). Together, the drug susceptibilities depend on their diffusion rates, efflux by membrane pump proteins, and the local membrane environment (Balzi and Goffeau 1995; Prasad and Singh 2013).

Recent advances in high throughput mass spectrometry-based strategies for a complete analysis of cellular lipids have been developed and employed in fungi (Singh and Del Poeta 2016). By employing high throughput mass spectrometry approach, we have earlier characterized the lipidome of various *Candida* spp. to show that while all *Candida* species comprise similar levels of various phospholipid classes, they exhibit distinct molecular lipid species imprint (Singh *et al.* 2010). The comparative lipidomics study that followed between susceptible and resistant clinical genetically matched isolates of *C. albicans*, presented evidence that changes in lipid homeostasis can not only influence drug resistance phenotypes but also impacts the cell wall integrity and mitochondrial function (Singh and Prasad 2011; Singh, Yadav and Prasad 2012).

That the prevalence of highly drug-resistant clinical isolates of *C. auris*, which cannot be explained based on the contributions of established resistance mechanisms (Kim *et al.* 2019; Rybak *et al.* 2019), makes it imperative to seek new alternatives which could also be important in presenting such level of drug resistance. For this, the present study, using the ESI-MS/MS (electrospray ionization tandem mass spectrometry) approach, has focused on analyzing comparative lipidome between drug-resistant and susceptible *C. auris* isolates. Our analyses quantified five major lipid groups of *C. auris*, namely PGLs, sphingolipids (SL), sterols, diacylglycerols (DAG) and triacylglycerols (TAG) along with the composition of their molecular lipid species. The comparative lipid profiles of *C. auris* strain CBS10913T (drug-susceptible) and NCCPF_470033 (drug-resistant) revealed marked changes in their compositions, suggesting a major remodeling of polar lipids in drug resistant *C. auris*.

MATERIALS AND METHODS

Materials

Lipid standards were purchased from Sigma-Aldrich, USA and Avanti polar lipids Inc., USA. All solvents and chemicals were mass spectrometry grade and purchased from Sigma-Aldrich, USA and Fisher Scientific, UK.

Strains and culture conditions

Candida auris strain CBS10913T was purchased from CBS database, Westerdijk Fungal Biodiversity Institute, Utrecht, the Netherlands. The drug-resistant *C. auris* NCCPF_470033 strain (this study) is a hospital isolate from India and was obtained from the National Culture Collection of Pathogenic Fungi, Postgraduate Institute of Medical Education & Research, Chandigarh, India. Cultures were maintained on YEPD agar plates at 30°C. For lipid extraction, 10^6 cells (1.0 O.D.) were inoculated in 50 mL YEPD medium and grown for 6 hrs, and approximately 5×10^8 cells were harvested, washed with dH_2O thrice before lipid extraction (Singh, Yadav and Prasad 2012).

Drug susceptibility assessment

Minimum inhibitory concentrations (MIC) of fluconazole (FLC), itraconazole (ITZ), ketoconazole (KTZ), miconazole (MCZ), amphotericin B (AmB), nystatin (NYS), caspofungin (CSP) and micafungin (MICA) against the *C. auris* strains were determined as described in method M27-A3 by the Clinical and Laboratory Standards Institute (CLSI, formerly NCCLS, USA) (Pfaller *et al.* 2008).

Lipid extraction

Harvested cells were broken in methanol using glass beads (Glaperlon, 0.4–0.6 mm), and lipids were extracted by the Folch extraction method using chloroform: methanol (2:1, v/v), as described earlier (Folch, Lees and Sloane Stanley 1957). Lipid extracts were dried in N_2 and kept in −20°C until analyzed. Lipid dry weights were recorded at this step for the normalization of mass spectral data.

Mass spectrometry analysis

Lipid extracts were dissolved in 1 mL chloroform. To the 2–3 μL aliquots of these dissolved lipids, internal standards were added as described previously (Singh *et al.* 2010; Singh and

Prasad 2011; Singh, Yadav and Prasad 2012), and volume made up to 1.4 mL using chloroform: methanol: 300 mM ammonium acetate (100:5:26, v/v/v). Lipid extracts were then analyzed on Xevo TQ-XS triple quadrupole mass spectrometer (XEVO-TQS#WAA627, Waters, UK, Milford, MA). Levels of various lipid classes and individual molecular lipid species were determined using the neutral loss, negative and positive multiple precursor ion scans as described earlier (Singh *et al.* 2010; Singh and Prasad 2011; Singh, Yadav and Prasad 2012).Instrument parameters settings are listed in supplementary sheet S1. Data processing was performed using the TargetLynx XS^{TM} software (Waters, UK, Milford, MA) and data normalized to lipid dry weight and represented as nmol/mg lipid dry weight. Lipid structures and their nomenclature were annotated according to previously published studies (Bowden *et al.* 2017) (www.lipidmaps.org, www.k-state.edu/lipid).

Gas chromatography mass spectrometry (GC-MS)

For free sterol analysis, base hydrolyzed lipid extract were derivatized with N,O-Bis (trimethylsilyl) trifluoroacetamide with trimethyl-chlorosilane (BSTFA/TMCS, Sigma, USA) and analyzed on DB5-MS column (30 m × 0.2 mm × 0.20 μm) as described previously (Singh, Yadav and Prasad 2012). The retention time and mass spectral patterns of external standards were used for identification of sterol species. For fatty acid (FA) analyses, base hydrolyzed lipid extract were derivatized with BF_3-Methanol and analyzed on Omegawax column (30 m × 250 μm × 0.25 μm) as described previously (Singh *et al.* 2017). The retention time and mass spectral patterns of fatty acid methyl ester standard mix (Sigma, USA) were used as a reference to identify respective FAs (Sharma *et al.* 2012).

Statistical analysis

Experiments were performed in triplicates, and all the lipid data sets are represented as mean ± standard error mean (SEM). Statistical significance was determined using student's *t*-test and *P*-values < 0.05 were considered significant. The principal component analysis (PCA) was performed using the XLSTAT software (Addinsoft, US) on Microsoft Excel platform. PCA between *C. auris* strains CBS10913T and NCCPF_470033 was performed using the whole lipidome data sets (582 lipid species as nmol/mg lipid dry weight, supplementary sheet S2) as well as the phospholipid species data (144 lipid species as % of total PGL + SL). However, for comparative PCA of *C. auris* with other *Candida* strains, we have used the data for only phospholipid species (as % of total PGL + SL, supplementary sheet S3), which are reported in the previously published lipidomic studies by our group (Singh and Prasad 2011; Singh, Mahto and Prasad 2013). We chose the mole% data of 144 phospholipid species for comparative purposes as these were detectable in the current study as well as in the earlier published lipidomes of *Candida*.

RESULTS AND DISCUSSION

NCCPF_470033 strain is highly resistant to azoles

For the lipidome analysis, we selected two strains of *C. auris*; CBS10913T, which was highly susceptible to antifungals and resistant hospital isolate NCCPF_470033. The CBS10913T strain was susceptible to all the tested drugs that included azoles, polyenes, and echinocandins. However, in comparison with the susceptible CBS10913T strain, NCCPF_470033 isolate showed high resistance towards FLC ($MIC_{80} > 256.0$ μg/mL), ITZ ($MIC_{80} > 0.25$ μg/mL), KTZ ($MIC_{80} > 0.125$ μg/mL) and MCZ ($MIC_{80} > 2.0$ μg/mL) and showed no change in susceptibility towards AmB (MIC_{80} 0.5 μg/mL), NYS ($MIC_{80} > 2.0$ μg/mL), CSP (MIC_{80} 75 ng/mL) and MICA (MIC_{80} 62.5 ng/mL) (Fig. 1). The differences in drug susceptibilities between CBS10913T and NCCPF_470033 isolates allowed us to make comparisons of their lipid profiles.

Azole resistant NCCPF_470033 show elevated levels of polar lipids

A comparative lipidomics was performed to underscore the importance of lipids in influencing drug resistance in *C. auris*. For this, lipids were extracted as described earlier from FLC susceptible CBS10913T and FLC resistant NCCPF_470033 strains. Lipid dry weights of extracts in triplicates obtained from 5 × 10^8 CBS10913T and NCCPF_470033 cells were 1.86 ± 0.03 and 2.23 ± 0.08 mg, respectively. The extracted lipids were subjected to mass spectrometry analysis on ESI-MS/MS (Electrospray Ionization mass spectrometry) and GC-MS as described earlier. In our analysis, 582 lipid species were detected belonging to five different lipid groups namely, PGLs, SLs, sterols, DAGs and TAGs. Moreover PGLs further divided into eight different lipid subclasses, namely lysophosphatidylcholine (LPC, 1-acyl-sn-glycero-3-phosphocholine) phosphatidylcholine (PC, 1,2-diacyl-sn-glycero-3-phosphocholine), lysophosphatidylethanolamine (LPE, 1acyl-sn-glycero-3-phosphoethanolamine), phosphatidylethanolamine (PE,1,2-diacyl-sn-glycero-3-phosphoethanolamine) phosphatidylinositol (PI, 1,2-diacyl-sn-glycero-3-phospho-(1'-myo-inositol), phosphatidylserine (PS, 1,2-diacyl-sn-glycero-3-phosphoserine), phosphatidylglycerol (PG, 1,2-diacyl-sn-glycero-3-phospho-(1'-sn-glycerol), phosphatidic acid (PA, 1,2-diacyl-sn-glycero-3-phosphate).

The quantitation of lipids revealed that the azole-resistant isolate NCCPF_470033 had 1.9 folds higher PGLs amounting to 467.6 ± 2.1 nmol/mg lipid dry weight when compared with the CBS10913T strain (Fig. 2A). This data coincided well with the increased levels of various PGL subclasses like PC, PE, LPE, PI, PS, and PG were as much as 2.9-fold higher in NCCPF_470033, compared to the CBS10913T strain. The contents of PA and LPC did not show any change between these isolates (Fig. 2A). PC was the most abundant PGL in the *C. auris* followed by PE. Interestingly PC was 1.7-fold higher in azole-resistant isolates, but PE showed the maximum change (2.9-fold) between the tested isolates among PGLs.

Our analysis of SLs was limited, and only two classes of SL were detected, which displayed no significant difference between the CBS10913T and NCCPF_470033 strains (Fig. 2B). The neutral lipids are the storage lipids and contain two major subclasses DAG and TAG. The total neutral lipid content was ~39% lower in NCCPF_470033 compared to the CBS10913T strain (Fig. 2B). While we observed as much as 2.1 folds increase in 16:1-DAG and 16:0-DAG content of NCCPF_470033, there were as much as 3.6 folds decrease in 18:1-TAG and 18:0-TAG content of NCCPF_470033, compared to the CBS10913T strain (Fig. 2B). In corroboration to these data, our GC-MS analysis showed that the content of 16C FA was 8% higher, and the content of 18C FA was 45% lower in NCCPF_470033 compared to the CBS10913T strain (Supplementary Fig. S1). However, composition of ergosterol esters showed no significant difference between the two strains (Fig. 2B). A recent multiomics study of Zamith-Miranda

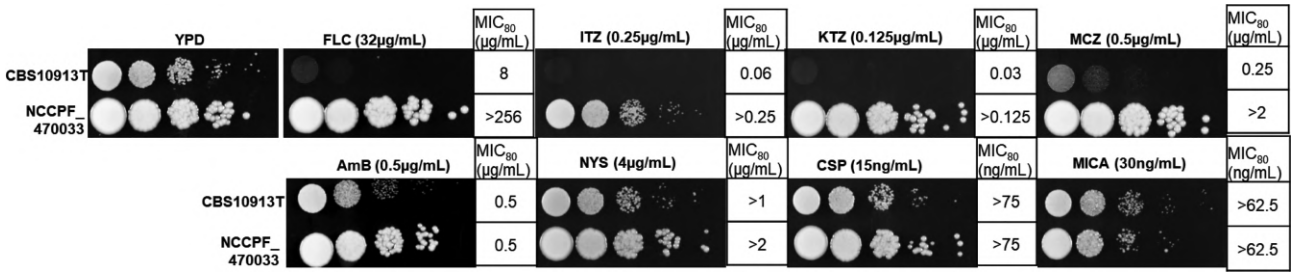

Figure 1. Drug susceptibility profiling of CBS10913T and NCCPF_470033 strains. The panels show the drug susceptibility of *C. auris* strains on FLC, ITZ, KTZ, MCZ, AmB, NYS, CSP and MICA using the spot assays. The MIC values, as determined by the broth dilution method (Pfaller *et al.* 2008), are also depicted.

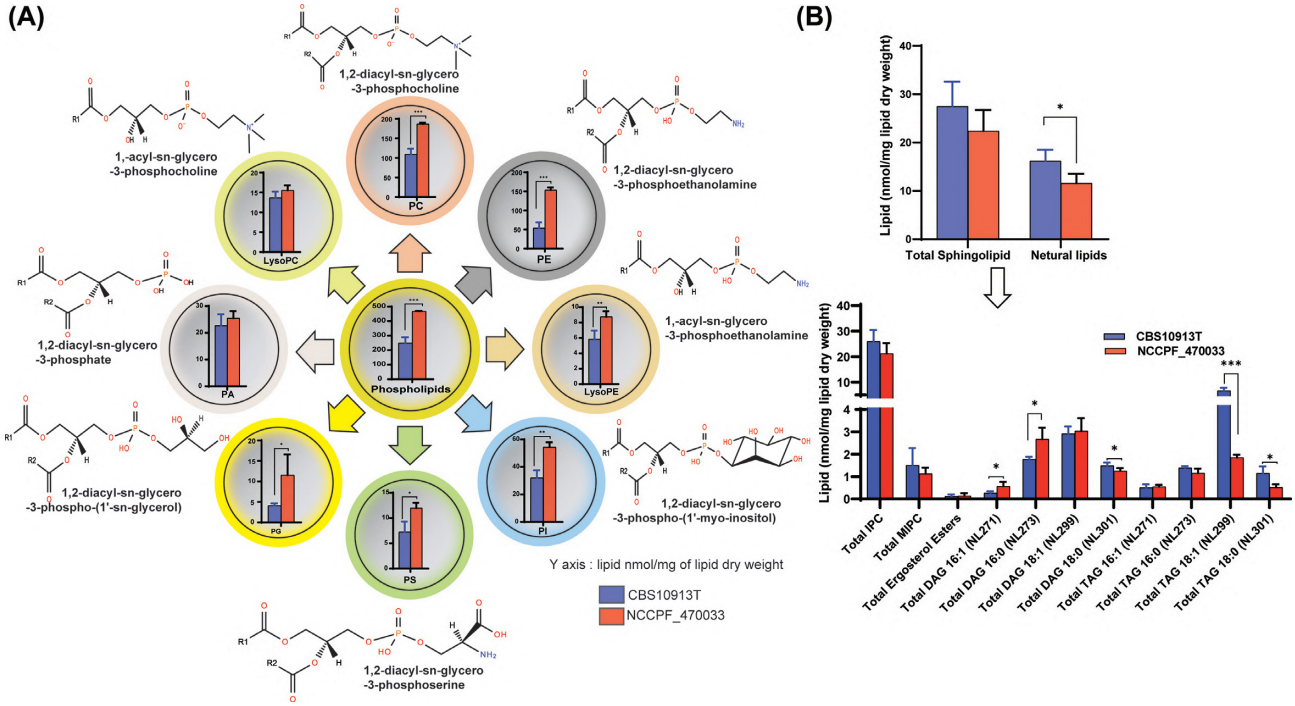

Figure 2. The total content of different lipid classes between CBS10913T and NCCPF_470033 strains. **(A)**, The total PGL content, along with the total class contents of PC, LPC PE, LPE, PI, PS, PG and PA, in CBS10913T and NCCPF_470033 strains of *C. auris* is depicted. **(B)**, The total SL and neutral lipid contents, along with the total class contents of IPC, MIPC, DAG and TAG, in CBS10913T and NCCPF_470033 strains of *C. auris* is depicted. The DAG and TAG content were determined based on the attached FA chain, as described earlier, For example, NL271, NL273, NL299 and NL301 scans were used to detect 16:1, 16:0, 18:1 and 18:0 -FA containing DAG or TAG species, respectively. Data represents nmol per mg lipid dry weight and can be found in supplementary sheet S2. Mean ± SEM of 3 replicates are plotted. The *P*-values of < 0.05, <0.01 and < 0.001 are represented by *, ** and ***, respectively.

et al. also reported that PC and TAG were most diverse lipid classes between resistant and sensitive *C. auris* isolates. However, lipids with unsaturation C16:1 FA was lower in resistant isolate (Zamith-Miranda *et al.* 2019). This is in accordance to our present data set of lipid profiles of resistant and susceptible *C. auris* isolates.

Molecular lipid species of PGLs show distinct imprint between susceptible and resistant strains

Alterations in membrane fluidity by changes in lipid homeostasis are known to affect drug resistance in *Candida* species (Mukhopadhyay, Kohli and Prasad 2002; Prasad *et al.* 2005). These alterations include changes in FA chain lengths, number of double bonds, hydroxylations, methylations, and backbone structure. We monitored these changes by quantifying the variations in molecular lipid species compositions between the CBS10913T and NCCPF_470033 strains. We identified and quantitated a total of 582 molecular species of various classes of lipids in *C. auris*.

Among 149 PGL species that were detected, lipid species with 34C and 36C containing 1 to 3 double bonds in their FA chains were most abundant in NCCPF_470033 isolate. For example, lipid species 34:3, 34:2, 34:1, 36:3, 36:2, 36:1 were abundant in all PC, PE, PI, PS, PG and PA classes (Figs. 3 and 4). Majority of mono- and poly- unsaturated lipid species were present in high abundance in NCCPF_470033 strain. For example, PC (30:1, 32:2, 32:1, 33:2, 33:1, 34:3, 34:2, 34:1, 36:3), PE (32:2, 32:1, 33:2, 33:1, 34:3, 34:2, 34:1, 35:1, 36:3, 36:2, 36:1), PI (32:2, 32:1, 34:3, 34:2, 34:1, 36:1), PS (32:1, 34:1), PG (34:2, 34:1) and PA (34:3, 34:1), were in higher amounts in NCCPF_470033 as compared to CBS10913T strain (Figs. 3 and 4). Among the lysophosphoglycerides (lyso-PGL), LPC (16:1, 18:1) and LPE (16:1, 18:2, 18:1) were higher while LPC (18:0) and LPE (16:0) were lower in NCCPF_470033. (Fig. 3).

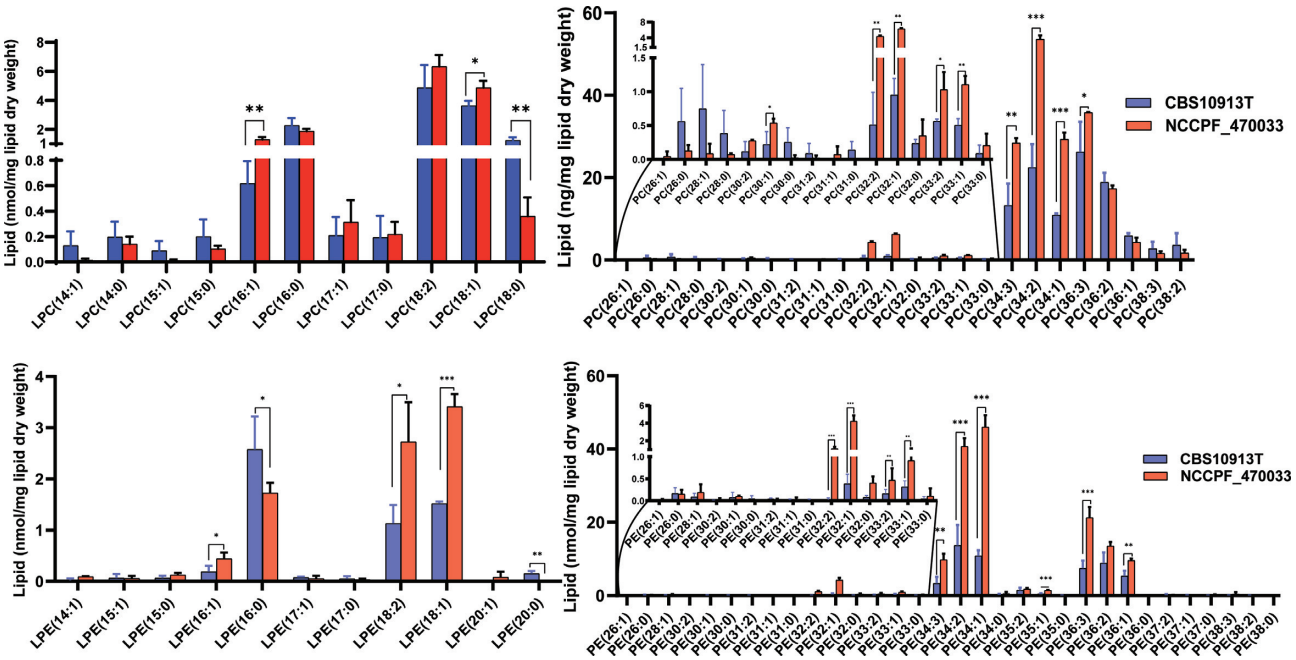

Figure 3. Comparison of LPC, PC, LPE and PE molecular lipid species compositions between CBS10913T and NCCPF_470033 strains. The PGL species are represented as 'total number of carbons in the acyl chains: total number of carbon-carbon double bonds in the acyl chains'. Data represents nmol per mg lipid dry weight and can be found in supplementary sheet S2. Mean ± SEM of 3 replicates is plotted. The *P*-values of < 0.05, <0.01 and < 0.001 are represented by *, ** and ***, respectively.

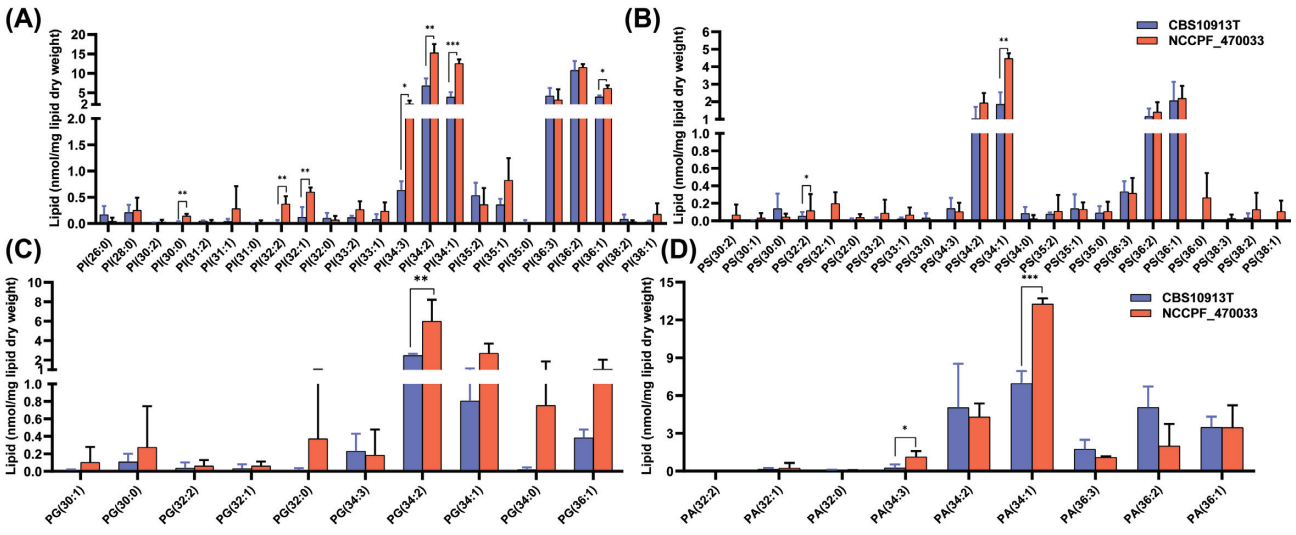

Figure 4. Comparison of PI, PS, PG, and PA molecular lipid species compositions between CBS10913T and NCCPF_470033 strains. The PGL species are represented as 'total number of carbons in the acyl chains: total number of carbon-carbon double bonds in the acyl chains'. Data represents nmol per mg lipid dry weight and can be found in supplementary sheet S2. Mean ± SEM of 3 replicates is plotted. The *P*-values of < 0.05, <0.01 and < 0.001 are represented by *, ** and ***, respectively.

Azole resistant *C. auris* present higher unsaturation index

A closer look at the PGL species revealed several interesting changes between NCCPF_470033 and CBS10913T strains. For example, the presence of odd chain fatty acids that have previously been also detected in other *Candida* species and yeasts (Singh and Prasad 2011; Kondo *et al.* 2014). Notably, the content of odd chain FA containing PGLs was higher in NCCPF_470033 as compared to CBS10913T strain (Fig. 5A). Although the levels of saturated PGL species did not change, the levels of unsaturated PGLs were higher in NCCPF_470033 compared to CBS10913T strain, resulting in a higher unsaturation index in NCCPF_470033 (Fig. 5B–D). The lipid ratios of PC(36:3/36:1), PE(32:2/32:1) and PE(36:3/36:1) were higher, while the ratios PE(34:2/34:1) and PE(36:2/36:1) were lower in NCCPF_470033 compared to CBS10913T strain (Fig. 5E). The changes in lipid ratios and odd chain FAs are good predictors of alteration in the membrane lipid environment (Singh and Prasad 2011).

Independent reports from others and us show that the metabolic pathways, including lipid metabolism, involved in the development of drug resistance, are often conserved in pathogenic fungi (Mukhopadhyay, Kohli and Prasad 2002; Singh and Prasad 2011; Singh, Mahto and Prasad 2013; Sharma *et al.* 2014; Gao *et al.* 2018). In this context, the available data provide credible evidence to point that imbalance in lipid homeostasis

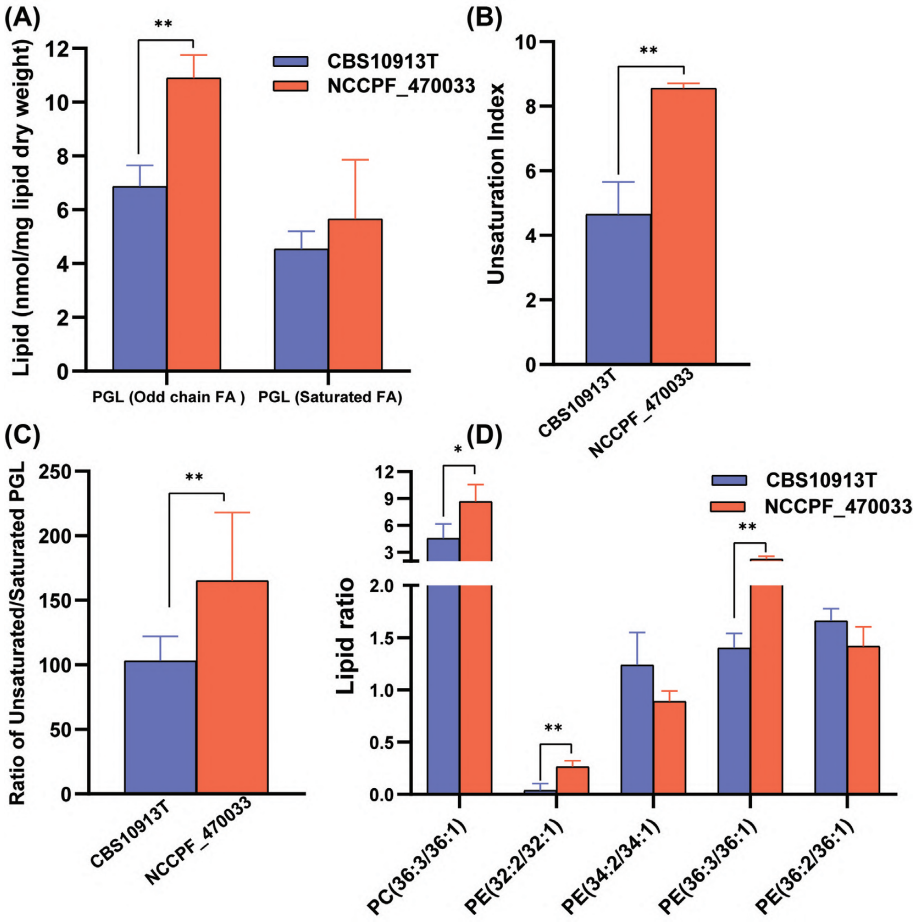

Figure 5. Alterations in PGL species levels of *C. auris* CBS10913T and NCCPF_470033 strains. **(A)**, Total levels of odd-chain fatty acyl containing PGLs and saturated fatty acyl containing PGLs. **(B)**, The degree of unsaturation represented as unsaturation index. The unsaturation index was calculated using the following formula: UI = [(1 × % monoene-PGL) + (2 × % diene-PGL) + (3 × % triene-PGL) + (4 × % tetraene-PGL) + (5 × % pentaene-PGL) + (6 × % hexaene-PGL)]/100. **(C)**, Ratio of unsaturated and saturated PGLs. **(D)**, Ratios of select PC and PE species levels. Mean ± SEM are shown (n = 3). The P-values of < 0.05, <0.01 and < 0.001 are represented by *, ** and ***, respectively.

influence drug susceptibility of fungal cells (Supplementary Table S1). Notable compositional changes were recorded in earlier published comparative lipidomics between isogenic matched pair of AS/AR (azole susceptible/azole-resistant) isolates of *C. albicans* (Singh and Prasad 2011). In Gu4/Gu5, G2/G5, YOI-16/YOI-64 isolates representing AS (azole sensitive/AR (azole resistant) isogenic pairs of *C. albicans* hospital isolates showed consistent increase in odd chain FA containing PGLs and unsaturation index in AR G5, Gu5, and YOI-64 isolates as compared to susceptible Gu4, G2 and YOI-16, respectively (Singh and Prasad 2011; Singh, Mahto and Prasad 2013). The odd chain FAs have a better advantage in influencing the membrane fluidity as compared to the polyunsaturated FAs (Jenkins, West and Koulman 2015), probably due to its low melting temperature (Ibarguren, López and Escribá 2014; Beppu *et al.* 2017). The compromised PGL biosynthesis with resulting changes in membrane fluidity affects was shown to affect the drug diffusion, accumulation and drug susceptibility of *C. albicans* cells highlighting a strong link between PGL homeostasis and azole resistance (Singh and Prasad 2011). The raised unsaturated lipids content in the present study is another common compositional change between resistant *C. auris* (present study) and *C. albicans* cells (Singh and Prasad 2011).

NCCPF_470033 shows variations in DAG and TAG metabolism

Among the neutral lipids, of a majority of DAG species that showed statistically significant changes, 16:1-DAG (32:2, 32:1, 34:3), 16:0-DAG (34:2, 34:1) and 18:1-DAG (34:2, 34:1) species were abundant in NCCPF_470033 compared to CBS10913T strain (Fig. 6). In contrast, of a majority of TAG species that showed statistically significant changes, 16:1-TAG (52:3), 16:0-TAG (46:2, 52:2), 18:1-TAG (48:3, 52:4, 52:3, 52:2, 54:3, 52:2) and 18:0-TAG (54:2) were present in much low in NCCPF_470033 compared to CBS10913T strain (Fig. 6).

Resistant *C. auris* possess a higher level of free ergosterol

Sterols and SLs are the other two essential components of the membranes that directly influence membrane fluidity (Dufourc 2008; Guan *et al.* 2009). Azole resistance in *C. auris* is caused by alteration in the ergosterol pathway and ergosterol content (Kean and Ramage 2019; Zamith-Miranda *et al.* 2019). We examined ergosterol and its intermediates by employing GC-MS and identified seven key intermediates of ergosterol biosynthesis pathway. Upon analyzing the free ergosterol biosynthe-

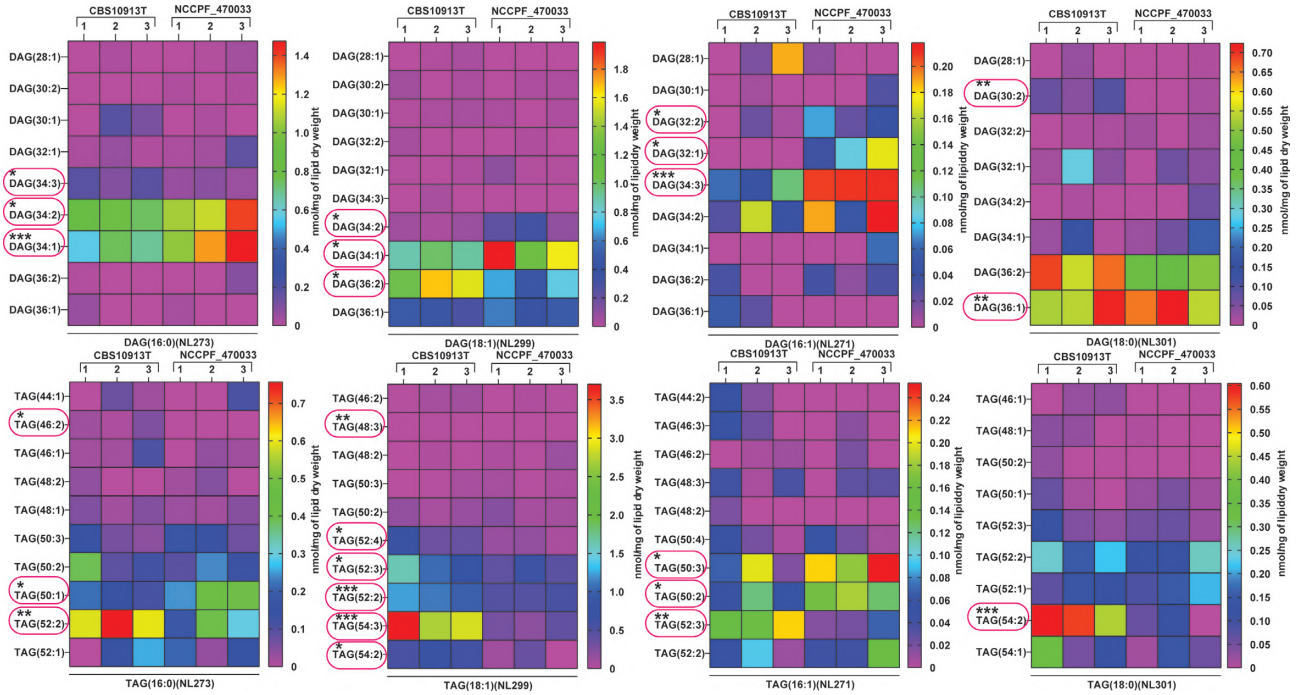

Figure 6. Comparison of DAG and TAG molecular lipid species compositions in CBS10913T and NCCPF_470033 strains. The DAG and TAG molecular species were analyzed as described earlier (Singh and Prasad 2011), also see Figure 2). DAG and TAG species are represented 'total number of carbons in the acyl chains: total number of carbon-carbon double bonds in the acyl chains'. DAG and TAG species boxed in red represents statistically significant changes. Data represents nmol per mg lipid dry weight and can be found in supplementary sheet S2. All the 3 replicates are plotted for each strain. The P-values of < 0.05, <0.01 and < 0.001 are represented by *, ** and ***, respectively.

sis intermediates, we observed that, most were significantly lower in NCCPF_470033 as compared to CBS10913T. Remarkably both fungisterol and squalene were below the detection limit and showed a drastic reduction in NCCPF_470033 (Fig. 7A). The end products ergostatetraenol and ergosterol levels, however, were significantly higher in NCCPF_470033 as compared to CBS10913T strain. In contrast, the levels of ergosteryl esters remained unchanged between the two isolates (Fig. 7B). similarly, total ergosterol was found higher in azole resistant *C. auris* isolate (Zamith-Miranda *et al.* 2019). The higher ergosterol content in NCCPF_470033 well correlated with observed higher resistance towards azoles of NCCPF_470033 isolate (Fig. 7A). The lowering of ergosterol under hypoxic *C. albicans* cells reported recently corroborates earlier studies. It highlights its role in governing FLC resistance (Burgain *et al.* 2020).

Few complex SL species show alteration in NCCPF_470033

Although the detailed analysis of SLs requires different protocol of extraction, the method employed in the present study let identification of some of the SL structures. Our analysis revealed that the levels of IPC (44:0–2), IPC (46:0–3) and MIPC (44:0–2) species were significantly lowered in NCCPF_47033 compared to CBS10913T strain (Fig. 7C). Some of IPC structures detected did show variation between CBS10913T and NCCPF_470033 strains, and whether these changes are related to drug susceptibilities will require further studies. A detailed and targeted sphingolipidomic study is required to understand the relevance of SLs in drug resistance in *C. auris*.

PCA analysis reveals the distinctness of the susceptible and resistant isolate

The comparative lipidome data described above hints towards a massive remodeling of lipid species in NCCPF_470033 when compared to the CBS10913T strain. We performed PCA analysis to further examine the statistical significance of remodeling of lipids associated with high azole resistance. PCA analysis allows the extraction and visualization of statistically significant variations from larger data sets. The extracted data are described by the principal components which account for the possible variations within the data. PCA was performed, using the lipid species data in nmol/mg lipid weight, between NCCPF_470033 and CBS10913T strains to highlight the statistically significant SL variations amongst them. The PCA analysis allowed the extraction of 5 principal components, of which the principal component 1, 2 and 3 accounted for ~83% variance in the data sets and were plotted (Fig. 8). Also, the associated loading values of each lipid species are decisive in the allocation of each principal component.

The plot of principal components 1 and 2 exhibited segregation of CBS10913T and NCCPF_470033 strains from each other (Fig. 8). An inspection of the loading values linked to principal component 1 confirmed that the lipid species with less abundance (like TAG(52:3)-16:1, TAG(54:2)-18:0, TAG(54:3)-18:1) and those with high abundance (like DAG(32:1)-16:1 and DAG(34:1)-18:1) in azole resistant NCCPF_470033 strain (compared to CBS10913T), are key to the separation of CBS10913T and NCCPF_470033 strains on principal component 1 axis. Analysis of loading values linked to principal component 2 reveals that the lipid species with less abundance (like TAG(54:2)-18:0, TAG(52:2)-16:0, TAG(52:3)-16:1) and those with high abun-

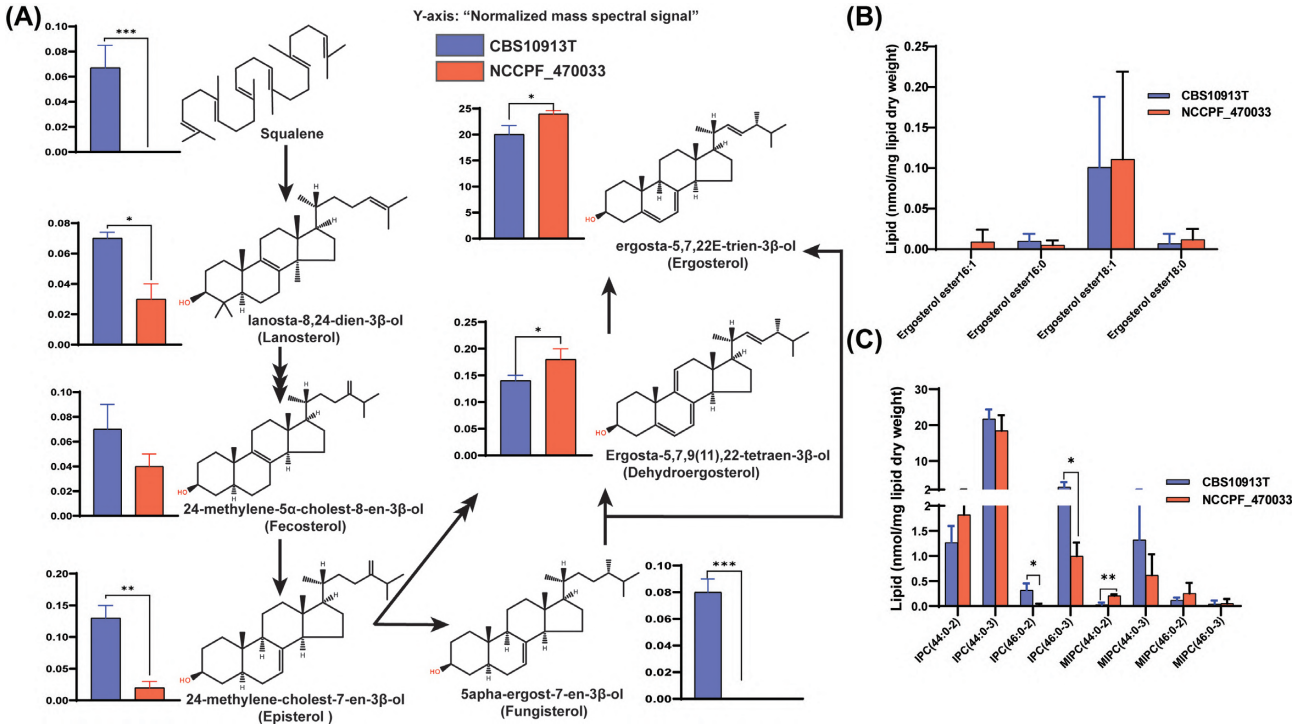

Figure 7. Comparison of sterols and sphingolipid compositions in CBS10913T and NCCPF_470033 strains. **(A)**, Analysis of free sterol species. **(B)**, Analysis of steryl esters. **(C)**, Analysis of IPC's and MIPC's. IPC and MIPC species are represented as 'total number of carbons in the sphingoid base and acyl chains: total number of carbon-carbon double bonds in the sphingoid base and acyl chains- number of hydroxyl groups present in the sphingoid base and acyl chains'. Data in (A) is represented as the normalized mass spectral signal. Data in (B) and (C) are represented as nmol per mg lipid dry weight and can be found in supplementary sheet S2. Mean ± SEM of 3 replicates is plotted. The *P*-values of < 0.05, <0.01 and < 0.001 are represented by *, ** and ***, respectively.

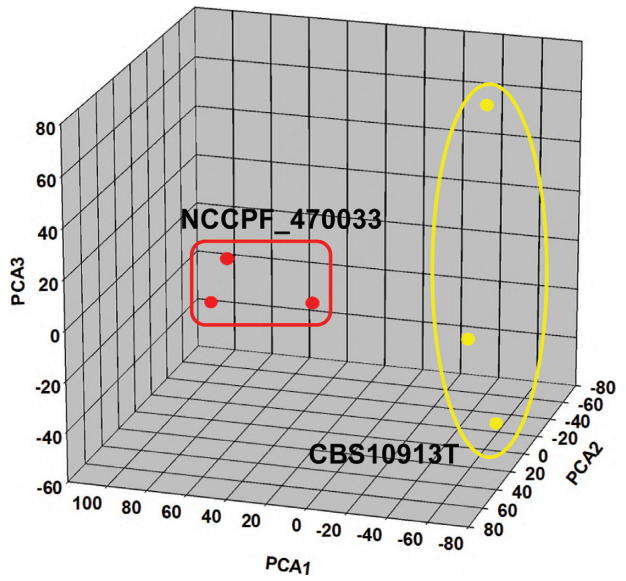

Figure 8. PCA analysis of lipid species compositions of CBS10913T and NCCPF_470033 strains of *C. auris*. PCA analysis was performed using the XLSTAT software described in methods. The scores of the top 3 principal components (factors) are plotted, demonstrating more than 83% of the variance in the data sets. The principal component 1 (factor 1), principal component 2 (factor 2) and principal component 3 (factor 3) contribute 43.33%, 24.5% and 15.5% variances respectively. A blind analysis was performed using 3 replicate data sets of each strain (Supplementary sheet S2). A list of factors loading values associated with each principal component is shown in supplementary sheet S4.

dance (like DAG(34:1)-18:1, DAG(34:3)-16:1, DAG(32:1)-16:1) in NCCPF_470033 (compared to CBS10913T), are key to separation of CBS10913T and NCCPF_470033 strains on principal component 2 axis. Similar variations were also observed across principal component 3 axis among the DAG and TAG species

However, the PCA analysis using the complete lipid species data set could not highlight the significant changes in the phospholipid group. To resolve this issue, we performed yet another PCA analysis using the lipid species data as mole% (% of total PGL + SL, supplementary sheet S3). In these analyses, five principal components were extracted, where the principal component 1 and 2 accounted for more than 95% variation in the data sets (Fig. S2a, Supporting Information). The loading values of principal component 1 show that PC (36:3, 36:2, 36:1, 38:3), PA (36:2, 36:1), PI (36:3), IPC (44:0–3), LPE (16:0) are deficient, while PE (32:1, 34:1, 34:2, 34:3, 36:3), PC (32:1, 32:2, 34:1, 34:2) are abundant, in NCCPF_470033 strain and important for segregation of CBS10913T and NCCPF_470033 strains on principal component 1 axis (Fig. S2a and b, Supporting Information). The loading values of principal component 2 show that the mono-unsaturated lipid species like PC (28:1, 36:1), PI (36:1), IPC (44:0–3), LPC (16:0) are deficient. In contrast, poly-unsaturated lipid species like PE (34:2, 34:3, 36:3), PC (34:2, 34:3) are abundant, in NCCPF_470033 strain and important for segregation of CBS10913T and NCCPF_470033 strains on principal component 2 axis (Fig. S2a and b, Supporting Information). Together, these PCA analyses highlight the specific subset of lipid species associated specifically with the azole resistant *C. auris*.

A comparative PCA analysis between the lipid profiles of *C. auris* strains (this study) with those of other *Candida* species (published previously, (Singh *et al.* 2010) shows a distinct lipid

imprint of *C. auris* (Fig. S2c and d, Supporting Information). Further, using the PCA analysis, we could also highlight similarities and differences in lipid profiles of *C. auris* strains and the previously published lipidomes of clinical isolates of *C. albicans* (Singh and Prasad 2011; Singh, Yadav and Prasad 2012; Singh, Mahto and Prasad 2013) (Supplementary Fig. S2e and S2f).

Although the PCA analyses did highlight certain lipid species that show significant changes between data sets, however, lipid changes consistent with drug resistance are difficult to often understand. For simplification, we have summarized the lipid variations reported in earlier published studies involving AS/AR isolates of *C. albicans* and *C. auris* and the present study (Table S1, Supporting Information). A comparison of these data sets shows that the lipid changes occurring between different AS/AR isolates are quite divergent and could impact drug susceptibilities in different ways, and demand further studies for better understanding.

CONCLUSION

Overall, in this study we were able to: (i) quantify major lipid groups and determine molecular lipid species compositions; (ii) highlight specific changes among the lipid species associated with azole resistance in *C. auris*; (iii) underline the commonalities of lipid compositional changes between AR *C. auris* and other *Candida* spp.; (iv) identify that specific lipid species variations could be a feature to distinguish *C. auris* strains from the other species of *Candida*. In future, we aim to expand our spectrum of analysis by including several susceptible and resistant isolates that are resistant to fluconazole and show collateral resistance to other class of drugs to pave way for better insight into the relevance of lipids in drug resistance in this important pathogenic yeast.

SUPPLEMENTARY DATA

Supplementary data are available at *FEMSYR* online.

AUTHORSHIP

Lipid experimentation and data analysis: GS, MK and AS; Strain curation and drug susceptibility: SK, MK, SMR and AC; Manuscript writing and review editing: MK, AS, AC, NAG and RP; Funding: AS, NAG and RP; Conceptualization: AS and RP. All authors read and approved the final manuscript.

ACKNOWLEDGMENTS

RP acknowledges support from the Indian Council of Medical Research, ICMR (AMR/149 (2)-2018-ECD-II). AS thanks support from ICMR (No.52/08/2019-BIO/BMS), DST-PURSE program (SR/PURSE Phase 2/29(C)) and the University of Lucknow. AS recognizes the support of Amity University, Haryana, during a mini-sabbatical stay. NAG acknowledges ICGEB, New Delhi, and Department of Biotechnology (DBT), Government of India for financial support (Grant No.: BT/PB/Centre/03/ICGEB/2011-PhaseII). The lipid analyses described in this work were performed in parts at the Kansas Lipidomics Research Center Analytical Laboratory, Kansas State University, USA (funded by NSF grants EPS 0236913, MCB 1413036, MCB 0920663, DBI 0521587, DBI1228622 and K-INBRE of NIH P20GM103418) and Amity Lipidomics Research Facility (ALRF), Amity University Haryana, India. MK and SK acknowledge the Department of Biotechnology (DBT) and the Council of Scientific and Industrial Research (CSIR) for providing fellowship support.

Conflict of interest. None declared.

REFERENCES

Anderson JB. Evolution of antifungal-drug resistance: mechanisms and pathogen fitness. *Nat Rev Microbiol* 2005;**3**:547–56.

Balzi E, Goffeau A. Yeast multidrug resistance: the PDR network. *J Bioenerg Biomembr* 1995;**27**:71–6.

Beppu F, Yasuda K, Okada A *et al.*. Comparison of the Distribution of Unsaturated Fatty Acids at the Sn-2 Position of Phospholipids and Triacylglycerols in Marine Fishes and Mammals. *J Oleo Sci* 2017;**66**:1217–27.

Bowden JA, Heckert A, Ulmer CZ *et al.* Harmonizing lipidomics: NIST interlaboratory comparison exercise for lipidomics using SRM 1950-Metabolites in Frozen Human Plasma. *J Lipid Res* 2017;**58**:2275–88.

Brown GD, Denning DW, Gow NAR *et al.* Hidden Killers: Human Fungal Infections. *Sci Transl Med* 2012;**4**:165rv13.

Burgain A, Tebbji F, Khemiri I *et al.* Metabolic Reprogramming in the Opportunistic Yeast Candida albicans in Response to Hypoxia. *mSphere* 2020;**5**, DOI: 10.1128/mSphere.00913-19.

Chowdhary A, Sharma C, Meis JF. Candida auris: A rapidly emerging cause of hospital-acquired multidrug-resistant fungal infections globally. Hogan DA (ed). *PLoS Pathog* 2017;**13**:e1006290.

Dufourc EJ. Sterols and membrane dynamics. *J Chem Biol* 2008;**1**:63–77.

Fairlamb AH, Gow NA, Matthews KR *et al.* Stop neglecting fungi. *Nat Microbiol* 2017;**2**:17120.

Folch J, Lees M, Sloane Stanley GH. A simple method for the isolation and purification of total lipides from animal tissues. *J Biol Chem* 1957;**226**:497–509.

Gao J, Wang H, Li Z *et al.* Candida albicans gains azole resistance by altering sphingolipid composition. *Nat Commun* 2018;**9**:4495.

Gonçalves S, Silva PM, Felício MR *et al.* Psd1 Effects on Candida albicans Planktonic Cells and Biofilms. *Front Cell Infect Microbiol* 2017;**7**:249.

Guan XL, Souza CM, Pichler H *et al.* Functional Interactions between Sphingolipids and Sterols in Biological Membranes Regulating Cell Physiology. *Mol Biol Cell* 2009;**20**:2083–95.

Hou X, Healey KR, Shor E *et al.* Novel *FKS1* and *FKS2* modifications in a high-level echinocandin resistant clinical isolate of *Candida glabrata*. *Emer Microb Infect* 2019;**8**:1619–25.

Ibarguren M, López DJ, Escribá PV. The effect of natural and synthetic fatty acids on membrane structure, microdomain organization, cellular functions and human health. *Biochim Biophys Acta BBA - Biomembr* 2014;**1838**:1518–28.

Jenkins B, West JA, Koulman A. A Review of Odd-Chain Fatty Acid Metabolism and the Role of Pentadecanoic Acid (C15:0) and Heptadecanoic Acid (C17:0) in Health and Disease. *Molecules* 2015;**20**:2425–44.

Kathuria S, Singh PK, Sharma C *et al.* Multidrug-Resistant Candida auris Misidentified as Candida haemulonii: Characterization by Matrix-Assisted Laser Desorption Ionization–Time of Flight Mass Spectrometry and DNA Sequencing and Its Antifungal Susceptibility Profile Variability by Vitek 2, CLSI Broth Microdilution, and Etest Method. Warnock DW (ed.). *J Clin Microbiol* 2015;**53**:1823–30.

Kean R, Ramage G. Combined Antifungal Resistance and Biofilm Tolerance: the Global Threat of Candida auris. *mSphere* 2019;**4**, DOI: 10.1128/mSphere.00458-19.

Khandelwal NK, Sarkar P, Gaur NA *et al.* Phosphatidylserine decarboxylase governs plasma membrane fluidity and impacts drug susceptibilities of Candida albicans cells. *Biochimica et Biophysica Acta (BBA) - Biomembranes* 2018;**1860**:2308–19.

Kim SH, Iyer KR, Pardeshi L *et al.* Genetic Analysis of *Candida auris* Implicates Hsp90 in Morphogenesis and Azole Tolerance and Cdr1 in Azole Resistance. Kronstad JW (ed). *mBio* 2019;**10**:e02529–18.

Kondo N, Ohno Y, Yamagata M *et al.* Identification of the phytosphingosine metabolic pathway leading to odd-numbered fatty acids. *Nat Commun* 2014;**5**:1–13.

Kumari S, Kumar M, Khandelwal NK *et al.* ABC transportome inventory of human pathogenic yeast Candida glabrata: Phylogenetic and expression analysis. *PLoS One* 2018;**13**:e0202993.

Lattif AA, Mukherjee PK, Chandra J *et al.* Lipidomics of Candida albicans biofilms reveals phase-dependent production of phospholipid molecular classes and role for lipid rafts in biofilm formation. *Microbiology* 2011;**157**:3232–42.

Lockhart SR, Etienne KA, Vallabhaneni S *et al.* Simultaneous Emergence of Multidrug-Resistant *Candida auris* on 3 Continents Confirmed by Whole-Genome Sequencing and Epidemiological Analyses. *CLINID* 2017;**64**:134–40.

Lone SA, Ahmad A. *Candida auris* —the growing menace to global health. *Mycoses* 2019;**62**:620–37.

Lupetti A, Danesi R, Campa M *et al.* Molecular basis of resistance to azole antifungals. *Trends Mol Med* 2002;**8**:76–81.

Mukhopadhyay K, Kohli A, Prasad R. Drug Susceptibilities of Yeast Cells Are Affected by Membrane Lipid Composition. *Antimicrob Agents Chemother* 2002;**46**:3695–705.

Pfaller MA, Boyken LB, Hollis RJ *et al.* Validation of 24-Hour Fluconazole MIC Readings versus the CLSI 48-Hour Broth Microdilution Reference Method: Results from a Global Candida Antifungal Surveillance Program. *J Clin Microbiol* 2008;**46**:3585–90.

Prasad R, Singh A. Lipids of Candida albicans and their role in multidrug resistance. *Curr Genet* 2013;**59**:243–50.

Prasad T, Saini P, Gaur NA *et al.* Functional Analysis of CaIPT1, a Sphingolipid Biosynthetic Gene Involved in Multidrug Resistance and Morphogenesis of Candida albicans. *Antimicrob Agents Chemother* 2005;**49**:3442–52.

Rybak JM, Doorley LA, Nishimoto AT *et al.* Abrogation of Triazole Resistance upon Deletion of CDR1 in a Clinical Isolate of Candida auris. *Antimicrob Agents Chemother* 2019;**63**, DOI: 10.1128/AAC.00057-19.

Satoh K, Makimura K, Hasumi Y *et al.* Candida auris sp. nov., a novel ascomycetous yeast isolated from the external ear canal of an inpatient in a Japanese hospital. *Microbiol Immunol* 2009;**53**:41–4.

Sharma M, Dhamgaye S, Singh A *et al.* Lipidome analysis reveals antifungal polyphenol curcumin affects membrane lipid homeostasis. *Front Biosci (Elite Ed)* 2012;**4**:1195–209.

Sharma S, Alfatah, Bari VK *et al.* Sphingolipid Biosynthetic Pathway Genes FEN1 and SUR4 Modulate Amphotericin B Resistance. *Antimicrob Agents Chemother* 2014;**58**:2409–14.

Shor E, Perlin DS. Coping with stress and the emergence of multidrug resistance in fungi. *PLoS Pathog* 2015;**11**:e1004668.

Singh A, Del Poeta M. Sphingolipidomics: An Important Mechanistic Tool for Studying Fungal Pathogens. *Front Microbiol* 2016;**7**, DOI: 10.3389/fmicb.2016.00501.

Singh A, MacKenzie A, Girnun G *et al.* Analysis of sphingolipids, sterols, and phospholipids in human pathogenic Cryptococcus strains. *J Lipid Res* 2017;**58**:2017–36.

Singh A, Mahto KK, Prasad R. Lipidomics and in Vitro Azole Resistance in Candida albicans. *OMICS: J Int Biol* 2013;**17**:84–93.

Singh A, Prasad R. Comparative Lipidomics of Azole Sensitive and Resistant Clinical Isolates of Candida albicans Reveals Unexpected Diversity in Molecular Lipid Imprints. *PLoS One* 2011;**6**:e19266.

Singh A, Prasad T, Kapoor K *et al.* Phospholipidome of Candida: Each Species of Candida Has Distinctive Phospholipid Molecular Species. *OMICS: J Int Biol* 2010;**14**:665–77.

Singh A, Yadav V, Prasad R. Comparative Lipidomics in Clinical Isolates of Candida albicans Reveal Crosstalk between Mitochondria, Cell Wall Integrity and Azole Resistance. *PLoS One* 2012;**7**:e39812.

Wasi M, Khandelwal NK, Moorhouse AJ *et al.* ABC Transporter Genes Show Upregulated Expression in Drug-Resistant Clinical Isolates of Candida auris: A Genome-Wide Characterization of ATP-Binding Cassette (ABC) Transporter Genes. *Front Microbiol* 2019;**10**:1445.

Zamith-Miranda D, Heyman HM, Cleare LG *et al.* Multi-omics Signature of *Candida auris*, an Emerging and Multidrug-Resistant Pathogen. Elias J (ed). *mSystems* 2019;**4**:e00257–19, /msystems/4/4/mSys.00257-19.atom.

Pandey *et al. Biotechnol Biofuels* (2019) 12:40
https://doi.org/10.1186/s13068-019-1379-x

Biotechnology for Biofuels

RESEARCH Open Access

Evaluation of divergent yeast genera for fermentation-associated stresses and identification of a robust sugarcane distillery waste isolate *Saccharomyces cerevisiae* NGY10 for lignocellulosic ethanol production in SHF and SSF

Ajay Kumar Pandey, Mohit Kumar, Sonam Kumari, Priya Kumari, Farnaz Yusuf, Shaik Jakeer, Sumera Naz, Piyush Chandna, Ishita Bhatnagar and Naseem A. Gaur*

Abstract

Background: Lignocellulosic hydrolysates contain a mixture of hexose (C6)/pentose (C5) sugars and pretreatment-generated inhibitors (furans, weak acids and phenolics). Therefore, robust yeast isolates with characteristics of C6/C5 fermentation and tolerance to pretreatment-derived inhibitors are pre-requisite for efficient lignocellulosic material based biorefineries. Moreover, use of thermotolerant yeast isolates will further reduce cooling cost, contamination during fermentation, and required for developing simultaneous saccharification and fermentation (SSF), simultaneous saccharification and co-fermentation (SScF), and consolidated bio-processing (CBP) strategies.

Results: In this study, we evaluated thirty-five yeast isolates (belonging to six genera including *Saccharomyces, Kluyveromyces, Candida*, *Scheffersomyces, Ogatea* and *Wickerhamomyces*) for pretreatment-generated inhibitors {furfural, 5-hydroxymethyl furfural (5-HMF) and acetic acid} and thermotolerant phenotypes along with the fermentation performances at 40 °C. Among them, a sugarcane distillery waste isolate, *Saccharomyces cerevisiae* NGY10 produced maximum 49.77 ± 0.34 g/l and 46.81 ± 21.98 g/l ethanol with the efficiency of 97.39% and 93.54% at 30 °C and 40 °C, respectively, in 24 h using glucose as a carbon source. Furthermore, isolate NGY10 produced 12.25 ± 0.09 g/l and 7.18 ± 0.14 g/l of ethanol with 92.81% and 91.58% efficiency via SHF, and 30.22 g/l and 25.77 g/l ethanol with 86.43% and 73.29% efficiency via SSF using acid- and alkali-pretreated rice straw as carbon sources, respectively, at 40 °C. In addition, isolate NGY10 also produced 92.31 ± 3.39 g/l (11.7% v/v) and 33.66 ± 1.04 g/l (4.26% v/v) ethanol at 40 °C with the yields of 81.49% and 73.87% in the presence of 30% w/v glucose or 4× concentrated acid-pretreated rice straw hydrolysate, respectively. Moreover, isolate NGY10 displayed furfural- (1.5 g/l), 5-HMF (3.0 g/l), acetic acid- (0.2% v/v) and ethanol-(10.0% v/v) tolerant phenotypes.

Conclusion: A sugarcane distillery waste isolate NGY10 demonstrated high potential for ethanol production, C5 metabolic engineering and developing strategies for SSF, SScF and CBP.

Keywords: Thermo-tolerance, Inhibitors, SHF, SSF, Fermentation, Ethanol

*Correspondence: naseem@icgeb.res.in; nasgaur@hotmail.com
Yeast Biofuel Group, DBT-ICGEB Center for Advanced Bioenergy Research, International Center for Genetic Engineering and Biotechnology (ICGEB), New Delhi 110067, India

Biomass Conversion and Biorefinery
https://doi.org/10.1007/s13399-020-00935-3

ORIGINAL ARTICLE

Secretome produced by a newly isolated *Aspergillus flavus* strain in engineered medium shows synergy for biomass saccharification with a commercial cellulase

Mohit Kumar[1,2] · Ajay Kumar Pandey[1] · Sonam Kumari[1] · Shahid Ali Wani[1] · Shaik Jakeer[1] · Rameshwar Tiwari[1] · Rajendra Prasad[2] · Naseem A Gaur[1]

Received: 21 May 2020 / Revised: 17 July 2020 / Accepted: 31 July 2020

Abstract

In this study, we evaluated the saccharification potential of the secretome produced by a new elephant faeces isolate *Aspergillus flavus* (AF-NGF1), alone as well as in combination with a commercial enzyme (CTec2). Medium engineering (involving sequential Taguchi design, response surface methodology and one factor at a time approaches) enhanced the cellulase (FPase) secretion in the secretome of isolate AF-NGF1 (AF-S) by 3.89-folds. AF-S showed a maximum increase of 7.1- and 8.69-folds in exo-glucanase (avicellase) and endo-glucanase (CMCase) activities, respectively. Equal enzyme loading (20 FPU/g of biomass) of AF-S and CTec2 showed comparable saccharification potential with acid pre-treated paddy straw (APPS). However, a 1:1 combination of AF-S and CTec2 showed 67.84% and 37.21% increased saccharification of APPS as compared with AF-S or CTec2 alone at 50 °C and 40 °C, respectively. During simultaneous saccharification and fermentation (SSF) at 40 °C, a 1:1 combination produced > 2-folds increased ethanol titre as compared with AF-S or CTec2 alone. When equal FPU of AF-S and CTec2 were mixed for a total of 20 FPU, the degree of synergy (DOS) for APPS saccharification was 1.79 ± 0.06 and ~ 30.49% increased FPase activity was detected, which suggested the synergistic correlation between AF-S and CTec2. Therefore, the combination of AF-S and CTec2 could be considered as a potential cellulolytic enzyme formulation for efficient biomass hydrolysis and SSF process for lignocellulosic ethanol production.

Mohit Kumar and Ajay Kumar Pandey contributed equally to this work as first author.

Highlights

- A 3.89-folds enhanced FPase activity was achieved by medium engineering in AF-S.
- Endo- and exo-glucanase activities were most influenced by medium engineering.
- AF-S and CTec2 (1:1) showed 67.84% enhanced saccharification than CTec2/AF-S.
- AF-S and CTec2 (1:1) produced 54.1% higher ethanol than CTec2/AF-S during SSF.
- AF-S showed synergy with CTec2 for FPase activity and APPS saccharification.

Electronic supplementary material The online version of this article (https://doi.org/10.1007/s13399-020-00935-3) contains supplementary material, which is available to authorized users.

✉ Naseem A Gaur
naseem@icgeb.res.in; nasgaur@hotmail.com

[1] Yeast Biofuel Group, DBT-ICGEB Centre for Advanced Bioenergy Research, International Centre for Genetic Engineering and Biotechnology, New Delhi, India

[2] Amity Institute of integrative science and health, Amity University Gurugram, Gurgaon, Haryana, India

Published online: 11 August 2020